STUDIES OF THE EFFECTS ON CANCER CELLS OF CISPLATIN IN COMBINATION WITH THE G-QUADRUPLEX STABILISING AGENT BRACO19.

A thesis submitted for the degree of Doctor of Philosophy of the University of London

Olga Greciano

Cancer Research UK Biomolecular Structure Group
The School of Pharmacy
University of London

January 2008

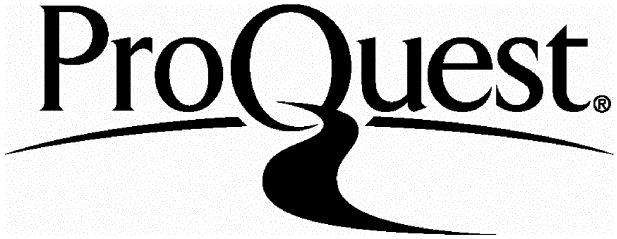

This thesis describes research conducted in the School of Pharmacy, University of London between October 2004 and January 2008 under the supervision of Prof. Stephen Neidle and Dr. Mekala Gunaratnam. I certify that the research described is original and that any parts of the work that have been conducted by collaboration are clearly indicated. I also certify that I have written all the text herein and have clearly indicated by suitable citation any part of this dissertation that has already appeared in publication.

Olga Genilloud

Signature

18/01/2008

Date

ACKOWLEDGMENTS

I would like to thank my supervisors Prof. Stephen Neidle and Dr. Mekala Gunaratnam for all the help and advice during the last years. In addition, I would also like to thank all my colleagues within the Biomolecular Structure Group and the School of Pharmacy for all their support during my PhD.

I also wish to thank Antisoma and Cancer Research UK for funding my PhD.

The FACS work was achieved in collaboration with Derek Davis and Lola Martinez for which I am very grateful.

Por último, quería dar las gracias a mis padres y a mis hermanos Felipe y Virginia que siempre me apoyan y me ayudan pero sobre todo cuando más los necesito.

CONTENTS

ABSTRACT 9

LIST OF FIGURES AND TABLES 11

LIST OF ABBREVIATIONS 16

Chapter 1- INTRODUCTION 19

1.1 Telomeres 19

1.1.1 End replication problem 19

1.1.2 Telomere associated proteins 21

1.2 Telomerase 25

1.2.1 Telomerase RNA component (TR) 25

1.2.2 Telomerase catalytic subunit (TERT) 26

1.2.2 Targeting telomerase in cancer therapy 28

1.3 Quadruplex 29

1.3.1 Quadruplex stabilising agents 30

1.3.2 Mechanism of action of G-quadruplex stabilising agents 34

1.4 Platinum compounds 36

1.4.1 Mechanism of action of platinum compounds 37

1.4.2 Resistance to platinum compounds 43

1.4.3 Telomeres and telomerase are possible targets of cisplatin 45

1.5 Combination therapy 46

AIMS OF THE THESIS 48

Chapter 2- COMBINATION TREATMENT OF BRACO19 AND CISPLATIN *IN VITRO*

2.1 INTRODUCTION 50

2.1.1 Drug combination studies 50

2.1.2 Drug combination studies using the combination index method of Chou and Talay 51

2.1.3 Response to chemotherapeutic agents in cancer cells. *In vitro* assays. 55

2.2 MATERIALS AND METHODS 56

2.2.1 Cell culture 56

2.2.2 Mycoplasma testing 56

2.2.3 Preparation of drugs 56

2.2.4 Short-term cytotoxicity studies: the sulphorhodamine B assay (SRB). 57

2.2.5 Determination of synergy by SRB 58

2.2.6 Long-term treatment 58

2.2.7 Statistical analysis 59

2.3 RESULTS 60

2.3.1 Combination index analysis in the epidermis carcinoma cell line A431 60

2.3.2 Long-term viability studies in A431 cells 63

2.3.3 Combination index analysis in the ovarian cell lines A2780 and A2780cis 66

2.3.4 Long-term viability studies in A2780 and A2780cis cells 71

2.3.5 Combination index analysis in the MCF-7 breast cancer cell line 74

2.3.6 Long-term viability studies in MCF-7 cells 77

2.4 DISCUSSION 79

Chapter 3- MECHANISM OF CELL GROWTH INHIBITION AFTER TREATMENT WITH BRACO19, CISPLATIN OR THE COMBINATION

3.1 INTRODUCTION 84

3.1.1 Senescence 84

3.1.2 Apoptosis 85

3.1.3 Necrosis 87

3.2 METHODS 88

3.2.1 Detection of cellular senescence (β-galactosidase activity) 88

3.2.2 Cell cycle analysis for sub G1 population 88

3.2.3 Bromodeoxyuridine (BrdU) staining 89

3.2.4 Annexin V and mitochondrial membrane potential 90

3.2.5 Detection of caspase 3 90

3.2.6 Detection of DNA strand-breaks using the Terminal deoxynucleotide transferase dUTP Nick End Labeling (TUNEL) assay 90

3.2.7 Dye exclusion method using trypan blue 91

3.3 RESULTS 92

3.3.1 Detection of cellular senescence (β-galactosidase activity) 92

3.3.2 Cell cycle analysis for sub-G1 97

3.3.3 Viability study. Bromodeoxyuridine incorporation 99

3.3.4 Annexin V 101

3.3.5 Tetramethyl rhodamine ethyl ester (TMRE) 104

3.3.6 Detection of caspase 3 activation 107

3.3.7 Detection of DNA strand breaks by TUNEL assay 110

3.3.8 Dye exclusion method using trypan blue 113

3.4 DISCUSSION 115

Chapter 4- EFFECTS OF BRACO19 AND CISPLATIN ON GENES AND PROTEINS INVOLVED IN APOPTOSIS

4.1 INTRODUCTION 122

4.1.1 p53 tumour suppressor signalling 122

4.1.2 The p53 independent pathway 124

4.2 METHODS 127

4.2.1 Reverse Transcriptase Polymerase Chain Reaction (RT-PCR) 127

4.2.2 Western blotting protocol 130

4.3 RESULTS 133

4.4 DISCUSSION 139

Chapter 5- EFFECTS OF BRACO19 AND CISPLATIN ON TELOMERES, TELOMERASE AND DNA DAMAGE RESPONSE

5.1 INTRODUCTION 143

5.1.1 DNA damage response 143

5.1.2 Telomere associated DNA damage 144

5.2 METHODS 145

5.2.1 Detection of gamma-H2AX 145

5.2.2 Chromosome banding and metaphase spreads 145

5.2.3 Measurement of telomere length 147

5.2.4 Measurement of telomerase activity 148

5.2.5 Reverse transcriptase polymerase chain reaction (h-TERT) 149

5.3 RESULTS 150

5.3.1 Detection of gamma-H2AX in A431 cells 150

5.3.2 Effect on chromosomes 160

5.3.3 Effect on telomere length 162

5.3.4 Effect on telomerase activity and h-TERT expression 167

5.4 DISCUSSION 170

Chapter 6- CONCLUSIONS 177

REFERENCES 183

Cisplatin is one of the most widely used drugs in the clinic in a variety of cancers such as ovarian, lung, head and neck, and is especially active in testicular cancer. Nevertheless, its side effects, principally nephrotoxicity, limit its use. Therefore it is important to combine this agent with drugs that can potentiate its effect, so that doses can be reduced and side-effects minimised.

A series of 3,6,9-trisubstituted acridines has been developed which act by binding to the 3'-single strand telomeric DNA overhang, stabilising G-quadruplex structures and producing inhibition of telomerase activity and subsequent arrest of cell growth. It has been previously shown that the lead compound from this series, BRACO19, is able to produce telomerase inhibition, which leads to telomere attrition and senescence phenotype *in vitro* in different human cancer cell lines, and *in vivo* in human tumour xenografts.

Cisplatin reacts preferentially with purine residues, especially with the N7 atom of guanines, producing DNA interstrand and intrastrand adducts, making telomeric DNA potentially a target of cisplatin. It is known that inhibition of telomerase activity enhances the effect of cisplatin in different cell lines. Therefore the combination of cisplatin with a G-quadruplex stabilising agent could be used as a new improved strategy of therapy.

The aim of this study was to establish the mechanism of action of this combination therapy at the molecular and cellular levels in different human cancer cell lines representing phenotypically varied cancers. Initially, determination of the grade of synergism using short-term cytotoxicity combination studies was carried out with both agents in the following cell lines: A2780, A2780cis, A431 and MCF7, using the Calcusyn program. All the cell lines followed the same pattern at the ratios used in this study, when the concentration of BRACO19 compared to cisplatin was greater the combination was better and synergistic for all of them. Following this, long-term viability studies were performed to investigate the effect after longer period of exposures. The results of these studies were definitely showing synergism for A431 and MCF-7 cells whereas for the ovarian cell lines the effects were additive at the concentrations used in this study. Subsequently, detailed molecular and cellular studies were carried out to determine the type of cell death using specific markers for apoptosis such as caspase 3 and cell cycle. Induction of senescence was studied assessing cells

for β-galactosidase activity. Gene and protein expression studies of important cell cycle regulators such as p53 and p21 were assessed. Also, an early DNA damage response was shown by the detection of γH2AX after treatment with both compounds in combination and alone. Inhibition of telomerase activity was observed for both agents and down-regulation of h-TERT in the case of BRACO19 and in the combination. However the compounds did not have an effect on telomere length.

This study has revealed that G-quadruplex stabilising ligands such as BRACO19 can be effectively used in combination with cisplatin to produce antitumour activity in various cancer cell lines. This can be of significant therapeutic utility in cancers that do not respond well to cisplatin.

Chapter 1- INTRODUCTION

Figure 1.1 DNA replication problem 20

Figure 1.2 Telomere-protein complex formed in human cells, the interaction between proteins and also the structure of t-loop/D-loop 23

Figure 1.3 Secondary structure of telomerase RNA 26

Figure 1.4 Telomerase structure 27

Figure 1.5 Scheme showing the telomerase mode of action 27

Figure 1.6 Schematic representation of a G-quartet and G-quadruplexes 30

Figure 1.7 Structures of G-quadruplex stabilising agents 33

Figure 1.8 Cisplatin structure 36

Figure 1.9 Carboplatin and oxaliplatin structures 37

Figure 1.10 Reaction of cisplatin with water molecules 38

Figure 1.11 Schematic representation of different cross-link formed by cisplatin 39

Figure 1.12 Structure of different adducts formed by cisplatin 42

Chapter 2- COMBINATION TREATMENT OF BRACO19 AND CISPLATIN *IN VITRO*

Figure 2.1 Median-effect plots for the two compounds and the combination at different drug ratios in A431 cells 62

Figure 2.2 Graphs showing long-term antitumour activity in A431 cells treated with BRACO19, cisplatin or the combination 64

Figure 2.3 A431 cells after one week treatment 65

Figure 2.4 Median-effect plots for the two compounds and the combination at different drug ratios in A2780 and A2780cis cells 70

Figure 2.5 Graphs showing long-term antitumour activity in A2780 cells treated with BRACO19, cisplatin or the combination 72

Figure 2.6 Graphs showing long-term antitumour activity in A2780cis cells treated with BRACO19, cisplatin or the combination 74

Figure 2.7 Median-effect plots for the two compounds and the combination at different drug ratios in MCF-7 cells 76

Figure 2.8 Graphs showing long-term antitumour activity in MCF-7 cells treated with BRACO19, cisplatin or the combination 78

Table 2.1 Combination index values in A431 cells 62

Table 2.2 Combination index values in A2780 and A2780cis cells 70

Table 2.3 Combination index values in MCF-7 cells 76

Chapter 3- MECHANISM OF CELL GROWTH INHIBITION AFTER TREATMENT WITH BRACO19, CISPLATIN OR THE COMBINATION

Figure 3.1 IMR-90 cells stained for β-galactosidase activity 93

Figure 3.2 A431 cells stained for β-galactosidase activity 94

Figure 3.3 MCF-7 cells stained for β-galactosidase activity 95

Figure 3.4 % of MCF-7 senescent cells after one, two or three weeks treatment with BRACO19, cisplatin or the combination 96

Figure 3.5 Cell cycle analysis in A431 cells after one week of treatment 98

Figure 3.6 Bromodeoxyuridine incorporation following a 30 minutes pulse in A431 cells treated for one week 100

Figure 3.7 Annexin V changes detected in A431 cells after one week of treatment 103

Figure 3.8 Tetramethyl rhodamine ethyl ester changes detected in A431 cells after one week treatment 106

Figure 3.9 Caspase 3 activation observed in jurkat cells 108

Figure 3.10 Detection of caspase 3 in A431 cells after one week treatment 109

Figure 3.11 Detection of DNA strand breaks in A431 cells after one week treatment 112

Figure 3.12 Graph representing % of non-viable A431 cells after one week treatment 114

Figure 3.13 Scheme of possible mechanism of cell death in A431cells following treatment with cisplatin, BRACO19 or the combination of both compounds 120

Table 3.1 Summary of the methods used for the study of the mechanism of cell growth inhibition 91

Table 3.2 Summary of changes observed in cell cycle in A431 cells after 1 week of treatment 97

Table 3.3 Summary of changes observed in bromodeoxyuridine incorporation in A431 cells after one week treatment 99

Table 3.4 Summary of changes observed in annexin V in A431 cells after one week treatment 104

Table 3.5 Summary of changes observed in tetramethlyl rhodamine ethyl ester in A431 cells after one week treatment 107

Table 3.6 Summary of changes observed in caspase 3 in A431 cells after one week treatment 108

Table 3.7 Summary of changes in % of apoptotic cells in A431 cells after one week treatment using TUNEL assay 110

Chapter 4- EFFECTS OF BRACO19 AND CISPLATIN ON GENES AND PROTEINS INVOLVED IN APOPTOSIS

Figure 4.1 Scheme showing different possible pathways a cell may undergo after DNA damage 126

Figure 4.2 p53, p21, p73 and GAPDH gene expression using RT-PCR 135

Figure 4.3 Graphs showing changes observed in p53, p21 and p73 normalized using GAPDH as a housekeeping gene 136

Figure 4.4 p53, p21 and α-actin protein expression using western blotting 137

Figure 4.5 Graphs showing changes observed in p53 and p21 normalized using α-actin as a housekeeping protein 137

Figure 4.6 PARP1 and GAPDH gene expression using RT-PCR 138

Figure 4.7 Graphs showing changes observed in PARP1 normalized using GAPDH as a housekeeping gene 138

Table 4.1 PCR conditions for the different primers used 129

Table 4.2 Dilution factors of primary and secondary antibodies 132

Table 4.3 Details of primary and secondary antibodies 132

Chapter 5- EFFECTS OF BRACO19 AND CISPLATIN ON TELOMERES, TELOMERASE AND DNA DAMAGE RESPONSE

Figure 5.1 γH2AX changes detected in A431 cells treated for different time points with BRACO19, cisplatin or the combination using FACS analysis 157

Figure 5.2 Immunofluorescence γH2AX detection in A431 cells 159

Figure 5.3 % of chromosome fusions in A431 cells treated with BRACO19, cisplatin or the combination 160

Figure 5.4 Metaphase spreads of A431 cells stained with giemsa. 161

Figure 5.5 Study of telomere length in A431 cells treated with BRACO19, cisplatin or the combination 163

Figure 5.6 Study of telomere length in A431 cells treated with BRACO19, cisplatin or the combination 164

Figure 5.7 Study of telomere length in A431 cells treated with BRACO19 165

Figure 5.8 Study of telomere length in A2780 cells treated with BRACO19 166

Figure 5.9 h-TERT gene expression using RT-PCR 168

Figure 5.10 Telomerase activity in A431 cells treated with BRACO19, cisplatin or the combination 169

Figure 5.11 Scheme of telomere associated DNA damage response in A431cells following treatment with cisplatin, BRACO19 or the combination of both compounds 175

Table 5.1 PCR conditions for the h-TERT primers used 149

Table 5.2 Summary of changes observed in γH2AX 157

Table 5.3 Summary of changes observed in γH2AX after treatment with 50 μM cisplatin used as a positive control 157

ALT	alternative lengthening of telomeres
ANOVA	Analysis of variance
ATM	ataxia telangiectasia mutated
ATP	adenosine triphosphate
ATR	ATM and Rad 3 related
BrdU	bromodeoxyuridine
C	cytosine
CI	combination index
DAPI	4',6-diamidino-2-phenylindole
D-loop	displacement loop
DNA	deoxyribonucleic acid
dNTP	deoxyribonucleotide triphosphate
dUTP	deoxyuridine triphosphate
ED	effective dose
FACS	fluorescence activated cell sorter
FITC	fluorescein
FRET	fluorescence resonance energy transfer
G	guanine
G1	gap 1 phase
G2	gap 2 phase
HR	homologous recombination
h-TERT	human telomerase reverse transcriptase
h-TR	human telomerase RNA
IC_{50}	concentration that produces 50% cell growth inhibition
NER	nucleotide excision repair

PARP1/2	poly(ADP-ribose) polymerase
PBS	phosphate buffered saline
PCR	polymerase chain reaction
POT1	human protection of telomeres 1
RNA	ribonucleic acid
RT-PCR	reverse transcriptase-PCR
SRB	sulphorhodamine B
S-phase	synthesis phase
TBS	tris-buffered saline
TERT	telomerase reverse transcriptase
T-loop	telomere loop
TMRE	tetramethyl rhodamine ethyl ester
TR	telomerase RNA
TRAP	telomere repeat amplification protocol
TRF1/TRF2	telomere repeat binding factors 1/2
TUNEL	Terminal deoxynucleotide transferase dUTP Nick End Labeling
X-gal	5-bromo-4-chloro-3-indolyl-β-D-galactopyranoside

Chapter 1- INTRODUCTION

1.1 Telomeres.

1.1.1 End Replication problem.

Telomeres are nucleoprotein complexes at the end of eukaryotic chromosomes comprising tandem repeat DNA sequences [TTAGGG of 6 to 12 kb and a short single-stranded G-rich 3′-overhang of 100 to 200 bases in mammals *(Makarov et al, 1997)*]. These sequences are associated with specific proteins. Telomeres protect chromosome ends from recombination, end-to-end fusions, and recognition as DNA damage, and need to be maintained in a "capped" status. The most accepted model proposes that telomeres in mammalian cells end in specific terminal loops termed telomere-loops (T-loops) (Figure 1.2). The 3'-telomeric overhang invades the double strand region forming a displacement-loop (D-loop), then protecting the end of the chromosome and avoiding being recognized as a DNA strand break *(Griffith et al, 1999; Greider, 1999)*. The integrity of the single strand telomeric overhang is essential for cell survival and loss of the capped status of the chromosome will lead to genomic instability and senescence *(Blackburn, 2001)*. The uncapping of telomeres is recognised as a DNA strand break or DNA damage, consequently DNA damage machinery is activated, cells exit cell cycle arrest in G1 and enter a non-replicative state.

Cells present telomere erosion varying from 50 to 200 bases at each round of replication *(Harley et al, 1990)* due to the "end replication problem". DNA replication is semiconservative, therefore every helix of DNA acts as a template for its own duplication. DNA synthesis starts with the formation of a replication fork, and then DNA is synthesised by the DNA polymerases which need a primer and add nucleotides in the 5′ to 3′direction. Because of the antiparallel orientation of the two strands in the double helix of DNA, one of the strands has to be synthesised in the 5′ to 3′direction and the other in the 3′ to 5′direction, called the leading and lagging strand respectively. Due to the nature of DNA polymerases synthesis in the 3′ to 5′direction is not possible. The lagging strand is synthesised discontinuously in small fragments called Okazaki fragments, each primed by a short RNA molecule. These primers are subsequently digested and replaced with DNA. Therefore while the replication of the leading strand is not expected to result in DNA loss, during the synthesis of the lagging strand due to the removal of the distal RNA primer, there is a small loss of DNA (Figure 1.1). This loss of DNA leads to the formation of the 3′-telomeric overhang. This model predicts the existence of overhangs in 50% of chromosome ends. However this is not the case and

therefore there must be other processes involved. It has been postulated that the origin of the G-rich tails is the result of a C-rich strand degradation mechanism carried out by a specific endonuclease at both chromosome ends *(Makarov et al, 1997)*.

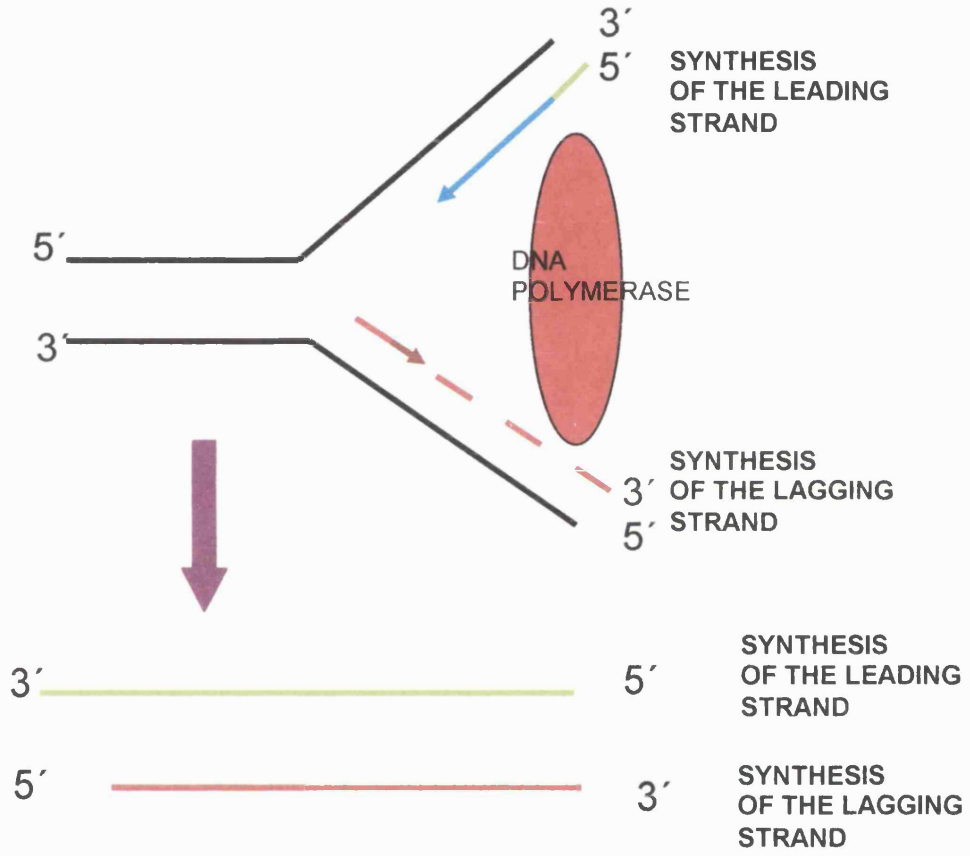

Figure 1.1. Mechanism of shortening of the leading strand due to the DNA replication problem (for further details see text).

Telomere shortening occurs in most somatic human cells, such as dermal fibroblasts, mucosal keratinocytes, peripheral blood cells, gastrointestinal epithelial cells, adrenocortical cells, renal cortex, liver, spleen. Most of these cells have in common that they are mitotically active *(Djojosubroto, 2003)*. Telomere shortening occurs after successive cell divisions. Furthermore, cells that are non-mitotically active such as brain and myocardium cells have stable telomere lengths *(Tabuko et al, 2002)* However, it has

been shown that cells with very little mitotic activity such as liver and renal cortex cells present telomere attrition, therefore there are other factors regulating telomere shortening. And it has also been demonstrated that the kinetics of telomere shortening are not linear, and vary with type and age of the cell *(Djojosubroto, 2003)*. Different mechanisms of telomere elongation have been proposed. Maintenance of telomere length is performed principally by a specific reverse transcriptase enzyme, telomerase. Telomerase is active in the germline and in some stem cells, but it is inactive in most somatic cells *(Chiu et al, 1996; Hiyama and Hiyama, 2007)*. In order to prevent progressive DNA loss in every round of replication, 90-95% of cancer cells have reactivated telomerase *(Shay and Bacchetti, 1997)*. Although this is the main mechanism developed by cancer cells to maintain their telomeres, some cancer cells can use an alternative lengthening of telomeres (ALT) mechanism. ALT involves recombinational telomere elongation and appears to occur frequently in astrocytic brain tumours and osteosarcomas *(Muntoni and Reddel, 2005)*. This mechanism has been proposed to occur by the invasion of the 3′-single strand telomeric overhang of one telomere into another telomere allowing consequently the extension of this 3′-end by a DNA polymerase *(Tomaska et al, 2004)*. Approximately 5-10% of human cancer cells use this mechanism.

1.1.2 Telomere associated proteins.

Telomeres act to protect chromosome ends from recombination processes, fusion and also avoiding being recognised as damaged DNA. Furthermore, they have to be able to allow the access and action of telomerase. They are associated with specific proteins (Figure 1. 2). The telomeric DNA forms a telomeric protein complex formed by six different proteins: TRF1, TRF2, TIN2, TPP1 (previously called PIP1, PTOP or TINT1), Rap1 and POT1. This complex has been termed "shelterin". The shelterin complex has two main functions, which are protection of chromosome ends and regulation of telomerase activity *(de Lange, 2005)*. Duplex telomeric DNA is bound by the TTAGGG repeat binding factors TRF1 and TRF2 which have C-terminal Myb-related DNA binding motifs and an internal dimerization domain that is required for homodimerization. TRF1 and TRF2 bind to double stranded telomeric DNA, and TRF2 has been reported to bind to the D-loop at the junction. TRF2 is important for the formation and stabilisation of the T-loop *(Griffith et al, 1999)*. Both factors participate in the regulation of telomere length *(Smogorzewska et al, 2000)*. Introduction of mutant

TRF1 into the HTC75 human fibrosarcoma cell line results in loss of TRF1 from telomeres. These changes affect telomere length. Cells that over-express wild-type TRF1 have progressive telomere shortening whereas cells that over-express mutated TRF1 show an increase in telomere length; therefore TRF1 produces negative feedback on telomerase activity *(van Steensel and de Lange, 1997)*. Similarly TRF2 has also been reported to regulate telomere length. Introduction of mutant TRF2 into HeLa cells leads to the induction of apoptosis. The expression of mutant TRF2 in this cell line produces disruption of the 3′-telomeric overhang that activates the DNA damage response and the apoptosis outcome. However in other cell lines such as IMR-90 or MCF-7, the inhibition of TRF2 function fails to produce apoptosis. Therefore telomere attrition may cause apoptosis or senescence depending on cell type *(Karlseder et al, 1999)*. Most recently, it was shown that the expression of a mutant TRF2 in IMR-90 cells induces premature senescence *(Smogorzewska and de Lange, 2002)*. It has been demonstrated that DNA damage induces phosphorylation of TRF2 probably through the ATM-kinase-mediated pathway. This phosphorylated protein does not bind to telomeres and it is rapidly localised in damage sites indicating the link between telomere maintenance and DNA damage response and repair *(Tanaka et al, 2005)*. TRF1 and TRF2 are linked via their associated factors TPP1 and TIN2 which form a complex. Over-expression of mutated TIN2 does not produce loss of TRF1, however it does produce telomere elongation, indicating the connexion between TRF1 and telomerase that result in the activation of telomerase activity *(Houghtaling et al, 2004)*. POT1 is the telomeric single-strand DNA binding protein 1. It binds directly to the single strand telomeric overhang, and also to the TRF1 complex through protein-protein interactions with TIN2 and TPP1. POT1 acts as a negative regulator of telomere length. Apparently it acts by regulating the access of telomerase to the primer *(Kelleher et al, 2005)*. POT1 defines how the C-rich telomeric DNA strand ends (ATC-5′). One possible theory is that POT1 recruits a nuclease that cleaves the C-strand at the 3′-AATC^CC-5′position *(Hockemeyer et al, 2005)*. Also, this explains the formation of the 3′-telomeric overhangs *(Makarov et al, 1997)*. The second theory is that POT1 protects the sequence (ATC-5′) from nucleolytic attack, therefore the nuclease does not have to be specific for this sequence, and attrition of the C-rich sequence occurs until an ATC-5′sequence is reached that POT1 is protecting *(Hockemeyer et al, 2005)*. Most recently it has been discovered that even POT1-TPP1 forms part of a complex that controls telomere length through a negative feedback mechanism; unexpectedly these proteins also can enhance

telomerase activity. A possible explanation is that the complex POT1-TPP1 binds to the 3'-overhang and prevents the binding and action of telomerase by negative feedback, but then by an unidentified mechanism there is disruption of this complex, and finally the POT1-TPP1 complex serves as a telomerase processivity factor *(Wang et al, 2007)*. The transcriptional repressor/activator protein Rap1 binds mostly to TRF2 *(Li et al, 2000)*.

In addition this DNA-protein complex interacts with factors involved in DNA recombination and repair such as tankyrase 1 and 2, poly(ADP-ribose)polymerase (PARP), the excision repair protein ERCC1/XPF, the helicases WRN and BLM, DNA protein kinase, ataxia-telangiectasia mutated (ATM), the ATM and Rad-3 related proteins (ATR), and the DNA-repair protein RAD51D, Ku70 and Ku86 *(Reviewed in Verdun and Karlseder, 2007)*.

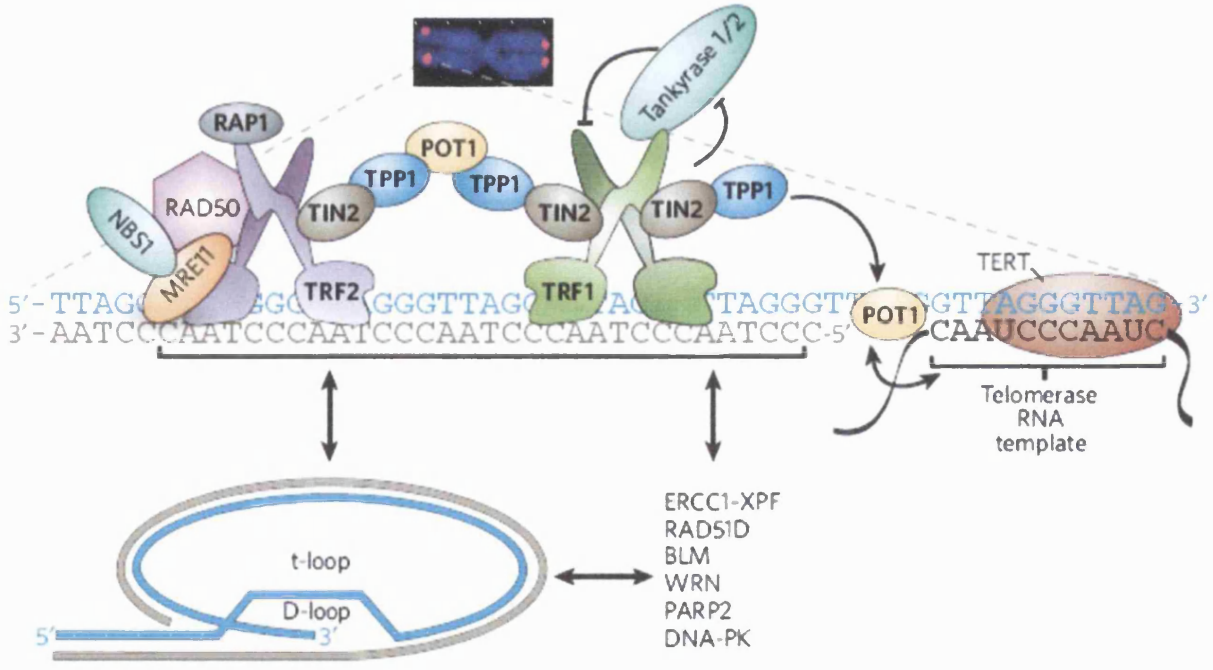

Figure 1.2. Telomere-proteins complex formed in human cells. The scheme shows the interaction between proteins and also the structure of t-loop/D-loop that DNA forms at the end of the telomeres *(Taken from Verdun and Karlseder, 2007)*.

The excision repair ERCC1/XPF complex acts as a structure specific endonuclease that has been shown to be associated with TRF2 in the telomeres. The introduction of a

mutant TRF2 into XPF deficient cells and to XPF wild type showed that when TRF2 activity was established again there was overhang loss only in the XPF wild-type cells. It is concluded that XPF may act as a nuclease that removes G-overhangs from damaged telomeres *(Zhu et al, 2003)*.

RAD51-D is also connected to telomeres. It has been shown that it participates in recombinational repair of double-strand breaks and telomere maintenance through the stabilisation of the T-loop *(Tarsounas et al, 2004)*.

The poly-ADP ribosylases PARP1 and PARP2 have been associated with TRF2. Moreover, PARP2 binds to TRF2 *(Dantzer et al, 2004)*. After telomere damage both enzymes poly(ADP-ribosyl)ate TRF2, and this modification releases it from telomeres. Consequently, it facilitates access of repair proteins to the damage site *(Dantzer et al, 2004; Gomez et al, 2006)*.

The member of the PARP family, tankyrase 1 interacts with TRF1. It poly(ADP-ribosyl)ates TRF1, which produces loss of its DNA binding activity and releases it from telomeres. TRF1 is degraded and as a consequence of the negative feedback there is telomere elongation *(Seimiya et al, 2005)*.

The RecQ family helicases, WRN and BLM have also been associated with telomeres. They have been connected with TRF2. Both helicases interact with TRF2 through its RecQ conserved domain located in the C-terminal region. This interaction produces the activation of its helicase activity *(Opresko et al, 2002)*. More recently, a link between WRN and BLM and POT1 has been proposed. POT1 seems to activate both helicases, inducing the unwinding of telomeric duplex and D-loop structures. A recent model proposes that POT-1 protects the single strand telomeric tail which is released by the helicases during DNA replication *(Opresko, 2005)*.

Decrease in Ku86 expression in human cells using small interference RNA has been related to telomere shortening and the appearance of chromosome aberrations such as chromosome fusions. Therefore, it seems that Ku86 in humans acts regulating telomere maintenance *(Jaco et al, 2004)*.

1.2. Telomerase

The enzyme telomerase was discovered in 1985 by Greider and Blackburn *(Greider and Blackburn, 1985)*. Telomerase is a ribonucleoprotein which functions as a reverse transcriptase or RNA dependent DNA polymerase, adding telomeric repeats to the single stranded 3'-ends of linear chromosomes. The telomerase complex has two key components, the catalytic protein subunit (TERT) responsible for the enzymatic elongation and the RNA component (TR) which provides a template which is essential and both have been identified in a big variety of organisms.

1.2.1 Telomerase RNA component (TR)

The RNA component of telomerase is not highly conserved during evolution. The size of TR can vary from 160 nucleotides in ciliates, 400-600 in vertebrates, to 1400 nucleotides in yeast. The primary sequence also changes in different species (Figure 1.3). However, recently it has been determined that all the different RNAs conserve a core secondary structure *(Chen and Greider, 2004)*. In vertebrates four conserved domains have been described; the pseudoknot domain, the boxH/ACA domain, the CR4/CR5 (conserved region 4 and conserved region 5 domain) and the CR7 (conserved region 7 domain) *(Chen et al, 2000)*. An important difference between telomerase compared to other retrotranscriptases is that the TR motif secondary structure is essential for the activity of this enzyme, while other reverse transcriptases use a small RNA template that is not a structural component of the enzyme *(Legassie and Jarstfer, 2005)*. The pseudoknot is absolutely necessary for the association of the TERT catalytic subunit with the RNA subunit *(Gilley and Blackburn, 1999; Lin et al, 2004; Theimer et al, 2005)*. The CR4-CR5 domains are also essential for telomerase activity *(Chen et al 2002)*, and boxH/ACA and CR7 are important to maintain RNA *(Chen et al, 2004)*. The pseudoknot contains an 11 nucleotide template (5′-CUAACCCUAAC-3′) which is located near its 5′-terminus. This region therefore has the template sequence for the synthesis of GGTTAG and an alignment domain is necessary to hybridize to the 3′-terminus of the DNA substrate *(Greider and Blackburn, 1989)*.

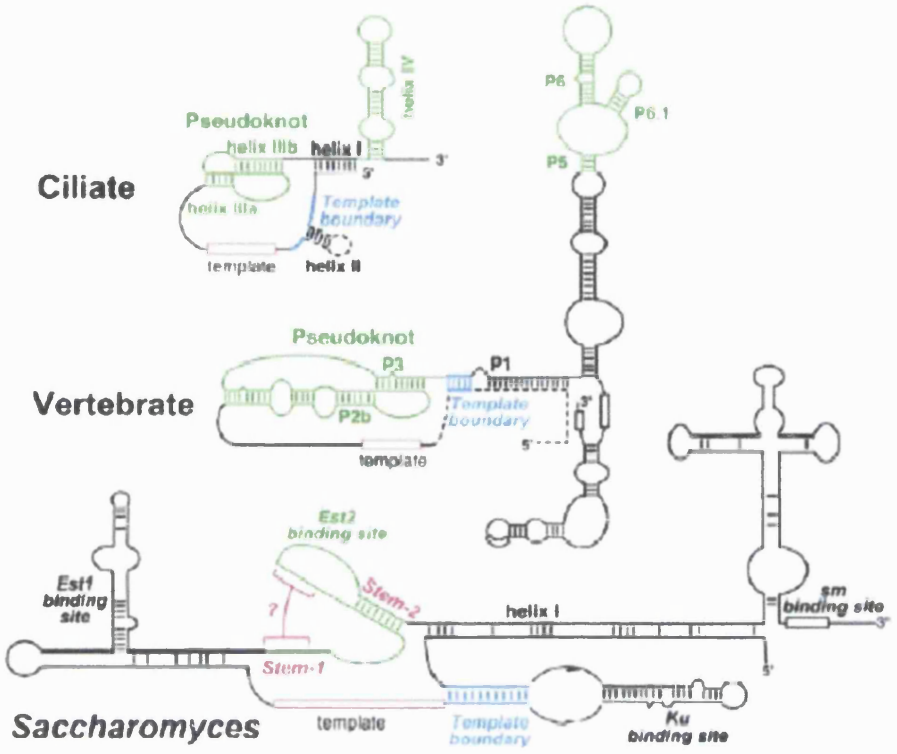

Figure 1.3. Secondary structures of telomerase RNA in different species *(Chen and Greider, 2004)*.

1.2.2 Telomerase catalytic subunit (TERT)

TERT is the catalytic subunit that mediates the addition of nucleotides and is homologous to reverse transcriptases (Figure 1.4). Therefore it contains several conserved retrotranscriptase motifs that are essential for its activity *(Lingner et al, 1997; Lee et al, 2003)*. The introduction of a mutation in the yeast homologue Est2p protein led to inactivation of telomerase and consequently produced telomere shortening indicating that these conserved retrotranscriptase motifs are necessary for the activity of telomerase *(Lingner et al, 1997)*. The TERT N-terminus has motifs that are important to bind to telomerase RNA and therefore are also essential for its activity. The C-terminus, although not very conserved during evolution, is also necessary for telomerase activity in vivo *(Huard et al, 2003)*.

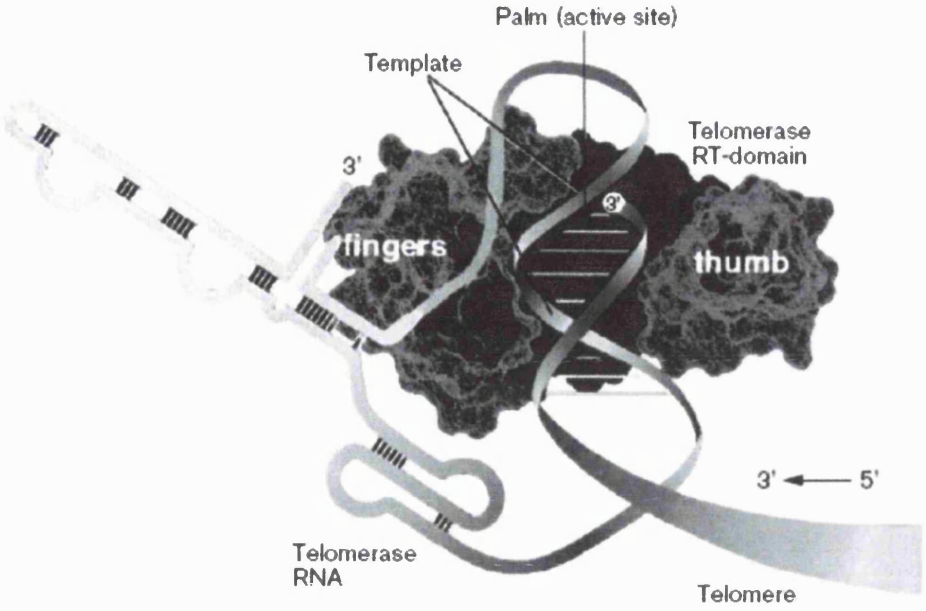

Figure 1.4. Model showing the telomerase structure *(Lingner and Cech,1998)*

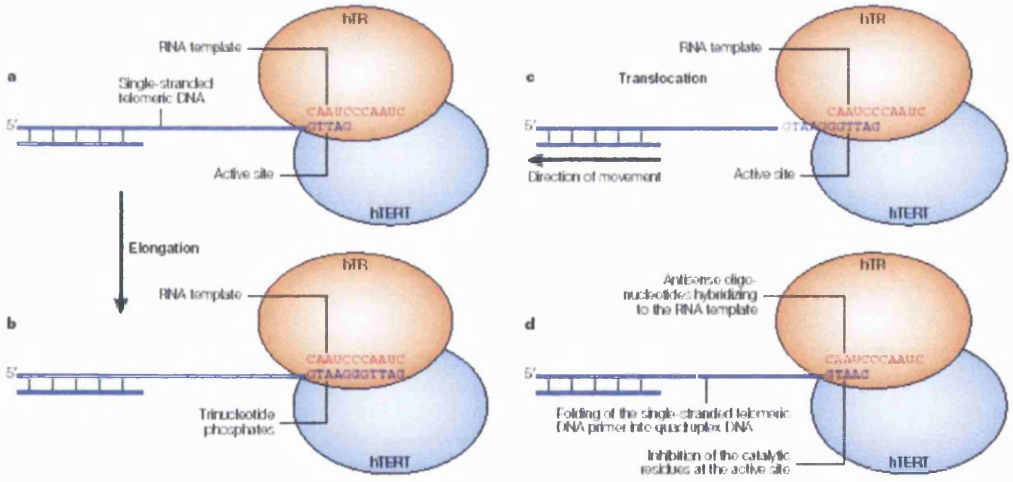

Figure 1. 5. Scheme showing the telomerase mode of action *(Neidle and Parkinson, 2002)*. a. The extreme of the 3´-telomeric overhang hybridizes with the end of the RNA template in the h-TR subunit. b. Telomerase starts adding nucleotides until the gap at the end of the template is filled. c. There is translocation of the telomerase enzyme in the 5´direction; therefore there is a new gap to be filled in the RNA template. d. scheme showing different mechanisms to target telomere maintenance.

1.2.3 Targeting telomerase in cancer therapy

Normal human somatic cells have a limited replicative lifespan due to the "end replication problem" added to other mechanisms such as nuclease degradation *(Harley et al, 1990; Makarov et al, 1997)* that lead to the replicative senescence phenotype, crisis and cell death. The fact that one of the characteristics of cancer cells is that they have unlimited capacity for replication and they have their telomere length stabilised *(Counter et al, 1992)* indicates that they have overcome this obstacle. Most human cancer cells overcome this obstacle through the reactivation of telomerase *(Shay and Bacchetti, 1997)*. Introduction of h-TERT in addition with two oncogenes (the simian virus 40 large-T oncoprotein and an oncogenic allele of H-ras) leads to the transformation of normal human epithelial and fibroblast cells into tumorigenic cells *(Hahn et al, 1999)*. Therefore, telomerase expression is essential for the unlimited replicative capacity for most human cancer cells. Introduction of a catalytically inactive dominant negative form of the catalytic subunit of telomerase h-TERT into human immortalized cells and cancer cells produced a disruption in telomerase activity that had an effect on telomere length that led to chromosomal fusions. This effect also produced the induction of apoptosis in p53 mutated cells indicating that it can be mediated by a p53-independent pathway *(Hahn et al, 1999)*. Consequently, in the absence of telomerase activity, cancer cells also shorten their telomeres in every round of replication that finally leads to telomere instability, senescence phenotype, and crisis and cell death. For that reason, inhibition of telomerase has been shown to be a good strategy for anticancer therapy.

There are different possible strategies for therapeutic intervention *(Neidle and Parkinson, 2002; Rezler et al, 2002; Shay and Wright, 2006)*; these include the direct inhibition of telomerase through the interaction with h-TERT or h-TR, or the indirect telomerase inhibition with G-quadruplex stabilising agents (Figure 1.5 d).

GRN163L is a lipid conjugate with a 13-mer oligonucleotide which targets the h-TR component of telomerase. As a consequence h-TERT cannot hybridise h-TR and there is telomerase inhibition *(Dikmen et al, 2005)*. BIBR1532 is a non-nucleosidic inhibitor of telomerase. It produces a delayed growth arrest in different leukaemia cell lines due to the effect on telomerase inhibition and consequent telomere erosion *(El-Daly et al, 2005)*.

1.3. Quadruplexes

DNA may be folded in regions which are rich in guanine bases into four-stranded structures called G-quadruplexes (Figure 1.6). The G-quartet is the basic unit that forms the G-quadruplex. Guanines are held together by Hoogsten hydrogen bonding forming planar structures *(Review in Davis, 2004)*. Those G-quartets stack one on top of the other, and are maintained by aromatic π-π interactions and monovalent ion interactions forming the G-quadruplexes *(Sundquist and Klug, 1989)*. These guanine rich sequences are found at the end of the chromosomes, in telomeric regions, in transcriptional regions in some oncogenes such as c-myc *(Simonsson et al, 1998)* and also promoter sites of many genes *(Huppert and Balasubramian, 2007)*. In fact, the human genome contains around 370,000 potential quadruplexes *(Huppert and Balasubramian, 2005; Todd et al, 2005)*. In vitro, the diversity is very large, they can be formed between different DNA strands, intermolecular quadruplex or a single DNA strand can fold and form an intramolecular unimolecular quadruplex. The intermolecular quadruplexes can be dimeric, formed by two strands or tetrameric formed by four strands. Also, the DNA strand orientation can be parallel, antiparallel or mixed. Furthermore, the different loops (the DNA sequences that join the G-runs) can have different locations, lateral, diagonal or propeller *(Burge et al, 2006)*. Although it has not been completely demonstrated, there is evidence for the existence of these structures *in vivo*. It has been shown by the production of specific antibodies against telomeric G-quadruplex that these antibodies react with the parallel G-quadruplex of Stylonychia. Furthermore, they react with the macronuclei and not with the micronuclei, showing that the presence of G-quadruplexes during DNA replication is very unlikely *(Schaffitzel et al, 2001)*. More recently, the existence of G-quadruplexes *in vivo* has been suggested in the transcription of G-rich regions in plasmid genomes, with the characterization of G-loops containing a stable RNA/DNA hybrid on one strand and possible G-quadruplex DNA on the other strand *(Duquette et al, 2004)*

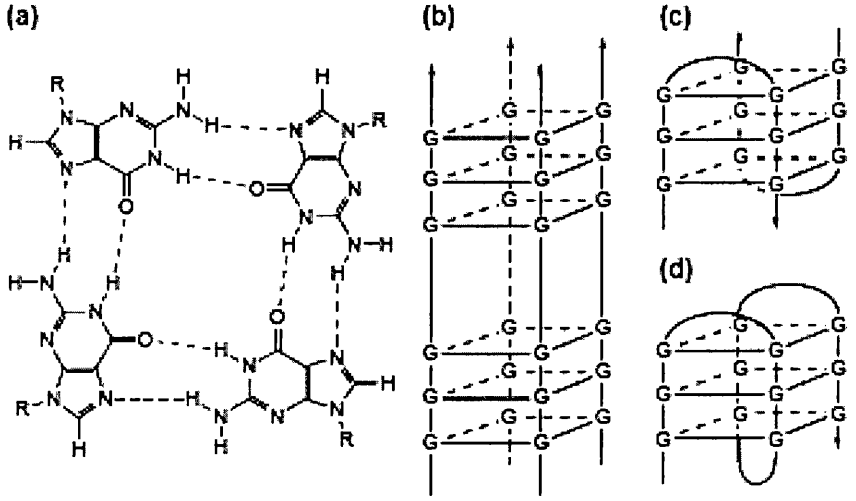

Figure 1.6. Schematic representation of a G-quartet and G-quadruplexes. a. G-quartet structure. b. intermolecular parallel G-quadruplex. c. intermolecular antiparallel G-quadruplex. d. intramolecular G-quadruplex *(Han and Hurley, 2000).*

1.3.2 G-quadruplex stabilising agents

Telomerase requires the 3′-single strand overhang to hybridise with the RNA template to initiate the synthesis of telomeres. A model has been proposed to explain how telomerase maintains telomere length. The telomeric DNA-protein complex can present two physical states. First, the uncapped state where it is accessible for telomerase to bind and consequently telomerase can add telomeric repeats. Secondly, the capped state where the complex is inaccessible to telomerase. Under physiological conditions there is equilibrium between the two states in order to maintain telomere length. On the other hand, if telomerase does not act there is telomere shortening. As a consequence there is a high chance that the telomere becomes uncapped *(Blackburn, 2001).* It has been shown that the folding of the 3′-single strand overhang into G-quadruplex structures leads to inhibition of telomerase *in vitro (Zahler et al, 1991).* Therefore compounds that preferably bind and stabilise G-quadruplex structures and avoid the action of telomerase are potential anticancer drugs. *(Han and Hurley, 2000; White et al, 2001; Rezler et al, 2002; Shay and Wright, 2006; Oganesian and Bryan, 2007).*

Many small molecules have been shown to act directly on this structure and inhibit telomerase (Figure 1.7). At present, most G-quadruplex binding compounds studied show affinity for duplex DNA as conventional cytotoxic compounds and therefore, apart from the effects on telomerase activity, they also have non-selective cytotoxic

effects. Consequently, a real need exists to design compounds with absolute selectivity for G-quadruplex, and to improve their selectivity against cancer cells.

Different types of compounds have been shown to interact with and stabilise G-quadruplexes. A series of nickel (II) and manganese (III) porphyrins were designed which are able to interact with G-quadruplex structures and stabilise them leading to telomerase inhibition *(Dixon et al, 2005).* Telomestatin, one of the most potent G-quadruplex stabilising agents, has been shown to bind preferably to the telomeric overhang DNA, and produces telomerase inhibition followed by telomere shortening in leukemia cells. It has been shown to activate the ATM-dependent DNA damage response *(Tauchi et al, 2006; Shammas et al, 2004).* Also, more recently telomestatin has been shown to bind to 3′-single strand telomeric DNA producing dissociation of the TRF2 protein and interfering with the capped status of the telomere and producing chromosome fusions *(Tahara et al, 2006).* Perylene derivatives bind to G-quadruplex DNA structures with different affinities according to the size and charge of the side chains and produce telomerase inhibition in a cell free assay *(Rossetti et al, 2005).* Ethidium has affinity for duplex DNA but also for triplexes and quadruplexes. Subsequently, ethidium derivatives were designed in order to increase the selectivity against quadruplexes. These ligands are capable of stabilising G-quadruplexes and inhibit telomerase. They also have fluorescent characteristics which enables them to be used as fluorescent probes for quadruplex structures *(Koeppel et al, 2001).* The triazine derivative, ligand 12459 was shown to produce down-regulation of telomerase activity and induce telomere shortening and apoptosis in the lung carcinoma A549 cell line. Also, the down-regulation of telomerase activity has been related to an alteration of the h-TERT splicing pattern. h-TERT presents several motifs able to form G-quadruplex structures, and ligand 12459 has been shown to have selectivity against these G-quadruplex by the PCR-stop assay *(Gomez et al, 2003; Gomez et al, 2004).* Quindoline derivatives, another type of ligands that have been designed in order to have selectivity against G-quadruplex, show inhibition of telomerase activity in K562 cells in a cell-free assay, and also telomerase inhibition in K562 and SW620 cell cultures. The effect on those cell lines was also followed by induction of senescence phenotype and telomere shortening *(Zhou et al, 2005).* The pentacyclic acridine derivative RHPS4 is able to interact with G-quadruplex structures and produce telomerase inhibition *in vitro*, and growth inhibition independent of telomere shortening accompanied by decrease in h-

TERT expression in 21NT cells. This compound also has effects on the telomerase negative ALT cell line, GM847 *(Gowan et al, 2001).* RHPS4 has been shown to displace the telomerase catalytic subunit from the nucleus and it also delocalises POT1 from the telomeres and as a consequence induces DNA damage response and chromosomal fusions *(Phatak et al, 2007; Salvati et al, 2007).*

BRACO19, which belongs to a group of novel small molecules established by Neidle's group, stabilises G-quadruplexes structures, as it has been showed by a FRET assay *(Schultes et al, 2004; Martins et al, 2007).* It is able to inhibit telomerase *in vitro* as has been demonstrated in a cell-free TRAP assay. The concentration required to inhibit telomerase activity by 50% is 6.3μM ($^{tel}EC_{50}$=6.3μM) *(Reed et al, 2008).* BRACO19 has been associated with the induction of senescence phenotype *in vitro* in DU145 prostate cancer cells with up-regulation of p21 and p16, accompanied by chromosome end-to-end fusions *(Incles et al, 2004).* It produces a rapid and progressive decrease in tumour volume in UXF1138LX xenografts models, telomere shortening at non-cytotoxic concentrations, and also almost complete inhibition of h-TERT expression *(Burger et al, 2005).* Furthermore, BRACO19 has been shown to produce delocalisation of POT1 in the HT1080 tumour cell line transfected with GFP-hPOT1 and as consequence chromosomes abnormalities *(Gunaratnam et al, 2007).* BRACO19 presents cytoxicity towards IMR-90 (normal fibroblast cell line) >5-fold lower than towards other tumour cell lines *(Incles et al, 2004).* Combination studies of BRACO19 and paclitaxel in A431 human vulval carcinoma xenografts models showed synergism between the two agents. The effect was significantly greater when the cells were treated with both agents *(Gowan et al, 2002).*

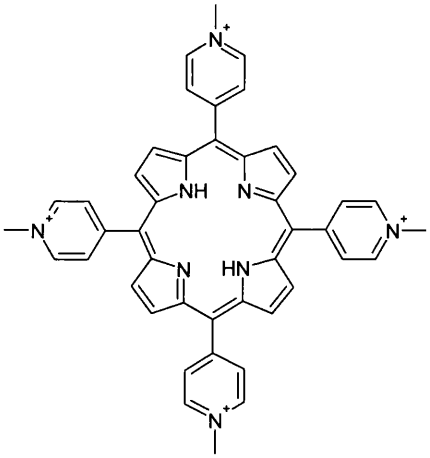

1

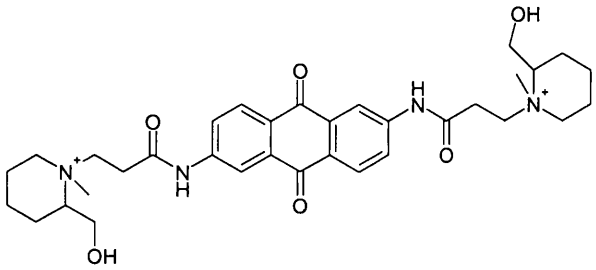

2

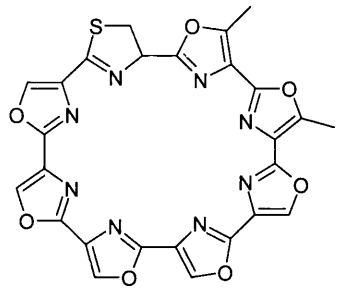

3

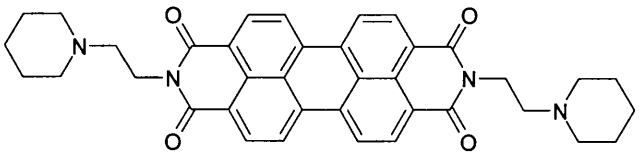

4

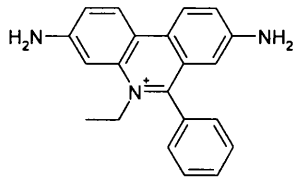

5

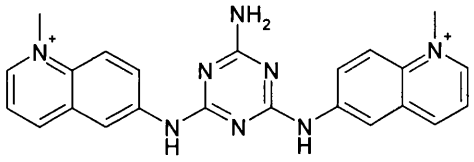

6

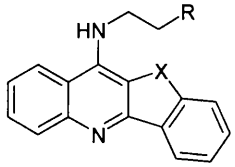

7

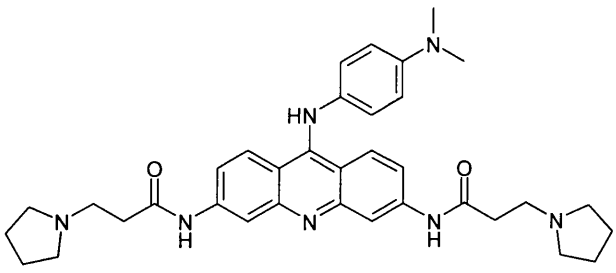

8

Figure 1.7. Structures of G-quadruplex stabilising agents. 1. Cationic porphyrin, 2. Diamido anthraquinones, 3. Telomestatin, 4. Perylenes, 5. Ethidium bromide derivatives, 6. Triazine compounds, 7. Quindoline derivatives, 8. the acridine derivative 9-(4-(N,N-dimethylamino)phenylamino)-3,6-bis(3-pyrrolodinopropionamido) acridine.

1.3.3 Mechanism of action of G-quadruplex stabilising agents.

The mechanism of action of this type of compound is based on the requirement to maintain the 3′-telomeric overhang as a single strand structure to be recognized by the complementary sequence of the RNA template in the h-TR subunit. This is a critical step which is necessary to occur for the h-TERT to start the synthesis of telomeric DNA. Folding of the 3′-telomeric overhang into G-quadruplex structures has been shown to inhibit the action of telomerase because of the impediment of this step to occur *(Zahler et al, 1991)*. Stabilisation of these quadruplexes *in vivo* can therefore inhibit the action of telomerase, indirectly leading to anticancer effects.

The classical model adopted for inhibitors of telomerase itself, suggests that telomere shortening occurs in every round of replication, 50-60 bases at each round. Normal somatic cells possess very long telomeres (6 to 12 kb) compared with cancer cells expressing telomerase, with 3 to 6 kb as an average telomere length. Due to cancer cells present shorter telomeres than normal cells, telomere attrition as a consequence of telomerase inhibition until a critical telomere length will occur much more rapidly in cancer cells than in normal somatic cells. But, there is a problem with the time required before telomeres reach the length required for senescence or apoptosis. The lag phase is the time between the administration of a telomerase inhibitor and the appearance of a response. Therefore a possibility exists where patients with large tumours would develop metastasis before the compounds start to be effective. For this reason, these agents could probably only be used in combination with other anticancer agents or after surgery or radiotherapy.

In the case of G-quadruplex binders, they show much more rapid effects at higher concentrations. These compounds target the telomere itself. There is evidence indicating that the capping of the single-strand telomeric overhang is important to avoid cells undergoing senescence. There is also increasing evidence suggesting that these ligands provoke uncapping of the telomeric overhang *(Riou, 2004)*. One of the advantages of these compounds is that they have effects against those cancer cells without telomerase activity which possess an alternative mechanism to maintain their telomeres. However, this can also be seen as a down-side due to the action being targeted towards telomeres and therefore the adverse effects could be extended to non-cancerous cells. Nevertheless, due to the differences between normal and cancer cells, it is possible to

find selectivity against cancer cells, with the benefit that these agents have activity also in telomerase negative cells *(Gowan et al, 2001; Pennarun et al, 2005; Kim et al, 2003).*

Therefore, many compounds have been shown to present selectivity towards G-quadruplex, and also to have effects on telomerase, telomeres and proteins associated with telomeres. However, there are still many aspects related to these agents that need to be investigated in order to find better ligands. As it has been previously discussed the human genome contains around 370,000 potential quadruplexes *(Huppert and Balasubramian, 2005; Todd et al, 2005).* Therefore, these guanine-rich sequences are not only found in telomeric regions, but also in transcriptional regions in some oncogenes such as c-myc *(Simonsson et al, 1998)* and c-kit *(Todd et al, 2007)* and also at promoter sites of many genes *(Huppert and Balasubramian, 2007).* These G-quadruplexes may be involved in the regulation of gene expression *(Du et al, 2008)*, and as a consequence non-selective G-quadruplex ligands can bind indiscriminately to different G-quadruplexes in the genome and may produce undesirable effects. Furthermore, the topologies of different quadruplex structures can vary significantly *(Burge et al, 2006)*; therefore it may be possible to design compounds that bind to specific G-quadruplexes. However, the frequency of occurrence of different quadruplexes *in vivo* and their roles in cell survival/function is not known clearly. Further studies are needed to understand the roles of these G-quadruplexes *in vivo*. This information will be vital to generate quadruplex ligands which can target selectively.

1.4. Platinum compounds

The first platinum compound cis-diamminedichloroplatinum(II) or cisplatin (Figure 1.8) was discovered by Barnett Rosenberg in 1965 during his studies on the effects of an electric current on bacterial growth. The electrical field caused cell division inhibition in *E.coli*. Further investigation indicated that cisplatin produced at the electrode during electrolysis was the active agent. Subsequent studies revealed that cisplatin has anticancer properties *(Rosenberg, 1985)*. At the present time, after more than 30 years of the discovery of its antitumour activity, it is still one of the most important drugs used in chemotherapy. Cisplatin is widely used in a variety of cancers such as ovarian, lung and head & neck. It is especially active in testicular cancer. Combination therapies with cisplatin in testicular cancer can have cure rates greater than 95% *(di Prieto et al, 2005)*.

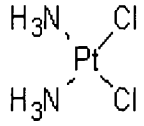

Figure 1.8. Cisplatin

Cisplatin is a planar coordination complex of platinum (II). It is coordinated to two chloride and two ammonia groups, where the chloride ligands are in a cis-geometry, ie: they are on the same side of the platinum atom and the two ammonia groups are on the opposite side. The trans isomer has one ammonia molecule and one chlorine atom on each of the two sides. The two ammonia groups are strongly coordinated to platinum (II), and the two chlorides are easily substituted by nucleophiles such as DNA. Inside the cell, chloride ligands are displaced by water molecules to allow the formation of aquated species which are the reactive forms.

Although cisplatin has high activity in chemotherapy, it has toxic side effects such as nausea, vomiting, nephrotoxicity and neurotoxicity. Cisplatin toxicity in addition with the appearance of drug resistance has limited its use. In order to try to overcome these problems and increase the spectrum of activity, other platinum compounds have been synthesised.

Even though many platinum drugs have been synthesised, only two of them have been approved by the U.S Food and Drug Administration (FDA): carboplatin (cis-diammine (1, 1-cyclobutanedicarboxylato) platinum(II)) (Figure 1.9) which has less toxicity than cisplatin *(Paccagnella et al, 2004)* and oxaliplatin (trans-R, R cyclohexane-1, 2-diamine) oxalaplatinum (Figure 1.9) which has been shown to have activity against some cisplatin and carboplatin resistant tumours. It has been used as a single agent and also in combination with other chemotherapeutic agents, and it seems to produce a better outcome when used in combination due to the different toxicity profile compared to cisplatin that permits combination with other anticancer drugs *(Stordal et al, 2007)*.

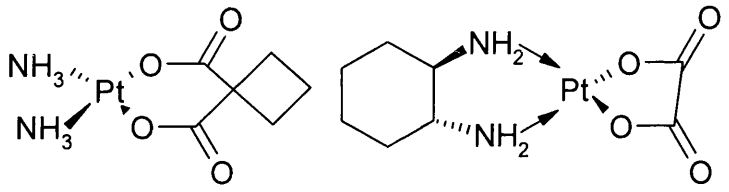

Figure 1.9. Carboplatin Oxaliplatin

1.4.1 Mechanism of action of platinum compounds.

Although previous studies suggested that cisplatin enters cells mainly by passive diffusion, more recently, copper and cisplatin uptake have been related. The major copper (Cu) influx transporter (CTR1) and copper-transporting P-type adenosine triphosphate (ATP7B) control the uptake of cisplatin. Furthermore the efflux of cisplatin is related to the ATP-binding cassette, sub-family C2 *(Wang and Lippard, 2005)*.

It has been demonstrated that cisplatin, due to the high chloride ion concentration (100mM) in blood suppresses the formation of the aqua species, and it is in its neutral form until it penetrates the cell membrane. Once inside the cell, where the chloride concentration is very low (4mM), it is hydrolysed and the two chloro ligands are replaced by two water molecules (Figure 1.10). These hydrolysis products, which have two positive charges, are the reactive species, as shown by a kinetic study of the affinity of the different aquated derivatives of cisplatin. The water molecule possesses higher hydrogen-bond donating ability; therefore the reaction with the nucleophilic guanine molecule occurs more easily *(Legendre et al, 2000)*.

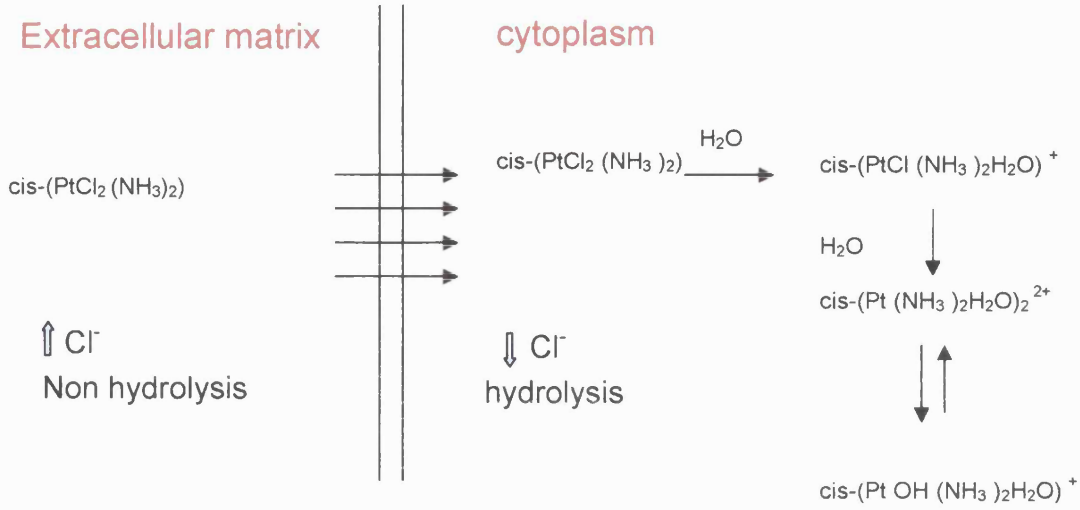

Figure 1.10. Reaction of cisplatin with water molecules and formation of the actual reactive forms (see text for details).

Cellular DNA is the main target of cisplatin *(Reedijk, 1999)*. It forms various types of adducts with DNA (Figure 1.11), and reacts preferentially with purine residues in DNA, mostly with guanine bases. Cisplatin forms 90% 1,2-intrastrand cross-links of which 65% are with two adjacent N7 guanine sites (5`-d(GG)) and about 25% are to adjacent N7 guanine and N7 adenine sites (5`-d(AG)). 10% are 1,3-intrastrand cross links at the d(GpNpG). Cisplatin also forms interstrand cross-links, about 1-2% between two guanines d(GpC)d(GpC).

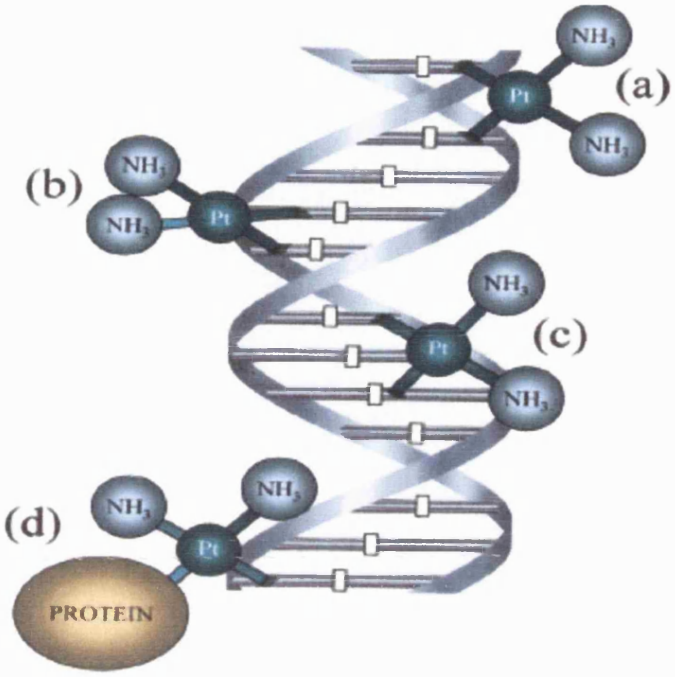

Figure 1.11. (a)interstrand cross-link, (b)1,2-intrastrand cross-link, (c)1,3-intrastrand cross-link, (d) protein-DNA cross-link *(Gonzalez et al, 2001)*.

The trans isomer interacts with DNA in quite different ways. It is sterically unable to form 1,2-intrastrand cross-links but it does form 1,3-intrastrand crosslinks and interstrand crosslinks. It forms 60% of intrastrand crosslinks at the d(GpNpG) and 40% of interstrand cross-links, principally d(GpC)d(GpC) *(Eastman et al, 1988)*. Studies of adduct profiles of cisplatin treated patients have demonstrated that tumour response correlates with levels of 1,2-intrastrand d(GpG) crosslinks, the most common adducts formed by cisplatin. Thus transplatin may be less cytotoxic than cisplatin because of the different DNA adducts it forms, and it has no use in the clinic *(Zamble and Lippard, 1995)*.

Coordination compounds similar to cisplatin have been synthesised using other metals such as Ni or Pd, but they are not active. The explanation of why cisplatin compounds are active, also relates to ligand-exchange kinetics. The Pt-ligand bond in platinum coordination compounds as expected, is much weaker than the covalent bond, however ligand exchange of platinum compounds is slow, from minutes to days, and this gives them a high kinetic stability. Whereas other coordination compounds react in

microseconds to seconds *(Reedijk, 2003)*. Another interesting point is that platinum compounds have a strong preference for binding to S-donor ligands, therefore it should be considered that due to the high amount of S-donors *in vivo*, these compounds may interact with many other biomolecules, especially with those containing methionine and cysteine residues *(Reedijk, 1999)*. Although platinum compounds have a thermodynamic preference for binding to S-donor ligands, the binding of Pt with guanine N7 is often thermodynamically favoured, and Pt-sulfur interactions could serve as a reservoir for platination at DNA. Finally, platinum compounds target N7 atoms of guanine in DNA. Nevertheless, interaction of cisplatin with sulfur containing biomolecules has been associated with resistance; increased level of glutathione has been associated with cisplatin resistance *(Rudin et al, 2003)*.

Cisplatin adducts are specifically recognised by different proteins. First of all, they are recognised by proteins that belong to the nucleotide excision repair (NER) pathway and the mismatch repair pathway which are the principal mechanisms that repair cisplatin adducts, and secondly by proteins such as non-histone proteins for example: from the high mobility group (HMG) family which act by stabilising these DNA-protein complexes *(Kartalou and Essigmann, 2001; Wozniak and Blasiak, 2002)*. Cisplatin adducts are repaired principally by the NER pathway *(Zamble et Lippard, 1995; Moggs et al, 1997)*. This mechanism removes intrastrand crosslinks. The first step is the recognition of the lesion by factors such as *Xeroderma Pigmentosum* (XP) complementation group A (XPA) and the single stranded binding proteins (RPA) and the separation of the double helix at the DNA lesion site. The second step is incision by the structure-specific endonucleases. The incision on the 3′side of the lesion is carried out by the XPG nuclease and on the 5′side of a lesion by the Excision repair complementation group 1 and *Xeroderma Pigmentosum* complementation group F (ERCC1/XPF) nuclease. The incisions are made asymmetrically around the lesion, followed by the excision of the single stranded DNA fragment containing the lesion. The last step is the repair of the lesion by a proliferating cell nuclear antigen (PCNA) dependent DNA polymerase *(de Laat et al, 1999)*. The status of the NER mechanism is important in the sensitivity towards cisplatin. *Xerodema Pigmentosum* fibroblasts are hypersensitive towards cisplatin due to a deficiency in the nucleotide excision repair machinery. These fibroblasts are unable to repair cisplatin adducts, consequently the number of adducts after treatment is higher than in normal cells *(Dijt et al, 1988; Plooy*

et al, 1985). Disturbing the nucleotide excision repair pathway as a strategy to overcome cisplatin resistance in ovarian cancer was carried out by decreasing the expression of ERCC1 protein using antisense ERCC1 RNA in ovarian resistant cells. The result was an enhancement in cytotoxicity to cisplatin due to the reduced capacity of DNA damage repair *(Selvakumaran et al, 2003).* The NER mechanism has different efficiencies towards the different types of cisplatin adducts. 1,3-d(GpNpG) intrastrand crosslinks are repaired more efficiently, 15-20 fold better than 1,2-(GpG) intrastrand crosslinks. This is in relation to the diverse structural alterations caused in the helix by the different cisplatin adducts that lead to a different response *(Moggs et al, 1997).* The fact that cell lines deficient in mismatch repair proteins h-MLH1 and h-MSH2 are more resistant to cisplatin, lead to the conclusion that the DNA mismatch repair pathway contributes to the effect of cisplatin *(Samimi et al, 2000).* This is a post-replication repair system that corrects single base mispairs that occur in DNA during replication, through the recognition of the damage by one of the mismatch recognition complexes. An *in vitro* study demonstrated that cisplatin intrastrand crosslinks are recognised by these complexes *(Yamada et al, 1997).* In addition, cisplatin sensitivity has been associated with the expression of the mismatch repair gene MLH1. The study of MLH1 expression in patient samples demonstrated that low expression of MLH1 was associated with poor prognosis *(Kishi et al, 2003).* The mismatch repair pathway contributes to the effect of cisplatin by activating the apoptosis pathways; this effect seems to occur through the oncogenic tyrosine kinase c-Abl and the p53 related protein p73 *(Sedletska et al, 2005).*

All cisplatin adducts bend and unwind the DNA helix. The 1,2-d(GpG) intrastrand cross-links cisplatin adduct bends the DNA helix towards the major groove and produces unwinding of the double helix *(Takahara et al, 1995; Elizondo-Riojas and Kozelka, 2001).* However it is of interest that the 1,2-d(GpG) interstrand cross-links produces bending towards the minor groove and produces a different degree of unwinding of the helix comparing to others adducts *(Coste et al, 1999).* Each cisplatin adduct distorts and unwinds the DNA helix in a different manner, and the diverse preference of platinum compounds to form different adducts explains the diverse efficacy of these compounds (Figure 1.12). This is consequently another reason why cisplatin and transplatin do not show the same efficacy *(Brabec and Kasparkova, 2005).* These adducts are recognised and processed by different cellular proteins *(Kartalou and*

Essigmann, 2001). These proteins include the non-histone chromatin associated high-mobility group (HMG) box protein, repair proteins, transcription factors and other proteins such as histone H1 *(Kartalou and Essigmann, 2001)*. The effect of HMG box proteins can be explained with two models. The first is the "hijacking model" in which HMG proteins recognise cisplatin adducts and produces the induction of apoptosis. HMG1 protein interacts directly with the p53 tumour-suppressor protein *in vitro* and activates p53 DNA binding. The effect on p53 induces cell cycle arrest or apoptosis depending on the grade of DNA damage *(Jayaraman et al, 1998)*. The second is the "repair shielding model" in which the HMG proteins shield the cisplatin adducts and that avoids them from being recognised by the NER DNA repair system, hence they are not repaired *(Gonzalez et al, 2001)*. It has been shown that the treatment of MCF-7 cells with steroid hormones that induce over-expression of HMG1 also sensitises these cells to cisplatin due to the protection that these proteins provide towards NER proteins *(He et al, 2000)*. However there have been observed discrepancies about the effect of these proteins in cisplatin sensitivity *(Reviewed in Wang and Lippard, 2005)*. As an example, it has been demonstrated that cisplatin resistant cell lines show over-expression of the HMG1 gene. Therefore there is a relation between HMG1 and cisplatin resistance which is completely controversial to the "hijacking" or the "repair shielding model" *(Nagatani et al, 2001)*.

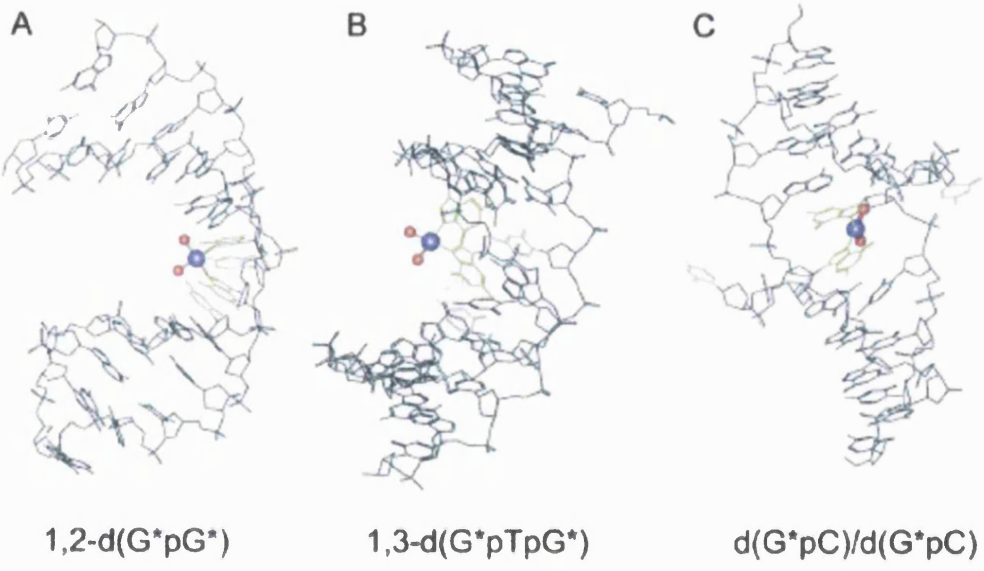

Figure. 1.12. Structure of different adducts formed by cisplatin and the effect on the DNA double helix. A. 1,2-d(GpG) intrastrand cross-link. B. 1,3-d(GpTpG) intranstrand cross-link. C. inter-d(GpC)/d(GpC) adduct. *(Review in Kartalou and Essigmann , 2001)*.

DNA adducts induced by cisplatin produce a DNA damage response which is modulated by several signal transduction pathways, leading to cell cycle arrest, repair or death. Cisplatin cell death has been associated with apoptosis *(Gonzalez el al, 2001, Sedletska et al, 2005)*. It has also been associated with necrosis, and the mode of cell death seems to be concentration dependent. Very high concentration of cisplatin (800μM) produces necrosis in mouse proximal tubular cells whereas lower concentration (8μM) leads to apoptosis *(Wang, 2005)*. Cisplatin has also been shown to induce premature senescence in the WI38 fibroblast cell line. It produces up-regulation of p53 protein and G1 arrest. The senescent phenotype is followed by the induction of apoptosis *(Zhao et al, 2004)*.

The p53 tumour suppressor protein mediates the cellular response that occurs after DNA damage produced by different DNA damaging agents such as cisplatin. The p53 protein has two main roles following DNA damage. First, it induces cell cycle arrest that permits the cell to activate DNA repair systems and repair the damage. And secondly, it is able to induce apoptosis. p53 status and cisplatin sensitivity have been widely studied, however, their roles are still controversial. While cisplatin induced apoptosis seems to be related to p53, cisplatin is also able to produce tumour response in p53 mutant cells. An investigation using a mouse tumour model of the role of p53 in cisplatin response showed that the different protein status did not interfere with the induction of apoptosis and sensitivity towards cisplatin *(Petit et al, 2003)*. Furthermore, another study has demonstrated that inactivation of p53 protein through the expression of the human papilloma virus 16E6 or 16E7 produced an increase in sensitivity towards cisplatin. This effect seems to be related to the role of p53 in DNA repair of cisplatin adducts *(Hawkins et al, 1996)*.

1.4.2 Resistance to platinum compounds.

The main mechanisms of resistance to cisplatin therapy are: deficient drug uptake, decrease in apoptosis, increased DNA repair mechanisms and altered metabolism of cisplatin.

Deficient drug uptake leads to resistance to cisplatin due to reduced intracellular accumulation. Cisplatin produces down-regulation of its major influx transporter in human ovarian carcinoma cells and that effect is related to the appearance of resistance

(Holzer et al, 2004). A431 cisplatin resistant cells show a decrease in cisplatin uptake when compared to the wild type cell line which leads to decreased drug accumulation and more tolerance towards cisplatin *(Lanzi et al, 1998).* The study of the mechanism of resistance following exposure of cisplatin or its analogue oxaliplatin showed decreased drug uptake in the human teratocarcinoma cell line 2102EP *(Rennicke et al, 2005).* Alteration in cisplatin metabolism can be carried out through the inactivation of cisplatin by glutathione, metallothionein or other sulphur-containing molecules. Cisplatin produces up-regulation of frataxin mRNA and protein expression in the A2780 cisplatin resistant cell line. Frataxin acts by detoxifying reactive oxygen species via activation of glutathione peroxidase. As a result, an increase in frataxin levels is related to cisplatin resistance *(Ghazizadeh, 2003).* Furthermore, inhibition of glutathione synthesis with the glutathione synthesis inhibitor buthionine sulfoximine in MCF-7 breast cancer cells transfected with the antiapoptotic protein Bcl-2, reverses cisplatin resistance *(Rudin et al, 2003).* The mutation of the homologous recombination repair (HR) pathway through XRCC3 or Rad54 resulted in increased cisplatin sensitivity in chicken cells *(Raaphorst et al, 2005).* The human endometrial cancer cell line HEC59 which has a mutation in the h-MSH2 mismatch protein presented resistance towards cisplatin and its analogue carboplatin compared to the wild type cell line. The resistance mechanism in this case is due to the failure of this protein to recognise the damage and consequently to generate signals that lead to the apoptosis outcome *(Fink et al, 1996).* Human ovarian cancer cells lines deficient in h-MLH1 and h-MSH2 have also been shown to be more resistant to cisplatin due to the contribution of the DNA mismatch repair pathway in the recognition of the adducts by the mismatch recognition complexes *(Samimi et al, 2000).* This repair pathway corrects single base mispairs that occur in DNA during replication, through the recognition of the damage by one of the mismatch recognition complexes. Apoptosis modulation is also an important mechanism of resistance. Over-expression of antiapoptotic proteins such as Bcl-2 and Bcl-X_L and down-regulation of caspase 3 have been associated with cisplatin resistance in the A2780 human ovarian cancer cell line *(Williams et al, 2005).* A comparative apoptosis study of A431 wild type cells and their counterpart A431 cisplatin-resistant cell line after cisplatin treatment demonstrated that there was reduced induction of apoptosis in the resistant cell line, which was correlated with an increase in antiapoptotic protein Bcl-2 and inhibition of the effector caspase 3 (CPP32) *(Mese et al, 2000).*

The use of platinum compounds in combination with other drugs that target important cellular pathways related to DNA damage and DNA repair can be a good strategy in order to avoid the appearance of drug resistance.

1.4.3 Telomeres and telomerase are possible targets of cisplatin.

Cisplatin reacts preferably with guanine bases in double stranded DNA forming mostly intrastrand crosslinks, therefore G-rich regions in the genome such as telomeres are possible targets of cisplatin. Single-stranded sequences containing at least four repeats of three or four guanines fold into intramolecular G-quadruplex structures *in vitro* in the presence of monocationic ions. There is also evidence that these regions also form G-quadruplexes *in vivo (Schaffitzel et al, 2001; Duquete et al, 2004)*. Platinum compounds bind covalently specially to the N7 atom of guanines *(Reedijk, 1999)*. The four guanines of a G-quartet have their N7 atoms involved in hydrogen bonding, therefore only the guanines out of the stack can react with platinum compounds. Platination experiments of the Tetrahymena telomeric sequence $(T_2G_4)_4$ in aqueous solutions containing Li, Na or K showed that cisplatin only binds to the guanines located in the loops, these are the guanines that have the N7 un-coordinated *(Redon et al 2001)*. Later experiments with the human telomere sequences $AG_3(T_2AG_3)_3$ and $(T_2AG_3)_4$ also showed that cisplatin is able to platinate its folded structure *(Redon et al, 2003)*. Studies comparing the rate of reaction between cisplatin and human telomeric quadruplex structure, duplex DNA and single stranded DNA with one platination GG site, showed that all reactive cisplatin species react faster with double stranded DNA than with single strand oligonucleotides and the quadruplex structure is platinated twice faster than the duplex DNA. These two forms react three times faster than single strand DNA. The explanation for this is that the quadruplex structures used for this study had ten possible platination sites whereas the duplex only had two sites. Furthermore, the accessibility of cisplatin to these guanines is greater in the quadruplex structure. Therefore the conclusion of this study was that quadruplex DNA is a possible target of cisplatin *(Garnier and Bombard, 2007)*.

Another important point is that telomerase has an RNA moiety rich in guanine bases, consequently it is another possible target for cisplatin *(Sedletska et al, 2005)*. Inhibition of telomerase activity has been shown in different cell lines and it is thought to be dependent on cell type *(Zhang et al, 2002)*. It has been found that cisplatin produces

inhibition in telomerase activity in several human cell lines such as hepatoma cell line *(Furuta et al, 2003, Zhang et al, 2002)*, ovarian cancer cells *(Kunifuji, 2002)*, testicular cancer *(Burger et al, 1997)* and produces a decrease in telomere length in HeLa cancer cells *(Ishibashi, 1998),* and in BEL-7404 hepatoma cells *(Zhang et al, 2002)*. One possible explanation is that cisplatin binds to this guanine rich motif in the RNA subunit of telomerase, avoiding the action of telomerase. The second possible theory is that cisplatin binds to the G-quadruplex in the loop regions and prevents the unfolding of the DNA single strand telomeric sequences, producing also inhibition of telomerase *(Redon et al, 2003)*. However, the results published on the effect of cisplatin in telomerase activity and telomere length are inconsistent; cisplatin does not produce telomerase inhibition in nasopharyngeal cancer cells *(Ku et al, 1997)*, furthermore, the effect of cisplatin in the SHSY5Y neuroblastoma cells, 1301 lymphoblastic T cells and the HeLa 229 cells was shown to be telomere independent as it was demonstrated that the DNA damage γ-H2AX foci did not co-localise with telomeres, indicating that telomeres are not the only target of cisplatin *(Jeyapalan et al, 2006)*.

1.5 Combination therapy

Since the beginning of the use of cisplatin as a chemotherapeutic agent in clinic, its toxicity and the appearance of resistance have limited its use. As a strategy in order to solve the problem, many different analogues have been designed and synthesised. However, only two of them carboplatin and oxaliplatin are used in the clinic. The combination of these compounds with other chemotherapeutic agents has shown an improvement in the strategy of therapy. Different agents have shown synergy when combined with cisplatin, and also importantly overcome the resistance induced by platinum compounds *(Adjei et al, 1997; To et al, 2005; Yunmbam et al, 2004; Rodrigues et al, 2004)*. The aim of combination therapy is to find compounds that act synergistically, that means their effects are potentiated in order to be able to reduce doses of both compounds and consequently reduce secondary effects. For this reason it is also important to take into consideration that the agents used in combination do not overlap toxicities and consequently they do not potentiate their toxic effects.

There are many different combinations used in the clinic that have demonstrated to improve the effect of cisplatin. Cisplatin combined with bortezomib and gemcitabine has been used as first-line treatment in patients with advanced solid tumours. The results observed in a study with 34 patients were very promising and the conclusions

were that this combination is recommended and constitutes a safe treatment *(Voortman et al, 2007)*. The treatment of osteogenic sarcoma is a combination of methotrexate, cisplatin, doxorubicin and ifosfamide. Although, research is mostly focused in finding new agents, it is also focused in improving the combination of these compounds *(Ferrari and Palmerini, 2007)*. These are examples of the latest combinations that show the importance of the study of possible combinations in order to find better treatments, more effective, less toxic and successful against resistant cancers.

The aim of this thesis was to investigate the *in vitro* combination treatment of G-quadruplex stabilising agent BRACO19 with cisplatin, an anticancer agent widely used in the clinic.

The first goal was to study how effective are these two compounds when used in combination. The purpose was to investigate if G-quadruplex stabilising ligands such as BRACO19 can be effectively used in combination with cisplatin to produce antitumour activity in human cancer cell lines at low concentration ratios, where unwanted toxicity can be avoided.

The second goal was to investigate the mechanism of action of this combination therapy at the molecular and cellular levels in order to understand the effects observed during cell growth inhibition studies.

Chapter 2- COMBINATION TREATMENT OF BRACO 19 AND CISPLATIN *IN VITRO*

2.1. INTRODUCTION

The aim of this chapter was to investigate how effective BRACO19 and cisplatin are when used in combination. For that purpose, the Combination Index of Chou and Talalay was used and four different cell lines were tested following 4 days of exposure with these agents. Furthermore, long-term cell growth inhibition studies up to four weeks were carried out in order to verify if growth inhibitory effect was maintained along with time.

2.1.1 Drug combination studies.

There are many different methods to determine the interaction between different drugs and most importantly to calculate the effect of combinatorial treatment outcomes *(Greco et al, 1995)*. This leads to the description of three important concepts which define how effective the combination is. These are: synergism, antagonism and additivity. However, there has not been a consensus to give them a unique definition *(Merlin, 1994)*. The most accepted methods are the Loewe additivity model, the Bliss independent criterion and the median-effect plot *(Boik et al, 2007)*.

2.1.1.a Loewe additivity model

The Loewe additivity model is based on the following equation *(Goldoni and Johansson, 2007)*:

$$\Sigma\, x_i/X_i=1$$

x_i: dose of compound i in the combination

X_i: dose compound i in the single treatment

When the value of $\Sigma\, x_i/X_i$ is less than 1, the compounds are synergistic, whereas when the value is more than 1, the compounds are antagonistic.

This model has a significant limitation; it can only be applied when all the compounds tested have the same mechanism of action *(Greco et al, 1996: Goldoni and Johansson, 2007)*.

2.1.1.b Bliss independent criterion

The Bliss independent or non-interaction criterion is based on the following equation *(Goldoni and Johansson, 2007)*:

$$E(x,y)=E(x)+E(y)-E(x)*E(y)$$

E: fractional effect (between 0 and 1)

x: dose of compound 1

y: dose of compound 2

E(x,y): expected fractional effect for the combination treatment of compound 1 and 2 at x and y doses respectively.

When the experimental value of the combination fractional effect is higher than the expected value the compounds are synergistic, whereas when the experimental value is lower, the compounds are antagonistic.

This model also has a significant limitation; it can only be applied when the compounds tested have different mechanisms of action *(Greco et al, 1996: Goldoni and Johansson, 2007)*.

2.1.2 Drug combination studies using the Combination Index method of Chou and Talalay.

The Loewe additivity method can only be used with compounds that have the same mechanism of action that means they are mutually exclusive, whereas the Bliss independence criterion is only applicable when the compounds used in combination have different mechanism of action that means they are mutually nonexclusive *(Greco et al, 1995; Chou and Talalay, 1984)*. The median-effect plot method overcomes the limitations of previous methods. For that reason and due to the existence of a user-friendly computer program to analyse the data, in practice the median-effect plot method is widely used *(Reynolds and Maurer, 2005; Chou, 2006)*.

2.1.2.a Combination Index

The method used here is the median-effect plot based on the multiple drug-effect equation of Chou-Talalay *(Chou and Talalay, 1984)* using the Calcusyn program from Biosoft. The concept of combination index (CI) was introduced by Chou and Talalay

(Chou and Talalay, 1983) and it is basically a quantitative approach to calculate the quality of a drug combination, that assign CI=1 for an additive effect, CI<1 for synergism and CI>1 for an antagonistic effect.

2.1.2.b The Median-Effect principle

The median-effect principle is based on the mass-action law using the mathematical principle of induction and deduction *(Chou, 2006)*.

2.1.2.b.1 The Median-Effect equation of Chou

This equation correlates the doses and effects of a drug in a simple manner:

$$f_a/f_u=(D/D_m)^m \quad \text{or} \quad D = D_m(f_a/(1-f_a))^{1/m} \quad \text{or} \quad f_a = 1/(1+(D_m/D)^m)$$

D: dose of drug

D_m: the median-effect dose

f_a: fraction affected

f_u: fraction unaffected

m: an exponent signifying the sigmoidicity of the dose effect curve, where m=1, >1 and <1 indicate hyperbolic, sigmoidal, and flat sigmoidal dose-effects curves

2.1.2.b.2 The Median-Effect plot of Chou

The median-effect plot of Chou, is the plot of the logarithmic form of Chou's median-effect equation:

$$Log\ (f_a/f_u) = m\ log\ (D) - m\ log\ (D_m)$$

Where the linear correlation coefficient r has to be >0.9 for tissue culture

2.1.2.b.3 The Combination Index equation of Chou-Talalay.

The multiple drug-effect equation was derived from the median effect plot *(Chou and Talalay, 1984)*.

For mutually exclusive compounds:

$$(f_a/f_u)_1^{1/m}+(f_a/f_u)_2^{1/m}=(D)_1/(D_m)_1 + (D)_2/(D_m)_2$$

$(D)_1$: dose of drug 1

$(D)_2$: dose of drug 2

$(Dm)_1$: the median-effect dose of drug 1

$(Dm)_2$: the median-effect dose of drug 2

(When the dose-effect relationship of both drugs in single treatments and in combination are all parallel in the median-effect plot, this correspond to compounds presenting similar mechanism of action)

For mutually nonexclusive compounds:

$$(f_a/f_u)_1^{1/m}+(f_a/f_u)_2^{1/m}=(D)_1/(D_m)_1 + (D)_2/(D_m)_2+ (D)_1(D_2)/ (D_m)_1(D_m)_2$$

(When the plots of both drugs as single treatments are parallel but the plot of their combination is concave upward and can intercept the plot of the more active compound the compounds have different mechanisms of action)

The combination index equation and the term combination index (CI) were derived from the multiple drug-effect equation *(Chou and Talalay, 1984)*.

For mutually exclusive compounds:

$$CI= (D)_1/(D_x)_1 + (D)_2/(D_x)_2= (D)_1/ D_m(f_a /(1-f_a))^{1/m1} + (D)_2/ D_m(f_a /(1-f_a))^{1/m2}$$

For mutually nonexclusive compounds:

$$CI = (D)_1/(D_x)_1 + (D)_2/(D_x)_2 + (D)_1(D_2)/ (D_x)_1(D_x)_2$$

$(D)_1$, $(D)_2$ in the numerators are the doses for the drugs in combination producing x% effect in the experiment.

$(D_x)_1$, $(D_x)_2$ in the denominators are the doses for the drugs alone producing x% effect.

Chou and Talalay defined three steps to determine the combination index *(Chou and Talalay, 1984)*:

1. Calculate the median-effect plot and determine m and D_m values for the two drugs and the combination.
2. For a particular f_a calculate the corresponding dose for each drug and the combination:

   $$D_x = D_m(f_a /(1-f_a))^{1/m}$$

3. Calculate the combination index using combination index equations.

They calculated $(D)_1$ and $(D)_2$, by the known ratio A/B, that is the concentration of one of the drugs in respect to the other, which is constant for the total range of concentrations. $(D)_1 = (D_x)_{1,2} \times A / (A + B)$ and $(D)_2 = (D_x)_{1,2} \times B / (A + B)$

To facilitate this calculation, they developed a computer program to calculate combination index, which is available as Calcusyn from Biosoft. The program produces a range of CI values which are interpreted as below:

Degrees of synergism or antagonism:

<0.1	very strong synergism
0.1-0.3	strong synergism
0.3-0.7	synergism
0.7-0.85	moderate synergism
0.85-0.90	slight synergism
0.90-1.1	nearly additive
1.10-1.20	slight antagonism

2.1.2.b.4 The fraction affected-Combination Index Plot and Isobologram

Combination index values at different fraction affected can be calculated by the Calcusyn software. This can be represented with the fraction affected-combination index plot which represents f_a and the CI on the x- and y- axes, respectively, or with an isobologram *(Chou, 2006)*. An isobologram is a graph that represents the equipotent combinations of two compounds at different effective doses (isobol). This graph can be composed by different isobols at different effective doses (ED_{50}, ED_{75}, ED_{90}).

2.1.3 Response to chemotherapeutic agents in cancer cells. *In vitro* assays.

There are many different *in vitro* chemosensitivity assays *(Bellamy, 1992)* that can be used as predictors of therapeutic outcome. The sulphorhodamine B assay (SRB) *(Skehan et al, 1990)* is a rapid assay that permits the screening of many drugs in different cell lines and enables one to compare the activity of different anticancer agents in cell cultures. It is a rapid and economic assay that presents advantages compared to other similar cytotoxicity assays such as (3-(4,5-dimethylthiazol-2-yl)-2,5-diphenyltetrazolium bromide (MTT). It is faster, simple, less affected by environmental factors such as pH of the media, metabolic conditions and most importantly the complex formed between the SRB and the basic aminoacids of cellular proteins is stable and does not have to be read immediately *(Bellamy, 1992)*. The assay involves exposure of cells to drug for four days and enables one to calculate short-term cell death. The assay can be used in the same manner to predict the resistance of various cell lines to a wide range of compounds.

2.2 MATERIALS AND METHODS.

2.2.1 Cell culture

A431 human squamous carcinoma cell line, A2780 human ovarian cell line (wild type) and A2780cis (cisplatin resistant) and MCF-7 breast cancer cells were purchased from the European Collection of cell culture. The cell lines were grown in $75cm^2$ flask (TPP, Switzerland) in Dulbecco's Modified Eagles media (Invitrogen, UK) supplemented with 10%v/v foetal bovine serum (Invitrogen, UK), 0.5μg/ml hydrocortisone (Acros Chemicals, Loughborough, UK), 2mM L-glutamine (Invitrogen, Netherlands) and 2mM non-essential amino acids (Invitrogen, Netherlands) and maintained at 37^0C, 5% CO_2 in humidified atmosphere. A431 cells were passaged at 1:6 and A2780 and A2780cis at 1:20, twice a week.

2.2.2 Mycoplasma testing

All the cell lines were regularly tested for mycoplasma. Cells were grown in chamber slides. The number of cells seeded was chosen in order to give 50-60% confluence after 4-5 days of culture. The medium was removed and cells were washed with 2ml of phosphate buffered saline (PBS) (Invitrogen, UK). Then 2ml of 50% PBS in freshly prepared 4% paraformaldehyde was added to the cells, rinsed and discarded. Subsequently, the cells were washed with 4% paraformaldehyde, and then fixed for 10 minutes at room temperature. After the fixative, the plate was washed twice with distilled water. Consequently, 2ml of 50ng/ml Hoechst 33258 (Sigma, UK) in PBS was added and incubated for 10 minutes at room temperature. The dye was removed and the plate washed again twice with water. Afterwards, the slide was mounted with Vectashield (Vector Laboratories, UK), and visualized with fluorescence microscope, 330/380nm excitation and LP440 barrier filter.

2.2.3 Preparation of drugs

BRACO19 free base stock solution was prepared at a concentration of 10mM in dimethylsulfoxide (DMSO) and kept at 4^0C. Subsequently BRACO19 was dissolved at 1mM in 10mM HCl just before use.

Cisplatin or cis-diammineplatinum(II)dichloride (Sigma-Aldrich, Germany) was dissolved in 0.9% saline and sterilised by filtering through 0.22μM disc filters on the day of experiment.

2.2.4 Short-term cytotoxicity studies: the sulphorhodamine B (SRB) assay.

Short-term cytotoxicity was measured using the sulphorodamine B (SRB) assay *(Skehan et al, 1990).* SRB is a dye that binds to basic amino acids of cellular proteins and has absorbance at 540nm, that permits one to measure the total amount of protein which correlates with the total number of viable cells. This assay has several advantages compared to tetrazolium based assays such as better linearity, higher sensitivity and lower cost.

Adherent cells at a logarithmic growth phase were collected and counted using a Neybauer haemocytometer (Assistant, Germany). An appropriate dilution of the cells was made in medium, and 160μl (containing 4000 cells) were seeded into each well of a 96 well microtiter plate (Fisher scientific, UK) and incubated at 37^0C and 5% CO_2 overnight. Drugs were dissolved in media to required concentrations, and 40μl were pipetted into appropriate wells. The same volume of media was added to the positive and negative controls. Plates were incubated as described previously for further 96 hours. At the end of the 96 hours incubation, the medium was removed and cells were fixed with 160μl of 10% trichloroacetic acid (TCA) for 30 minutes on ice. Subsequently plates were washed 5 times with deionised water. Plates were then left to dry in the oven for approximately 1 hour at 60^0C. The plates were then stained with 0.4% SRB in 1% acetic acid for 15 minutes at room temperature. SRB was removed and the plates washed with 1% acetic acid before drying in the oven for approximately 1 hour at 60^0C. Bound SRB was solubilised by adding 100μl of 10mM unbuffered Tris-base solution (Sigma) and plates were left on a shaker for 5 minutes. Absorbance was read in a 96-well plate reader (Anthos 2010) at 540nm.

2.2.5 Determination of synergy by SRB.

Cells were exposed to BRACO19 and cisplatin as single agents or in combination at a constant molar ratio of 1:1, 1:2, 2:1, 3:1, 1:3, BRACO19:cisplatin for A431, MCF-7 and A2780, and 1:1, 1:2, 2:1, 1:4, 4:1 BRACO19:cisplatin for the A2780cis cell line. The experimental procedure was the same as described for the SRB assay, except when the cells were exposed to both agents, 20μl of each drug concentration was added to the appropriate well. The synergism between BRACO19 and cisplatin was determined by using combination index (CI) analysis using the method of Chou and Talalay *(Chou and Talalay, 1983)* based on the median-effect principle.

2.2.6 Long-term treatment.

Following the determination of synergy, long-term studies were set up with A431, MCF-7, A2780 and A2780cis to determine the effect of both drugs alone or in combination when the cells were treated at sub-cytotoxic concentrations (concentrations below the IC_{50}, which is the concentration necessary to produce 50% of cell growth inhibition during short-term exposure). These studies were carried out up to four weeks. These studies also had another aim that was to find out if the effect on viability was maintained along with time or the cells were becoming resistant to the treatment.

Furthermore, inhibitors of telomerase itself require a time lag between the administration of the compound and the appearance of a response. Introduction of a catalytically inactive dominant negative form of the catalytic subunit of telomerase h-TERT into different human cancer cells produced a disruption in telomerase activity. However, the effects on growth inhibition appeared after a few weeks of treatment. The time required for cell growth arrest was dependent on the initial telomere length *(Han et al, 1999)*. Therefore, these long-term cell growth studies are also of utility in order to investigate long-term effects due to inhibition of telomerase.

Cells were washed with 3ml of PBS and 4ml of trypsin was added to each flask and incubated at 37^0C for 10 minutes for A431 or 5 minutes for A2780 and A2780cis in order to bring cells into suspension. Once all the cells have detached, 4ml of media containing foetal bovine serum (FBS) was added in order to inactivate the action of trypsin. Cells were centrifuged at 8000rpm for 3 minutes, media was discarded and 10ml of fresh media was added to resuspend the pellet. Cells were counted using a

Neybauer haemocytometer. $1x10^5$ cells were seeded in $75cm^2$ flasks in 10mls of media and an appropriate concentration of drug was added. After 4 days of incubation media was discarded, cells were washed with PBS and fresh media and drug was added. Three days later medium was discarded and attached cells were harvested with trypsin and pelleted. The pellet was resuspended in 10mls of media and counted using a Neybauer haemocytometer. Cells were reseeded in a new flask as before with the appropriate amount of drug, and experiment was continued for further four weeks. Results were expressed as population doublings, calculated from the equation: $n= (\log P_n - \log P_0)/\log 2$ where P_n is the number of cells collected and P_0 is the initial seeding density, against time.

2.2.7 Statistical analysis.

Statistical significance for the long-term viability studies was evaluated by calculating analysis of variance (ANOVA) followed by Dunnetts test. The experiments were repeated 3 times and a critical value of $p<0.05$ was considered. The statistical analysis was carried out using the statistical computer program Minitab 14.

2.3. RESULTS

2.3.1 Combination Index analysis in the epidermis carcinoma cell line A431.

Exposure to BRACO19 and cisplatin as single agents for 96 hours produced 50% growth inhibition (IC_{50}) at concentrations of 3.2±0.2 and 3.15±0.35μM respectively in the A431 epidermis carcinoma cell line. Thus, in terms of potency both BRACO19 and cisplatin exert comparable growth inhibition in this particular cell line. Based on these sensitivity data, combination experiments were performed in order to measure the effect of the two compounds acting together. Combination studies were designed in which cells were first exposed to both drugs alone and then in combination. For this purpose, the appropriate range of concentrations was chosen for the single agents and then for the different combinations, including concentrations that produce minimum effect and concentrations that produce massive cell death. All the combinations were performed in a constant ratio, and the ratios chosen for this cell line were 1:1, 1:2, 2:1, 1:3 and 3:1 (BRACO19:cisplatin). Figure 2.1 shows the median-effect plots and the isobolograms for each of the ratios used in the combination. First of all, the concentration of both compounds was kept constant at a ratio 1:1 (equipotent concentration), and later the concentration of one of the drug relative to the other was increased or decreased in order to find out how this affects the combination. Combination index (CI) values at different effective doses (ED_{25}, ED_{50} and ED_{90}) are shown in Table 2.1. There is notable synergy when the compounds were administered in a constant ratio of 1:1, 2:1, 3:1 (BRACO19:cisplatin) whereas only a nearly additive-antagonistic effect was found when the ratio used was 1:2 and 1:3 (BRACO19:cisplatin). However, at these two ratios at ED_{90} the effect was slightly synergistic. We conclude that decreasing the concentration of BRACO19 has a negative effect in terms of synergism.

A

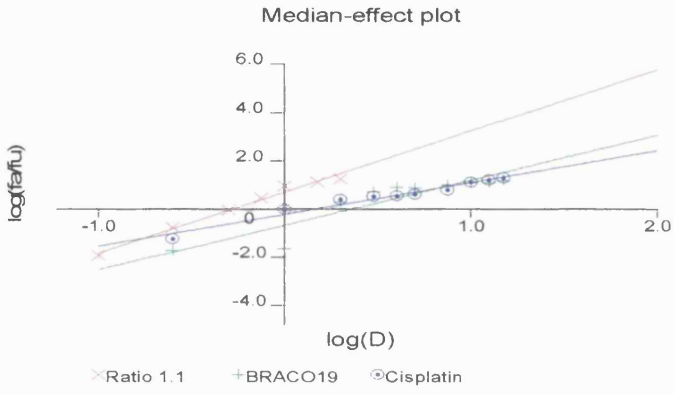
Median-effect plot
log(fa/fu)
log(D)
Ratio 1.1
BRACO19
Cisplatin

B

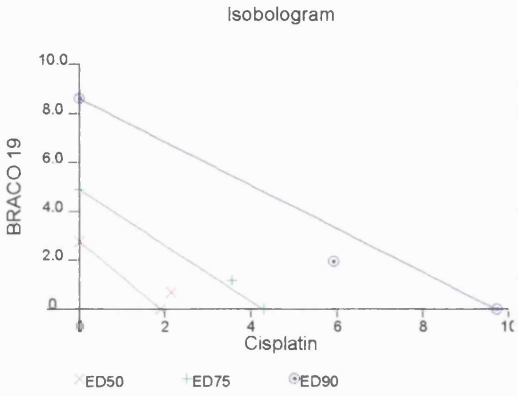
Isobologram
BRACO 19
Cisplatin
ED50
ED75
ED90

C

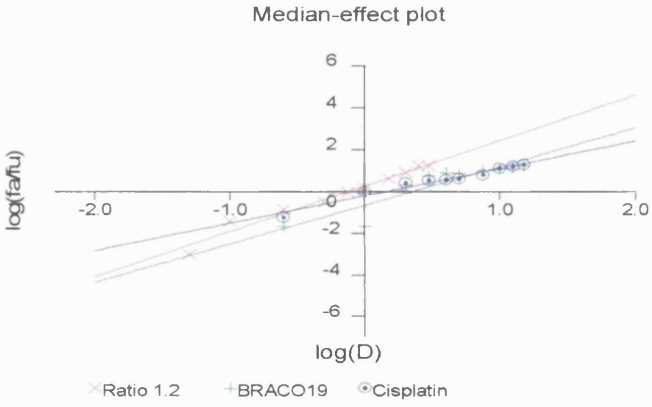
Median-effect plot
log(fa/fu)
log(D)
Ratio 1.2
BRACO19
Cisplatin

D

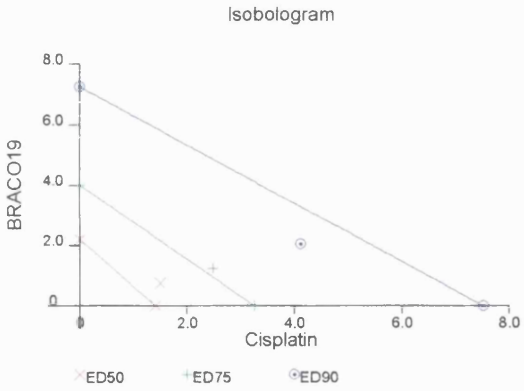
Isobologram
BRACO19
Cisplatin
ED50
ED75
ED90

E

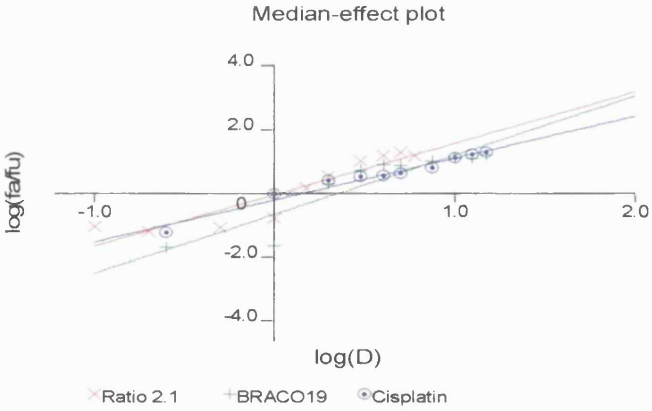
Median-effect plot
log(fa/fu)
log(D)
Ratio 2.1
BRACO19
Cisplatin

F

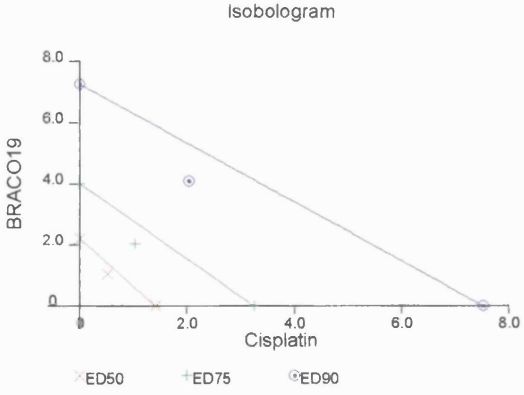
Isobologram
BRACO19
Cisplatin
ED50
ED75
ED90

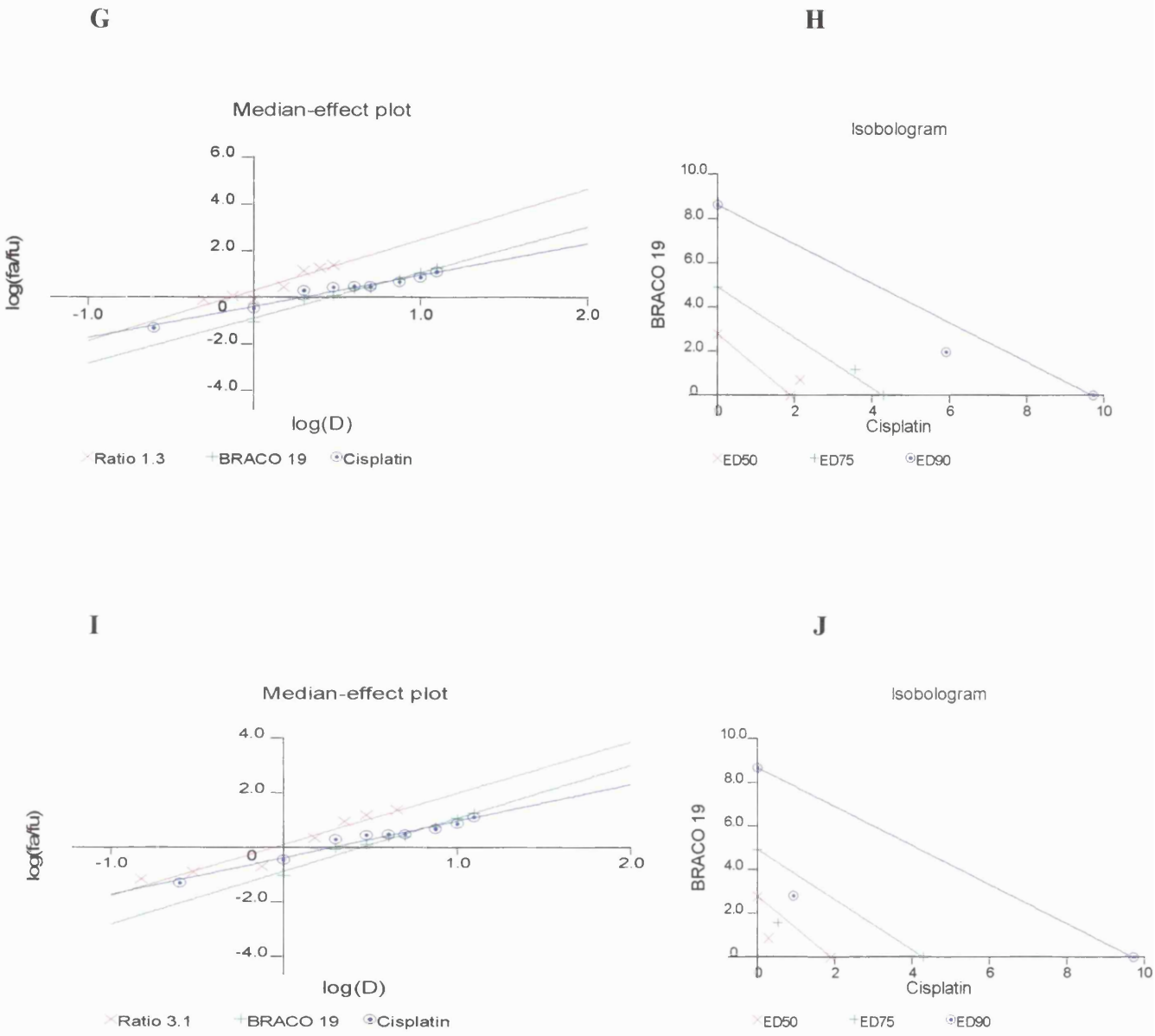

Figure 2.1. Median-effect plots for the two compounds and the combination at different drug ratios. Logarithm of dose (x axis) versus logarithm of fraction affected/ fraction unaffected (y axis). A: ratio 1:1, C: ratio 1:2, E: ratio 2:1, G: ratio 1:3, I: ratio 3:1 (BRACO19:cisplatin). Classic isobolograms of the two compounds at the different drug ratios. BRACO19 and cisplatin doses are represented on the y- and x-axis respectively. B: ratio 1:1, D: ratio 1:2, F: ratio 2:1, H: ratio 1:3, J: ratio 3:1 (BRACO19:cisplatin).

A431	ED_{25}	ED_{50}	ED_{90}
Ratio 1:1 (BRACO19:Cisplatin)	0.63±0.05	0.48±0.05	0.37±0.06
Ratio 1:2 "	1.48±0.12	1.10±0.04	0.83±0.16
Ratio 2:1 "	0.84±0.004	0.86±0.052	0.918±0.12
Ratio 1:3 "	1.37±0.01	1.102±0.04	0.88±0.07
Ratio 3:1 "	0.45±0.01	0.43±0.0007	0.42±0.001

Table 2.1. Combination index values at effective doses (ED) of 25, 50 and 90 in A431 cells.

2.3.2 Long-term viability studies in A431 cells.

A431 cells were exposed to BRACO19 and cisplatin alone and in combination at sub-cytotoxic concentrations up to four weeks. Cells were treated twice a week, and counted every 7 days. Results are expressed as population doublings (Figure 2.2). The effect observed with the two drugs was concentration and time dependent (Figures 2.2.A and 2.2.B). Notably, when using sub-cytotoxic concentrations in combination complete cessation of growth occurred after two weeks at concentrations that do not produce a significant effect when they were used as single agents (Figure 2.2.C). Remarkably lower cell density was observed after only one week of treatment for the combination compared to the single agents (Figure 2.3). Consequently, during long term exposure synergy is likely to be occurring.

A

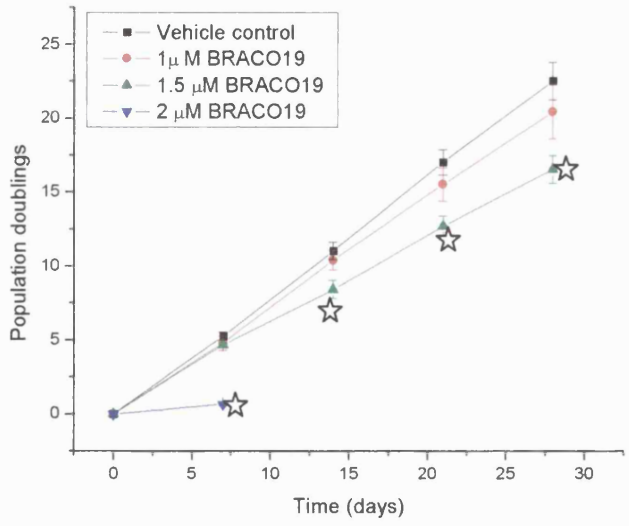

B

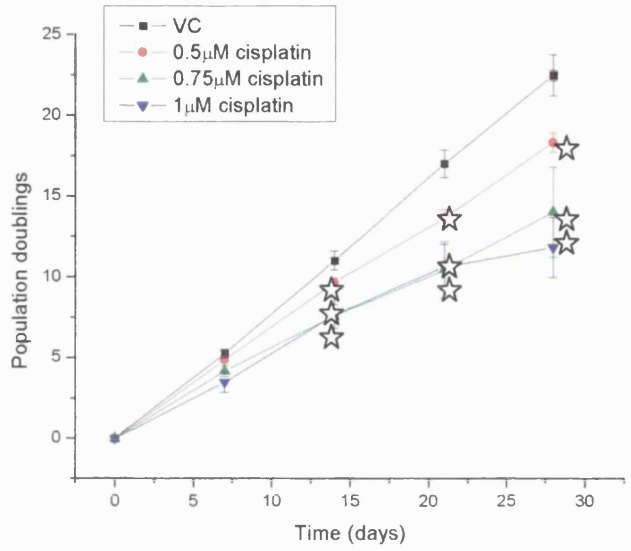

C

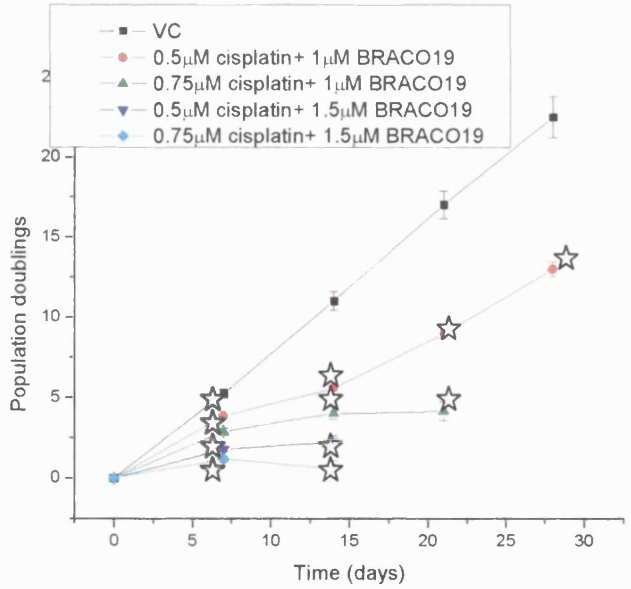

Figure 2.2. Graphs showing long-term antitumour activity expressed as population doublings in A431 cells treated with BRACO19 (A) or cisplatin (B) as single agents or as a combination (C) for four weeks. Cells were counted every week and reseeded with the initial seeding of $1x10^5$ cells. The drug was added twice a week. Data were analysed using Minitab statistical software version 14. ☆Statistically significant difference between treatments $p<0.05$ for n=3, ANOVA followed by Dunnetts test.

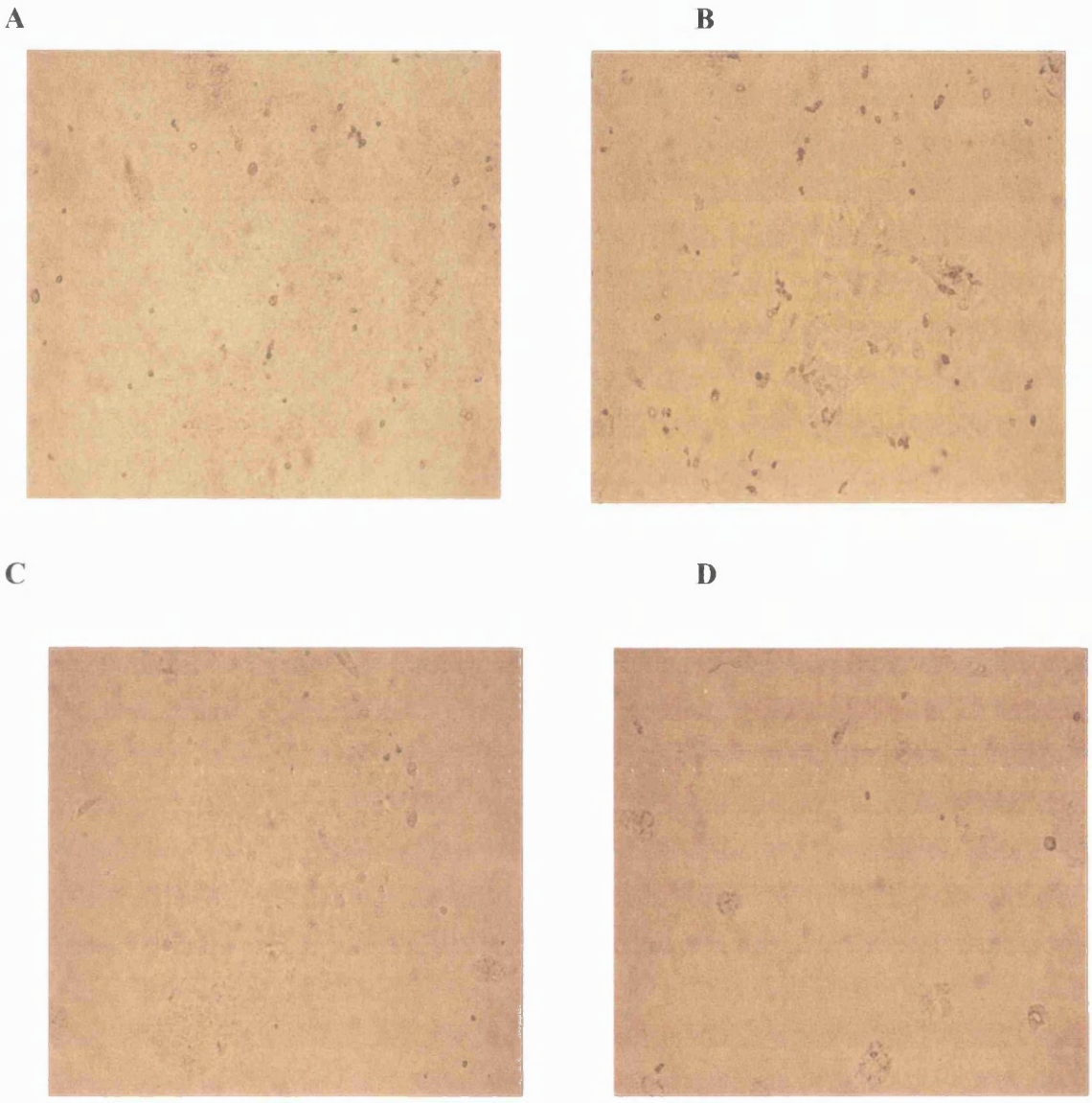

Figure 2.3. A431 cells after one week treatment. A. Vehicle control. B. 0.75μM cisplatin. C. 1.5μM BRACO19. D. 0.75μM cisplatin+1.5μM BRACO19.

2.3.3 Combination Index analysis in the ovarian cell lines A2780 and A2780cis.

Exposure to BRACO19 for 96 hours in A2780 and A2780cis produced an IC_{50} of 2.22±0.43 and 3.5±0.53μM respectively, while cisplatin produced an IC_{50} of 1.88±0.35 and 9.78±1.76μM in the same cell lines. BRACO19 and cisplatin exert comparable growth inhibition in A2780 whereas A2780cis presents 5-fold more resistance to cisplatin than the A2780 wild type as expected and hence this cell line is not very responsive to cisplatin. A2780cis also has a slightly higher value of IC_{50} for BRACO19 comparing with A2780 wild type, however the difference is not very significant, therefore some of the mechanism of resistance developed for this cell line against cisplatin may have an effect on BRACO19 sensitivity in short term exposure. Based on these sensitivity data, combination experiments were designed choosing again the appropriate range of concentrations in order to measure the effect of the two compounds acting together. Combination studies were planned in which cells were first exposed to both drugs alone and then in combination with a constant ratio of 1:1, 1:2, 2:1, for both cell lines and 1:3 and 3:1 for A2780 and 1:4 and 4:1 for A2780cis (BRACO19:cisplatin), in order to find out the best combination. Figure 2.4 shows the median-effect plots and isobolograms for each of the ratios used in the combination for both cell lines. Combination index (CI) values at different effective doses (ED_{25}, ED_{50} and ED_{90}) are shown in Table 2.2. In the case of the A2780 cell line, the ratio 1:1 was the worst combination, resulting in antagonistic. Ratio 1:2 (BRACO19:cisplatin) was additive and 1:3 (BRACO19:cisplatin) was nearly additive at ED90, but synergistic at ED25 and ED50. Ratios 2:1 and 3:1 (BRACO19:cisplatin) were the best combinations, and showed synergy for the whole range of concentrations chosen. For A2780cis the best combinations were 2:1 and 4:1 (BRACO19:cisplatin), both synergistic, the rest of the combinations were slightly antagonistic. Although the combination seems to be more effective in A431 cells, the results in the 3 cell lines followed the same pattern 2, 3 or 4 fold increases in the concentration of BRACO19 relative to cisplatin has a positive outcome for the effect.

A

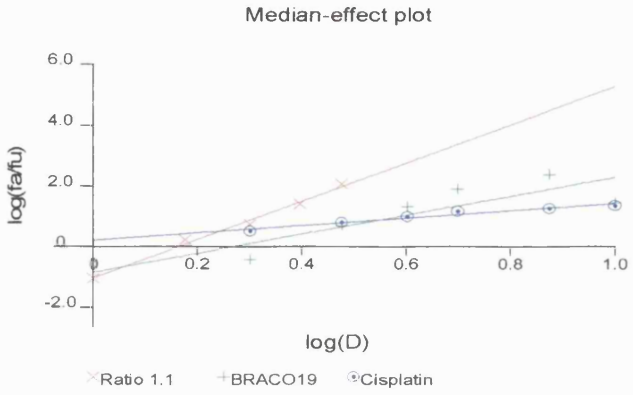
Median-effect plot
log(fa/fu)
log(D)
Ratio 1.1
BRACO19
Cisplatin

B

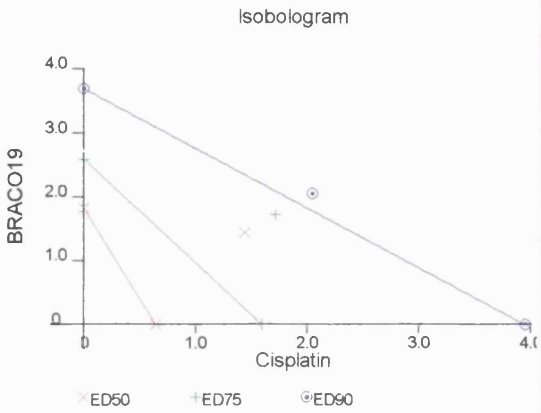
Isobologram
BRACO19
Cisplatin
ED50
ED75
ED90

C

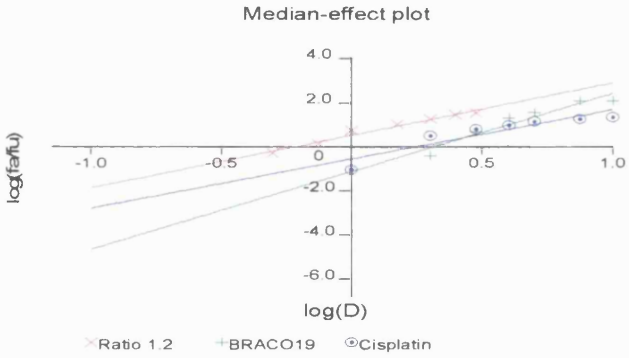
Median-effect plot
log(fa/fu)
log(D)
Ratio 1.2
BRACO19
Cisplatin

D

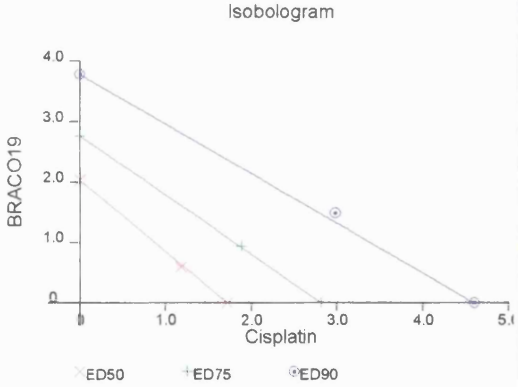
Isobologram
BRACO19
Cisplatin
ED50
ED75
ED90

E

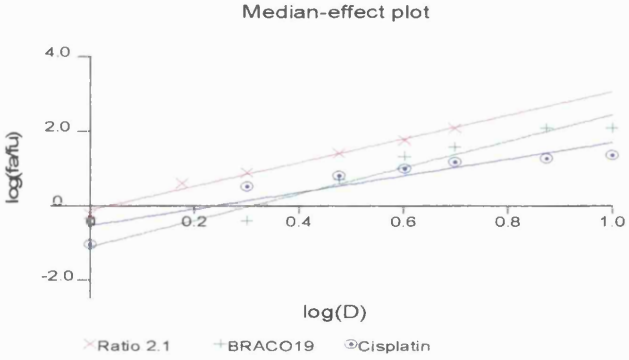
Median-effect plot
log(fa/fu)
log(D)
Ratio 2.1
BRACO19
Cisplatin

F

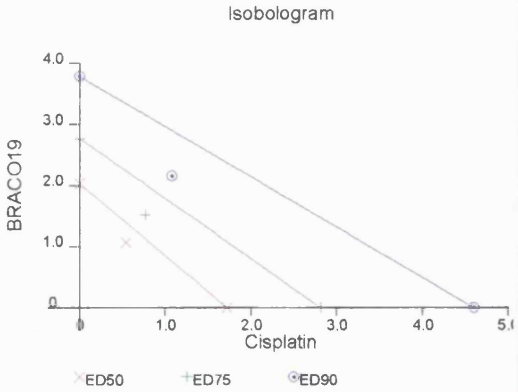
Isobologram
BRACO19
Cisplatin
ED50
ED75
ED90

G

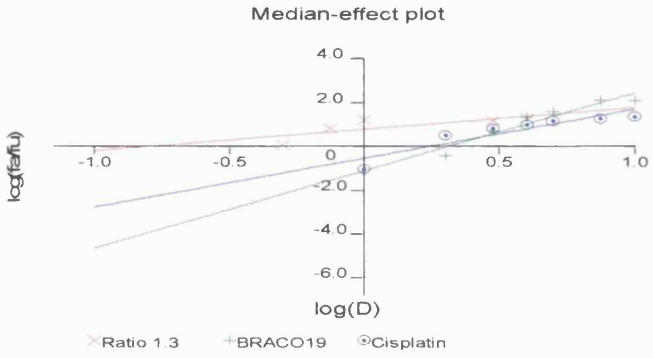
Median-effect plot
log(fa/fu)
log(D)
Ratio 1.3
BRACO19
Cisplatin

H

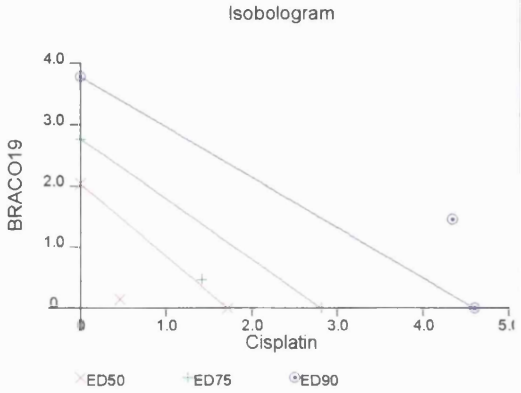
Isobologram
BRACO19
Cisplatin
ED50
ED75
ED90

I

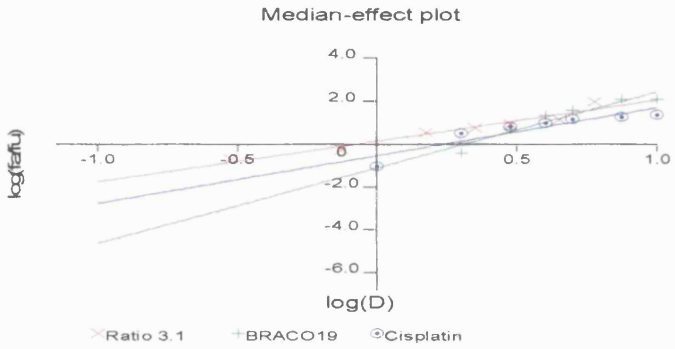
Median-effect plot
log(fa/fu)
log(D)
Ratio 3.1
BRACO19
Cisplatin

J

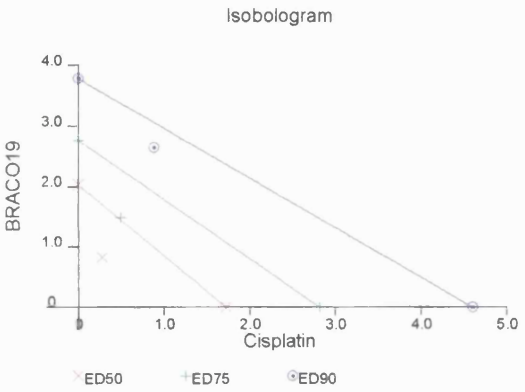
Isobologram
BRACO19
Cisplatin
ED50
ED75
ED90

K

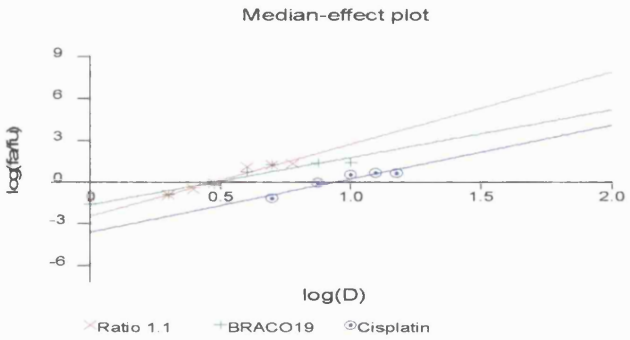
Median-effect plot
log(fa/fu)
log(D)
Ratio 1.1
BRACO19
Cisplatin

L

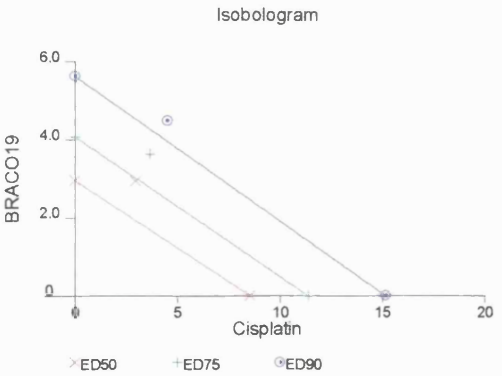
Isobologram
BRACO19
Cisplatin
ED50
ED75
ED90

M

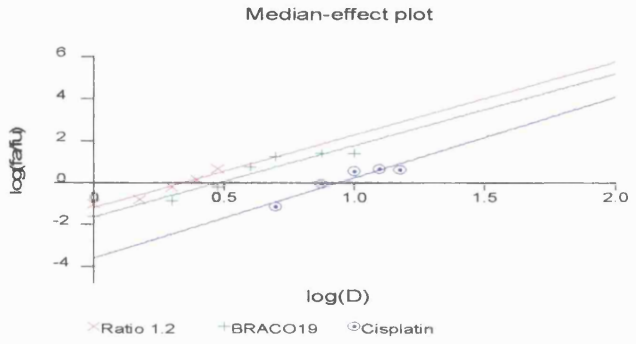
Median-effect plot
log(fa/fu)
log(D)
Ratio 1.2
BRACO19
Cisplatin

N

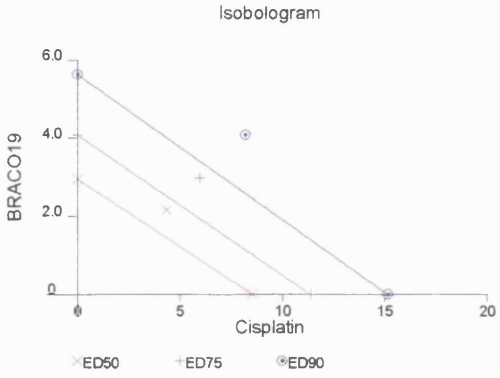
Isobologram
BRACO19
Cisplatin
ED50
ED75
ED90

O

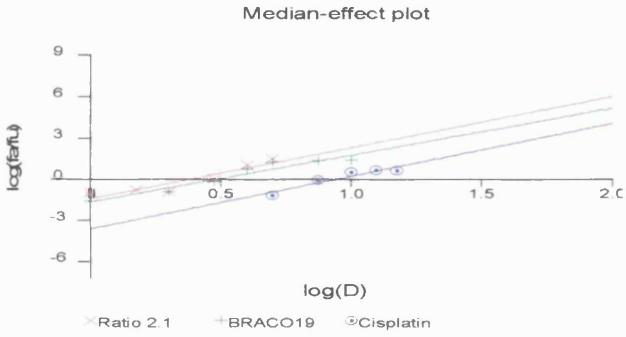
Median-effect plot
log(fa/fu)
log(D)
Ratio 2.1
BRACO19
Cisplatin

P

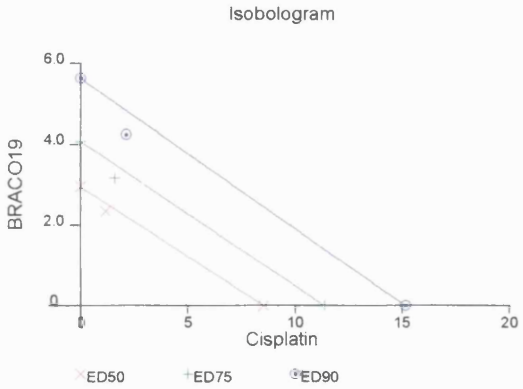
Isobologram
BRACO19
Cisplatin
ED50
ED75
ED90

Q

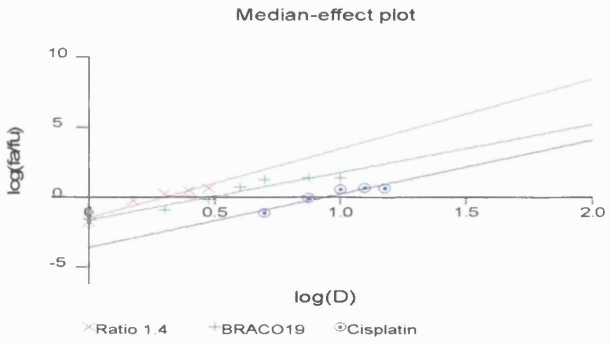
Median-effect plot
log(fa/fu)
log(D)
Ratio 1.4
BRACO19
Cisplatin

R

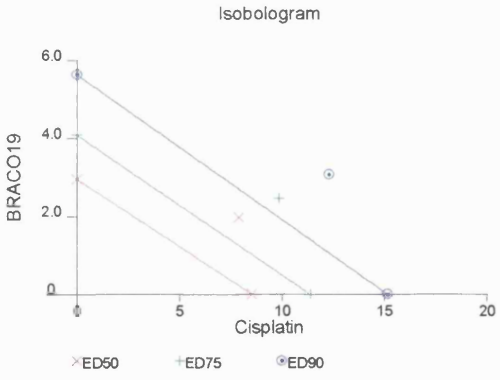
Isobologram
BRACO19
Cisplatin
ED50
ED75
ED90

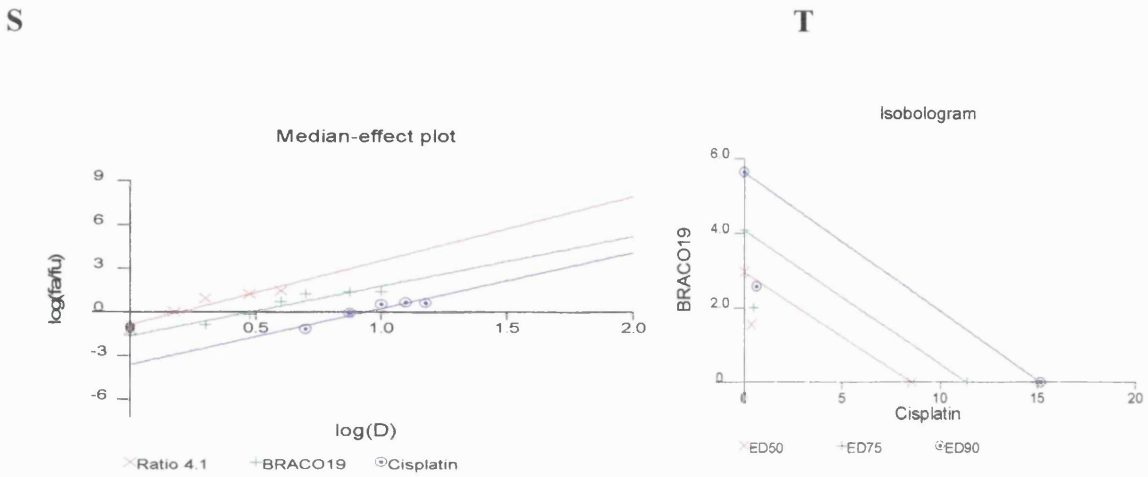

Figure 2.4. Median-effect plots for the two compounds and the combination at different drug ratios. Logarithm of dose (x axis) versus logarithm of fraction affected/ fraction unaffected (y axis). A2780 A: ratio 1:1, C: ratio 1:2, E: ratio 2:1, G: ratio 1:3, I: ratio 3:1 (BRACO19:cisplatin). A2780cis K: ratio 1:1, M: ratio 1:2, O: ratio 2:1, Q: ratio 1:4, S: ratio 4:1 (BRACO19:cisplatin). Classic isobolograms of the two compounds at the different drug ratios. BRACO19 and cisplatin doses are represented on the y- and x-axis respectively. A2780 B: ratio 1:1, D: ratio 1:2, F: ratio 2:1, H: ratio 1:3, J: ratio 3:1 (BRACO19:cisplatin). A2780cis L: ratio 1:1, N: ratio 1:2, P: ratio 2:1, R: ratio 1:4, T: ratio 4:1 (BRACO19:cisplatin)

A2780	**ED_{25}**	**ED_{50}**	**ED_{90}**
Ratio 1:1 (BRACO19:Cisplatin)	1.72±0.01	1.19±0.17	1.056±0.04
Ratio 1:2 "	1.03±0.07	1.008±0.002	0.99±0.06
Ratio 2:1 "	0.89±0.07	0.83±0.02	0.78±0.02
Ratio 1:3 "	0.51±0.24	0.75±0.11	1.17±0.21
Ratio 3:1 "	0.61±0.06	0.76±0.07	0.91±0.01
A2780cis	**ED_{25}**	**ED_{50}**	**ED_{90}**
Ratio 1:1 (BRACO19:Cisplatin)	1.32±0.029	1.16±0.07	1.02±0.096
Ratio 1:2 "	1.19±0.023	1.11±0.86	1.037±0.14
Ratio 2:1 "	0.91±0.02	0.86±0.07	0.81±0.10
Ratio 1:4 "	1.57±0.02	1.43±0.04	1.305±0.06
Ratio 4:1 "	0.67±0.13	0.64±0.15	0.624±0.17

Table 2.2. Combination index values at effective doses (ED) of 25, 50 and 90 in A2780 and A2780cis cells.

2.3.4 Long-term viability studies in A2780 and A2780cis cells.

A2780 and A2780cis cells were exposed to BRACO19 and cisplatin alone and in combination at sub-cytotoxic concentrations for up to four weeks. Results are expressed as population doublings (Figure 2.5 and 2.6). A2780 and A2780cis were not very responsive to BRACO19 even at concentrations close to IC_{50} and above the IC_{50} 3μM of BRACO19 in A2780. However, these two cell lines were more sensitive to cisplatin, and concentrations below IC_{50} produced significant growth inhibition which was both time and concentration dependent. The combination of both agents also produced significant growth inhibition, but comparing with the effect of both agents alone, the improvement was not very large and we concluded that only an additive effect and no synergy was observed in these cell lines. Short-term combination index studies were found to be synergistic when the concentration of BRACO19 was increased relative to cisplatin and it is possible that on increasing the concentration of BRACO19 the outcome would have been better.

A

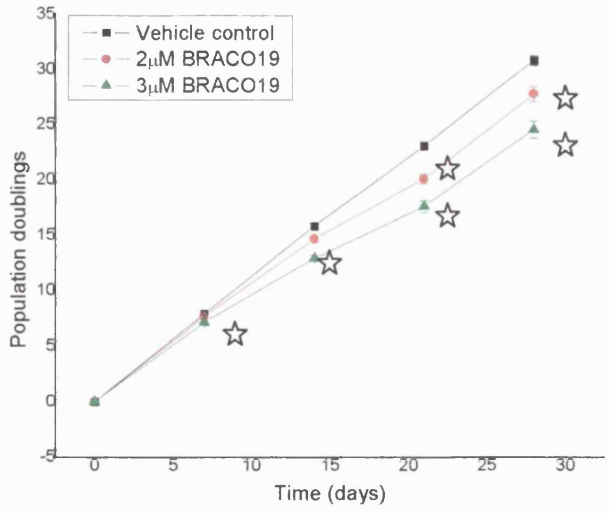

B

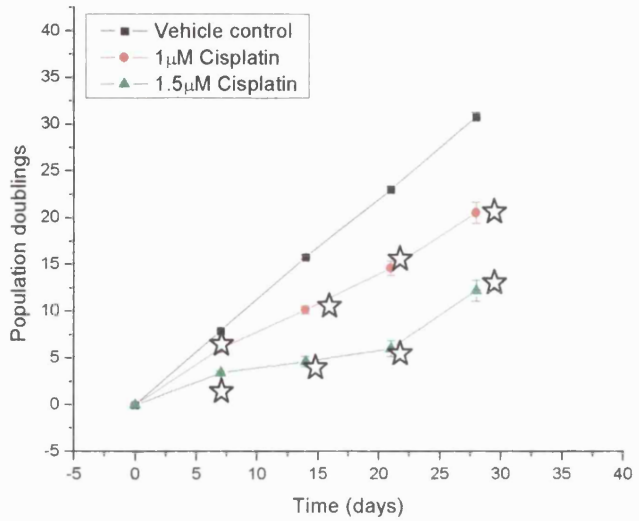

C

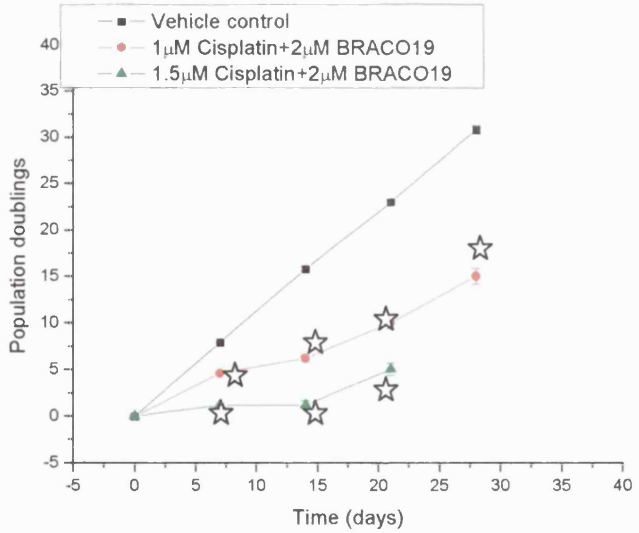

Figure 2.5. Graphs showing long-term antitumour activity expressed as population doublings in A2780 cells treated with BRACO19 (A) or cisplatin (B) as single agents or as a combination (C) for four weeks. Cells were counted every week and reseeded with the initial seeding of $1x10^5$ cells. The drug was added twice a week. Data were analysed using Minitab statistical software version 14. ☆Statistically significant difference between treatments $p<0.05$ for n=3, ANOVA followed by Dunnetts test.

A

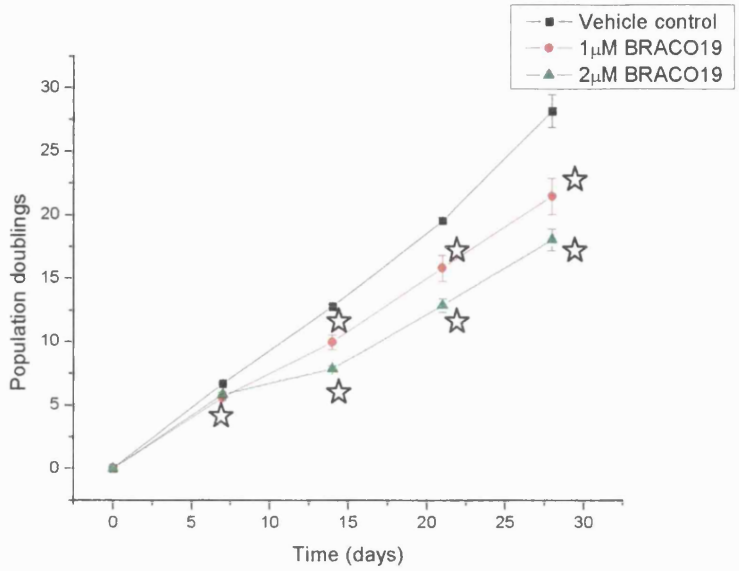
Vehicle control
1μM BRACO19
2μM BRACO19
Population doublings
Time (days)
0
5
10
15
20
25
30

B

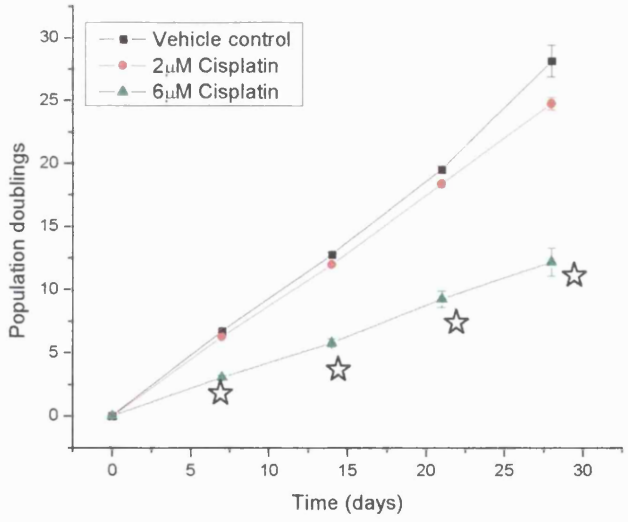
Vehicle control
2μM Cisplatin
6μM Cisplatin
Population doublings
Time (days)
0
5
10
15
20
25
30

C

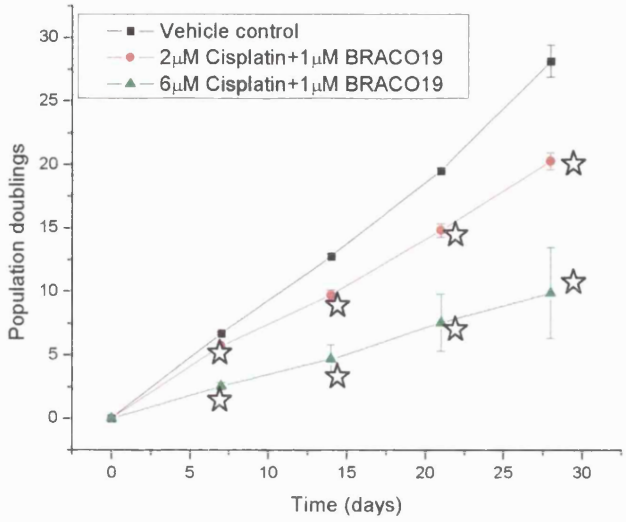

Figure 2.6. Graphs showing long-term antitumour activity expressed as population doublings in A2780cis cells treated with BRACO19 (A) or cisplatin (B) as single agents or as a combination (C) for four weeks. Cells were counted every week and reseeded with the initial seeding of $1x10^5$ cells. The drug was added twice a week. Data were analysed using Minitab statistical software version 14. ☆Statistically significant difference between treatments $p<0.05$ for N=3. ANOVA followed by Dunnetts test.

2.3.5 Combination Index analysis in the MCF-7 breast cancer cell line.

Exposure to BRACO19 and cisplatin as single agents for 96 hours produced 50% growth inhibition (IC_{50}) at concentrations of 2.83±0.41 and 0.55±0.03μM respectively in the MCF-7 breast cancer cell line. All the combinations were performed in a constant ratio, and the ratios chosen for this cell line were 1:1, 1:2, 2:1, 1:3 and 3:1 (BRACO19:cisplatin). Figure 2.7 shows the median-effect plots and isobolograms for each of the ratios used in the combination. First of all, the concentration of both compounds was kept constant 1:1, and later the concentration of one of the drug relative to the other was increased or decreased, in order to find out how this affects the combination in this cell line. Combination index (CI) values at different effective doses (ED_{25}, ED_{50} and ED_{90}) are shown in Table 2.3. There is notable synergy when the compounds were administered in a constant ratio of 1:1, 1:2, 2:1, 3:1 (BRACO19:cisplatin) whereas the effect was remarkably worse when the ratio used was 1:3 (BRACO19:cisplatin). Although the effect in short-term combination studies showed that the combination of BRACO19 and cisplatin is very effective in MCF-7

cells, it was demonstrated that decreasing the concentration of BRACO19 or increasing the concentration of cisplatin has a negative effect on synergy.

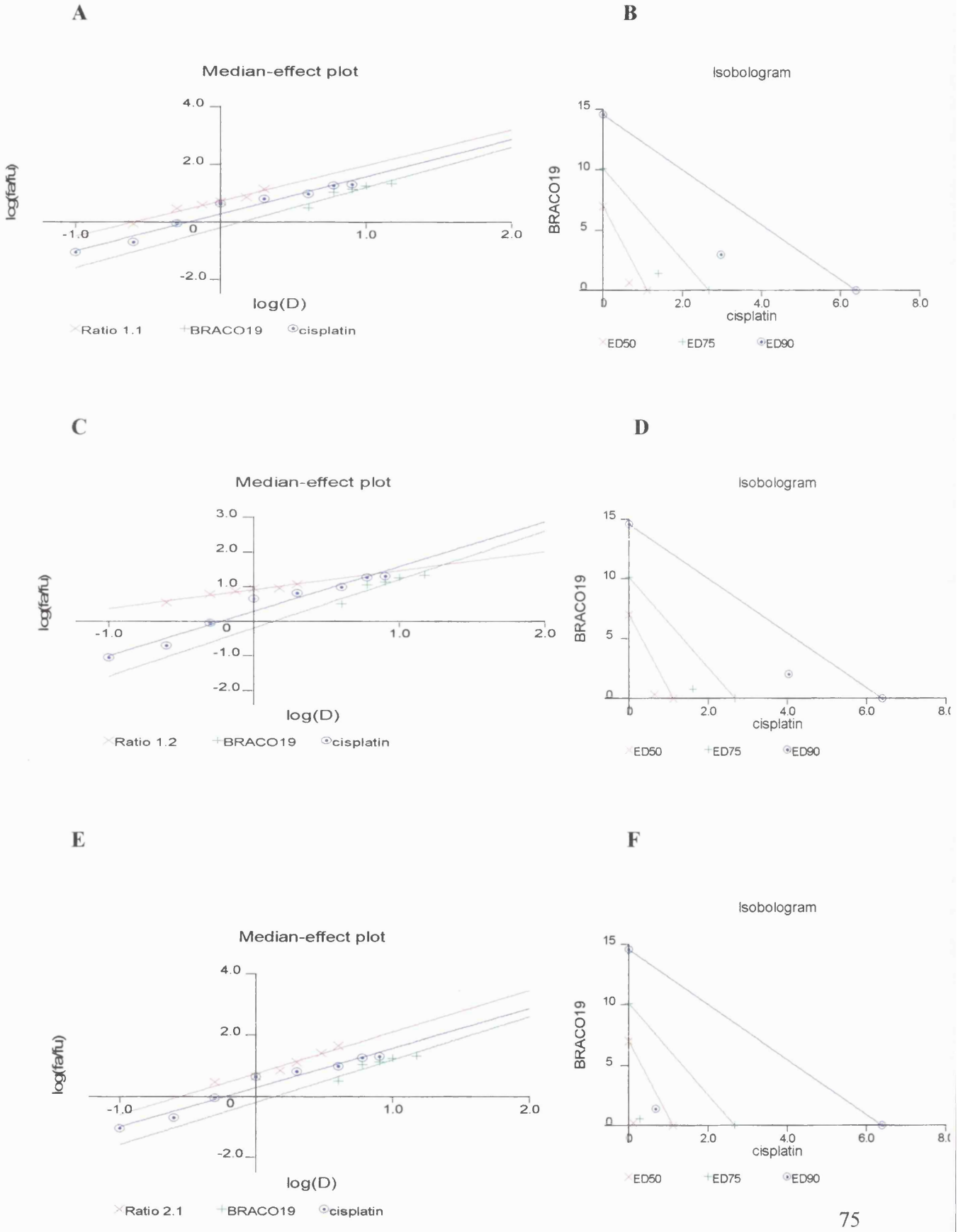

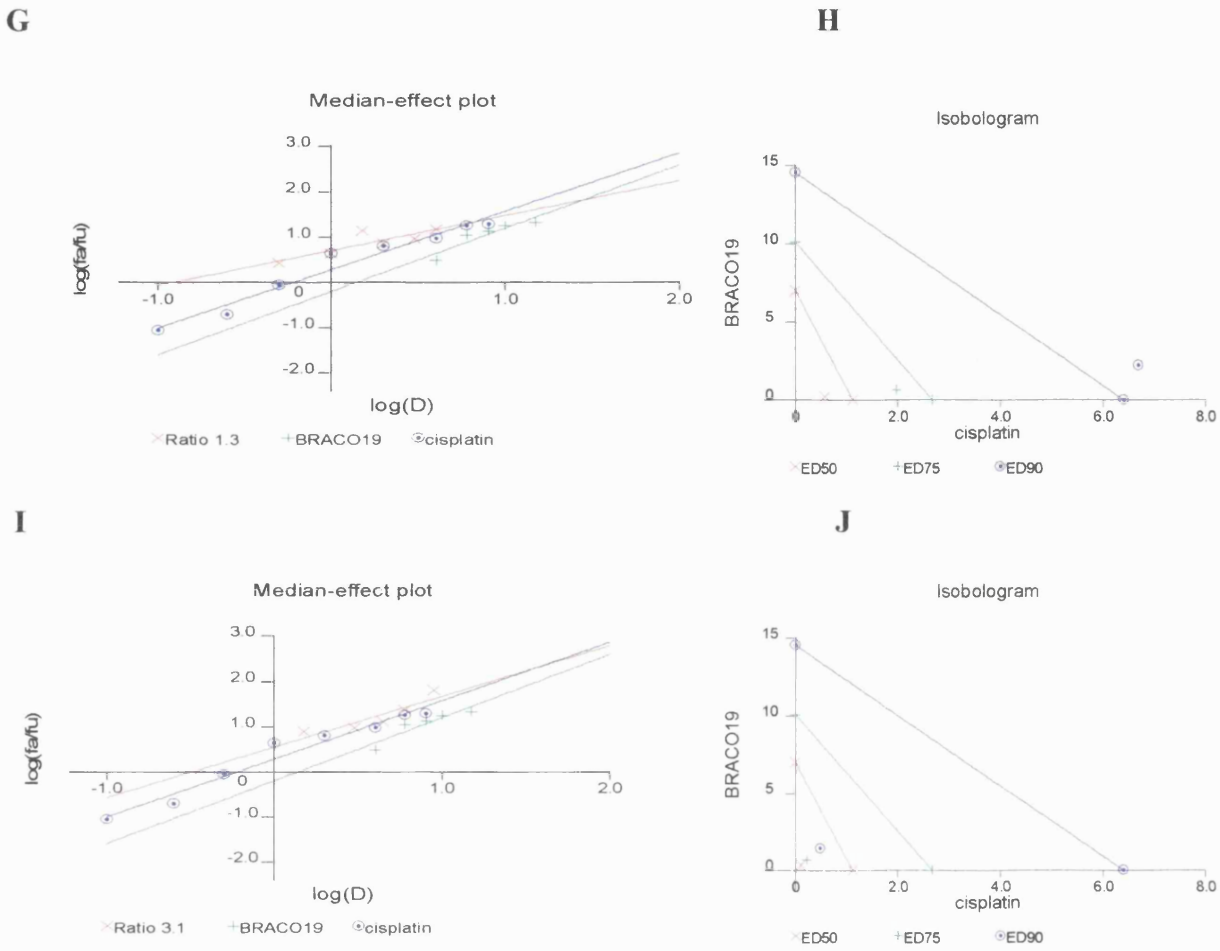

Figure 2.7. Median-effect plots for the two compounds and the combination at different drug ratios in the MCF-7 cell line. Logarithm of dose (x axis) versus logarithm of fraction affected/ fraction unaffected (y axis). A: ratio 1:1, C: ratio 1:2, E: ratio 2:1, G: ratio 1:3, I: ratio 3:1 (BRACO19:cisplatin). Classic isobolograms of the two compounds at the different drug ratios. BRACO19 and cisplatin doses are represented on the y- and x- axis respectively. B: ratio 1:1, D: ratio 1:2, F: ratio 2:1, H: ratio 1:3, J: ratio 3:1 (BRACO19:cisplatin).

MCF-7	ED_{25}	ED_{50}	ED_{90}
Ratio 1:1 (BRACO19:Cisplatin)	0.64±0.05	0.65±0.013	0.67±0.009
Ratio 1:2 "	0.54±0.129	0.66±0.035	0.84±0.09
Ratio 2:1 "	0.29±0.20	0.3±0.19	0.31±0.16
Ratio 1:3 "	2.05±0.156	1.482±0.31	1.074±0.03
Ratio 3:1 "	0.28±0.18	0.32±0.23	0.37±0.28

Table 2.3. Combination index values at effective doses (ED) of 25, 50 and 90 in MCF-7 cells.

2.3.6 Long-term viability studies in MCF-7 cells.

MCF-7 cells were exposed to BRACO19 and cisplatin alone and in combination at sub-cytotoxic concentrations for up to four weeks. Results are expressed as population doublings (Figure 2.8). The effect observed with the two compounds was again concentration and time dependent (Figures 2.8.A and 2.8.B). Notably, using sub-cytotoxic concentrations (0.25μM cisplatin and 1.5μM BRACO19) in combination complete cessation of growth occurred after two weeks of treatment, whereas these concentrations when used as single agents do not produce a significant effect (Figure 2.8.C). All the combinations used here showed a synergistic effect. However, the concentration of cisplatin was kept very low for all them. Cisplatin is very effective in this cell line therefore it was not possible to try a 3:1 ratio (cisplatin:BRACO19) in order to find out how this affect the combination.

A

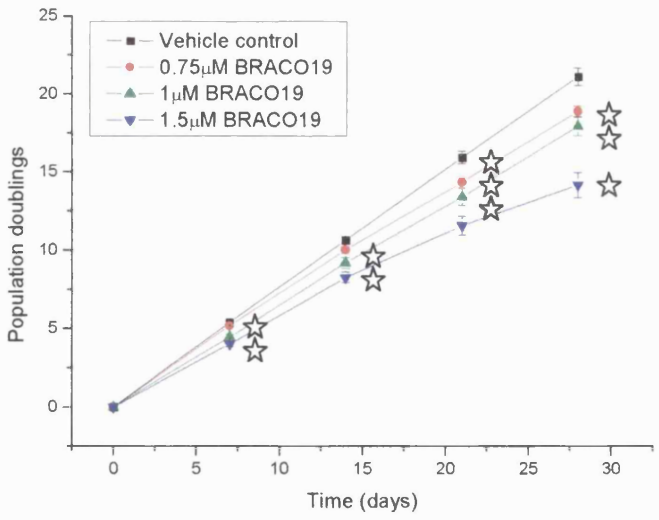

B

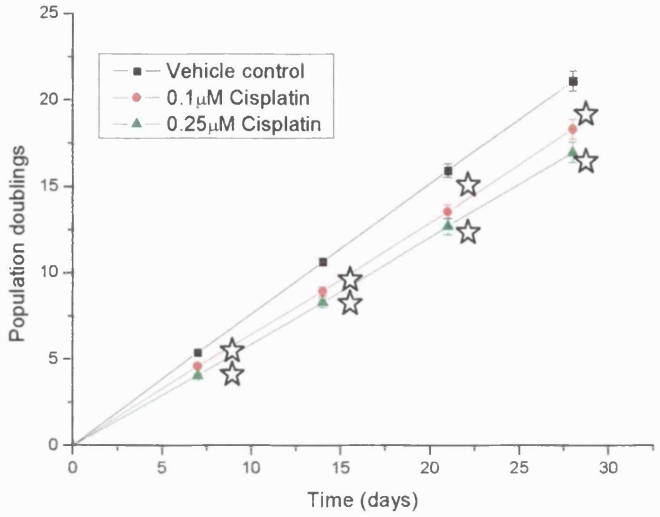

C

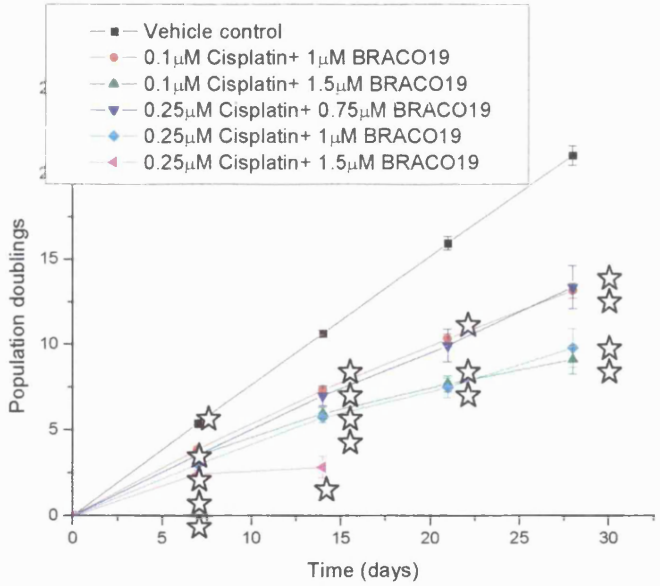

Figure 2.8. Graphs showing long-term antitumour activity expressed as population doublings in MCF-7 cells treated with BRACO19 (A) or cisplatin (B) as single agents or as a combination (C) for four weeks. Cells were counted every week and reseeded with the initial seeding of $1x10^5$ cells. The drug was added twice a week. Data were analysed using Minitab statistical software version 14. ☆Statistically significant difference between treatments $p<0.05$ for N=3. ANOVA followed by Dunnetts test.

2.4. Discussion.

The aim of combination therapy is to find compounds that act synergistically or even additively in order to reduce the doses of both agents, and minimize toxic effect. In this chapter it has been demonstrated using median-effect plot that the combination of cisplatin and BRACO19 produces synergistic cell kill in the epidermis carcinoma cell line A431 when the cells were exposed to both compounds in a constant ratio of 3:1, 2:1 and 1:1 (BRACO19:cisplatin) and nearly additive at the ratios of 1:3, 1:2 (BRACO19:cisplatin). In the case of the ovarian cell lines A2780 and A2780cis synergistic effects were only observed for the ratios of 2:1 and 3:1 for A2780 and 2:1 and 4:1 (BRACO19:cisplatin) for A2780cis and for the other ratios additive or nearly antagonistic effects were observed. MCF-7 cells showed synergistic effects for the ratios 1:1, 1:2, 2:1, 3:1 (BRACO19:cisplatin) and antagonistic effects for the ratio 1:3 (BRACO19:cisplatin). This shows that the combination treatment seems to be better for the MCF-7 breast cancer cell line, although decreasing the concentration of BRACO19 compared to cisplatin in a ratio 1:3 has a negative effect in the combination. However, we have to take into account that the sensitivity towards these two agents is not the same in the different cell lines. A431 and A2780 cells have very similar sensitivity against BRACO19 and cisplatin, therefore the ratio 1:1 in these cell lines is the equipotent concentration of these two agents. On the other hand, in MCF-7 cells the sensitivity towards cisplatin is higher than the sensitivity towards BRACO19 whereas in A2780cis BRACO19 is more effective than cisplatin. However, all the cell lines followed the same pattern at the ratios used in this study, when the concentration of BRACO19 compared to cisplatin was greater the combination was better and synergistic for all of them. Both compounds may act at the telomeres but in a different manner. BRACO19 shows selectivity towards G-quadruplex DNA compared to duplex DNA as has been previously shown *(Read et al, 2001; Harrison et al, 2003)*. Although the genome has many regions which have potential characteristics to form G-quadruplexes *(Shafer and Smirnov, 2001; Todd et al, 2005; Huppert and Balasubramanian, 2005)*, there is data to support the hypothesis that BRACO19 has selectivity towards G-rich single strand telomeric overhang. BRACO19 produces indirect telomerase inhibition due to the effect on the telomeric overhang as it has been shown *in vitro* and *in vivo*, by chromosome fusions and telomere shortening in various cell lines *(Gowan et al, 2002; Incles et al, 2004; Burger et al, 2005)*. On the other hand,

cisplatin reacts with double stranded DNA, having selectivity towards guanines *(Reedijk, 1999)*. Telomeric DNA is rich in guanines; therefore it may be one of the main targets of cisplatin. It has to be taken into consideration that both agents may act at the telomeres, and most importantly how they can interfere with each other. If cisplatin reacts with the guanines in the G-rich telomeric overhang, then the guanines are not free to coordinate with BRACO19, then cisplatin could antagonise the effect of BRACO19. In addition, other authors have published antagonism between cisplatin and another G-quadruplex stabilising agent, the pentacyclic acridine RHPS4 *(Cookson et al, 2005)*. They used the same method as here to calculate the combination index and they found antagonism when they treated the MCF-7 breast cancer cells with a constant ratio of 1:4 (RHPS4:cisplatin), which is exactly the same result as that presented here. Increasing the concentration of cisplatin relative to the G-quadruplex stabilizing agent has a negative outcome for the combination. Although they concluded that antagonism occurs between the two agents it could be that changing the ratio by increasing the concentration of RHPS4 would lead to an improved outcome. According to the results in the combination of BRACO19 and cisplatin, it could be that there is an interaction between the two compounds, and the fact that increasing the concentration of cisplatin, produces a negative effect which could be because cisplatin has an effect on the telomeric overhang, binding to the guanines and impeding the access of BRACO19. Other authors have studied whether cisplatin targets the G-rich single-strand telomeric overhang but it was reported that although cisplatin could bind the telomeric overhang its binding is weak *(Ishibashi and Lippard, 1998)*. Platination experiments on the Tetrahymena telomeric sequence $(T_2G_4)_4$ showed that cisplatin only binds to the guanines located in the loops, which have not coordinated the N7 *(Redon et al 2001)*. Later experiments with human telomere sequences $AG_3(T_2AG_3)_3$ and $(T_2AG_3)_4$ also demonstrated that cisplatin is able to platinate their folded structures *(Redon et al, 2003)*. Studies comparing the rate of reaction between cisplatin and human telomeric quadruplex structure, duplex DNA and single stranded DNA with one platination GG site, showed that all reactive cisplatin species react faster with double strand DNA than with single strand oligonucleotides and the quadruplex structure is platinated twice as fast as the duplex DNA and these two forms react three times faster than single strand DNA *(Garnier and Bombard, 2007)*. From these experiments, the conclusion is that cisplatin has an affinity for G-quadruplex structures and it can bind to the loops in the folded structure and at very high doses it may interfere with the action of BRACO19.

Therefore it is important to select the doses of both agents in order to obtain the desirable outcome.

On the other hand, a possible theory explaining the synergism between these compounds could be that the effect of BRACO19 in the cell potentiates the action of cisplatin interfering with DNA repair in the cell. The effectiveness of cisplatin is correlated with the number of adducts that forms, therefore if there is an agent that acts by interfering with the DNA repair machinery, then this agent will potentiate the effect of cisplatin *(Rodriges et al, 2004)*. The topoisomerase inhibitor pyrazoloacridine (NSC 366140) has been shown to inhibit the repair of platinum-DNA adducts in A549 leading to synergy between both compounds, whereas when NSC 366140 was combined with alkylating agents such as melphalan or 4-hydroperoxycyclophosphamide the effect was antagonistic, showing that the effect of adducts removal is essential for this outcome *(Adjei et al, 1997)*. It has been shown before that inhibition of telomerase activity enhances the effect of cisplatin in different cell lines *(Misawa et al, 2002)*. The effect on telomerase activity seems to have a relation to the DNA repair machinery. NHOF cells transfected with h-TERT have enhanced DNA repair compared to NHOF parental cells which do not express h-TERT. These transfected cells had faster nucleotide excision repair. Furthermore, when these NHOF transfected cells lose their capacity to express h-TERT, their capacity to repair DNA damage is also decreased *(Shin et al, 2004)*. Suppression of h-TERT has been also shown to reduce the capacity of DNA repair in human fibroblasts. h-TERT is up-regulated during S-phase, however, this up-regulation is not enough for telomere maintenance. For this reason, it has been postulated that h-TERT expression may have a role in DNA repair *(Masutomi et al, 2005)*. Consequently telomerase inhibition could produce a negative effect on DNA repair that leads to the accumulation of cisplatin adducts and explain the synergism observed. As a result the indirect effect of BRACO19 on telomerase has a positive effect on the combination. Other studies using human melanoma cells expressing mutant h-TERT characterized by telomere dysfunction showed an enhancement in cisplatin activity. Cell lines without telomerase activity were used with different telomere status and it was shown that greater telomere dysfunction leads to an improved outcome, suggesting that telomere dysfunction was the principal determinant of chemosensitivity *(Biroccio et al, 2003)*. Subsequently a G-quadruplex stabilising agent such as BRACO19 which has a direct effect on the telomere overhang would have a more rapid and effective effect, and it

would be more appropriate to combine cisplatin with a G-quadruplex stabilising agent than with a simple telomerase inhibitor.

Another important aspect to take into account is the resistance to treatment. Resistance to cisplatin has been related to telomere elongation, and telomerase activity is higher in A431 cisplatin resistant cell line compared with A431 wild type *(Mese, 2001)*, consequently, the effect of BRACO19 on telomerase activity and telomeres can be used as a good strategy to avoid the appearance of resistance towards cisplatin in this cell line.

The next was to look at the effect in viability at sub-cytotoxic concentrations during long-term exposure. The results of these studies were definitely showing synergism for A431 and MCF-7 cells, complete cessation of cell growth after two weeks of treatment for the combination at concentrations for both compounds that do not produce a significant effect when they were used as single agents. The importance of these long-term studies was to check out if there is a correlation between what was observed after short-term exposure and most importantly to ensure that the effect was maintained. Consequently reducing the doses of both agents that results in reducing the toxicity still produces synergy. For the ovarian cell lines nevertheless the effect is additive at the concentrations used for this study. On the other hand, this is only an *in vitro* approach, that gives an idea of effectiveness of this combination and other studies *in vivo* have to be carried out, to check if there is still correlation with what it was found here. It is necessary to distinguish between *in vitro* synergy and the *in vivo* efficacy *(Greco et al, 1996; Kaufmann et al, 1996)*. Although a combination of two agents show synergy *in vitro*, it could be that they may also potentiate their toxic effects *in vivo* and therefore they do not have clinical applicability. Therefore, it is important when combining anticancer agents that they do not overlap toxic effects.

Due to the differences found in the four cell lines, and the better result showed in MCF-7 and A431 cells, I decided to continue the mechanistic studies in these cell lines in order to determine the mechanism of action of the combination.

Chapter 3- MECHANISM OF CELL GROWTH INHIBITION AFTER TREATMENT WITH BRACO19, CISPLATIN OR THE COMBINATION

3.1. INTRODUCTION

In the previous chapter the effectiveness of combining BRACO19 and cisplatin was investigated following short and long-term exposure in different human cancer cell lines. The results of these studies were definitely showing synergy in A431 and MCF-7 cells. The aim of this chapter was to investigate the mechanism of cell growth inhibition in these two cell lines using different markers for senescence, apoptosis and necrosis. Furthermore, cell cycle and viability studies were also used to obtain more information about the mechanism.

3.1.1 Senescence.

Normal human somatic cells posses a limited capacity for replication (discussed in chapter 1). Telomeric DNA shortens in every replication cycle, leading to uncapping of telomeres and replicative senescence *(Smith and Pereira-Smith, 1996; Chiu and Harley, 1997; Cristofalo et al, 2004)*. The old idea was that telomeres erode until a certain critical length, when the cells enter a non-replicative state or senescence. However it has been demonstrated that it is not the critical length, but rather the status of uncapping of the end of the chromosome that makes the cell enter crisis *(Blackburn, 2000)*. The uncapping of telomeres is recognised as a DNA strand break or DNA damage, consequently DNA damage machinery is activated, and cells exit cell cycle, arrest in G1 and enter a non-replicative state while they try to repair the damage. Senescent cells have lost their ability to divide but they are metabolically active and have characteristic morphology: they are flattened, show cellular enlargement and are multinucleated cells *(Campisi, 2001)*.

Apart from telomere uncapping, there are other signals that can induce the senescence phenotype such as DNA damage, oxidative stress, oncogene activity, and lack of nutrients, etc *(Ben-Porath et al, 2005)*.

The cyclin dependent kinases inhibitors p21 and p16 are the main regulators of the G1 cell cycle arrest in senescence *(Herbig et al, 2006)*. p21 and p16 act by inhibiting the cyclin dependent kinases responsible for phosphorylating the retinoblastoma protein (Rb) and therefore inhibiting the transcription of genes required for DNA synthesis.

The majority of cancer cells have reactivated telomerase in order to avoid telomere attrition, however, this is not the only mechanism used (discussed in chapter 1). These mechanisms prevent cancer cells from undergoing replicative senescence. On the other hand, senescence can be induced in tumour cells by different mechanisms such as radiation, genetic manipulation or treatment with chemotherapeutic agents *(Roninson, 2003).*

3.1.2 Apoptosis.

Apoptosis is a genetically controlled and evolutionarily conserved mechanism of cell death. This mechanism of programmed cell death is used by multicellular organisms to maintain the homeostasis of tissues *(Fulda and Debatin, 2006).* There are two main pathways that lead to apoptosis: the extrinsic or receptor mediated pathway and the intrinsic or mitochondrial pathway. The extrinsic pathway is a mechanism used during organism development in order to eliminate unnecessary cells *(Khosravi-Far and Esposti, 2004)*, whereas the intrinsic pathway is activated by cellular stress signals *(Gogvadze and Orrenius, 2006).* Both pathways lead to the activation of cysteine-dependent aspartate-specific proteases called caspases.

3.1.2.a Extrinsic or receptor mediated pathway.

The extrinsic pathway is activated by death receptors as a consequence of extracellular death signals. These transmembrane death receptors which are activated by certain ligands, belong to the tumour necrosis factor receptor (TNFR) gene superfamily. They contain two important domains, one typical of this family of proteins, a cysteine-rich extracellular domain and a homologous cytoplasmic sequence or death domain *(Ashkenazi and Dixit, 1998).* An example of a very well studied death receptor is the CD95, also called Fas or Apo1. When the ligand that is a member of the tumour necrosis family binds the trimeric receptor, it produces the subsequent recruitment of adaptor proteins such as FADD (Fas-associated death domain) *(Siwkowski et al, 2004)*, forming the death inducing signalling complex (DISC). The adaptors bind to the cytoplasmic death domain in the death receptor through its own death domain, and they also produce the binding through their other death effectors domain (DED) to the death effectors domain (DED) in the initiator procaspase 8 inducing its own activation through self-cleaveage. Caspase 8 subsequently activates the effector caspases.

3.1.2.b Intrinsic or mitochondrial pathway.

The intrinsic pathway is activated by oxidative stress that can be produced by different factors such as DNA damage produced by cytotoxic agents in cancer therapy. During apoptosis there is mitochondrial damage, depolarization of mitochondrial membrane and subsequent cytochrome c release *(Matapurkar and Lazebnik, 2006)*. The release of cytochrome c and other proteins such as AIF (apoptosis-inducing factor) from mitochondria is mediated by Bax, Bid and Bcl-2. These proteins belong to the Bcl-2 family. Some of these family proteins are proapototic such as Bax and Bid, and others are antiapoptotic such as Bcl-2. Bcl-2 is located in the outer mitochondrial membrane. There is evidence that Bid and Bax are recruited to the mitochondria where they interact with Bcl-2, however is not known how these proteins produce the release of cytochrome c and AIF *(Crompton, 1999)*. There is an expansion of the matrix space and due to the area of the inner membrane being greater than the outer membrane the outer membrane collapses and produces the release of the apoptogenic factors. Cytochrome c in the cytoplasm forms a complex with the protein Apaf-1. Apaf-1 oligomerizes and binds to the initiator procaspase 9 and forms the apoptosome *(Kim et al, 2005; Shi, 2006)*. Procaspase 9 activates itself and subsequently caspase 9 activates the effector caspases 3, 6 and 7 *(Kumar et al, 2007)*. Apaf-1 has an amino terminal region with 12 or 13 WD-40 repeats, a central ATPase domain and a carboxy terminal caspase recruitment domain (CARD). Cytochrome c binds to the WD-40 region of Apaf-1, which produces hydrolysis of dATP to dADP and a conformational change in the Apaf-1 molecule. Apaf-1 activates procaspase 9 via this CARD-CARD interaction *(Kim et al, 2005)*.

Effector caspases produce their effects through different mechanisms. They inactivate antiapoptotic proteins such as the inhibitor of caspase activated deoxyribonuclease (ICAD) or Bcl-2 proteins, damage cell structures such as nuclear lamina, affect chromatin organization which leads to chromatin condensation, and they also cleave proteins involved in DNA repair and DNA replication affecting their function and therefore the homeostasis of the cells *(Thornberry and Lazebnik, 1998)*.

Finally, during apoptosis there is activation of endonucleases that cleave DNA into fragments. They induce internucleosomal DNA cleavage producing 180-200 base pair fragments, but they also produce large DNA fragments and single strand cleavage

(Bortner et al, 1995). The internucleosomal DNA cleavage seems to be a hallmark of apoptosis and it can be used to distinguish between apoptosis and necrosis.

3.1.3 Necrosis.

Necrosis is an unregulated mode of cell death. It has always been considered to be a passive mechanism that occurs as a consequence of depletion of energy adenosine triphosphate (ATP) in cells *(Kanduc et al, 2002)*. Following DNA damage, cells activate DNA repair proteins such as poly(ADP-ribose)polymerase (PARP). PARP activation induces β-nicotinamide adenine dinucleotide (NAD) depletion that leads also to ATP depletion and loss of cell homeostasis *(Ha et al, 1999; Zhong et al, 2004)*. ATP depletion affects ATP-dependent ion channels and produces disequilibrium of ions in the cell *(Barros et al, 2001)*. There is an increase in influx of Na^+ and water that produces cell swelling, membrane blebbing and finally collapse of the cell *(Carini et al, 1995)*. The latest event during necrosis is the release of lysosomal enzymes into the extracellular space. Necrotic cells share common morphologic characteristics with apoptotic cells such as changes in mitochondrial membrane integrity *(Bhatia, 2004)*. On the other hand, they present specific characteristics such as complete loss of plasma membrane integrity that can be detected with the use of vital dyes such as trypan blue.

3.2. METHODS

3.2.1 Detection of Cellular Senescence (β-galactosidase activity).

Cells were stained for β-galactosidase activity as a biomarker of cell senescence *(Dimri et al, 1995).* Senescent human cells express β-galactosidase, histochemically detectable at pH=6 which is the optimal pH for its activity, and this activity is not found in presenescent, quiescent or immortal cells. Cells expressing β-galactosidase activity metabolise 5-bromo-4-chloro-3-indolyl-βD-galactopyranoside (X-gal) and form a local blue precipitate.

Cells were stained with the senescence β-galactosidase staining kit (Cell Signalling Technology) according to manufacturer's instructions. Briefly, at the end of each week, $1x10^5$ cells from each treatment were seeded in a 6 well plate (Fisher scientific, UK) in 2ml of media with appropriate amounts of drug and incubated at 37^0C overnight. The following day, medium was removed, and cells were washed once with 2ml of 1X PBS. The cells were then fixed with 1ml of 1X fixative solution for 10 minutes at room temperature. Later, fixative solution was removed and cells were washed twice with 1X PBS. And finally, 1ml of staining solution containing X-gal was added to the plate and plates were incubated at 37^0C overnight. The next day, cells were visualised under the microscope at a magnification of 200X. Three different fields that were representative of the total population were counted and percentage of blue cells compared to non-stained cells was calculated.

3.2.2 Cell cycle analysis for sub-G1 population.

$1x10^5$ cells were treated with appropriate concentrations of compounds as before (see chapter 2). After one week, cells were counted and $1x10^6$ cells of each treatment were fixed in 70% ethanol. Samples at this point can be kept at -20^0C. Samples were washed twice in phosphate-citrate buffer (0.192M Na_2HPO_4, $4x10^{-3}$M citric acid, pH=7.8), spinned at 2000 rpm and supernatant was carefully discarded. The phosphate-citrate buffer helps to elute the small fragments of DNA. To ensure that only DNA was stained, cells were treated with 50μl of ribonuclease (Sigma, Germany) and 200μl of 50μg/ml propidium iodide (Invitrogen, UK). DNA content was measured using a

FACSCALIBUR flow cytometer (All the flowcytometric work reported in this thesis was carried out in the FACS laboratory CRUK, at Holborn). Histograms of the cell cycle phase distribution and calculations of the percentage in G1, S and G2 phases were obtained by analyzing at least 10^4 single events to perform statistical analysis. We used pulse processing signal to exclude clumps of cells from analysis.

3.2.3 Bromodeoxyuridine (BrdU) Staining.

$1x10^5$ cells were treated with appropriate concentrations of agents as before (see chapter 2). After one week of treatment, cells were treated with 10μM BrdU (Sigma, UK) for 30 minutes and incubated at 37^0C in order to allow the cells to incorporate the BrdU. After the incubation time the cells were harvested and fixed in cold 70% ethanol. Cells were centrifuged at 2000 rpm for 5 minutes and supernatant was carefully discarded and the pellet was washed twice in PBS (Invitrogen, UK). The cells were resuspended in 2M hydrochloric acid and incubated at room temperature for 30 minutes. Again, the cells were centrifuged at 2000 rpm for 5 minutes and carefully supernatant was discarded and the pellet was washed twice in PBS and once in PBS-T (PBS+0.1% bovine serum albumine (BSA) (Sigma, UK)+0.2% Tween 20, pH=7.4). Subsequently 2μl anti-BrdU mouse antibody (Becton Dickinson) was added directly in to the cells and incubated for 20 minutes in the dark at room temperature. Then the cells were washed twice in PBS-T, and stained with 50μl of FITC-conjugated rabbit anti-mouse F(ab')2 fragments (DAKO) for 20 minutes in the dark at room temperature. Afterwards, the samples were washed in PBS, centrifuged and resuspended in 50μl of 100μg/ml ribonuclease (Sigma, Germany) and 200μl of 50μg/ml of propidium iodide (Invitrogen, UK) for 20 minutes at room temperature.

3.2.4 Annexin V and mitochondrial membrane potential.

Cells were treated with appropriate concentrations of agents as before. After one week of treatment, cells were harvested and resuspended in fresh media. Tetramethyl rhodamine ethyl ester (TMRE) was added at a final concentration of 40nM, and cells were incubated for 10 minutes at 37^0C. Later on, cells were centrifuged at 1000 rpm for 4 minutes and carefully supernatant was discarded and the pellet was washed in PBS (Invitrogen, UK). Then centrifuged again at 1000 rpm for 4 minutes and resuspended in 500μl of annexin V buffer (Invitrogen, UK) per sample. Finally 5μl of annexin V-Alexa

647 conjugate (Invitrogen, UK) was added to each tube. The samples were incubated at room temperature for 15 minutes. And before analysis, 2µl of 4',6-diamidino-2-phenylindole (DAPI) was added to each sample to distinguish between death and alive cells.

3.2.5 Detection of caspase 3.

$1x10^5$ cells were treated with appropriate concentrations of compounds as before. After one week, cells were counted and $1x10^6$ cells of each treatment were fixed in 4% paraformadehyde in PBS (Invitrogen, UK) for 30 minutes at room temperature. Afterwards, cells were pelleted and washed in PBS. At this point samples were kept at 4^0C until further analysis. Cells were washed two times in PBS-T (PBS+0.1%BSA (Sigma, UK)+0.2% Tween 20, pH=7.4), spin at 2000 rpm and the supernatant was carefully discarded. Pellets were resuspended in 20µl of FITC-conjugated rabbit anti-active caspase 3 monoclonal antibody (BD Pharmingen, UK) and incubated at room temperature for 1 hour. The cells were washed again in PBS-T (PBS+0.1%BSA+0.2% Tween 20, pH=7.4), centrifuged and resuspended in 50µl of 100µg/ml ribonuclease (Sigma, Germany) and 200µl of 50µg/ml of propidium iodide (Invitrogen, UK), and analyzed by flow cytometry.

3.2.6 Detection of DNA strand-breaks using the Terminal deoxynucleotide transferase dUTP Nick End Labeling (TUNEL) assay.

This assay is based on labelling DNA strand breaks with brominated-dUTP using a terminal deoxynucleotidyl transferase. This enzyme catalyzes the incorporation of dUTPs to double or single stranded DNA breaks. These brominated-dUTP sites are then recognised by antiBrdU antibodies labelled with fluorochromes.

The TUNEL assay was performed using the APO-BRDU kit (eBiosciences, USA).
$1x10^5$ cells were treated with appropriate concentrations of compounds as before. After one week, cells were counted and $1x10^6$ cells of each treatment were fixed in 4% paraformadehyde in PBS for 30 minutes at room temperature. Afterwards, cells were pelleted and washed in PBS. Subsequently, cells were permeabilised by adding 1ml of 70% ethanol. Cells were kept at -20^0C for 1 hour. The rest of the protocol was carried

out according to manufacturer's instructions. The kit provides a FITC labelled antiBrdU antibody that allows the identification of DNA strand breaks, and a mix of propidium iodide and RNase for DNA profiling.

All the FACS results were analysed by Dolores Martinez from FACS laboratory, CRUK using the FlowJo programme version 8.5.

3.2.7 Dye exclusion method using Trypan Blue.

Cells were treated with appropriate concentrations of compounds as before for one week. Then cells were harvested. 200µl of each cell suspension were mixed with 200µl of 0.4% of tryptan blue (Sigma, UK), and incubated for 5 minutes at room temperature. Later on, blue cells (necrotic) and unstained cells (non necrotic) were counted using a Neybauer haemocytometer (Assistant, Germany).

Method	Detection	Advantages	Disadvantages
β-galactosidase activity	Senescence, G1 arrest		
Cell cycle for sub-G1	Late apoptosis. Activation of endonucleases	Information about cell cycle	Low sensitivity for the detection of apoptosis
BrdU incorporation	% of cells in S-phase	Detection of S-phase arrest	
Annexin V	Early apoptosis. Cell membrane damage		Translocation of phosphatidyl serine also occurs during necrosis
TMRE	Early apoptosis. Mitochondrial membrane damage	Specific marker for the intrinsic apoptotic pathway	Mitochondrial membrane damage also occurs during necrosis
Detection of caspase 3	Apoptosis	Specific marker for apoptosis	Detection of only one specific caspase
TUNEL	Apoptosis. Activation of endonucleases	Good sensitivity for the detection of apoptosis	
Trypan blue	Viability. Cell membrane damage	Discriminates early and non apoptotic cells from other forms of cell death	

Table 3.1 Summary of the methods used for the study of the mechanism of cell growth inhibition.

3.3. RESULTS

3.3.1 Detection of Cellular Senescence (β-galactosidase activity).

A431 cells were stained for β-galactosidase activity as a biomarker of cell senescence. All treatments including both compounds and the combination were assessed for β-galactosidase activity every week (see chapter 2). There was no senescence phenotype (blue staining) after BRACO19, cisplatin or combinations treatments for any of the concentrations used as show in Figure 3.2. Therefore in the A431 cell line, neither of these compounds or the combination lead to senescence. Since the concentrations used for the single agents did not produce a dramatic effect on cell viability after four weeks of treatment, higher concentrations of BRACO19 and cisplatin (2.5μM and 1.5μM respectively) were also investigated. These concentrations also failed to induce any senescence in A431 cells.

As a control, a non-cancerous fibroblast cell line, IMR-90, was used. IMR-90 cells were cultivated for two weeks, then stained for β-galactosidase activity and used as a negative control (Figure 3.1.A). These cells were maintained in culture for six weeks, stained for β-galactosidase activity and used as a positive control (Figure 3.1.B).

The senescence phenotype was also investigated in MCF-7 cells (Figure 3.3). All the treatments from long-term studies (see chapter 2) were stained for β-galactosidase activity up to three weeks. Figure 3.4 shows percentages of senescent cells observed after different treatments. The concentrations used for BRACO19 or cisplatin were also very low as with previous studies in A431 cells. However, senescence was observed for both agents. The induction of senescence was time and concentration dependent for both compounds. After three weeks of treatment, a significant effect was observed for all the treatments; 1.5μM BRACO19 and 0.5μM cisplatin induced 25% and 18% of senescent cells respectively. On the other hand, the combination of both agents showed a more marked effect. All the combinations used showed a dramatic increase in percentage of senescent cells after only one week of treatment. The combination of 1.5μM BRACO19 and 0.5μM cisplatin induced 40% senescence.

Cell cycle studies were carried out in A431 cells to determine the mechanism of cell death following BRACO19, cisplatin or the combination treatment.

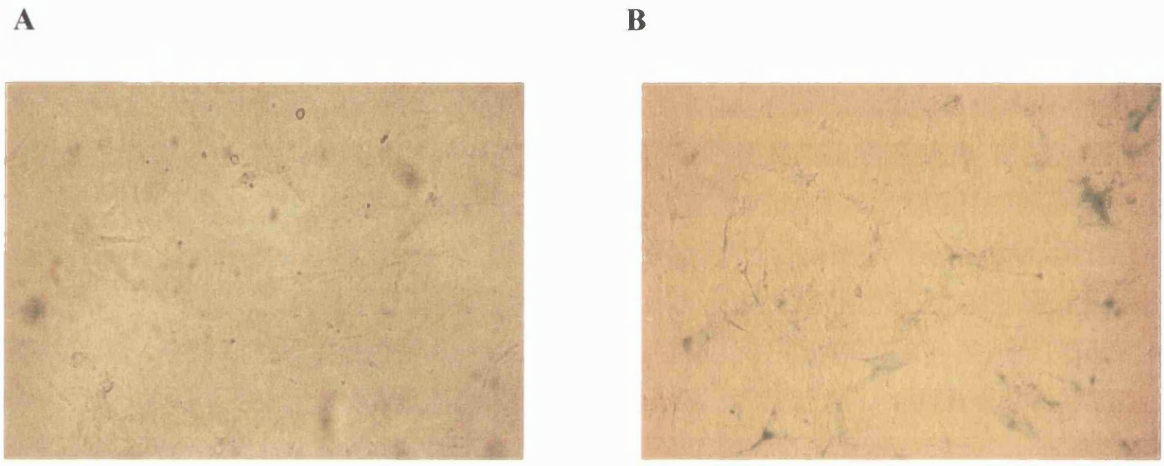

Figure 3.1. IMR-90 cells with β-galactosidase staining. A. Negative control (IMR-90 cells cultivated for two weeks), B. Positive control (IMR-90 cells cultivated for six weeks)

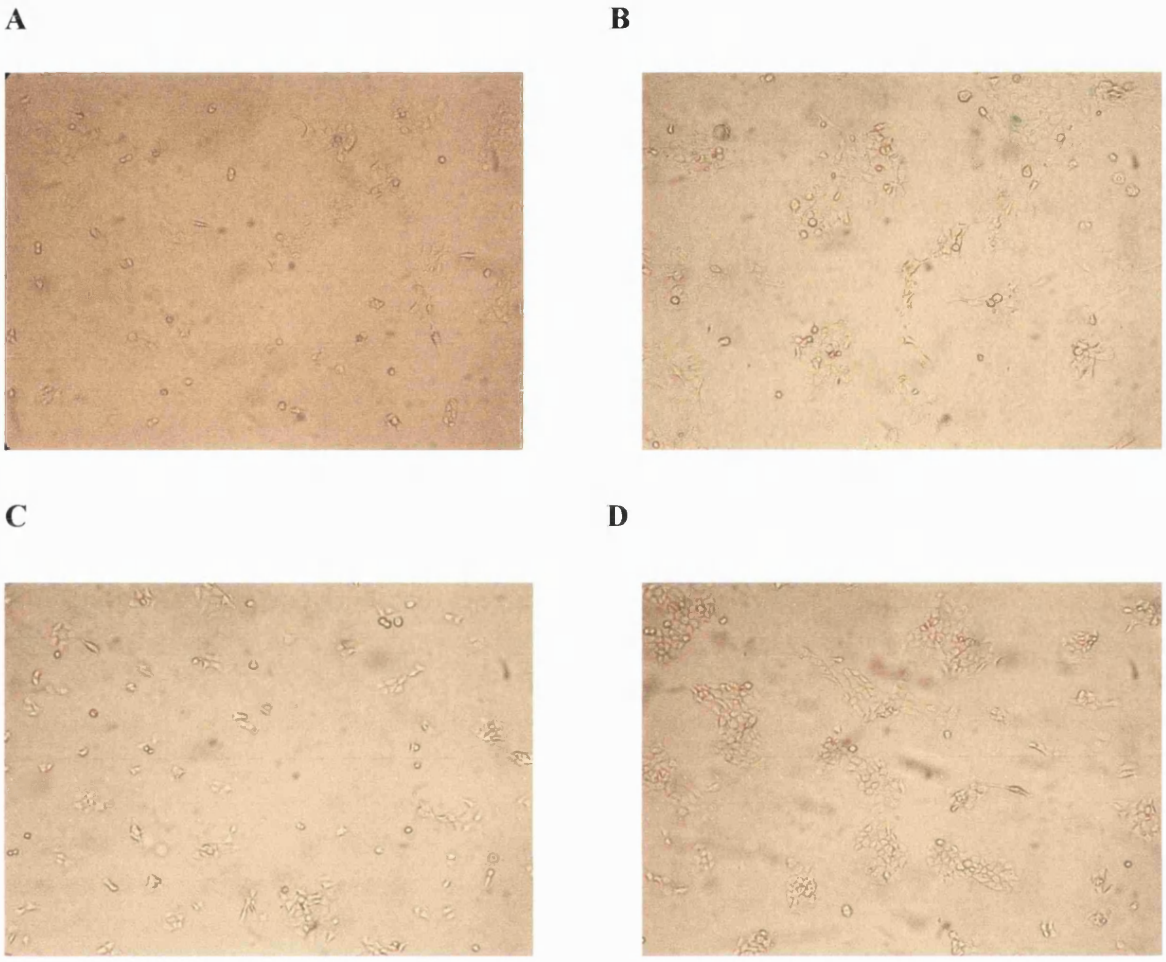

Figure 3.2. A431 cells stained for β-galactosidase after three weeks of treatment. A. Vehicle control, B. 1μM BRACO19, C. 0.5μM cisplatin, D. 1μM BRACO19+0.5 μM cisplatin.

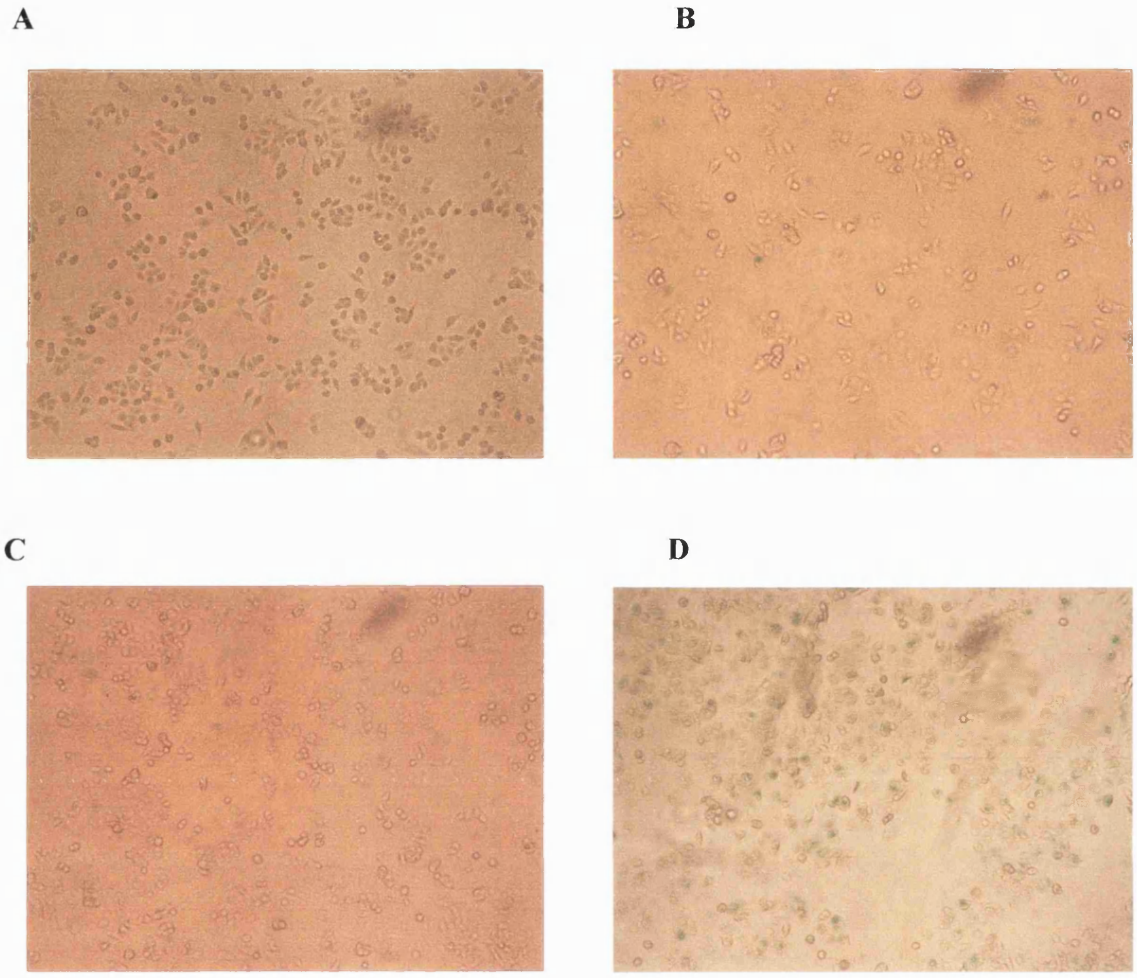

Figure 3.3. MCF-7 cells stained for β-galactosidase activity after one week of treatment. A. Vehicle control, B. 1.5μM BRACO19, C. 0.25 μM cisplatin, D. 1.5μM BRACO19+0.25 μM cisplatin.

A

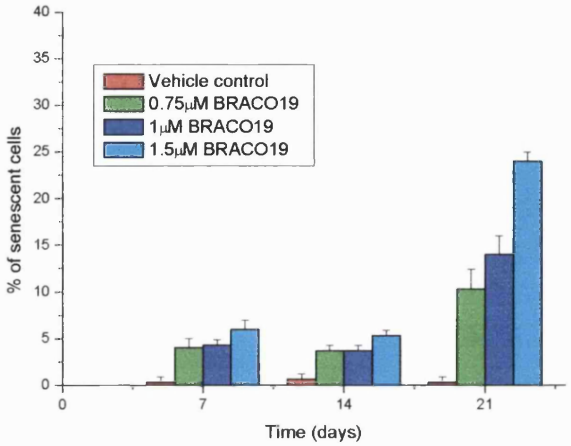

B

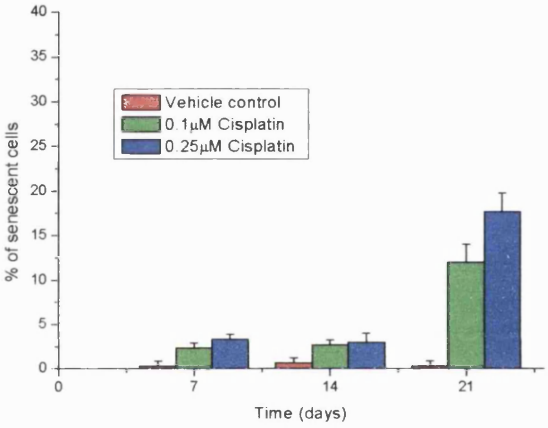

C

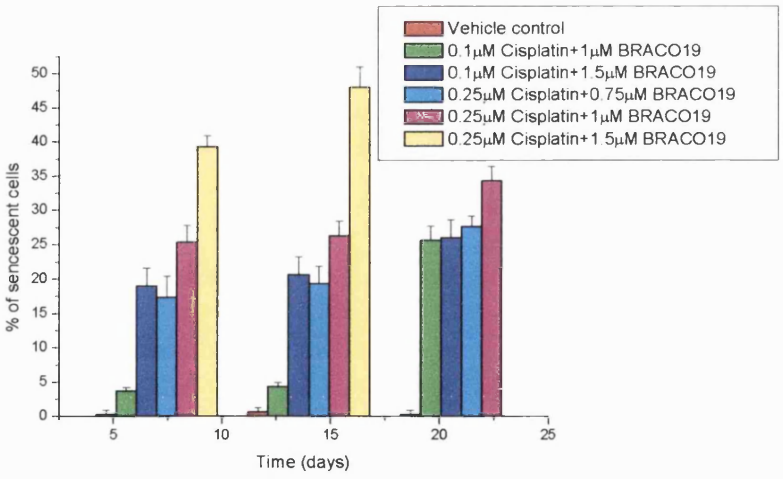

Figure 3.4. Percentage of senescent cells observed after treatment with various concentrations of BRACO19 (A), cisplatin (B) or the combination (C) after one, two and three weeks of exposure in MCF-7 cells.

3.3.2 Cell cycle analysis for sub-G1 population.

Activation of nucleases that produce DNA fragmentation occurs during apoptosis *(Bortner et al, 1995)*. Therefore, apoptotic cells would have smaller fragments of DNA. After staining of DNA with propidium iodide, these fragments would appear on the left of the G1 peak as sub-G1 population on the cell cycle histogram. However, detection of DNA fragmentation only allows detection of late apoptosis *(Cohen et al, 1992)*, when DNases have been activated. Furthermore, cells can also go through apoptosis and not be detected because there is not enough DNA lost.

A431 cells were treated with both compounds alone or in combination at concentrations of 0.75μM cisplatin and 1.5μM BRACO19 for one week. Cell cycle histograms are represented in Figure 3.5. Neither of these compounds at these concentrations or the combination showed a significant difference in sub-G1. The results are summarized in Table 3.2.

However, following treatment with cisplatin, BRACO19 and the combination an increase in the percentage of cells in S-phase and G2 was detected. Therefore, further investigation using BrdU incorporation (see 3.3.3) was necessary to determine if the changes detected were a consequence of an arrest in S-phase or G2 or on the contrary if the cells were proliferating faster as a consequence of the effect of these agents.

cell cycle	Sub-G1	G1	S	G2
Vehicle control	1.9	76	11.5	10.6
0.75μM cisplatin	2.1	46.9	29.9	21.1
1.5μM BRACO19	1.59	51.3	21	18.7
Combination	4.6	46.7	22.7	26

Table 3.2. Summary of changes observed after one week of treatment in A431 cells in cell cycle (results are expressed as percentage).

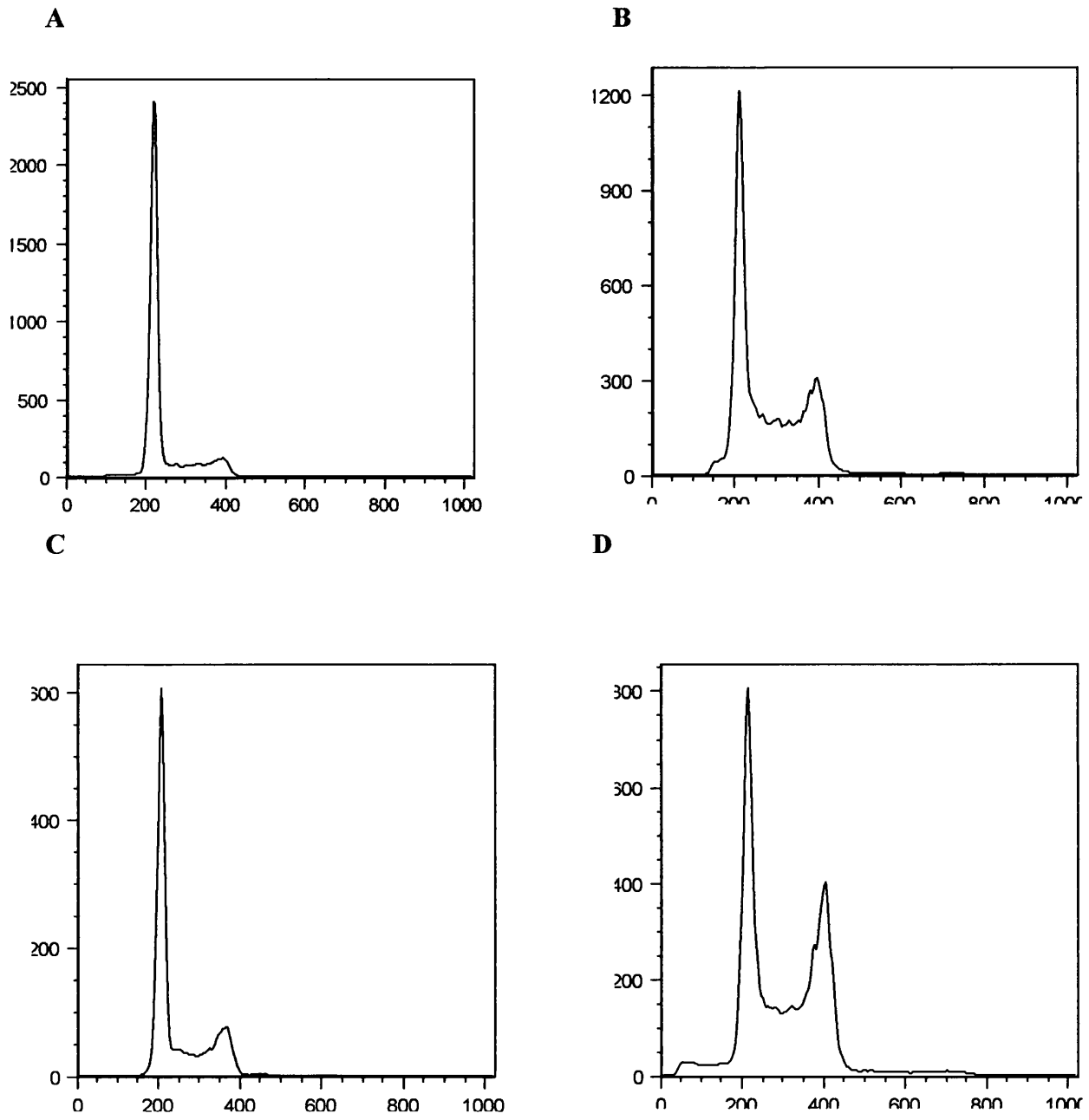

Figure 3.5. Cell cycle analysis after one week of treatment in A431 cells. A. Vehicle control, B. 0.75μM cisplatin, C. 1.5μM BRACO19, D. 0.75μM cisplatin+1.5μM BRACO19.

3.3.3 Viability study. Bromodeoxyuridine (BrdU) incorporation.

The study of incorporation of 5-bromo-2'-deoxyuridine (BrdU) was used in order to assess if there was any change in cell proliferation following different treatments. The amount of BrdU incorporated indicates the number of cells that have passed through S-phase during the time of exposure (Figure 3.6).

A remarkable result was observed after one week of treatment. When A431 cells were treated with both 0.75μM cisplatin and 1.5μM BRACO19, there was a notable decrease in BrdU incorporation, indicating that cells stopped proliferating (Table 3.3). However this change was not observed for the single agents. This is also in agreement with what was observed during long-term viability studies (see chapter 2), using sub-cytotoxic concentrations in combination, a dramatic decrease in population doubling occurred after one week and complete cessation of growth after two weeks of treatment at concentrations that do not produce a significant effect when they were used as single agents.

Upon cisplatin and BRACO19 treatments, it was observed an increase in BrdU incorporation compared to vehicle control. Interestingly, during previous cell cycle analysis, an increase in S-phase was also detected following these treatments.

Bromodeoxyuridine incorporation	**1 week**
Vehicle control	11.1
0.75μM cisplatin	19.7
1.5μM BRACO19	22.2
Combination	2.43

Table 3.3. Summary of changes observed in BrdU incorporation after one week of treatment in A431 cells (results are expressed as percentages).

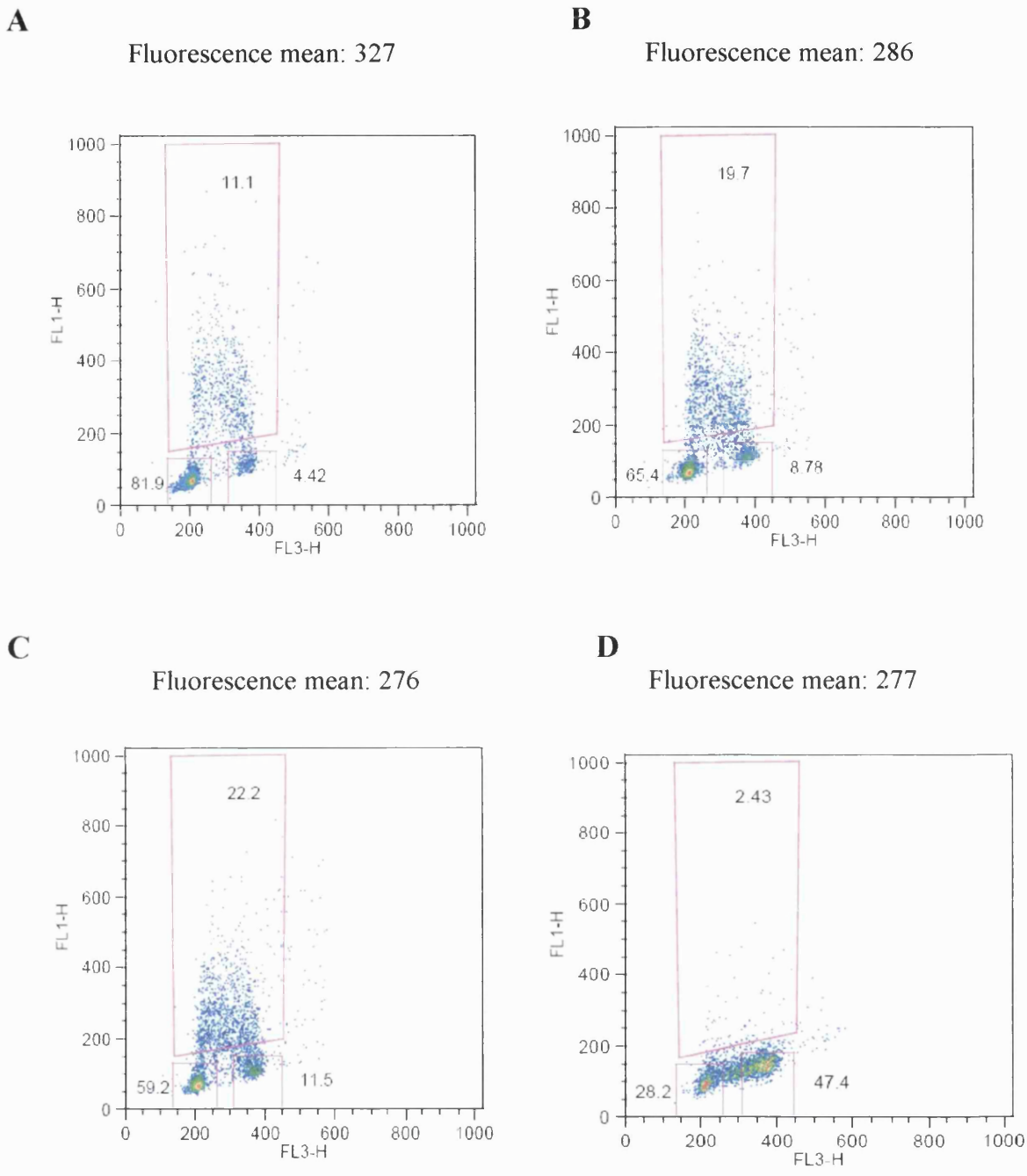

Figure 3.6. BrdU incorporation following a 30 minutes pulse treatment in A431 cells treated for one week. A. Vehicle control, B. 0.75μM cisplatin, C. 1.5μM BRACO19, D. 0.75μM cisplatin+1.5μM BRACO19.

3.3.4 Annexin V

One of the first indications of apoptosis is the loss of cell membrane integrity. During early apoptosis, there is translocation of the lipids of the inner membrane to the outer membrane, and as a consequence phospholipids such as phosphatidylserine are exposed to the extracellular environment. Annexin V is a protein that belongs to the annexin family. This protein specifically binds to phosphatidylserine whereas it does not have affinity for other phospholipids such as phosphatidylcholine and sphingomyeline. This property has been used to detect and quantify apoptotic cells by flow cytometry by conjugating fluorescein Alexa-647 to annexin V. Phosphatidylserine translocation also occurs during necrotic death, therefore, a vital dye such as DAPI is normally used in order to distinguish between necrotic and apoptotic cells. DAPI only binds to nucleic acids and after treatment with RNase only to DNA when plasma membrane integrity is completely lost, characteristic of necrotic cells.

Cells were treated with various concentrations of the single agents and combination of both compounds for one week. There was a notable change for all the treatments, single agents and the combinations after one week of treatment in the late apoptotic or necrotic cell population. Single agent cisplatin and BRACO19 produced similar effects at the concentrations used (Table 3.4). The combination of 0.5μM cisplatin+1μM BRACO19 also produced similar changes, whereas in the case of 0.75μM cisplatin+1.5μM BRACO19 the modification was greater. However, the cells that appear to stain for annexin V also stained for DAPI, indication that they had completely lost their membrane integrity, and they were either late apoptotic or necrotic cells (Figure 3.7) but rather necrotic for all treatments.

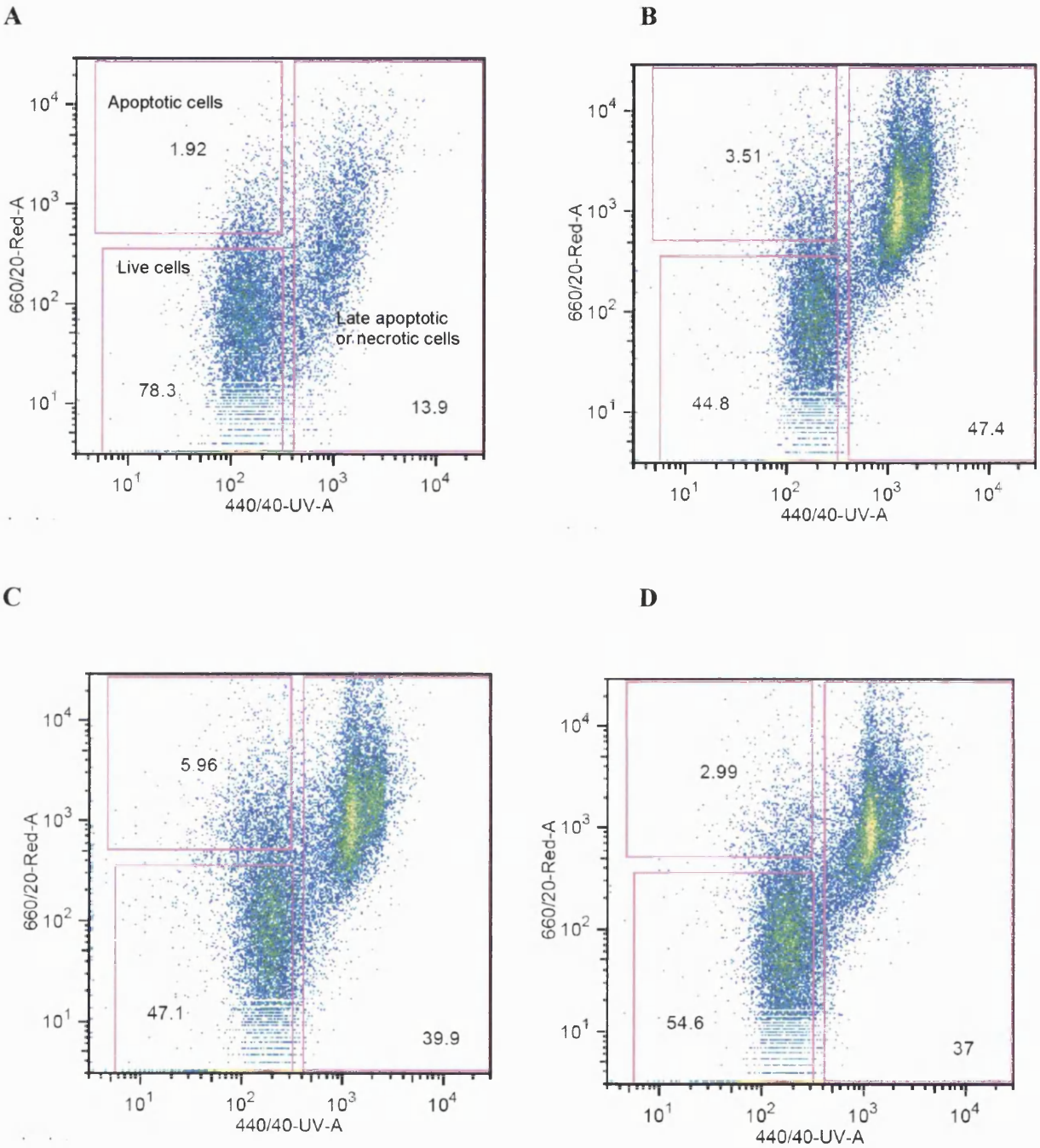
A
Apoptotic cells
1.92
Live cells
Late apoptotic
or necrotic cells
78.3
13.9
660/20-Red-A
440/40-UV-A
B
3.51
44.8
47.4
660/20-Red-A
440/40-UV-A
C
5.96
47.1
39.9
660/20-Red-A
440/40-UV-A
D
2.99
54.6
37
660/20-Red-A
440/40-UV-A

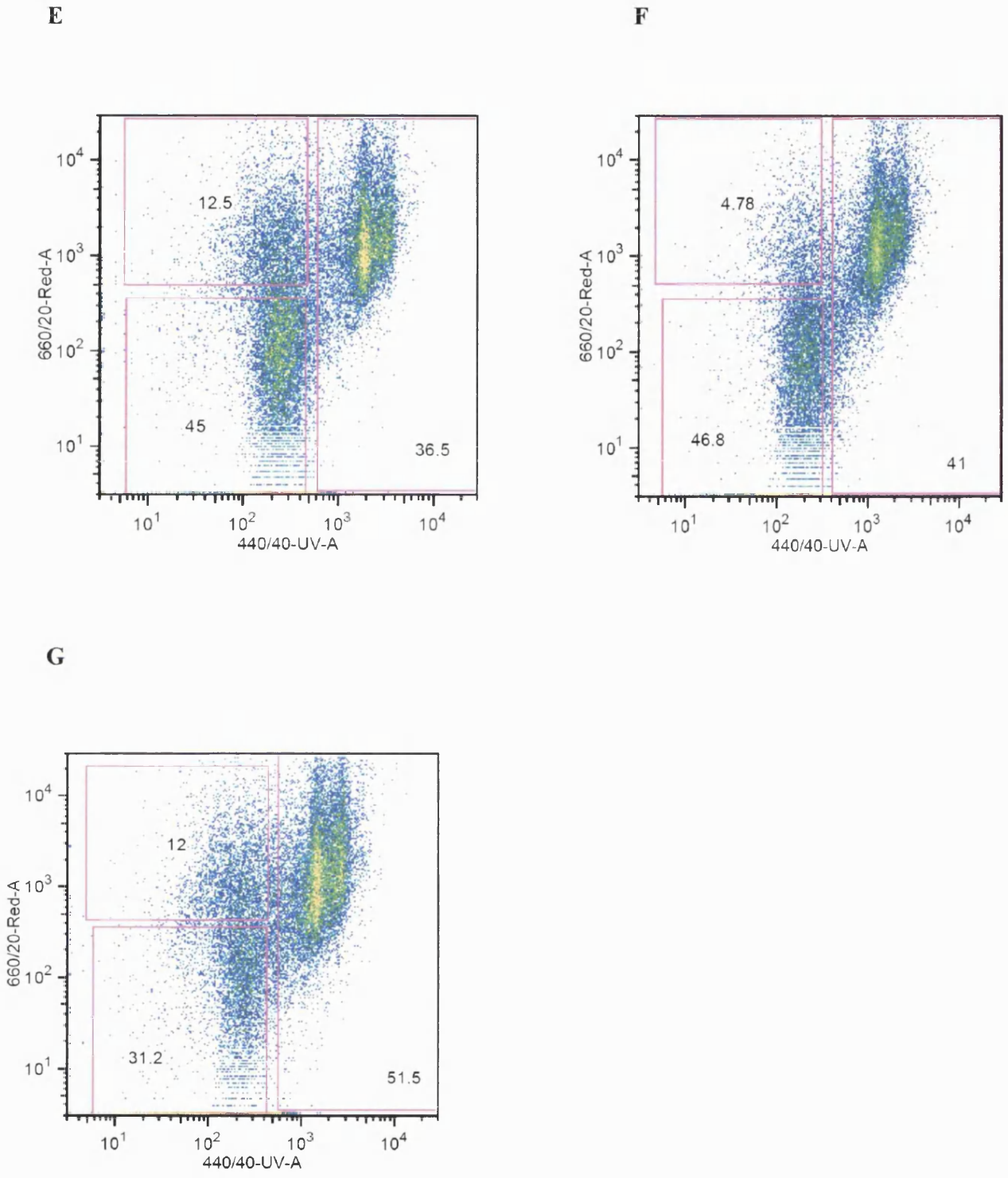

Figure 3.7. Annexin V changes detected after one week of treatment in A431 cells. A. Vehicle control, B. 0.5μM cisplatin, C. 0.75μM cisplatin, D. 1μM BRACO19. E. 1.5μM BRACO19, F. 0.5μM cisplatin+1μM BRACO19 19, G. 0.75μM cisplatin+1.5μM BRACO19.

Annexin V	Live cells	Apoptotic cells	Late apoptotic or necrotic cells
Vehicle control	78.3	1.92	13.9
0.5μM cisplatin	44.8	3.51	47.4
0.75μM cisplatin	47.1	5.96	39.9
1μM BRACO19	54.6	2.99	37
1.5μM BRACO19	45	12.5	36.5
0.5μM cisplatin+1μM BRACO19	46.8	4.78	41
0.75μM cisplatin+1.5μM BRACO19	31.2	12	51.5

Table 3.4. Summary of changes observed in annexin V after one week treatment in A431 cells (results are expressed as percentages).

3.3.5 Tetramethyl rhodamine ethyl ester (TMRE)

The loss of mitochondrial transmembrane potential is also one of the early events during apoptosis, and it is used as an early apoptosis marker. However, during necrosis there are also changes in the mitochondrial membrane *(Bhatia, 2004)*. The mithocondrial membrane potential ranges from 120 to 180mV and the intra-mitochondrial side is electronegative. Therefore, lipophilic cations accumulate in the mitochondrial matrix under physiological conditions, and there is rapid uptake and equilibration. Consequently, cationic lipophilic fluorochromes can be used to measure the mitochondrial membrane potential. One of these fluorochromes is Tetramethylrhodamine ethyl ester (TMRE). In early apoptosis, there is loss of these fluorochromes due to the loss of mitochondrial membrane integrity, and these changes can be detected by flow cytometry by decrease in fluorescence *(Galluzzi et al, 2007)*.

In the case of A431 cells treated for one week, a significant change was observed in the mitochondrial membrane potential for all single and combination treatments. Decrease in TMRE was detected by a decrease in fluorescence (Figure 3.8). However, a remarkable change in DAPI staining was also observed following all treatments. Therefore, the changes observed in mitochondrial membrane were not indicative of an apoptotic population; they were indicative of late apoptotic or necrotic cell population (Table 3.5). On the other hand, this is an *in vitro* study and therefore it is expected that cells undergo necrosis after apoptosis. Therefore, other studies had to be carried out to

determine the type of cell death. During apoptosis, there is mitochondrial membrane damage, release of cytochrome c and consequently activation of caspases. For that reason, the changes observed in TMRE could be interpreted as apoptosis if there were activation of caspases. As a consequence, the next step was to look at caspase 3 activation.

A

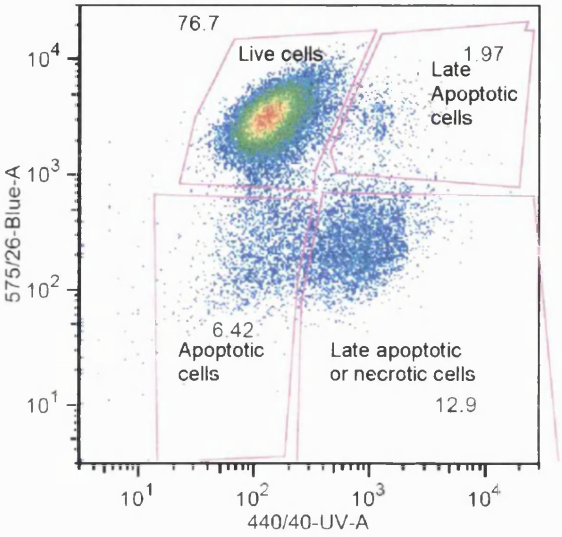

B

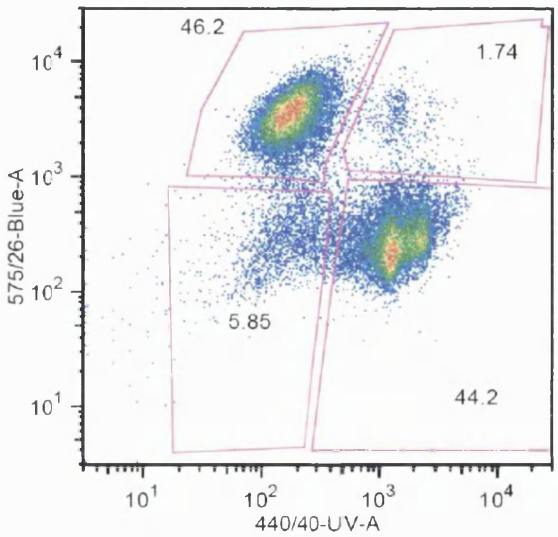

C

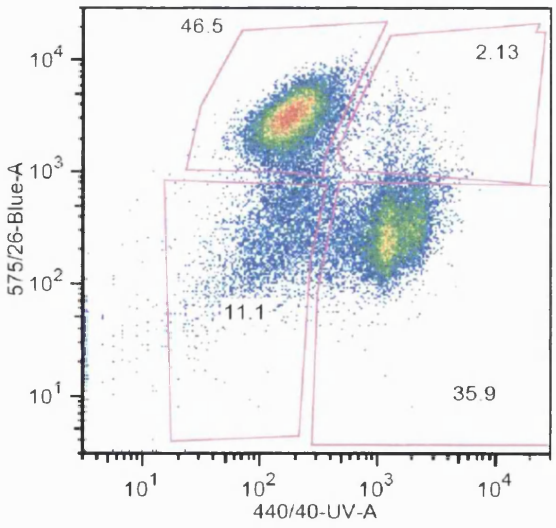

D

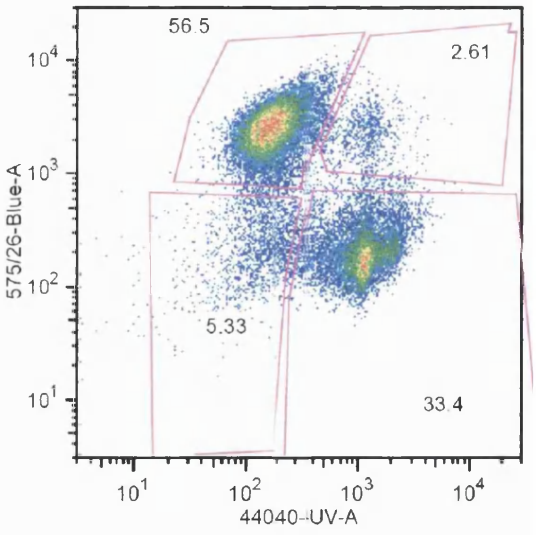

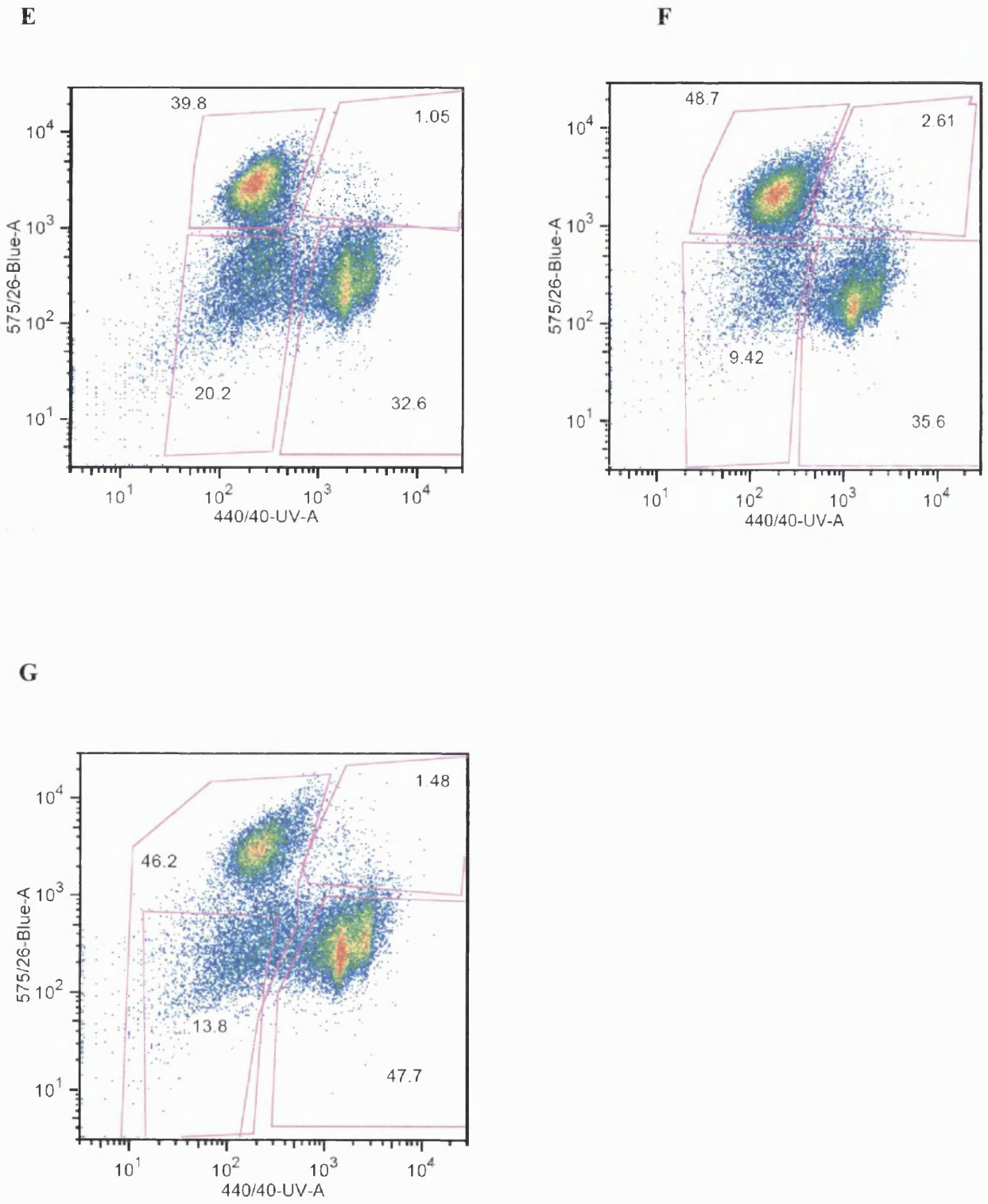

Figure 3.8. TMRE changes detected after one week of treatment in A431 cells. A. Vehicle control, B. 0.5μM cisplatin, C. 0.75μM cisplatin, D. 1μM BRACO19. E. 1.5μM BRACO19, F. 0.5μM cisplatin+1μM BRACO19, G. 0.75μM cisplatin+1.5μM BRACO19.

TMRE	Live cells	Apoptotic cells	Late apoptotic or necrotic cells
Vehicle control	76.7	6.42	14.82
0.5μM cisplatin	46.2	5.85	45.94
0.75μM cisplatin	46.5	11.1	38.03
1μM BRACO19	56.5	5.33	36.01
1.5μM BRACO19	39.8	20.2	33.65
0.5μM cisplatin+1μM BRACO19	48.7	9.42	38.21
0.75μM cisplatin+1.5μM BRACO19	46.2	13.8	49.18

Table 3.5. Summary of changes observed after one week treatment in A431 in TMRE (results are expressed as percentages).

3.3.6 Detection of caspase 3 activation.

Caspase 3 is a cysteine protease enzyme that belongs to the effector group of caspases. There is evidence that cellular changes that occur during apoptosis are promoted by effector caspases. These effector caspases produce their effects through three different mechanisms: first of all, they inactivate antiapoptotic proteins such as the inhibitor of caspase activated deoxyribonuclease (ICAD) or Bcl-2 proteins. Secondly, they produce damage to cell structures such as nuclear lamina, affecting chromatin organization and leading to chromatin condensation. And finally, they cleave proteins involved in DNA repair and DNA replication, affecting their function and therefore the homeostasis of the cells *(Thornberry and Lazebnik, 1998)*. Therefore, detection of caspase 3 activation is a definitive marker of apoptosis. Many different cytotoxic agents have been shown to induce activation of caspase 3 in different cell lines. As a positive control, the immortalized line of T lymphocyte jurkat cells were treated with 10μg/μl of staurosporine for 4 hours (Figure 3.9). Caspase 3 activation was investigated in A431 cells treated for one week (Table 3.6). 11% of the population of A431 cells treated with 0.75μM cisplatin showed caspase 3 activation whereas BRACO19 did not produce significant increase in caspase 3 activation. On the other hand, the combination showed very similar effect (8.88% increase in caspase 3 activation) compared to cisplatin treatment (Figure 3.10). Cisplatin single treatment did not produce a significant effect on cell growth (see chapter 2), whereas the combination treatment produce a massive effect on cell viability after one week treatment. Therefore, it seems that the main death mechanism following cisplatin treatment in A431 cells is apoptosis. However,

following combination treatment there is activation of caspase 3 probably due to the effect of cisplatin but there are also other events happening such as S-phase arrest (see 3.3) and necrosis (see 3.4 and 3.5).

	Caspase 3
Vehicle control	0.47
0.75μM cisplatin	11
1.5μM BRACO19	2.29
Combination	8.88

Table 3.6. Summary of changes observed after one week treatment in A431 in caspase 3 activation (results are expressed as percentages).

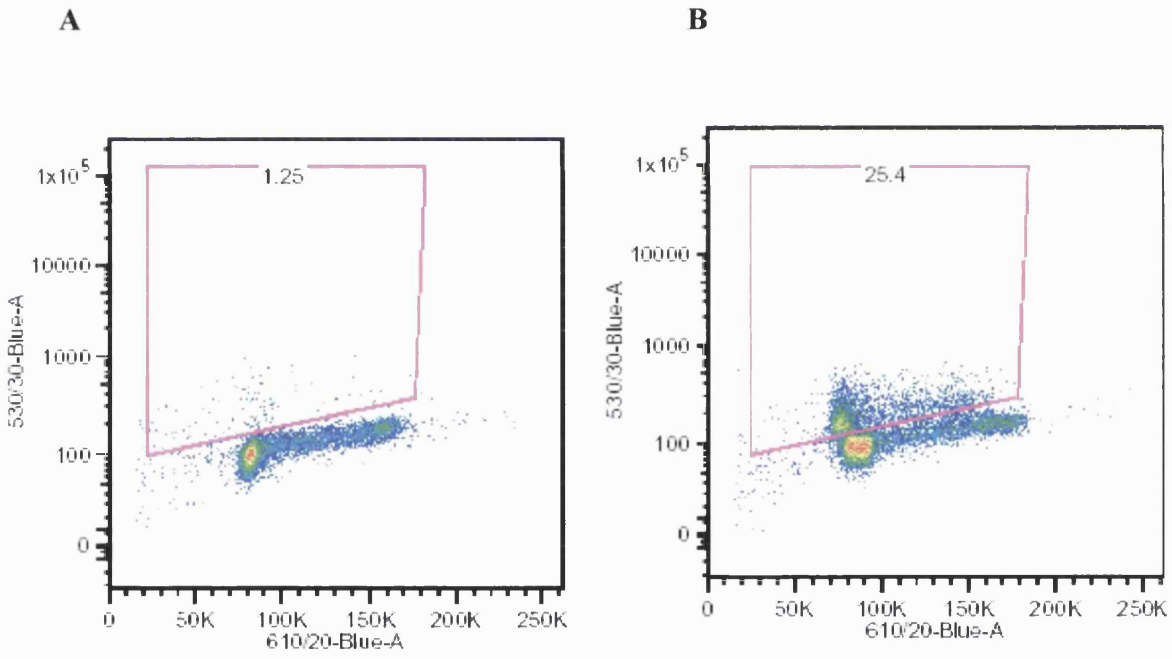

Figure 3.9. Caspase 3 activation observed in jurkat cells treated with 10μM stautosporine for 4 hours. A. Vehicle control, B. 10μM stautosporine.

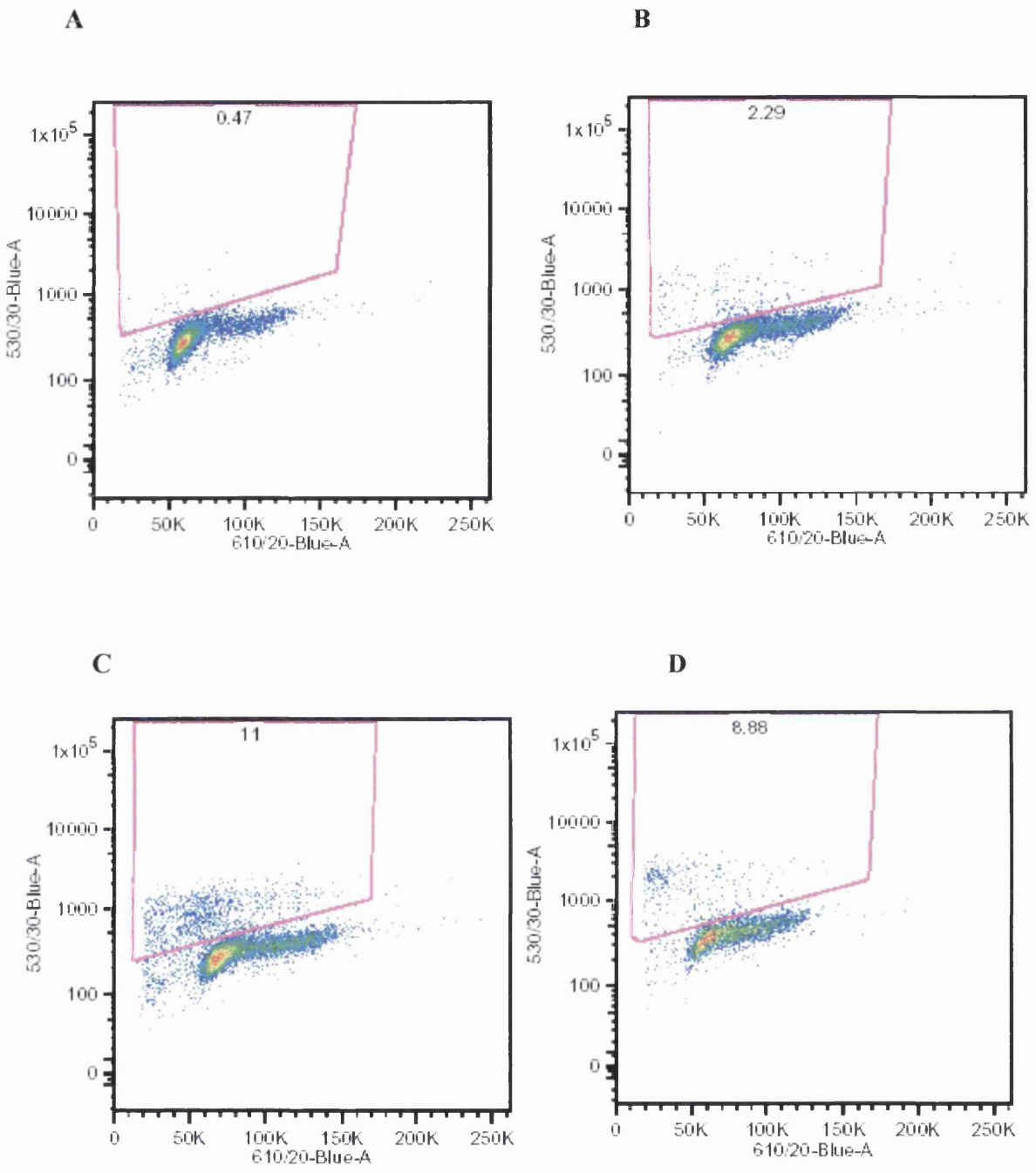

Figure 3.10. Detection of caspase 3 after one week of treatment in A431 cells. A. Vehicle control, B. 0.75μM cisplatin, C. 1.5μM BRACO19. D. 0.75μM cisplatin+1.5μM BRACO19

3.3.7 Detection of DNA strand breaks by TUNEL assay .

During late apoptosis there is activation of nucleases that produce internucleosomal DNA strand breaks; therefore, DNA laddering is another hallmark of apoptosis.

A431 cells were treated as before for one week. The kit provides a positive control, cells derived from a human lymphoma cell line in which DNA strand breaks have been induced and a negative control, untreated cells. Interestingly, BRACO19 did not produce DNA strand breaks even at 2μM concentration (Table 3.7). However, cisplatin induces a significant effect at 0.75μM and a more marked effect at 1μM concentration. On the other hand, the combination of 0.75μM cisplatin+1.5μM BRACO19 produces less DNA strand breaks than cisplatin alone (Figure 3.11). This is in agreement with what was found in caspase 3 activation. It seems that the main mechanism of cell death in the combination is not apoptosis.

TUNEL assay	**Apoptotic cells**
Vehicle control	1.41
0.75μM cisplatin	6.72
1μM cisplatin	12.4
1.5μM BRACO19	0.32
2μM BRACO19	0.73
0.75μM cisplatin+1.5μM BRACO19	4.19

Table 3.7. Percentage of apoptotic cells using TUNEL assay. Summary of changes observed after one week of treatment in A431.

A

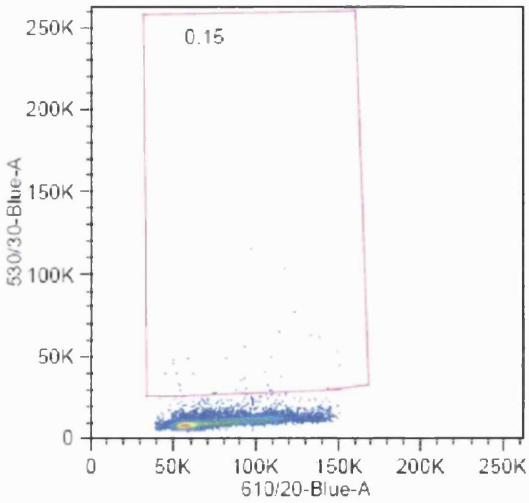
0.15
250K
200K
150K
100K
50K
0
530/30-Blue-A
0
50K
100K
150K
200K
250K
610/20-Blue-A

B

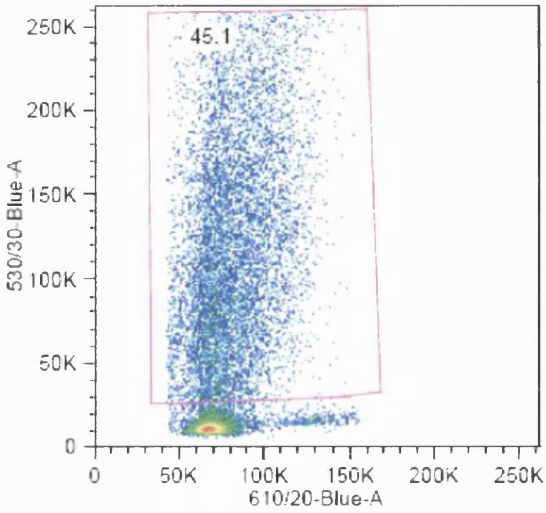
45.1
250K
200K
150K
100K
50K
0
530/30-Blue-A
0
50K
100K
150K
200K
250K
610/20-Blue-A

C

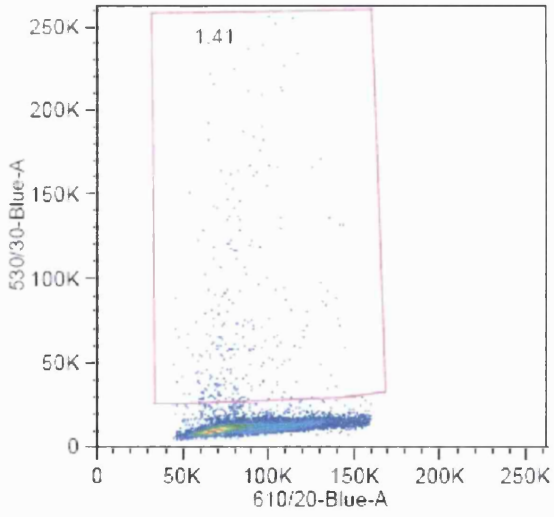
1.41
250K
200K
150K
100K
50K
0
530/30-Blue-A
0
50K
100K
150K
200K
250K
610/20-Blue-A

D

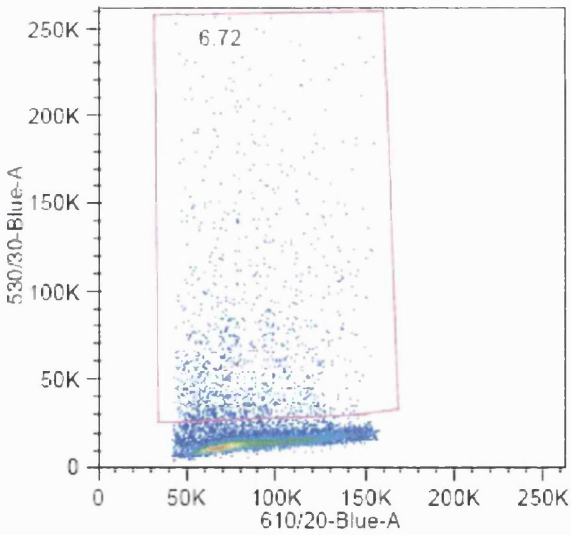
6.72
250K
200K
150K
100K
50K
0
530/30-Blue-A
0
50K
100K
150K
200K
250K
610/20-Blue-A

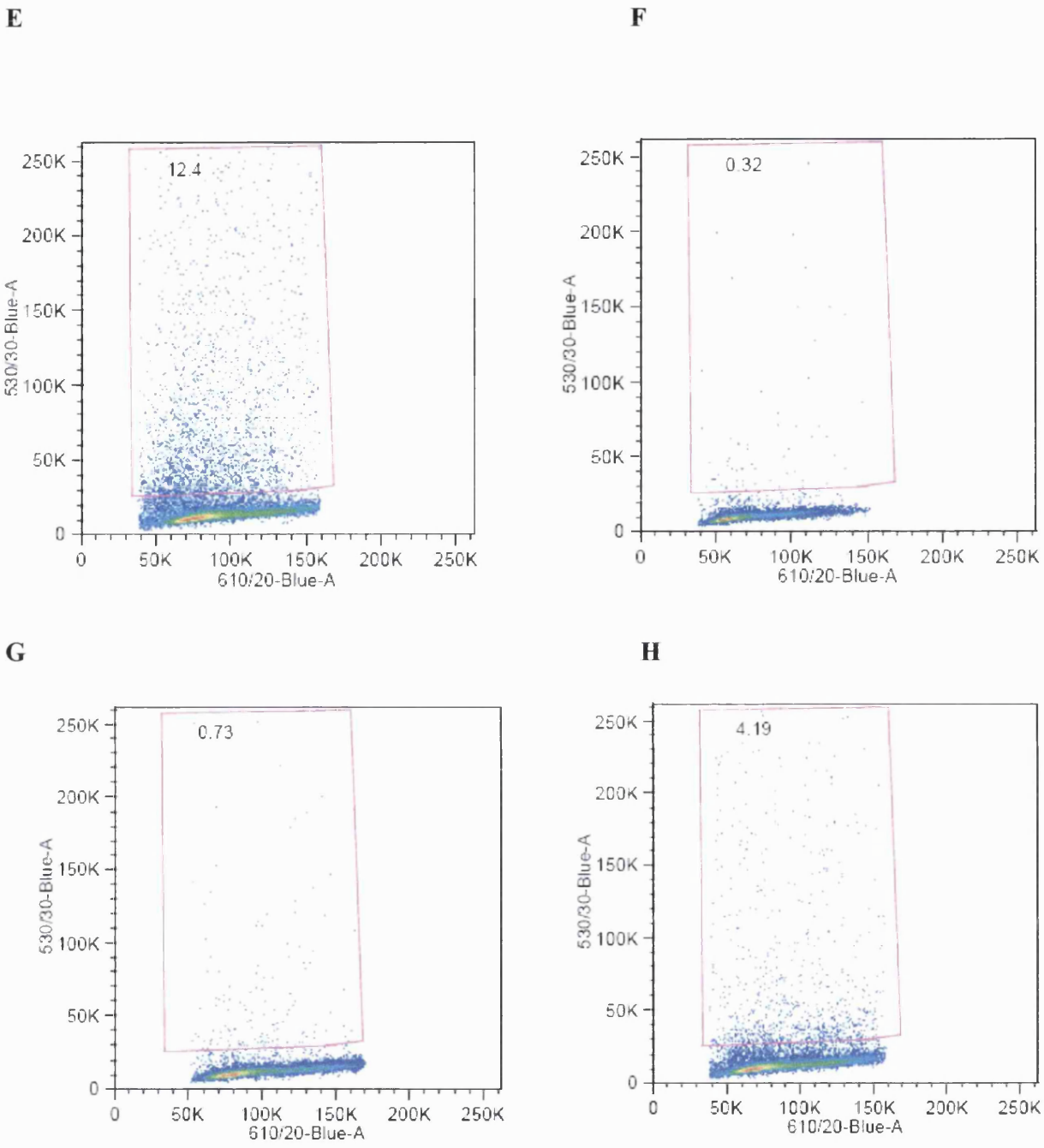

Figure 3.11. Detection of DNA strand breaks after one week of treatment in A431 cells using TUNEL assay. A. Negative control cells provided in APO-BRDU kit, B. Positive control cells provided in APO-BRDU kit, C. Vehicle control, D. 0.75μM cisplatin, E. 1μM cisplatin, F. 1.5μM BRACO19, G. 2μM BRACO19, H. 0.75μM cisplatin+1.5μM BRACO19.

3.3.8 Dye exclusion method using trypan blue.

Complete loss of cell membrane integrity is a hallmark of necrosis. A vital stain such as trypan blue can be used to distinguish necrotic cells. Viable cells exclude trypan blue whereas non-viable cells do not, therefore only non-viable will stain blue. One week experiment already showed a significant effect for the single agents (Figure 3.12).

Cisplatin treatment produced a considerable increase in percentage of non-viable cells. Previous caspase 3 detection studies showed that following this treatment there was activation of apoptotic pathways. On the other hand, this is an *in vitro* study and therefore it is expected that following apoptosis cells undergo necrosis.

Following BRACO19 treatment, an increase in percentage of non-viable cells was observed. Therefore, this is another sign that BRACO19 induces necrosis in A431 cells. BRACO19 at this concentration did not produce caspase 3 activation, but previous studies showed that there was an increase in the number of cells stained for annexin V and for DAPI, indication that they were necrotic. Furthermore, a decrease in TMRE accompanied by a remarkable change in DAPI staining was also detected. Consequently, the changes observed in mitochondrial membrane were not indicative of an apoptotic population, but of a late apoptotic or necrotic cell population.

The combination of cisplatin and BRACO19 produced a dramatic increase in the percentage of non-viable cells, 55% cell death. Although the combination showed very similar effects (8.88% increase in caspase 3 activation) compared to cisplatin treatment, due to the differences observed in cell growth studies (see chapter 2), it cannot be concluded that the main mechanism of cell death following combination treatment is apoptosis. As it has been previously discussed, caspase 3 activation following combination treatment must be due to the effect of cisplatin in A431 cells but there are also other events happening such as S-phase arrest and necrosis.

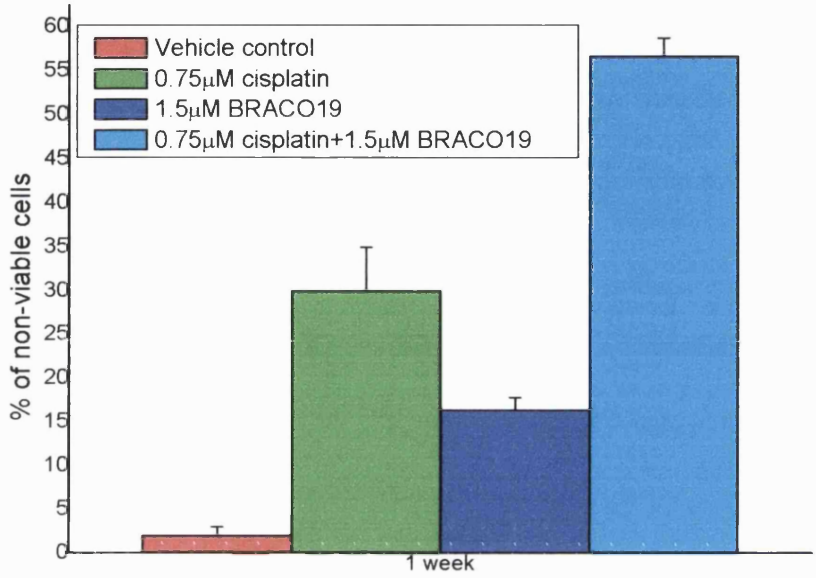

Figure 3.12. Percentage of non-viable A431 cells or cells stained with trypan blue after one week of treatment.

3.4. DISCUSSION

Diverse modes of cell death have been associated with different types of anticancer drugs *(Kim et al, 2006)*. Apoptosis is the most common, and generally induction of apoptosis has been linked with treatment response *(Morero et al, 2007)*. The apoptotic intrinsic pathway is related to DNA damaging agents, and is associated with mitochondrial disruption, cytochrome c release and activation of caspases *(Matapurkar and Lazebnik, 2006)*. The tumour suppressor p53 gene has been shown as the principal regulator of the apoptosis program *(Schuler and Green, 2005)*. Nevertheless, p53 independent apoptosis has been widely observed *(Oniscu et al, 2004; Irwin et al, 2003; Pennarun et al, 2005)*. On the other hand, necrosis is an unregulated mode of cell death that has been associated with greater cell damage *(Uezono et al, 2001; Michalakis et al, 2005)*. Alkylating agents such as the nitrogen mustard mechlorethamine hydrochloride and N-methyl-N′-nitro-N-nitrosoguanidine induced necrotic cell death in mouse embryofibroblast. The effects produced by these agents seem to be independent of p53 and Bax *(Zhong et al, 2004)*. Other agents, such as taxol, have been shown to induce necrosis at micromolar concentrations in Hela cancer cells after very short treatments (2 hours) *(Michalakis et al, 2005)*.

BRACO 19 is a G-quadruplex stabilising agent that has been shown to produce indirect telomerase inhibition, telomere shortening in several cell lines, and characteristics of a senescent phenotype *(Gowan et al, 2002; Burger et al, 2005; Incles et al, 2004)*. Although G-quadruplex stabilising agents produce indirect telomerase inhibition whether or not accompanied by telomere shortening, it is necessary to differentiate them from direct inhibitors that target the enzyme itself. The direct inhibitors produce a greater delayed effect on cell viability. As a consequence their effect is produced after telomerase inhibition, telomere shortening and eventual cell growth arrest and senescence like phenotype followed by apoptosis or necrosis depending on cell type. On the other hand G-quadruplex stabilising agents show much more rapid effects and also activity in telomerase-negative cancer cells *(Gowan et al, 2001; Pennarun et al, 2005; Kim et al, 2003)*. Therefore the mechanism of action of these ligands may be more related to the effect on the 3′-telomeric overhang and the proteins associated leading to the uncapping of the telomeres *(Riou, 2004)*. Nevertheless the mechanism of cell death

that cells undergo after DNA damage is more related to cell type and mutations in important cell cycle regulator genes that they contain.

Cisplatin reacts preferably with guanine bases in double stranded DNA *(Reedijk, 1999)*. Therefore G-regions in the genome such as telomeres are possible targets of cisplatin. DNA adducts induced by cisplatin produce a DNA damage response which is modulated by several signal transduction pathways, leading to cell cycle arrest, repair or death. Cisplatin induces two different modes of cell death: necrosis and apoptosis, and the types of cell death are concentration dependent. Very high concentrations of cisplatin (800μM) produce necrosis in mouse proximal tubular cells whereas a lower concentration (8μM) leads to apoptosis *(Reviewed in Wang and Lippard, 2005)*. However, it has been previously shown that cisplatin can also induce premature senescence in primary cultured fibroblast *(Zhao et al, 2004)* and this effect may be related to the effect of cisplatin on telomeres.

Telomere erosion has an important role in leading cells to the senescence phenotype. However, other types of external stress such as DNA damaging agents can induce senescence *(Ben-Porath and Weinberg, 2005)*. Senescence was investigated in the A431 epidermis carcinoma and in the MCF-7 breast cancer cell lines. In the MCF-7 cell line, there was induction of senescence for both agents and also for the combination. The onset of senescence was time and concentration dependent for both compounds. The combination showed a more marked effect. However, in the A431 cell line, there was no induction of senescence even at very high concentrations of BRACO19 or cisplatin. Senescence is regulated by two main genes p53 and Rb. In order to prevent senescence, it has been previously shown that these two genes have to be inactivated *(Smogorzewska and de Lange, 2002)*. However, the inactivation of p53 seems to be sufficient to avoid or delay the appearance of senescence in some cell lines *(Beauséjour et al, 2003)*. A431 cells have a p53 inactive protein mutated at codon 273 *(Lanzi et al, 1998)*, but they posses wild type Rb *(Ahmad et al, 1999)*. Remarkably, A431 cells with dominant-negative TERT do not undergo senescence after telomere shortening and chromosome breakage; instead the cells undergo apoptosis.

Consequently, different markers of apoptosis and necrosis were used to investigate the mechanism of death in A431 cells. In this study, it was demonstrated that one week treatment in the epidermis carcinoma cell line A431 did not produce a significant increase in the sub-G1 population, indicative of DNA strand breaks for the single agents or the combination treatments. However, this is not a definitive result; cells can go through apoptosis without an increase in sub-G1 population. The activation of endonucleases during apoptosis induces the appearance of DNA fragments which normally appear on the left of the G1 peak because they produce a fluorescence signal less intense than G1 population. However, if DNA loss occur during late S-phase, G2 or mitosis, it is possible that the DNA loss is not detected in the sub-G1 region.

Cell cycle studies showed that following treatment with cisplatin, BRACO19 and the combination there is an increase in the percentage of cells in S-phase compared to the vehicle control. These agents seem to produce an S-phase arrest. Furthermore, the study of cell viability using the BrdU incorporation showed a remarkable result after one week of treatment. When A431 cells were treated with 0.75μM cisplatin+1.5μM BRACO19, there was a notable decrease in BrdU incorporation, indicating that cells stopped proliferating. This result was not observed at the same concentrations for the single agents. This is in agreement with what was observed during the long-term viability studies (see chapter 2). Using sub-cytotoxic concentrations in combination a dramatic decrease in population doubling occurred after one week and complete cessation of growth after two weeks of treatment at concentrations that do not produce a significant effect when they were used as single agents. However, following BRACO19 and cisplatin treatment, there is an increase in the population of cells that are incorporating BrdU, and that could be interpreted as they are proliferating faster. On the other hand, if we consider the values of the fluorescence mean (Figure 3.6) that indicate how much BrdU is incorporated by the cells, we cannot conclude that after treatment with these agents there is an increase in cell proliferation. There is a decrease in fluorescence mean for all the treatments including the combination; therefore, cells treated with BRACO19 or cisplatin have incorporated less BrdU than untreated cells. An explanation could be that treated cells are incorporating BrdU slower than the untreated cells as a consequence of the DNA damage produced by these agents.

Other markers of early apoptosis such as annexin V and TMRE were studied. The staining with annexin V showed that the changes observed in the apoptotic population were not significant. However, there was a notable change for all the treatments, single agents and combinations in the late apoptotic or necrotic cell population after one week of treatment. A comparison between the different treatments, cisplatin and BRACO19 as single agents produces similar effects at the concentrations used. The combination of 0.5μM cisplatin+1μM BRACO19 also exert similar changes, whereas in the case of 0.75μM cisplatin+1.5μM BRACO19 the effect was greater. The changes observed in TMRE demonstrated that there was a change in mitochondrial potential membrane as a consequence of membrane disruption that could be indicative of apoptosis through the mitochondrial pathway. Nevertheless, changes in mitochondrial membrane are also indicative of necrosis *(Bhatia, 2004)*. On the other hand, most of the cell population that had lost TMRE was also stained with DAPI, suggesting that cells were in a late apoptotic phase or they were necrotic. During apoptosis, as a consequence of mitochondrial membrane disruption, cytochrome c is released and caspase cascade is activated. However, caspase 3 activation was only found in A431 cells treated with cisplatin. Caspase 3 activation has been earlier associated with cisplatin-induced apoptosis in A431 cells *(Mese et al, 2000)*. BRACO19 did not induce caspase 3 activation. Furthermore, the combination of both agents produced less caspase 3 activation than cisplatin. Interestingly, BRACO19 did not produce DNA strand breaks, and cisplatin induces a significant effect on DNA strand breaks already at 0.75μM and more markedly effect at 1μM concentration. In agreement with the result of caspase 3 activation, the combination of 0.75μM cisplatin+1.5μM BRACO19 produces less DNA strand breaks than cisplatin alone. It seems that the main mechanism of cell death for the combination is not apoptosis.

Moreover, necrotic cell death was studied using trypan blue staining. Complete loss of cell membrane integrity is a hallmark of necrosis. Both cisplatin and BRACO19 treatments produced a significant effect after one week. Although, A431 cells treated with cisplatin died through apoptosis, this is an *in vitro* experiment, therefore it is expected that cells in culture following apoptosis undergo necrosis. The combination of cisplatin and BRACO19 produced a dramatic increase in percentage of non-viable cells.

Consequently, it seems that the main mechanism of cell death for the combination is necrosis.

For these studies, I decided to use one week time point; therefore, I could compare these results with the cell growth studies (see chapter 2). However, because I did not study the mechanism after shorter periods of time, there is the limitation of not detecting early apoptosis occurring after treatment with cisplatin. As it has been mentioned above, this is an *in vitro* study and therefore it is expected that cells underwent apoptosis would become necrotic in culture. That is the reason we only detect late apoptosis or necrosis after treatment with cisplatin.

In conclusion, it was demonstrated in this study that A431 cells treated with cisplatin produced a very rapid apoptotic response which is caspase 3-dependent, whereas BRACO19 treatment produced necrotic cell death. The combination of both compounds produced the same type of effect as BRACO19 but it also led to dramatic decrease in cell proliferation with the onset of necrotic cell death.

Necrosis is an unregulated form of cell death that is completely independent of important apoptotic regulator genes such as p53, p73, p21, Bcl2 or Bax. However, this type of cell death has been related to increase in DNA repair enzymes such as PARP1. In the next chapter we investigated the most relevant genes and proteins involved in apoptosis (p53, p21, p73) and also PARP1 gene expression in order to elucidate the cell death pathway for the single agents and the combination.

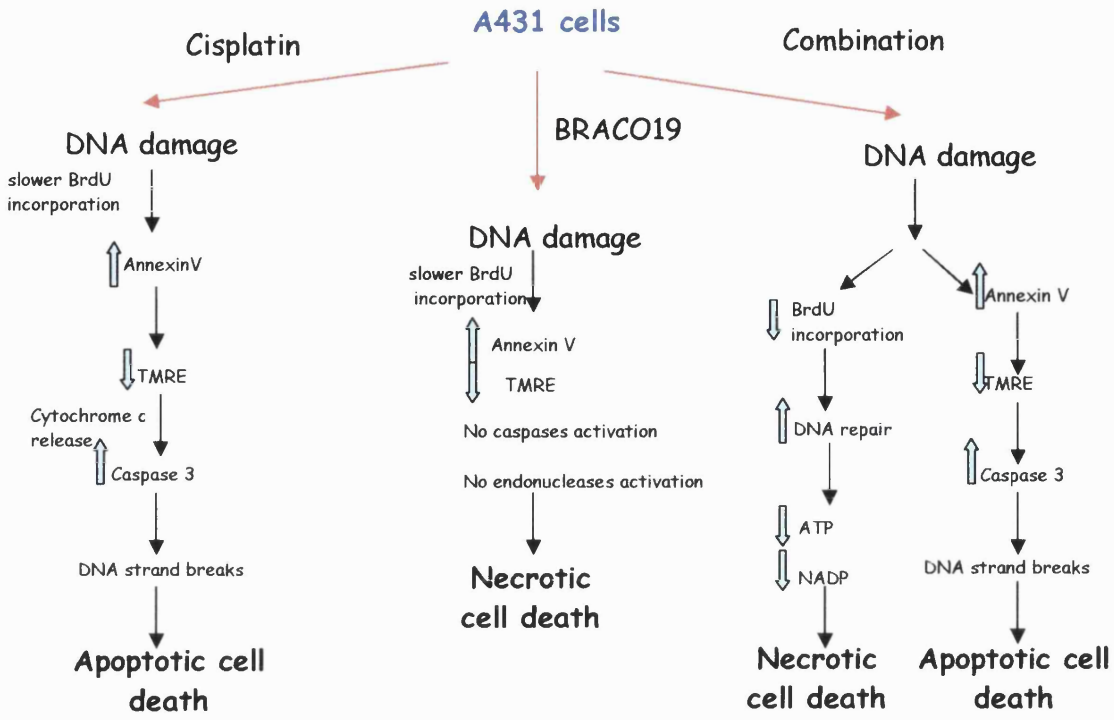

Figure 3.13 Scheme of possible mechanism of cell death in A431cells following treatment with cisplatin, BRACO19 or the combination of both compounds (see text for details).

Chapter 4- EFFECTS OF BRACO19 AND CISPLATIN ON GENES AND PROTEINS INVOLVED IN APOPTOSIS

4.1. INTRODUCTION

In the previous chapter the mode of cell death was investigated, and the conclusions were that A431 cells treated with cisplatin produced a very rapid apoptotic response which is caspase 3-dependent, whereas BRACO19 treatment produced necrotic cell death. The combination of both compounds produced the same type of effect as BRACO19 but it also led to a dramatic decrease in cell proliferation. The next step was to investigate important genes and proteins involved in apoptosis such as p53 and p21 to conclude if they are involved in cisplatin-induced apoptotic cell death, and also to look at changes in PARP1 which is involved in necrosis.

4.1.1 p53 tumour suppressor signalling.

After DNA damage, cells can undergo through two different pathways, cell cycle arrest or apoptosis *(Pietenpol and Stewart, 2002),* depending on the grade of damage, in order to protect genome integrity. First, the cell is arrested to repair the damage, and if the damage cannot be repaired properly the cell will undergo programmed cell death or apoptosis. The principal regulator of this process is the p53 tumour suppressor protein *(Vogiatzi et al, 2006).* Following DNA damage p53 is phosphorylated by one of the members of the phosphatidylinositol-3 kinase-like family (PI-3K) including DNA-PK, Ataxia telangiectasia mutated (ATM) or Ataxia telangiectasia related protein (ATR) *(Woo et al, 1998; Helt et al, 2005).* Phosphorylation of p53 induces transcription of the cyclin inhibitor p21 and this subsequently blocks the cell cycle in G1 in order to allow the repair of DNA through the DNA repair machinery. p21 upregulation produces inhibition of several cyclin-CDK complexes causing hypophosphorylation of the retinoblastoma protein (Rb). Rb needs to be phosphorylated in order to allow the progression from G1 to S-phase. Phosphorylated Rb is associated with E2F, but when it is hyperphosphorylated by specific cyclin-CDK kinases, it dissociates and E2F acts as a transcription factor allowing the transcription of several genes necessary for the progression of the cell cycle through the S-phase. However, when the cyclin-CDK kinases are inhibited Rb cannot be phosphorylated and E2F does not dissociate from Rb and subsequently its action as a transcription factor is lost. Consequently cells are arrested in G1 (Figure 4.1). Once DNA damage is repaired, the cell can enter the cell cycle, however, if the damage persists then p53 activates the intrinsic apoptotic

pathway. The intrinsic or cytotoxic agent related pathway is activated by p53 through the transrepression of the antiapoptotic protein Bcl-2 and the transcription of the proapoptotic protein Bcl-2 associated X (Bax). These factors induce the disruption of the mitochondrial membrane with the subsequent release of cytochrome c and activation of several caspases (Figure 4.1) *(Kim et al, 2005; Shi, 2006)*. Furthermore, p53 controls its own abundance through the induction of MDM2 *(Haupt et al, 1997)*. p53 is also able to induce apoptosis by a transcription independent pathway *(Schuler and Green, 2005)*. The importance of the p53 pathway in cell cycle and DNA damage repair is realised from several observations which indicate that more than 50% of cancers have p53 gene mutations, and these mutations could allow the cells to bypass this checkpoint allowing them to bypass cell death *(Vogelstein et al, 2000)*. Two homologues of p53, p63 and p73 have been discovered *(Kaghad et al, 1997)*. These proteins share similar characteristics with p53. They have DNA binding and transactivation domains and they are able to transactivate many p53 targets and therefore they are also able to induce cell cycle arrest or apoptosis. Consequently, since the discovery of these analogues, some of the p53 independent pathways that have been previously observed could be explained. It has been earlier demonstrated that cisplatin is able to upregulate p73 protein in a mismatch-repair-defective human cell line HCT116 combined with the induction of p53. The induction of p73 is also correlated with the activation of c-Abl and the activation of the apoptosis cascade *(Gong et al, 1999)*. The tyrosine kinase c-Abl is activated by DNA damaging agents, leading to cell cycle arrest or apoptosis. It was previously shown that p73 is a substrate of c-Abl. Cells that are defective in kinase c-Abl due to mutation were not able to induce apoptosis after transfection of p73, whereas wild type c-Abl cells underwent apoptosis when p73 was introduced, concluding that upregulation of p73 alone can not induce apoptosis *(Agami et al, 1999)*. Primary murine colonocytes which were p53 mutant transactivated p73 after cisplatin treatment followed by apoptotic response. This demonstrated that cisplatin induced-apoptosis in this cell line is independent of p53 and involves the p73 pathway *(Oniscu et al, 2004)*. p73 is activated by different DNA damaging agents such as campothecin, etoposide, doxorubicin and cisplatin *(Irwin et al, 2003)*. However, its upregulation is not consistent and may be dependent on cell type *(Vikhanskaya et al, 2000)*. Apparently, p73 is able to promote apoptosis by different mechanisms; p73 produces upregulation of Scotin which induces apoptosis by activating caspase cascade. Secondly, p73 is also able to activate

the mitochondrial apoptosis pathway but via PUMA and Bax. p73 transactivate PUMA which has an effect on Bax conformation which changes it to its active state, leading to the disruption of the mitochondrial membrane and formation of the apoptosome. And finally there is evidence that suggests that p73 is also capable of inducing apoptosis through the death receptor pathway *(Ramadan et al, 2005)*, and thus able to induce apoptosis in a p53-independent manner. However, results found in cell lines which are p53 mutated demonstrate that the interaction of p53 that have particular mutations with p73, could lead to the inactivation of such protein. In fact introduction of certain p53 mutations in p53 wild-type cells lead to the inactivation of p73 and the appearance of chemoresistance *(Irwin et al, 2003)*. Sensitivity to chemotherapeutic agents has been correlated with p53 status. p53 mutations have been correlated in many occasions with the appearance of resistance; however these findings are not definitive as this is not always the case *(Reles et al, 2001)*.

4.1.2 The p53 independent pathway.

The upregulation of the cyclin kinase inhibitor p21 that lead to cell cycle arrest, can be through one of the members of the p53 family or through a p53-independent pathway *(Burkhart et al, 1999; Spurgers et al, 2006)*. The serine-threonine kinase Chk2 is able to induce upregulation of p21 in p53 wild type and p53 mutant cells. After DNA damage, ATM and ATR kinases phosphorylate different proteins including Chk2, and this phosphorylation induces its activation *(Aliouat-Denis et al, 2005)*. Consequently, Chk2 can produce activation of p21 and cell cycle arrest in a p53-independent manner. Cell cycle arrest can also occur in both p53- and p21-independent pathways involving p16. p16 acts as an inhibitor of specific cyclin dependent kinases leading to hypophosphorylation of Rb and consequently cell growth arrest *(Rheinwald et al, 2002)*.

Existence of a p53-independent apoptotic pathway has been well established in recent years. Different anticancer drugs such as cisplatin, taxol, campothecin are able to induce apoptosis in a p53-independent way *(McDonald and Brown, 1998; Sugimura et al, 2004; Mese et al, 2000)*. As already mentioned, p53 is able to activate the mitochondrial apoptotic cascade leading to the activation of effectors caspases. However, the activation of caspases has been previously demonstrated in p53 inactive mutant cells. As an example, A431 cells used in this study possess an inactive p53 protein *(Lanzi et*

al, 1998); nevertheless they die through apoptosis after treatment with cisplatin. This apoptosis mechanism is caspase 3-dependent *(Mese et al, 2000)*. Cisplatin also produces apoptotic cell death in a transgenic mouse tumour model in which p53 has been inactivated. Using the same model other anticancer drugs such as paclitaxel or doxorubicin fail to induce apoptosis *(Petit et al, 2003)*. On the other hand, it has been earlier demonstrated that induction of DNA damage can produce necrotic cell death in p53 deficient cells. This necrotic death is completely independent of p53, Bax, Bak and caspases, and is dependent of polyADP ribosylase (PARP) activation *(Zhong et al, 2004)*. Induction of PARP as a consequence of DNA damage has been associated with necrotic cell death *(Ha and Snyder, 1999)*. Activation of PARP produces depletion of intracellular β-nicotinamide adenine dinucleotide (NADP) and adenosine 5′triphosphate (ATP) and therefore induces necrosis (Figure 4.1).

p53 mutations have been correlated in many occasions with the appearance of resistance; however there is a controversy about the effect of p53 mutations in sensitivity towards chemotherapeutic agents. Although it has been widely published that p53 mutations confer resistance towards DNA damaging agents *(Reles et al, 2001; Xue et al, 2007)*, there are an increasing number of publications showing that this correlation is not always true. Agents such as the antifolate anticancer drugs methotrexate or lometrexol showed similar effects in several p53 wild-type cell lines compared to their counterpart p53 mutated *(Lu et al, 2001)*. A study using a model of normal human fibroblast cells in which p53 was inactivated by expression of human papilloma virus showed that cisplatin and carboplatin have enhanced sensitivity toward this cell line. Furthermore, model using mouse embryonal fibroblast with p53 mutant confirmed increased sensitivity towards cisplatin compared to mouse fibroblast with p53 wild-type *(Hawkins et al, 1996)*. In addition apoptotic response has also been correlated with tumour response, however, other types of cell death such as necrosis or autophagy can be observed *(Kim et al, 2006)*.

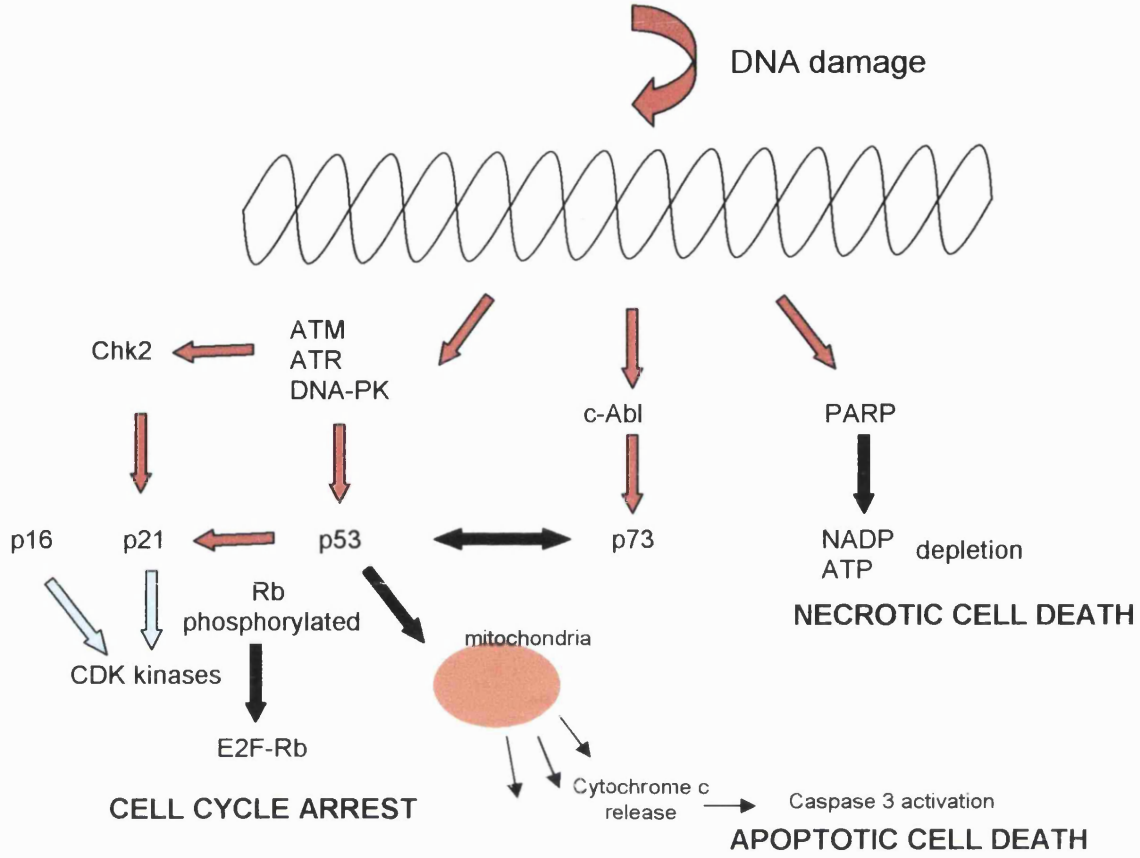

Figure 4.1. Scheme showing the different possible pathways a cell may undergo after DNA damage.

4.2. METHODS

4.2.1 Reverse Transcriptase Polymerase Chain Reaction (RT-PCR).

RT-PCR was carried out to analyse expression of various genes in order to determine the effect of these compounds at transcriptional level. Cells were treated in culture for one week as described previously (see chapter 2). Pellets were kept at -80^{0}C until ready to extract RNA. RNA was extracted from cell pellets using the QIAGEN RNeasy Minikit following manufacter's instructions. The RNA concentration was determined by absorbance at 260nm using a GeneQuant (Pharmacy Biotech, USA). Extracted RNA was kept at -20^{0}C until required. 600ng of total RNA was reverse transcribed using c-DNA cycle kit (Invitrogen, UK) as described below in a 2 step reaction.

1. RNA primer preparation

	For one reaction
Random hexamer	1µl
RNA	600ng
10mM dNTP mix	2µl
DEPC H_2O	up to 12µl

RNA and primer were denatured at 65^{0}C for 5 minutes. Following this the samples were kept in ice to cool down before adding c-DNA master mix, prepared as follows:

2. c-DNA synthesis

	For one reaction
5X c-DNA synthesis buffer	4µl
0.1M DTT	1µl
Rnase OUT	1µl
DEPC H_2O	1µl
AMV-RT (15U/µl)	1µl

8µl of the above mix was added to each tube while on ice. Samples were heated to 50^0C for 1 hour followed by 85^0C for 5 minutes. c-DNA was used for the polymerase chain reaction (PCR) using the conditions described in Table 4.1.

PCR reactions were carried out under the following conditions, using primers appropriate for the gene of interest. All primers were purchased from ATD Bio, UK.

	(1X)
DEPC H_2O	35.75µl
10X Reaction buffer IV	5µl
$MgCl_2$ (50mM)	2µl
dNTP mix (10mM)	2µl
Primer (10µM) Forward	2µl
Primer (10µM) Reverse	2µl
c-DNA	1µl
Taq polymerase (AB gene, UK)	0.25µl

RT-PCR	Primers	Conditions	Product size
GAPDH (Incles et al, 2004)	F' GGC AGT GAT GGC ATG GAC TG R' CGG GAA GCT TGT GAT CAA TGG	94^0 C 3 min 94^0 C 1 min 55^0 C 1 min 35X 72^0 C 2.5 min 72^0 C 10 min	358bp
P21	F'CTTCGACTTTGTCACCGAGACACCA R'GTTTTCGACCCTGAGAGTCTGCAG	94^0 C 3 min 94^0 C 1min 55^0 C 1 min 35X 72^0 C 1min 72^0 C 5min	275bp
P53	F' CCTTCCCAGAAAACCTACCA R' TCATABBBCACCACCACACT	94^0 C 3 min 94^0 C 1min 55^0 C 1 min 35X 72^0 C 1min 72^0 C 5min	371bp
p73 (Kartasheva et al, 2002)	F' TGG AAC CAG ACA GCA CCT ACT TCG R' TGC TGG AAA GTG ACC TCA AAG TGG	94^0 C 5min 94^0 C 30 sec 63^0 C 1 min 40X 72^0 C 1 min 72^0 C 5min	335bp
PARP1 (Tempera et al, 2005)	F' GCAGAGTATGCCAAGTCCAACAG R' ATCCACCTCATCGCCTTTTC	94^0 C 3 min 94^0 C 30 sec 59^0 C 30 sec 30X 72^0 C 30 sec 72^0 C 5 min	299bp

Table 4. 1. PCR conditions for the different primers used.

All gene products were run in 1.5% agarose gel in 1X Tris-Borate EDTA (TBE) buffer (Sigma, UK) at 80V for 90 minutes. Gels were prepared as follows: 1.5g of agarose was dissolved in 100mls of TBE by heating until boiling. When temperature was about 50^{0}C, ethidium bromide (Sigma, UK) was added until 0.5mg/ml final concentration. Gels were visualised using Gene Snap (Syngene, UK) and quantification was carried out using Gene Tools software (Syngene, UK). The 100 base pair DNA ladder was used as a molecular weight marker (Biolabs, UK). All gene products were normalised against GAPDH as a housekeeping gene.

4.2.1 Western blotting protocol.

$1x10^5$ cells were treated with appropriate concentrations of drug as before (see chapter 2), for 1 week. At the end of the week, pellets were collected and resuspended in cold PBS in order to wash, centrifuged at 8000rpm for 3 minutes and finally PBS was aspirated. Pellets were resuspended in 100µl of cold lysis buffer (this amount can vary depending on the number of cells in the pellet), and incubated on ice for 30 minutes. Pellets were then centrifuged at 14000rpm for 15 minutes at 4^0C, and the supernatants were transferred to clean eppendorfs in aliquots of 10µl and kept at -80^0C until use. Lysis buffer was prepared as below:

	For 10 ml	Stock solution
50mM HEPES	500µl	1M
25mM NaCl	500µl	5M
0.1% NP40/IGEPAL CA-630	100µl	10%

All stock solutions were kept at 4^0C. One tablet of protease inhibitor cocktail was added to the above just before use.

Protein concentration was determined using the Bradford assay, and 50µg of protein was used to detect p53 and α-actin, and 75µg of protein was used to detect p21 protein expression. The volume required for loading the appropriate concentration of protein was calculated and the same amount of sample buffer was added, mixed and heated at 95^0C for 5 minutes before loading. The sample buffer was prepared as below:

1 M Tris-base pH 6.8	100µl
50% glycerol	300µl
20% SDS	200µl
β-mercaptoethanol	20µl
1% bromophenol blue	15µl

Samples were run in a 13% SDS-PAGE which was prepared as described below:

	Separating	Stacking
40% acrylamide	3.475ml	750µl
H_2O	5.125ml	4.25ml
3M Tris pH=8.8	1.25ml	
0.5M Tris pH=6.8		2ml
10% SDS	100µ	80µl
10% APS	75µl	200µl
TEMED	10µ	6µl

The samples were run at 150V for 75 minutes using 1X NuPAGE MES SDS running buffer (Invitrogen, UK). A rainbow marker (Amersham Biosciences) was used to ensure transfer and a protein molecular weight standard for western blots (MagicMark XP protein standard) (Invitrogen, UK) to determine the molecular weight of the proteins. 10µl of each marker was loaded per lane.

At the end of 75 minutes the gels were carefully removed from the glass plates and soaked in transfer buffer for 5 minutes. A gel-membrane sandwich with filter pads and sponges were prepared and the proteins transferred at 50V for 60 minutes, in cold transfer buffer with a cold pad.

The components of the transfer buffer are described below:

10X TG	100ml
Methanol	200ml
dH_2O	700ml

10X TG

0.25M Tris-base

1.9M Glycine

Following transfer, membrane was blocked for 2 hours at room temperature in blocking solution (0.1% tween and 5% low fat dried milk in PBS). Later the membrane was incubated with the appropriate dilution of primary antibody in blocking buffer overnight at 4^0C. The next day, the membrane was washed 3 times in PBS for more than 10 minutes. Subsequently, the membrane was incubated with the secondary antibody diluted in blocking buffer for 1 hour at room temperature and washed as previously. Finally, the membrane was visualized using a Horseradish Peroxidase Luminiscent Visualization System (HRPL) kit (National Diagnostics, USA) following manufacture's instructions.

The dilution factors and details of primary and secondary antibodies are described in Tables 4.2 and 4.3.

Protein	Molecular weight (kDa)	Dilution 1st antibody	Dilution 2nd antibody
α- actin	42	1/500 overnight at 4^0 C	1/1000 1h at room temperature
P21	21	1/500 overnight at 4^0 C	1/1000 1h at room temperature
P53	53	1/200 overnight at 4^0 C	1/1000 1h at room temperature

4. 2. Dilution factors of primary and secondary antibodies.

Antibody (Ab)	Description
α-actin	Mouse monoclonal anti-α-actin (Abcam, UK)
P21	Mouse monoclonal anti-p21 (Invitrogen, UK)
P53	Mouse monoclonal anti-p53 (Abcam, UK)
Secondary Ab	Peroxidase-Goat anti-mouse IgG (H+L) (Invitrogen, UK)

4. 3. Details of primary and secondary antibodies.

4.3. RESULTS

A431 cells treated for one week showed no significant difference in p53 gene expression normalized against GAPDH as a housekeeping gene for either of the treatments used in this study (Figure 4. 2). The p53 downstream gene cyclin kinase inhibitor p21 also did not show a significant change (Figure 4. 2) after one week of treatment. This result correlates with the non-observance of senescence with β-galactosidase activity (see chapter 2). Subsequently the p53 family member p73 was also studied in order to investigate a possible p53-independent pathway. However, there was no significant change in p73 expression in any of the treatments studied, except with 1.5μM BRACO19 where 2-fold down-regulation was observed (Figure 4. 3). Following this gene expression study, a protein expression study was carried out using Western blotting in order to investigate if the treatments had any effect on the translation of these cell cycle proteins. p53 and p21 protein expressions were investigated using one week treatment samples. α-actin was used as a housekeeping protein to normalize expression levels. No change in protein expression of p21 or p53 was observed for any of the treatments used (Figure 4. 5). The result in p53 protein expression was expected due to A431 cells possessing a p53 inactive protein mutated at codon 273 *(Lanzi et al, 1998)*. However, A431 cells have a p21 wild-type protein *(Huang et al, 2006)*. The cyclin kinase inhibitor p21 can be up-regulated through one of the members of the p53 family or through a p53-independent pathway *(Burkhart et al, 1999; Spurgers et al, 2006)*. The Chk2 kinase is able to induce up-regulation of p21 in p53 wild-type and p53 mutant cells. Consequently, it was also necessary to investigate p21. Concluding, the effect of BRACO19, cisplatin or the combination of both compounds in this particular cell line seems to be independent of p53 and p21 proteins. The protein expression results obtained correlate with previous gene expression studies. A431 cells also have p16 and Rb wild-type proteins present *(Schmidt and Fan, 2001)*. Cell cycle arrest can also occur in both p53- and p21-independent pathway involving p16. p16 is also an inhibitor of specific cyclin dependent kinases and up-regulation of p16 leads to hypophosphorylation of Rb and consequently cell growth arrest *(Rheinwald et al, 2002)*. However, neither of the treatments used in A431 cells showed a senescence phenotype, therefore, it was not necessary to investigate these genes.

The cell death studies showed that BRACO19 and the combination produce necrotic cell death in A431 cells. It is well known that PARP1 gene expression is related to necrotic cell death *(Ha and Snyder, 1999; Zhong et al, 2004)*. Therefore, the effect on PARP1 gene expression was studied in A431 cells treated with cisplatin, BRACO19 and the combination (Figure 4. 6). Interestingly, the combination produces a significant up-regulation in PARP1 gene expression (Figure 4. 7), confirming that the combination induces necrotic cell death.

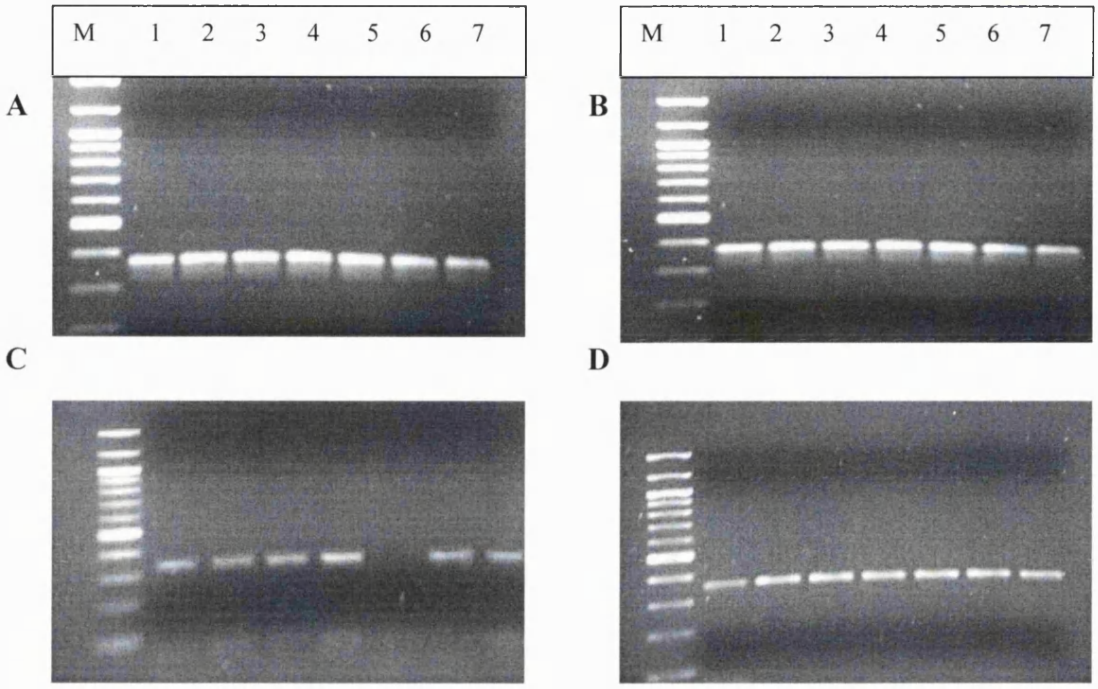

Figure 4. 2. Gene expression using RT-PCR, M (molecular weight marker), lane 1 (vehicle control), lane 2 (0.5 μM cisplatin), lane 3 (0.75 μM cisplatin), lane 4 (1 μM BRACO19), lane 5 (1.5 μM BRACO19), lane 6 (0.5 μM cisplatin+1 μM BRACO19), lane 7 (0.75 μM cisplatin+1.5 μM BRACO19). A. p53, B. p21, C. p73, D. GAPDH after one week treatment.

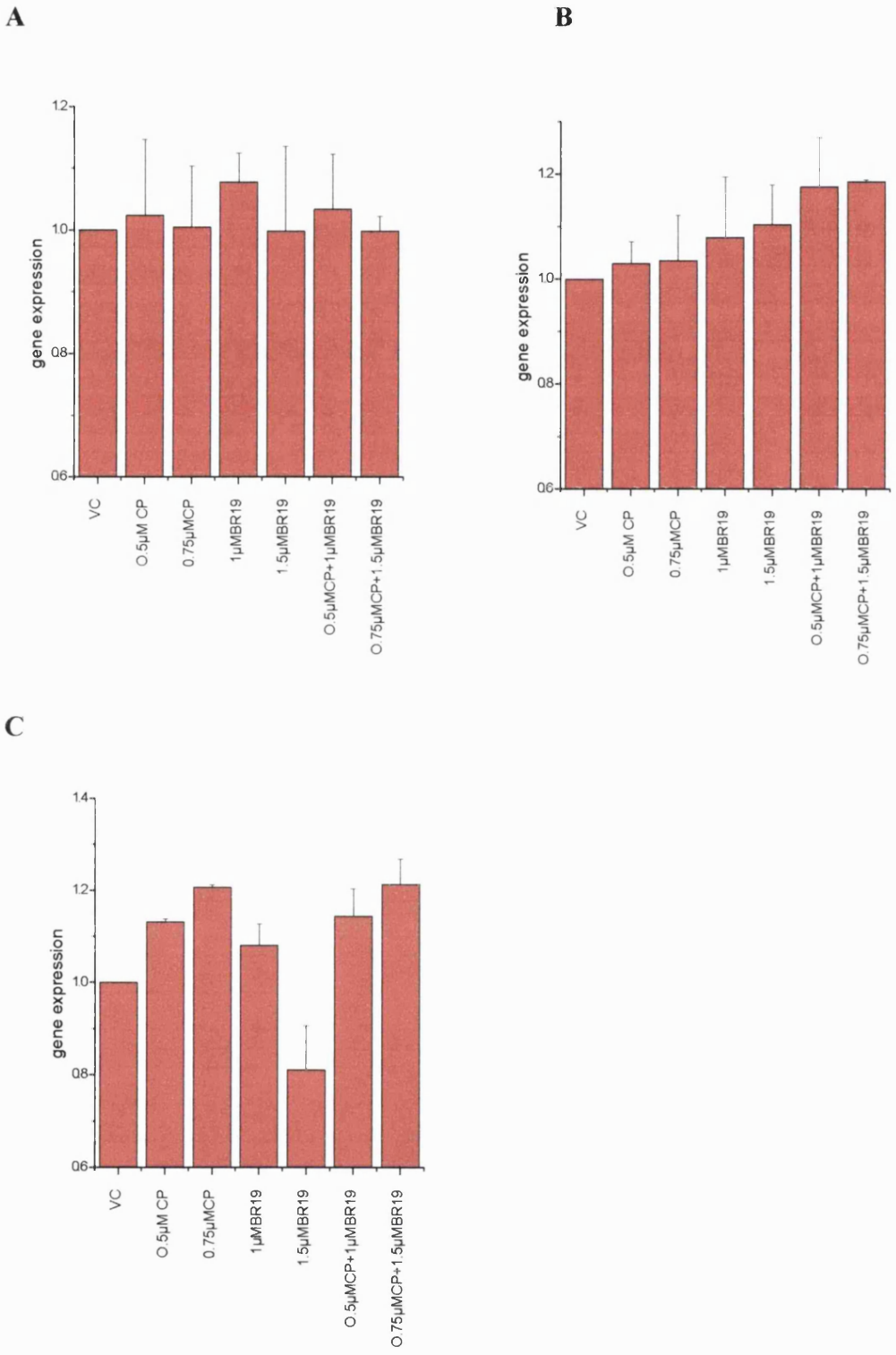

Figure 4. 3. Gene expression after one week of treatment of p53 (A), p21 (B) and p73 (C) normalized against GAPDH as a housekeeping gene. VC: vehicle control, CP: cisplatin, BR19: BRACO19.

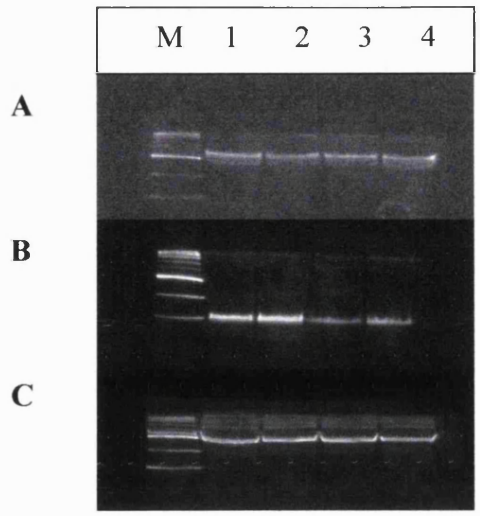

Figure 4. 4. Protein expression using western blotting after one week treatment. M (molecular weight marker), lane 1(0.75 μM cisplatin+1.5 μM BRACO19), lane 2 (1.5 μM BRACO19), lane 3 (0.75 μM cisplatin), lane 4 (vehicle control). A. p53, B. p21, C. α-actin used as a housekeeping protein.

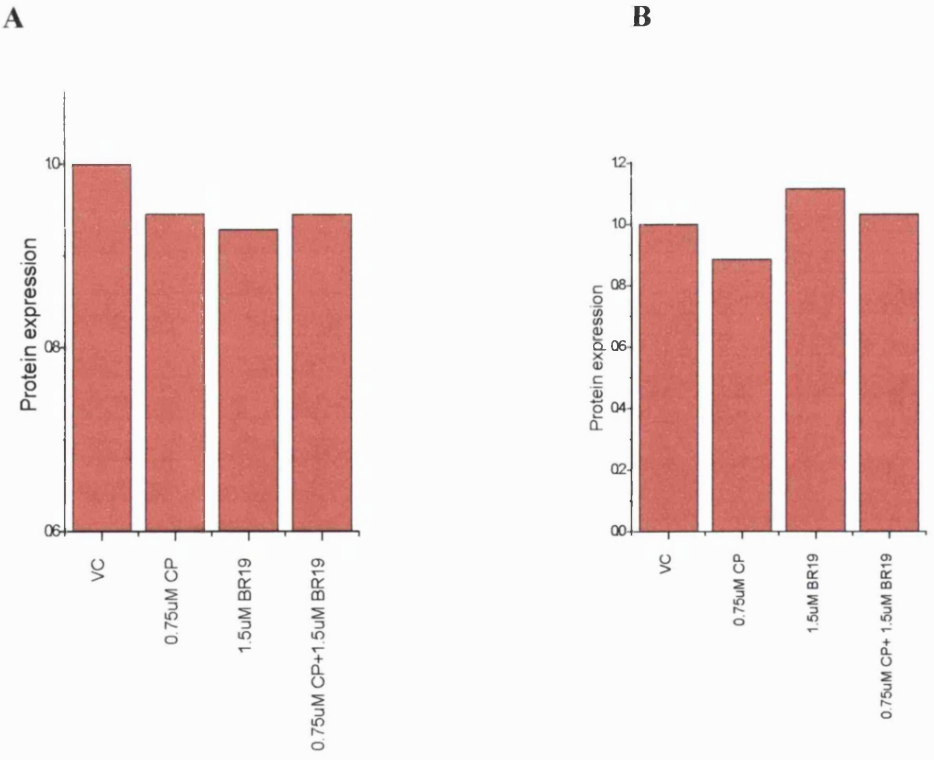

Figure 4. 5. Protein expression after one week of treatment of p53 (A) and p21 (B) normalized against α-actin as a control. VC: vehicle control, CP: cisplatin, BR19: BRACO19.

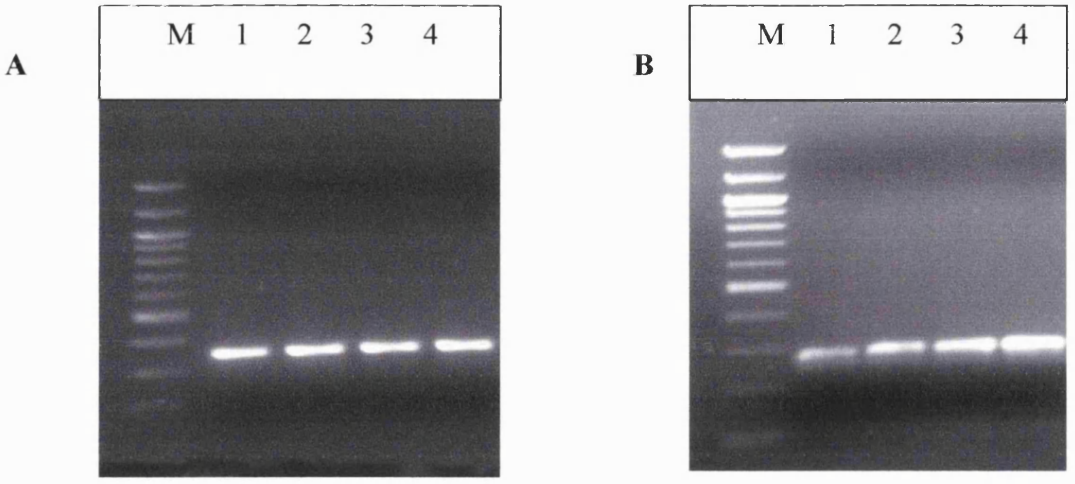

Figure 4. 6. The mRNA levels of GAPDH (A) and PARP1 (B) were determined by RT-PCR. Marker (M), Vehicle control (lane 1), cells treated during one week with 0.75 μM cisplatin (lane 2), 1.5 μM BRACO19 (lane 3), 0.75 μM cisplatin +1.5 μM BRACO19 (lane 4).

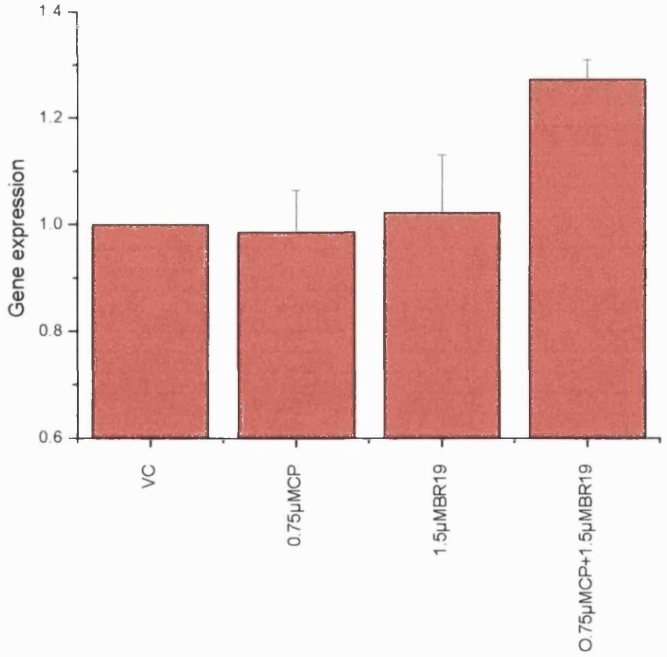

Figure 4. 7. Graph representing gene expression of PARP1 normalized against GAPDH as a control after one week of treatment. VC: vehicle control, CP: cisplatin, BR19: BRACO19.

4.4. DISCUSSION

It has been previously shown (see chapter 3) that cisplatin treatment in A431 cells produced a very rapid apoptotic response which is caspase 3-dependent, whereas BRACO19 treatment produced necrotic cell death. The combination of both compounds produced the same type of effect as BRACO19 but it also led to a dramatic decrease in cell proliferation. The study on p53 gene and protein expression showed that apoptotic cell death after treatment with cisplatin is independent of p53. Furthermore, a possible p73-dependent pathway was investigated; however, there were no changes in p73 gene expression. Diverse chemotherapeutic agents such as cisplatin have been shown to induce apoptosis in a p53-independent way *(McDonald and Brown, 1998; Sugimura et al, 2004; Mese et al, 2000)*. As has been mentioned above, p53 is able to activate the mitochondrial apoptotic cascade leading to the activation of effector caspases *(Kim et al, 2005; Shi, 2006)*. On the other hand, the activation of caspases has also been previously demonstrated in p53 inactive mutant cells. A431 posses an inactive p53 protein *(Lanzi et al, 1998)*, and treatment with cisplatin activates apoptotic machinery in this cell line indicating the existence of a p53-independent pathway able to activate caspases and therefore to induce apoptosis *(Mese et al, 2000)*. On the other hand, it has been earlier demonstrated that induction of DNA damage can produce necrotic cell death in p53 deficient cells. This necrotic cell death is completely independent of p53, Bax, Bak and caspases, and it is dependent on polyADP ribosylases (PARP) activation *(Zhong et al, 2004)*. The activation of PARP produces depletion of intracellular β-nicotinamide adenine dinucleotide (NADP) and adenosine 5′triphosphate (ATP) and therefore induces necrosis. BRACO19 treatment induced necrotic cell death in A431 cells. It produces loss of cell membrane integrity as it was demonstrated with the vital stain trypan blue and it did not produce caspase 3 activation (see chapter 3). However, the treatments used in this study did not produce a very significant change in cell growth and consequently in necrotic population. Consequently, BRACO19 treatment did not produce a significant change in PARP-1 gene expression. Upon BRACO19 treatment there was no change in p53 expression, but it produced down-regulation of p73 gene expression.

The promoter region of c-myc has sequences which can potentially form G-quadruplexes. These regions have been shown to participate in the transcriptional regulation of this gene. G-quadruplex stabilising agents such as quindoline derivatives have selectivity towards these G-quadruplexes as it has been shown by polymerase chain reaction stop assay and a molecular modelling study. Interestingly, these agents produce down-regulation of the oncogene c-myc in the hepatocarcinoma Hep G2 cell line *(Ou et al, 2007)*. At my request, Alan Todd searched for sequences which can potentially form G-quadruplexes on the pattern G_{3-5} $N_{1-7}G_{3-5}$ N_{1-7} G_{3-5} N_{1-7} G_{3-5} in the promoter region of p73. Three different regions were found:

-464 to -431 5' GGGCCGTCTGGGGGACAGCAGGGAGTCCGGGGG 3'
CCCGGCAGACCCCCTG TCGT CCCTCAGGCCCCC

-93 to -69 5' CCCCTCCCC GCG CCCATATAACCC 3'
GGGGAGGGGCGCGGGTATATTGGG

-52 to -20 5' CCCGCCC TGCC TCCCCGCCC GCGC ACCCGCCC 3'
GGGCGGGACGGAGGGGCGGGCGCGTGGGCGGG

It could be that these G-quadruplexes act by controlling the transcription of p73. Therefore, the down-regulation of p73 could be explained as a consequence of the stabilisation of these G-quadruplexes by BRACO19.

Thus, BRACO19 seems to produce unregulated necrotic cell death in A431 cells independently of p53 and p73. p73 is activated by different DNA damaging agents such as campothecin, etoposide, doxorubicin, cisplatin *(Irwin et al, 2003)*, and its upregulation seems to be cell type dependent *(Vikhanskaya et al, 2000)*. p73 is able to promote apoptosis by different mechanisms. Therefore, p73 acts as a tumour suppressor gene. Consequently, down-regulation in p73 could produce resistance to chemotherapy treatments. Resistance to apoptosis has been correlated with resistance to treatment. Introduction of certain p53 mutations in p53 wild type cells lead to the inactivation of p73 and the appearance of chemoresistance *(Irwin et al, 2003)*. However, the effect of the inactivation of p73 has not been extensively studied. On the other hand, p73 seems to have similar functions as p53. Sensitivity to chemotherapeutic agents has been correlated with the p53 wild-type cell status, as has been mentioned before. p53 mutations have been correlated on many occasions with the appearance of resistance

(Reles et al, 2001; Xue et al, 2007); however there is a controversy about the effect of p53 mutations on sensitivity towards chemotherapeutic agents. Although it has been widely shown that p53 mutations confer resistance towards DNA damaging agents, there are also increasing number of publications suggesting that this correlation is not always correct *(Hawkins et al, 1996; Brown et al, 1999; Petit et al, 2003, Lu et al, 2001)*. For example, alkylating agents such as the nitrogen mustard mechlorethamine hydrochloride showed similar sensitivity towards mouse embryofibroblast wild type compared to a modified line in which p53 and Bax genes were inactivated. This agent produced necrotic cell death in the modified cell line *(Zhong et al, 2004)*.

The combination of both agents also led to necrotic cell death. The treatment used in this study produces a very significant change in cell growth and consequently in necrotic population. This treatment did not show changes in p53 or in p73. Interestingly, the combination produced significant up-regulation of PARP1 gene expression. Furthermore, the treatment seems to arrest cells in S-phase as it has been shown with BrdU incorporation assay (see chapter 3). They have up-regulated PARP1 and possible other DNA repair proteins in order to repair the damage. Consequently, there is depletion of ATP energy that leads cells to undergo necrosis.

Following gene and protein expression study, the next step was to investigate DNA damage response and the effect of both compounds on telomeres and telomerase activity.

Chapter 5- EFFECTS OF BRACO19, CISPLATIN ON TELOMERES, TELOMERASE AND DNA DAMAGE RESPONSE

5.1 INTRODUCTION

In the two previous chapters the mechanism of cell growth inhibition was studied. In this chapter, I investigated the DNA damage response and the effect of both compounds on telomeres and telomerase activity to elucidate further mechanism of action.

5.1.1 DNA damage response.

The basic unit of chromatin, the nucleosome, is formed by 147 base pairs of DNA that involve an octamer of histone proteins. The octamer is formed by two copies each of the histones H2A, H2B, H3 and H4 *(Wood et al, 2005)*. Although these histones are highly conserved, there are different variants which have specialised biological functions. H2AX is a variant of the H2A histone that forms part of the protein core in the nucleosome. H2AX represents 2-10% of total H2A *(Rogakou et al, 1998)*. Its principal difference compared to other isoforms is that it has a conserved serine residue that is phosphorylated upon DNA damage *(Fernandez-Capetillo et al, 2004)*. One of the earliest responses after DNA damage is the phosphorylation of histone H2AX in its C-terminal tail at this conserved serine 139 *(Rogakou et al, 1998)*. The phosphorylated form is also called γH2AX and is detected during double stranded DNA breaks as discrete foci. The number of these foci is apparently comparable to the number of DNA double strand breaks *(Rogakou et al, 1999)*. It facilitates the recruitment of DNA repair proteins. There are different factors able to induce the phosphorylation of H2AX, including physical factors X-ray, UV, chemical factors, DNA damaging agents *(Takahashi and Ohnishi, 2006)*, apoptosis *(Rogakou et al, 2000)* or damaged telomeres *(Salvati et al, 2007)*. The kinases that phosphorylate H2AX in response to DNA damage belong to the phosphatidylinositol-3 kinase-like family of kinases (PI-3K), principally, ataxia telangiectasia mutated (ATM), the ATM and Rad3 related (ATR), the ATM related kinase (ATX), and DNA dependent protein kinase (DNA-PK). DNA-PK has been shown to be activated during late apoptotic DNA fragmentation. It seems to produce phosphorylation in H2AX and then is degraded by proteolysis. The H2AX phosphorylation at this state may be necessary to facilitate chromatin condensation *(Mukherjee et al, 2006)*. H2AX is also phosphorylated after DNA damage, then it recruits DNA repair proteins and facilitates DNA repair. Once DNA damage is repaired, γH2AX is removed from chromatin. The protein phosphatase 2A seems to be involved

in the dephosphorylation of γH2AX that occurs after DNA damage is repaired *(Chowdhury et al, 2005)*.

5.1.2 Telomere associated DNA damage response.

Telomeres protect chromosome ends and need to be maintained in a "capped" status (discussed in chapter 1). The integrity of the single strand telomeric overhang is essential and loss of the capped status will lead to genomic instability.

Disruption of the "capped" status of the chromosomes due to the action of a DNA damaging agent or a telomerase inhibitor is recognised as a DNA strand break and may lead to the activation of a DNA damage response that can be detected as γH2AX foci. G-quadruplex stabilising agents seem to have a dual mechanism of action *(Gunaratnam et al, 2007; Kelland, 2007)*. Firstly, they have long-term antiproliferative effects as a consequence of the inhibition of telomerase. And secondly, short-term effects due to the effect on the capping of the telomere.

Therefore, it is interesting to investigate both mechanisms of action by looking at telomere associated DNA damage, chromosome fusions and also long-term effects on telomere length and effect on telomerase activity.

5.2. METHODS

5.2.1 Detection of γH2AX

DNA damage therefore can be detected by the use of antibodies against H2AX.

5.2.1.a Detection of γH2AX using FACS analysis

$1x10^6$ cells were treated with appropriate concentrations of drugs as before for different time periods: 1, 6, 12 and 24 hours. Cells were fixed in 1ml of 70% ethanol, pelleted and washed with PBS. Later, cells were labelled using the H2AX Phosphorylation Assay Kit (Upstate, USA) following manufacter's instructions. The kit provides an anti-phospho-histone H2AX (Ser139) FITC conjugated in order to detect γH2AX. H2AX labelling was measured using FACSCALIBUR flow cytometer.

5.2.2.b Detection of γH2AX using immunohistochemistry

$2x10^5$ cells in 2ml of media were seeded in 2-well glass chamber slides (NUNC, UK). Cells were treated with the appropriate concentration of compound and incubated for 12 hours. After the incubation time, cells were washed once with 2mls of 1X Tris-buffered saline (TBS) (Sigma,UK). Later on, cells were fixed in 95% ethanol 5% acetic acid for 5 minutes. Then chamber slides were blocked with 3% bovine serum albumin (BSA) (Sigma,UK) in 1X TBS for 1 hour at room temperature. After blocking the slides, cells were incubated with 2μg/ml of mouse monoclonal antiphosphohistone H2AX (Upstate, UK) in blocking buffer for 1 hour at room temperature. Following, cells were washed 5 times with 1X TBS for 1 minute. Later, cells were incubated with the secondary antibody Alexa555-goat antimouse IgG (Molecular Probes, UK) (1/2000 dilution) for 1 hour at room temperature. Finally, each well was washed 5 times with 1X TBS and the slides were mounted with Vectashield medium (Vector Laboratories, UK).

5.2.2 Chromosome banding and Metaphase Spreads.

$1x10^5$ cells were incubated with appropriate concentrations of drug as before, during three weeks (see long-term studies, chapter 2). At the end of every week when cells were ready to harvest, 100μl of colcemid (GibcoBRL) was added to each flask and incubated at 37^0C for 1 hour. Cells were then trypsinised and pelleted at 1200rpm for 15

minutes. The supernatant from each tube was removed using a fresh Pasteur pipette. Pellets were resuspended in up to 12ml 0.075M potassium chloride. Tubes were mixed by immersion and incubated for 20 minutes at room temperature. Later on, cells were fixed with freshly made fixative solution containing a 3:1 ratio of methanol and acetic acid, first adding 5 drops of the fix solution and mixing by inversion 5 times and then incubate at room temperature for 15 minutes. After fixing, the samples were centrifuged for 15 minutes at 1200rpm, and then supernatant was removed with a fresh Pasteur pipette until just above the pellet. The pellet was sucked up using a fresh pipette and added to 9ml of fresh fix to each of the tubes and the pellet was dispersed by squeezing the Pasteur pipette up and down in the fix until there were no clumps. The tubes were then centrifuged for 15 minutes at 1200rpm. After centrifugation, the supernatant was removed and 5ml of fresh fix was added while vortexing the tube. Later the tubes were centrifuged again at 1200 rpm this time for 6 minutes. This last step was repeated this time adding 3ml of fix mix. After the last centrifugation the pellets were vortex for at least 30 seconds at maximum speed.

Preparation of slides

20µl of each sample was dropped onto a wet pre-washed superfrost slide (VWR, USA), and then slides were placed on the hotplate at 80^0C for a couple of seconds in order to dry them. Slides were incubated in the oven overnight at 60^0C to age.

G-banding staining

Chromosomes were stained for G-banding by placing the slides in 5% giemsa solution (VWR, UK) for 3 minutes and washing twice in buffer pH=6.8 (VWR, USA). Slides were dried by incubating overnight at 60^0C before visualisation using confocal microscopy. The slides were mounted with a coverslip, using Eukitt mounting medium (Agar scientific, Germany).

5.2.3 Measurement of telomere length.

DNA was extracted from cell pellets using the QIAGEN Blood and cell culture DNA Mini Kit following manufacter's instructions. The DNA concentration was determined by measurement of the absorbance at 260nm using a GeneQuant spectrophotometer. In order to determine the purity of each sample, the ratio of Abs 260/Abs 280 was calculated. The DNA was kept at -20^{0}C until required.

C-rich probe (CCCTAACCCTAACCCTAACCC) (Invitrogen, UK) was labelled with γP32-ATP. 20ρmol of C-rich oligonucleotide was incubated with 80μCi of γP32-ATP (Amersham Biosciences, UK), 1μl of T4PNK enzyme (BioLabs), 3μl of T4 Phosphonucleotide kinase buffer (BioLabs) and 16μl of TE buffer (10mM Tris-Cl, 1mM EDTA, pH=8) for 1 hour at 37^{0}C. Afterwards the oligonucleotide was purified using the QIAquick Nucleotide Removal Kit (Qiagen, UK) following manufacter's instructions. The oligonucleotide was resuspended in 100μl of EB buffer (10mM Tris-Cl, pH=8.5)

2μg of genomic DNA of each sample was digested with 1.5μl of Hinf I and 1.5μl Rsa I restriction enzymes (Roche, Germany) and labelled with 3.5μl of ^{32}P-C-rich probe, in 3μl of NEB buffer 2 (50mM NaCl, 10mM Tris-HCl, 10mM $MgCl_2$, 1mM DTT, pH=7.9) (BioLabs), and up to 30μl of TE buffer (pH=8) at 37^{0}C overnight. 5μl of loading buffer was added to each tube to stop the reaction and samples were electrophoresed in 0.7% agarose gels with 0.5μg/μl of ethidium bromide for 2.5 hours at 115V in 1X Tris-Borate-EDTA (TBE) buffer (Sigma, UK). As a molecular weight marker, the ^{35}S DNA Marker (Amersham Biosciences, UK) was used following manufacture's instructions. Subsequently, the gel was dried, firstly for 2 hours in filter paper and towel paper, followed by in a gel dryer for 20 minutes. The gel was then exposed to an X-ray film overnight (Molecular Dynamics). Telomeric smears were visualized using a phosphorimager (Molecular Dynamics).

5.2.4 Measurement of telomerase activity

$1x10^5$ cells were treated with appropriate concentrations of drug as before (see chapter 2). Total cellular protein was extracted from pellets using the Bradford assay and 500ng of protein was subsequently used to measure telomerase activity *in vitro*. In the first step of the assay, protein was incubated with the TS primer (0.1μg, 5'AATCCG TCG AGC AGA GTT 3') at 30°C for 10 min to enable elongation of primer by telomerase, followed by 4 minutes at 92^0C in order to denature telomerase.

1. Telomere elongation

	(1X)
H_2O	32μl
10X buffer	4μl
BSA (0.1mg/ml)	0.5μl
dNTPs (10mM)	0.5μl
TS primer (0.1μg/μl)	1μl

Following this, the elongated products were amplified using ACX primer (1μM, 5' GCG CGG $[CTTACC]_3$ CTA ACC 3') at 94°C for 5 minutes and 33 cycles of 94°C for 30 seconds, 61°C for 1 minute, 72°C for 1 minute.

2. PCR amplification of the telomerase products

	(1X)
H_2O	7.6μl
10x buffer	1μl
ACX (10μM)	1μl
Taq	0.4μl (2 units)

Both TS and ACX primers were purchased from Invitrogen. The PCR products were resolved on a 10% polyacrylamide gels, stained with SYBR green (Sigma) and quantified using gel scanner and gene tool software (Sygene, Cambridge, UK).

5.2.5 Reverse Transcriptase Polymerase Chain Reaction (RT-PCR).

RT-PCR was carried out to analyse expression of h-TERT in order to determine the effect of these compounds at transcriptional level. Cells were treated in culture for one week as described previously (see chapter 2). The RT-PCR method is described in chapter 4. PCR conditions are described in Table 5.1.

hTERT (Incles et al, 2004)	F' GCCAAGTTCCTGCACTGGCTGATG R'GTTCTGGGGTTTGATGATGCTGGCG	94^0 C 5 min 94^0 C 30 sec 56^0 C 1 min 35X 72^0 C 1 min 72^0 C 10min	588bp

Table 5.1. PCR conditions for the h-TERT primers used

5.3. RESULTS

5.3.1 Detection of γH2AX in A431 cells

Time course studies for cisplatin, BRACO19 and the combination showed phosphorylation of H2AX due to the effect on DNA by these compounds, as an early DNA damage response (Figure 5.1). Cisplatin produced the appearance of γH2AX after 6 hours, maximum response at 12 hours and the response decreased at 24 hours, whereas BRACO19 produced a more rapid response, with changes observed only after 1 hour of treatment, a maximum at 12 hours and decreased at 24 hours. In the case of the combination, the effect was already apparent and very similar to BRACO19 after 1 hour of treatment. However, the effect produced by the combination was greater than the single agents after 12 hours treatment (Table 5.2). In order to evaluate the extent of damage produced by these agents, A431 cells were treated with 50μM cisplatin at the same time points which served as positive control (Table 5.3). Considering that the IC_{50} for cisplatin in this cell line is 3.15±0.35μM, this concentration is very toxic. The maximum effect was observed again at 12 hours, 13.1% of cells were positive for γH2AX. Therefore, 6.02% observed for the combination seems to be a very significant response. Also as a positive control the immortalized line of T lymphocytes jurkat T cells was treated with the natural product staurosporine. Staurosporine is a non-selective protein kinase inhibitor that is a good example of an anticancer drug that induces apoptosis. 17% of the population of jurkat cells treated with stautosporine for 2 hours showed γH2AX.

FACS analysis showed that the largest γH2AX response in A431 cells occurred at 12 hours time point for all the treatments. Therefore, the 12 hours time point was chosen to detect γH2AX directly in the cells using immunofluorescence (Figure 5.2). A mouse anti-γH2AX antibody was used, followed by a goat anti-mouse secondary antibody labelled with the Alexa555 fluorochrome. In the untreated A431 cells used as a vehicle control, fluorescence was not detected. A431 cells treated with 1.5μM BRACO19 showed an increase in fluorescence detected. A more significant change in γH2AX was observed in cells treated with 0.75μM cisplatin. And finally A431 cells treated with the

combination of both compounds showed brighter fluorescence after treatment. Therefore, it was possible to reproduce the data observed with FACS analysis.

A

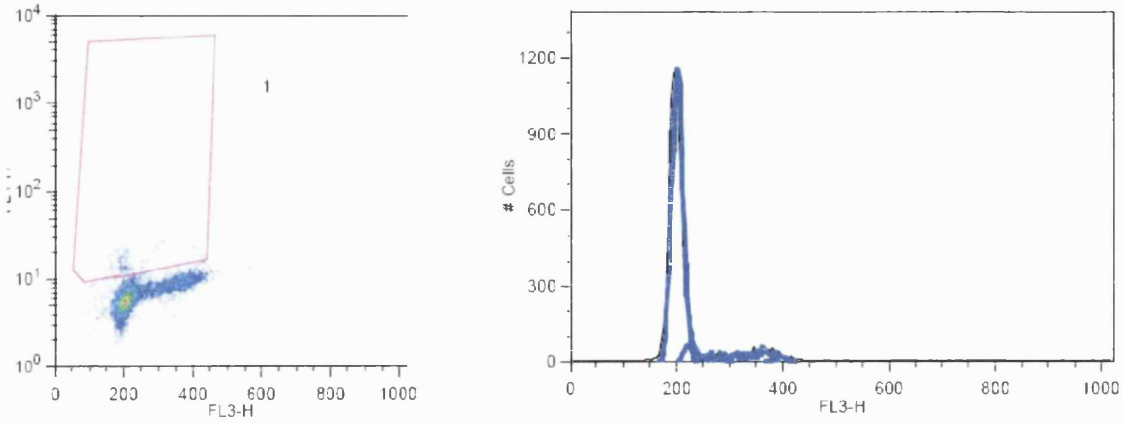

B

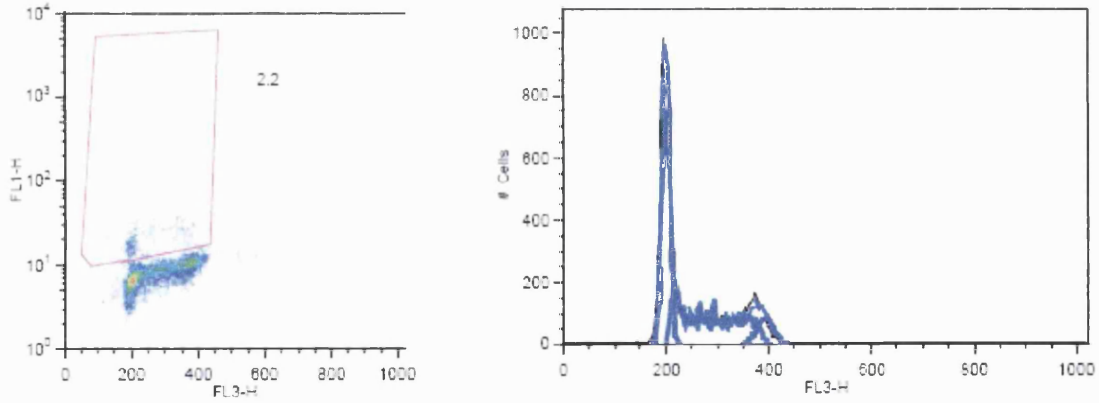

C

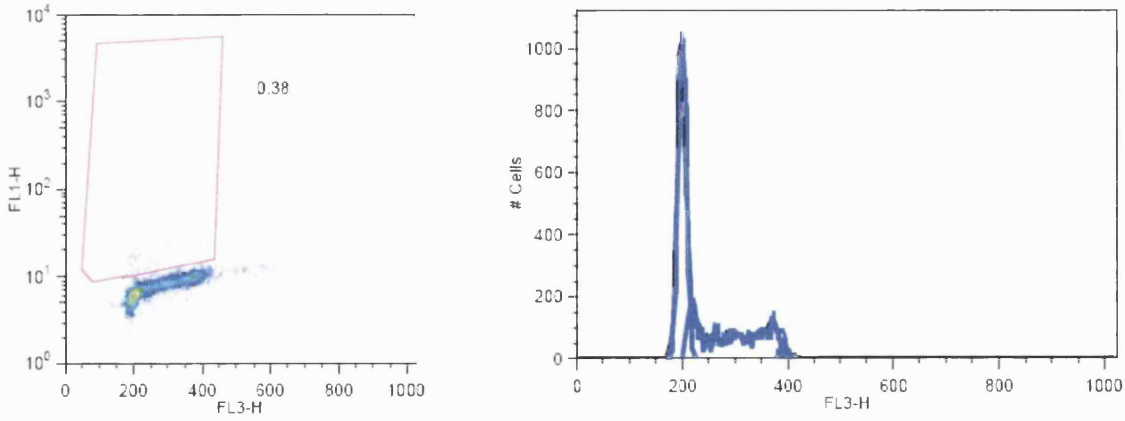

D

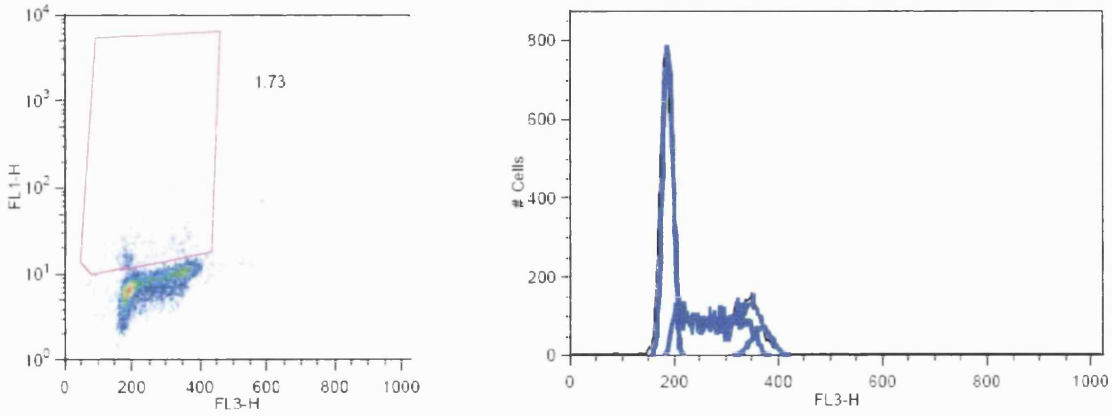

E

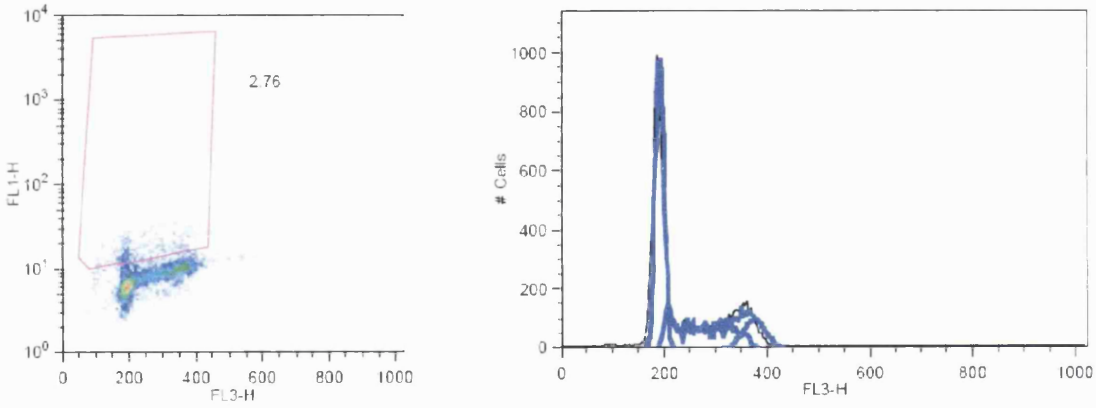

F

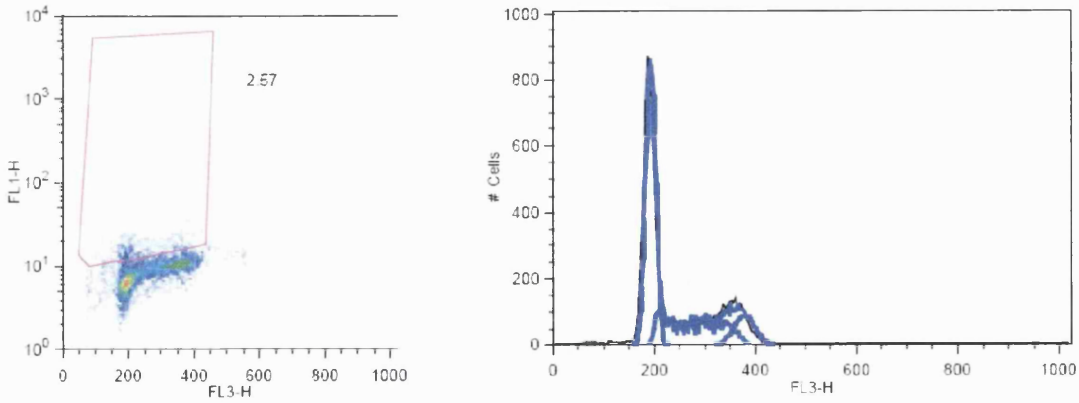

G

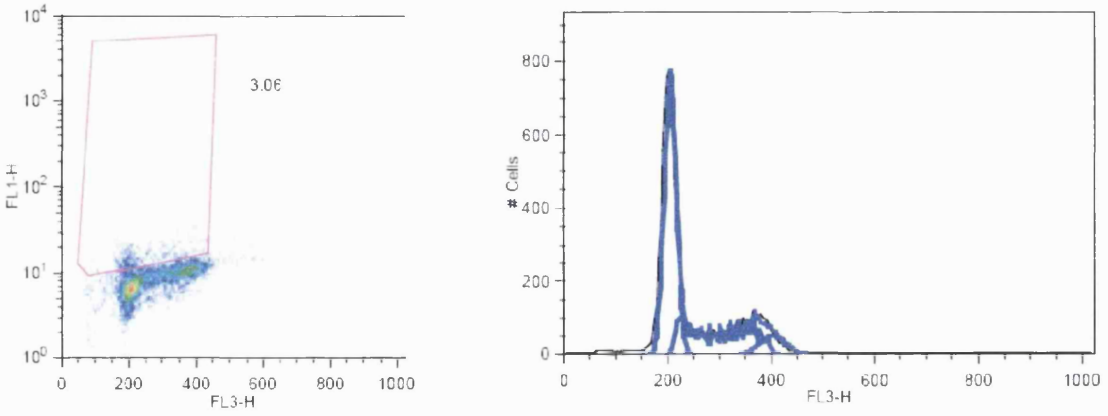

H

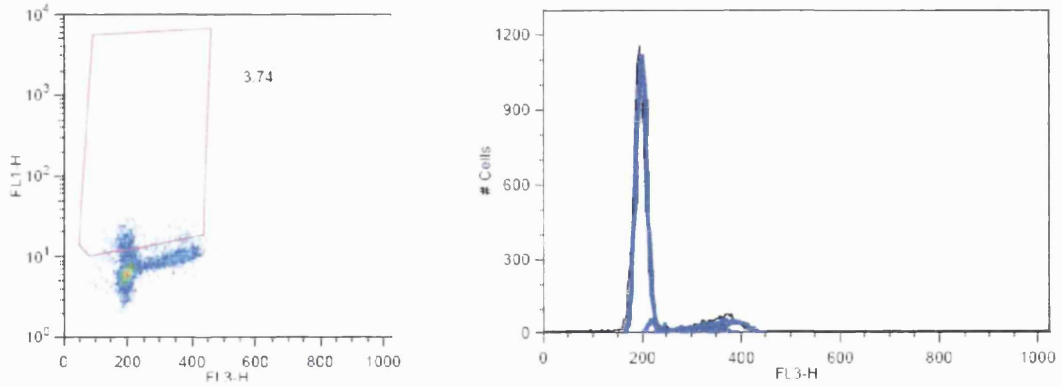

I

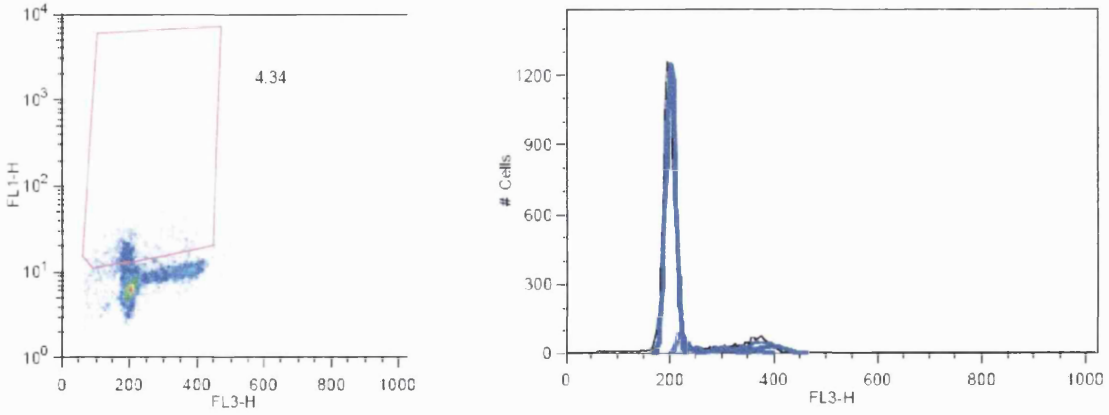

J

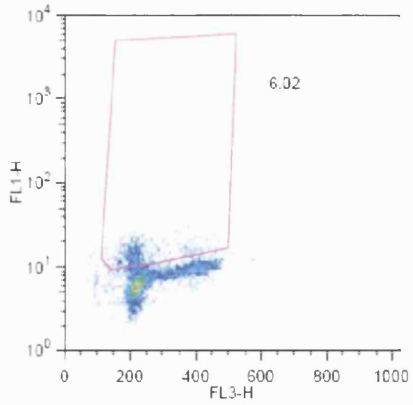
6.02
FL1-H
FL3-H

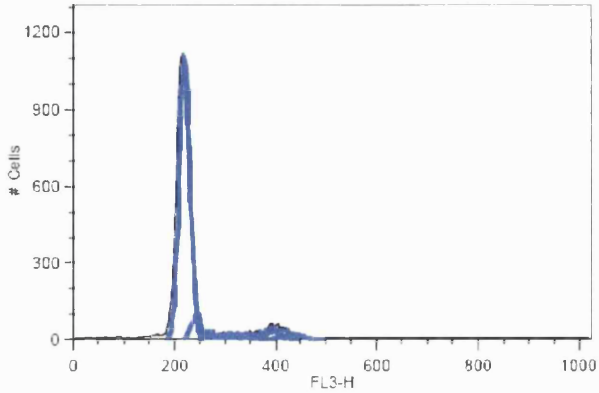
Cells
FL3-H

K

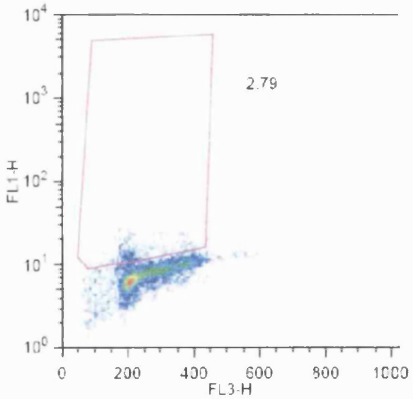
2.79
FL1-H
FL3-H

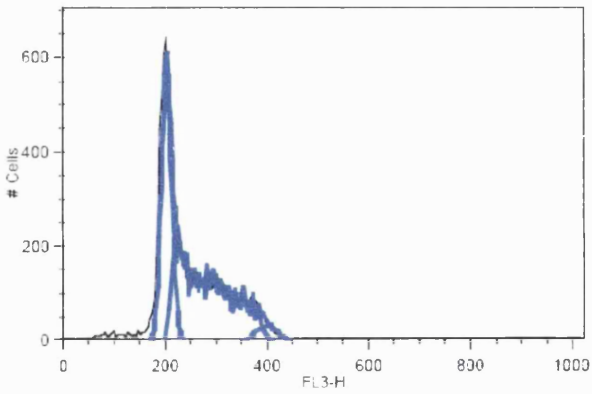
Cells
FL3-H

L

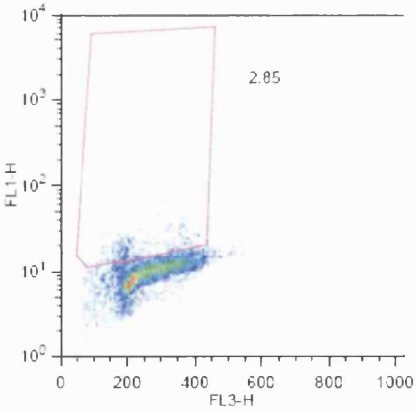
2.85
FL1-H
FL3-H

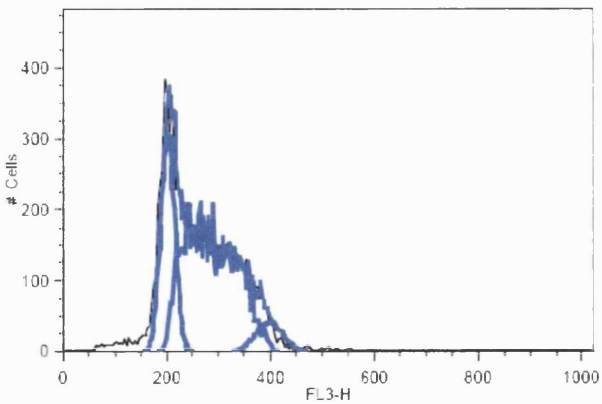
Cells
FL3-H

M

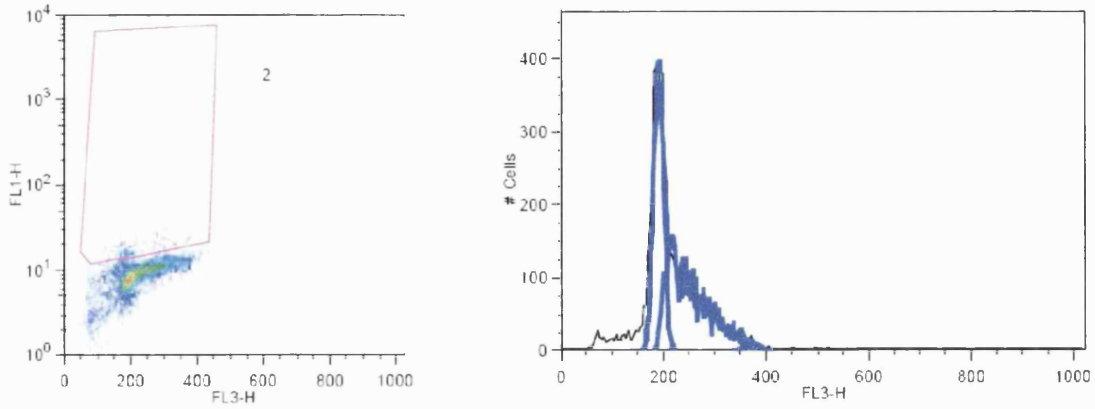

N

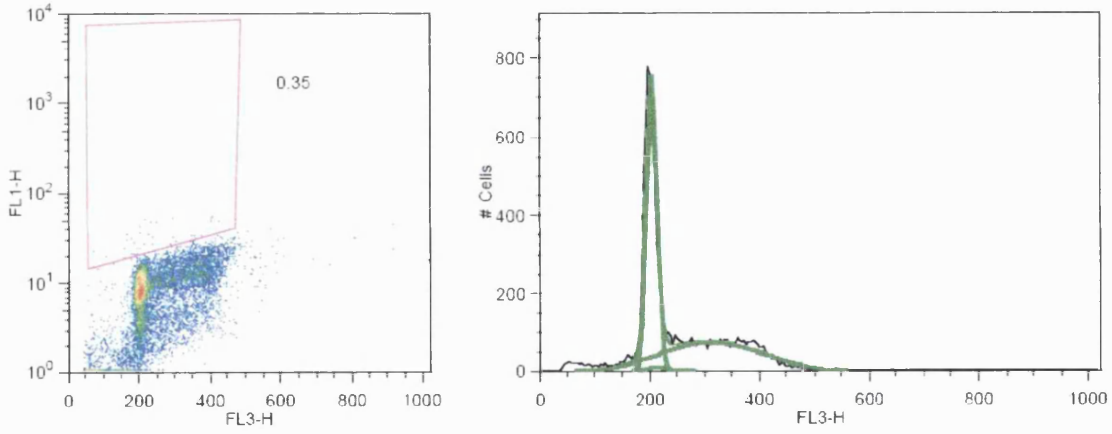

O

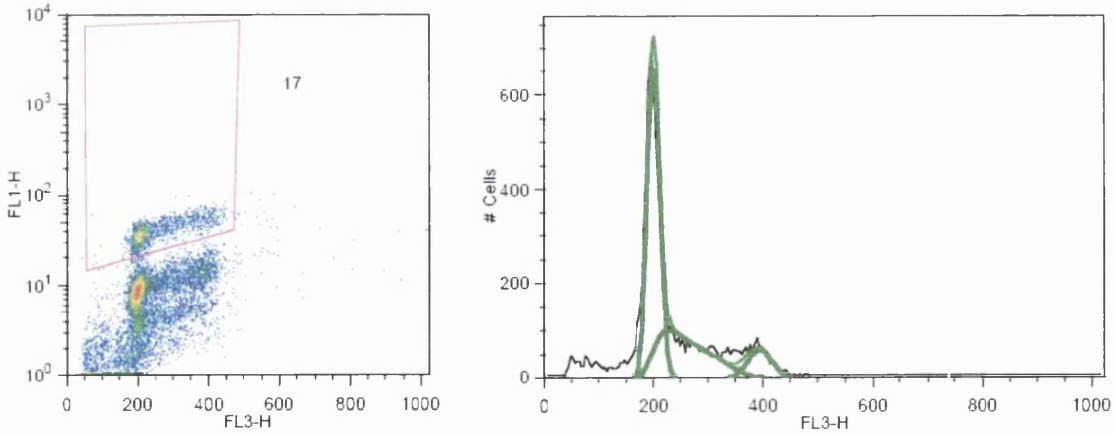

P

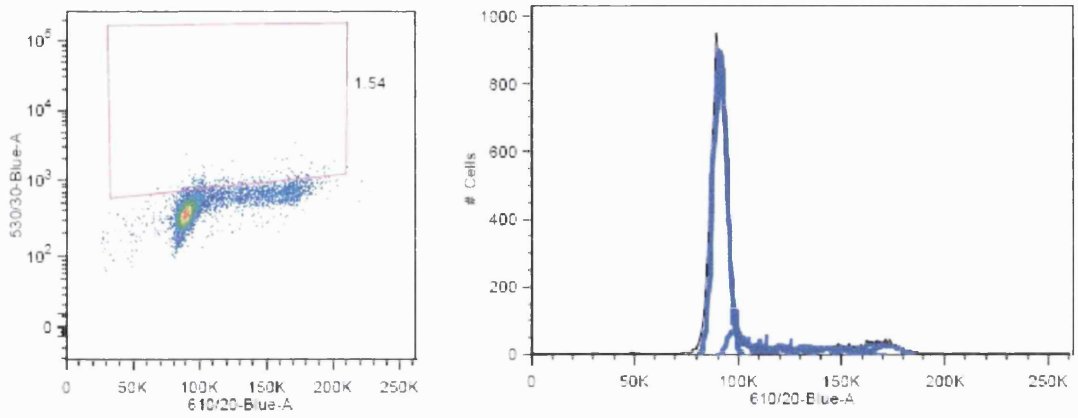
1.54
530/30-Blue-A
610/20-Blue-A
Cells

Q

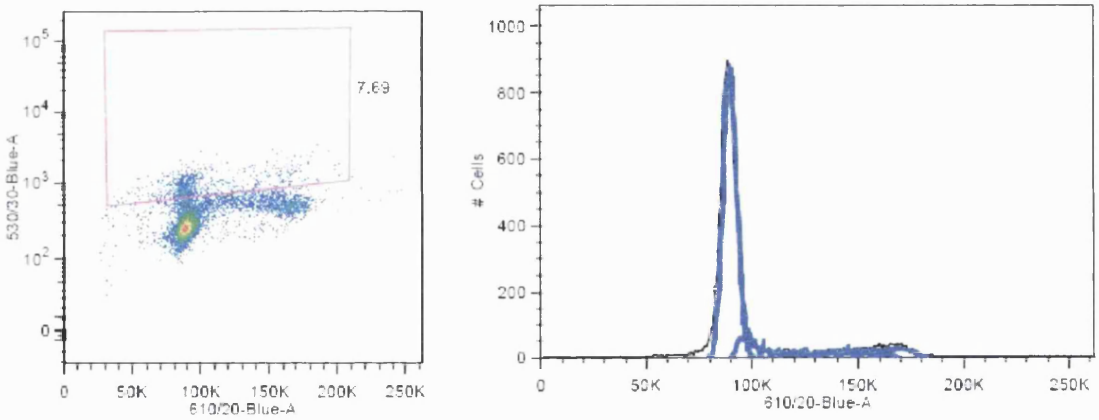
7.69
530/30-Blue-A
610/20-Blue-A
Cells

R

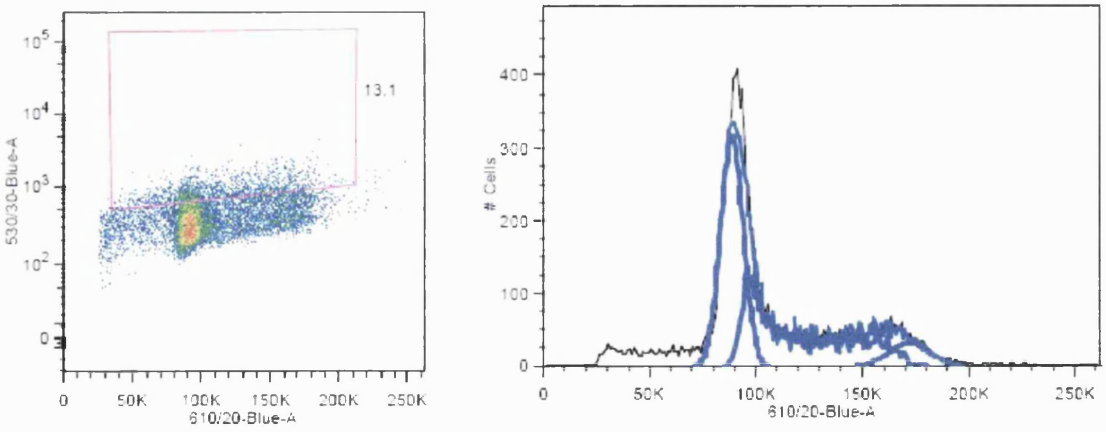
13.1
530/30-Blue-A
610/20-Blue-A
Cells

S

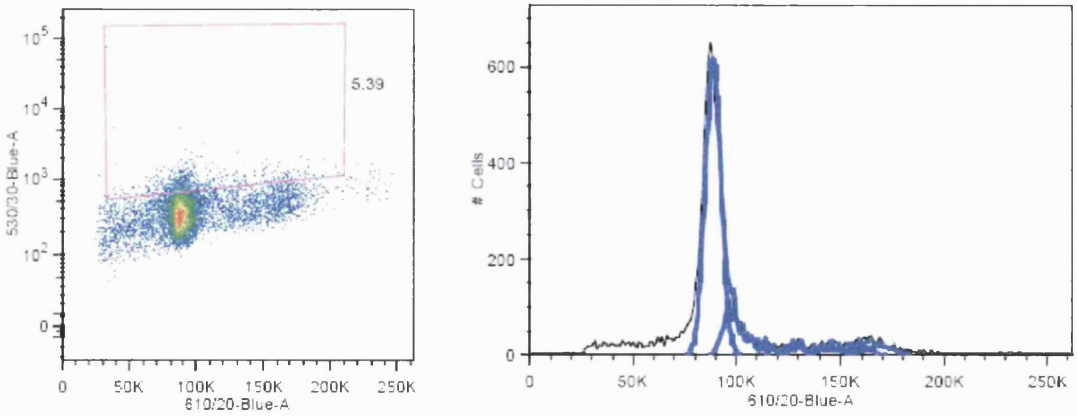

Figure 5. 1. γH2AX changes detected in A431 cells treated at different time points with 1.5μM BRACO19, 0.75μM cisplatin and 0.75μM cisplatin+1.5μM BRACO19. A. Vehicle control, B-D 1 hour treatment, E-G 6 hour treatment, H-J 12 hour treatment, K-M 24 hour treatment. N untreated jurkatt cells, O jurkatt cells treated with 10μg/ml stautosporine for 2 hours. P-S A431 cells treated with 50μM cisplatin for 1 hour, 6 hours, 12 hours and 24 hours respectively.

γH2AX	1.5μM BRACO19	0.75μM cisplatin	1.5μM BRACO19+ 0.75μM cisplatin
1 hour	2.2	0.38	1.73
6 hour	2.76	2.57	3.06
12 hour	3.74	4.34	6.02
24 hour	2.79	2.85	2

Table 5. 2. γH2AX changes detected in A431 cells treated at different time points with 1.5μM BRACO19, 0.75μM cisplatin and 0.75μM cisplatin+1.5μM BRACO19. (Results are expressed as percentage of cells).

γH2AX	50 μM cisplatin
1 hour	1.54
6 hour	7.69
12 hour	13.1
24 hour	5.39

Table 5. 3. γH2AX changes detected in A431 cells treated at different time points with 50μM cisplatin used as a positive control. (Results are expressed as percentage of cells).

A

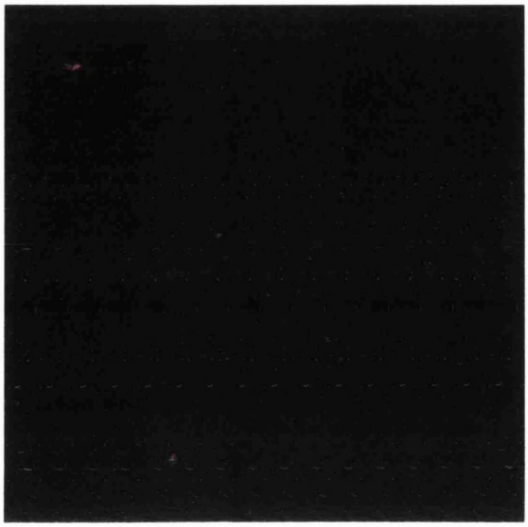

B

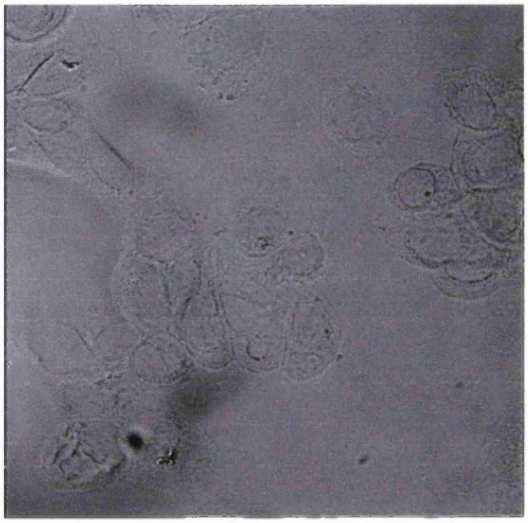

C

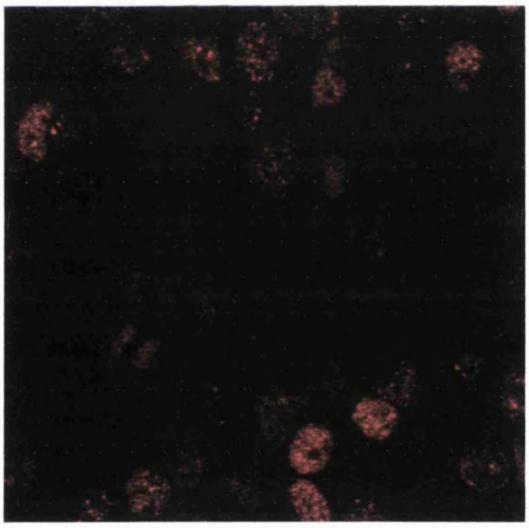

D

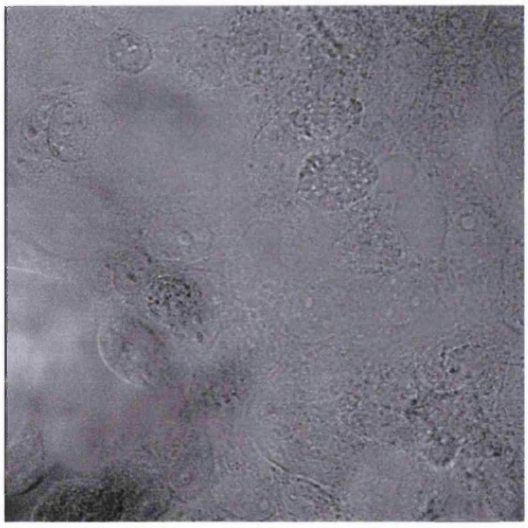

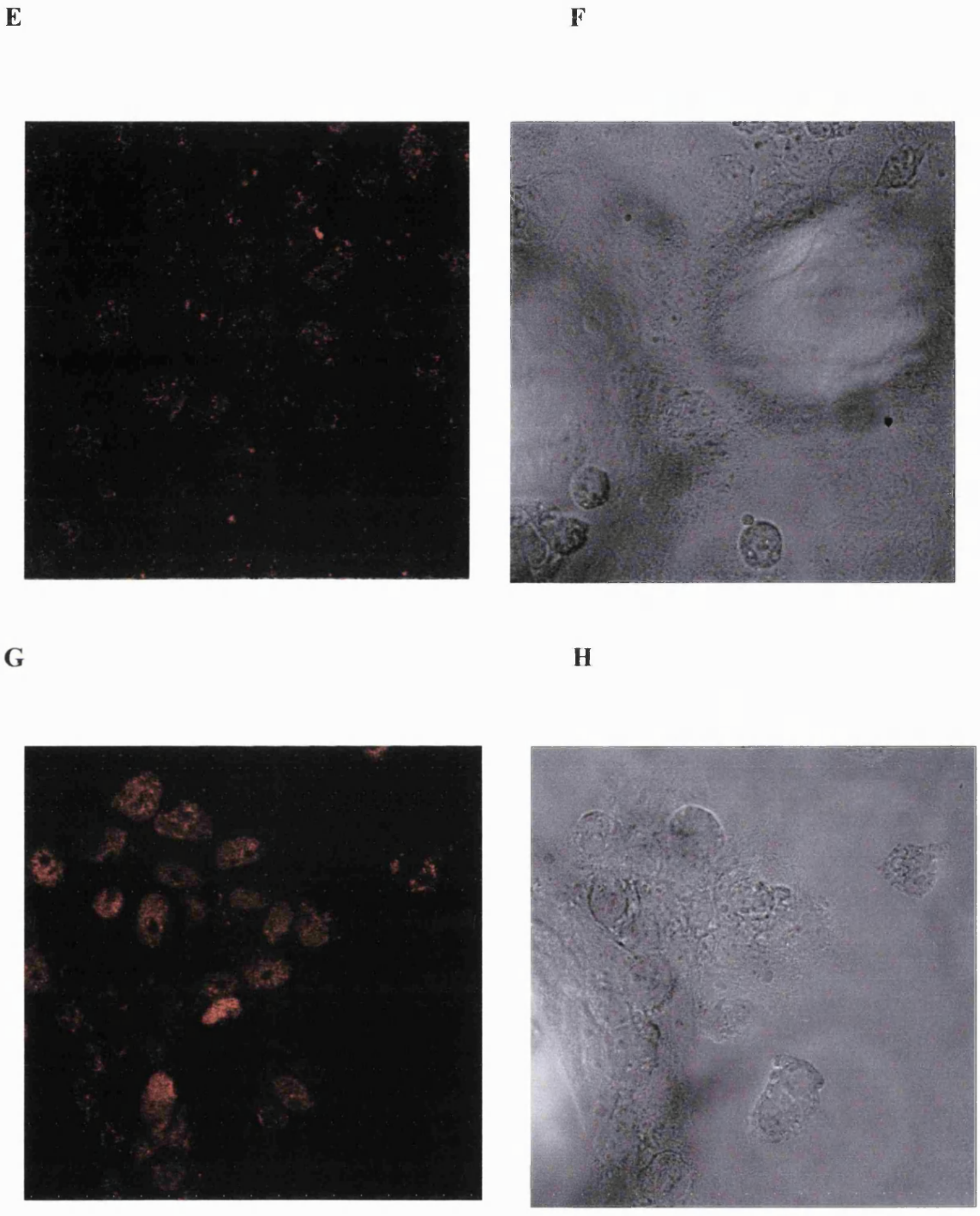

Figure 5.2. Immunofluorescence of γH2AX detection in A431 cells. A. Vehicle control, C. 0.75μM cisplatin, E. 1.5μM BRACO19 and G. 0.75μM cisplatin+1.5μM BRACO19 treated for 12 hours visualised using transmitted light. B. Vehicle control, D. 0.75μM cisplatin, F. 1.5μM BRACO19 and H. 0.75μM cisplatin+1.5μM BRACO19 treated for 12 hours visualised with Alexa555.

5.3.2 Effect on chromosomes

Chromosome abnormalities were studied with metaphase spreads. The uncapping of the telomere produces the formation of end-to-end fusions. Chromosomes that possess their telomeres unprotected tend to fuse their chromatids. Therefore, during anaphase when the chromatids are pulled apart by the microtubules, there is a double-strand break and both chromatids have cohesive ends. Consequently, they fuse with other chromosome forming an end-to-end fusion. If this cycle is repeated, long tails of fused chromosomes would be formed.

Cells were treated with 0.75μM cisplatin, 1.5μM BRACO19 or the combination for one week. After one week of treatment the number of chromosome abnormalities such as telomere fusions was not significant for the single treatments (Figure 5.3 and 5.4). The effect of both compounds alone at these concentrations did not produce the uncapping of the telomeres. These concentrations did not produce a significant effect on cell viability after one week of treatment. However, a dramatic increase (18%) in chromosome fusions in A431 cells treated with the combination was observed, as a result of the effect of both agents at the telomeres.

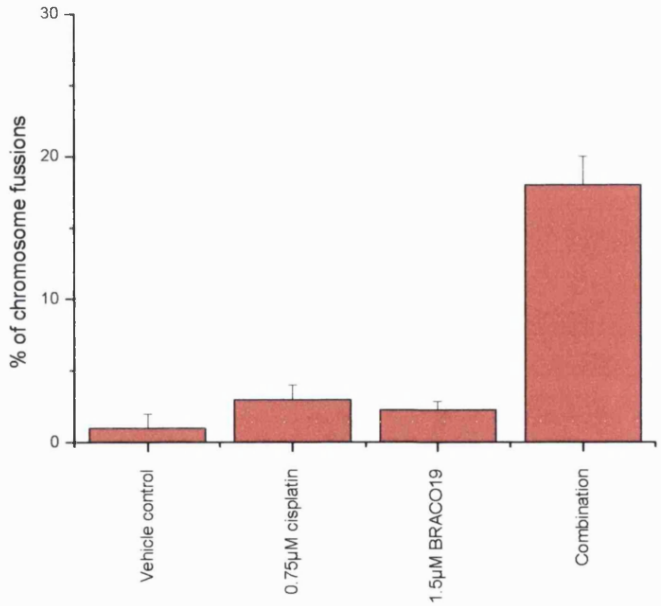

Figure 5.3. % of chromosome fusions in A431 cells after one week treatment.

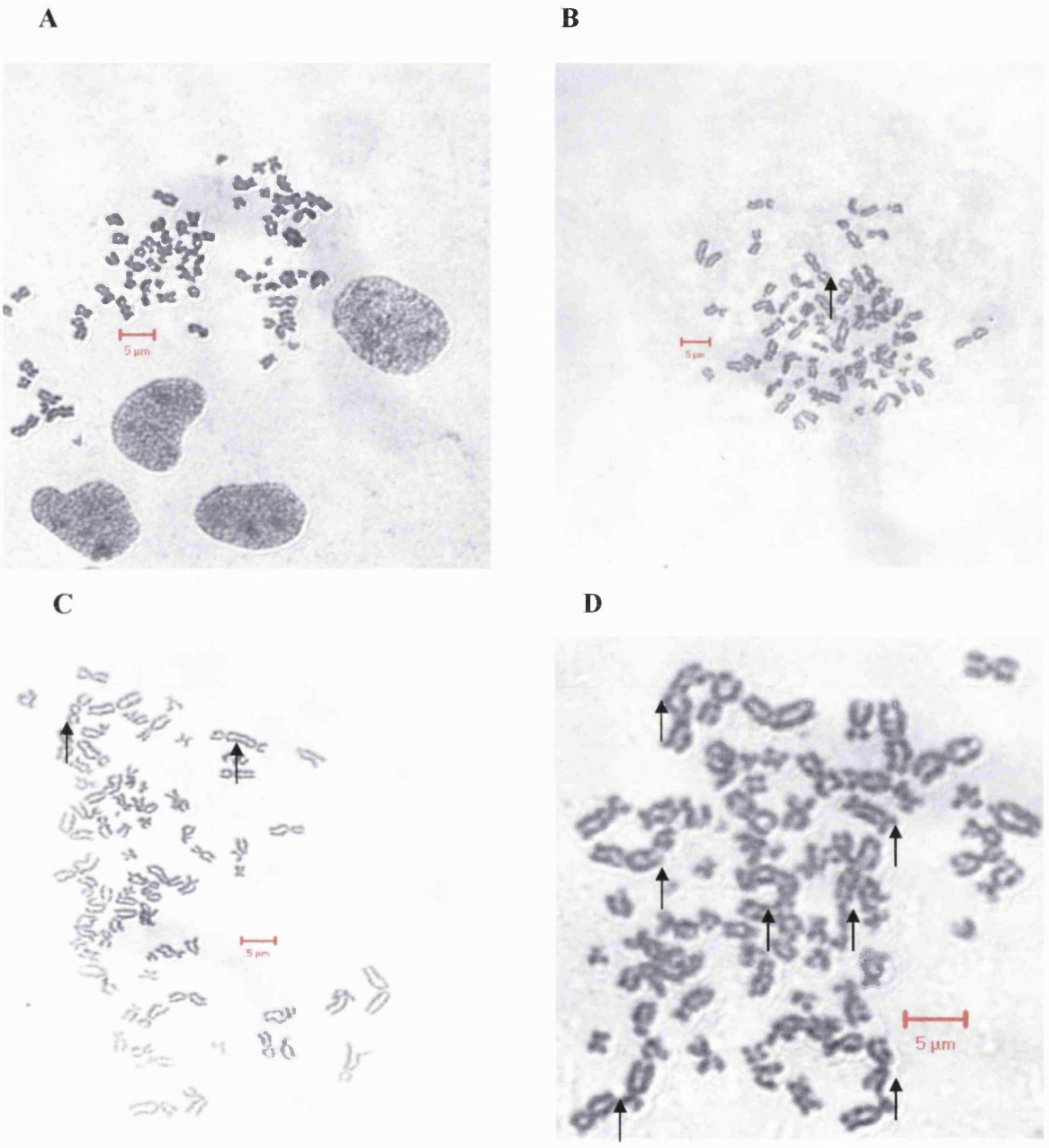

Figure 5.4. Metaphase spreads stained with giemsa from A431 cells. Cells were treated twice weekly during one week. A. Vehicle control, B. 1.5µM BRACO19, C. 0.75µM cisplatin, D. 1.5µM BRACO19+ 0.75µM cisplatin.

5.3.3 Effect on telomere length

The effect on telomere length was studied using southern blotting. A431 cells were treated with 0.75μM cisplatin, 1.5μM BRACO19 and the combination for one week. Changes in telomere length were not found for any of the treatments (Figure 5.5). A431 cells were also treated with 0.5μM cisplatin, 1μM BRACO19 and the combination for three weeks. This combination is very effective (see chapter 2) but it is not as aggressive and efficient as 0.75μM cisplatin+1.5μM BRACO19 combination. The reason for choosing the second combination is that it may allow the detection of a change in telomere length after a few weeks of treatment due to the effects on telomerase inhibition. DNA was extracted every week in order to study any possible difference along with time. However, no differences were observed for either BRACO19 or cisplatin as single agents or the combination (Figure 5.6). On the other hand BRACO19 produces telomere shortening in other cell lines as a consequence of the inhibition of telomerase. For that reason, A431 cells were treated with 1.5μM BRACO19 for a longer period of time, up to seven weeks. A431 cells have very short telomeres (average length restriction fragments ~2.5kb). Nevertheless, there was no telomere shortening after a long treatment with BRACO19 in the epidermis carcinoma cell line A431 (Figure 5.7). On the other hand, the long-term effect of BRACO19 in the ovarian carcinoma cell line A2780 was also studied. A2780 cells have longer telomeres than A431 cells (average restriction fragments ~6kb). A2780 cells were treated with 2μM BRACO19 up to five weeks. This concentration is not very effective in terms of cell growth inhibition (see chapter 2); however, it reduces telomere length by ~2kb after five weeks exposure (Figure 5.8).

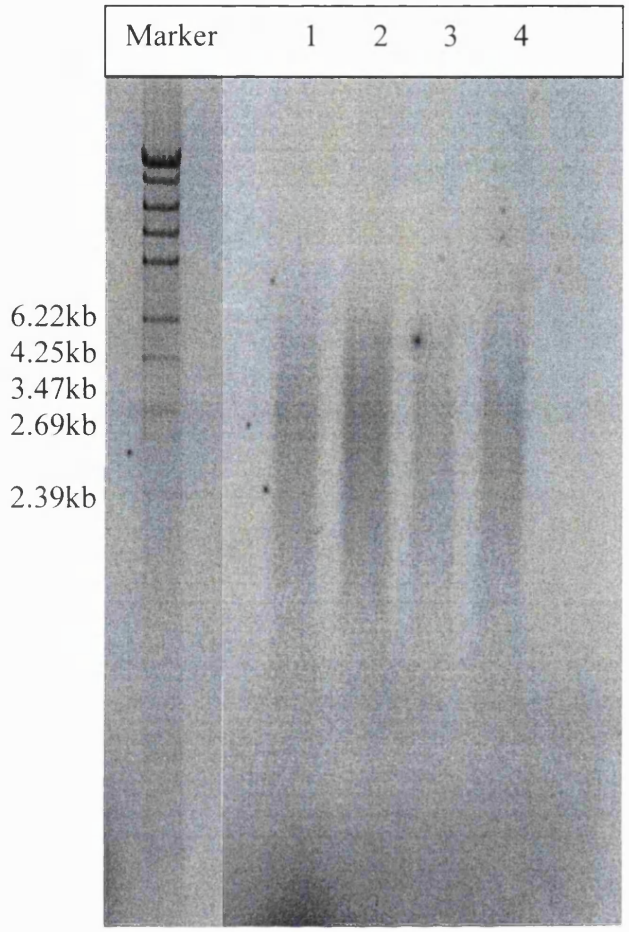

Figure 5.5. A431 DNA was harvested after one week from untreated cells (lane 1), culture treated with 0.75μM cisplatin (lane 2), 1.5 μM BRACO19 (lane 3) and 0.75μM cisplatin+1.5 μM BRACO19 (lane 4).

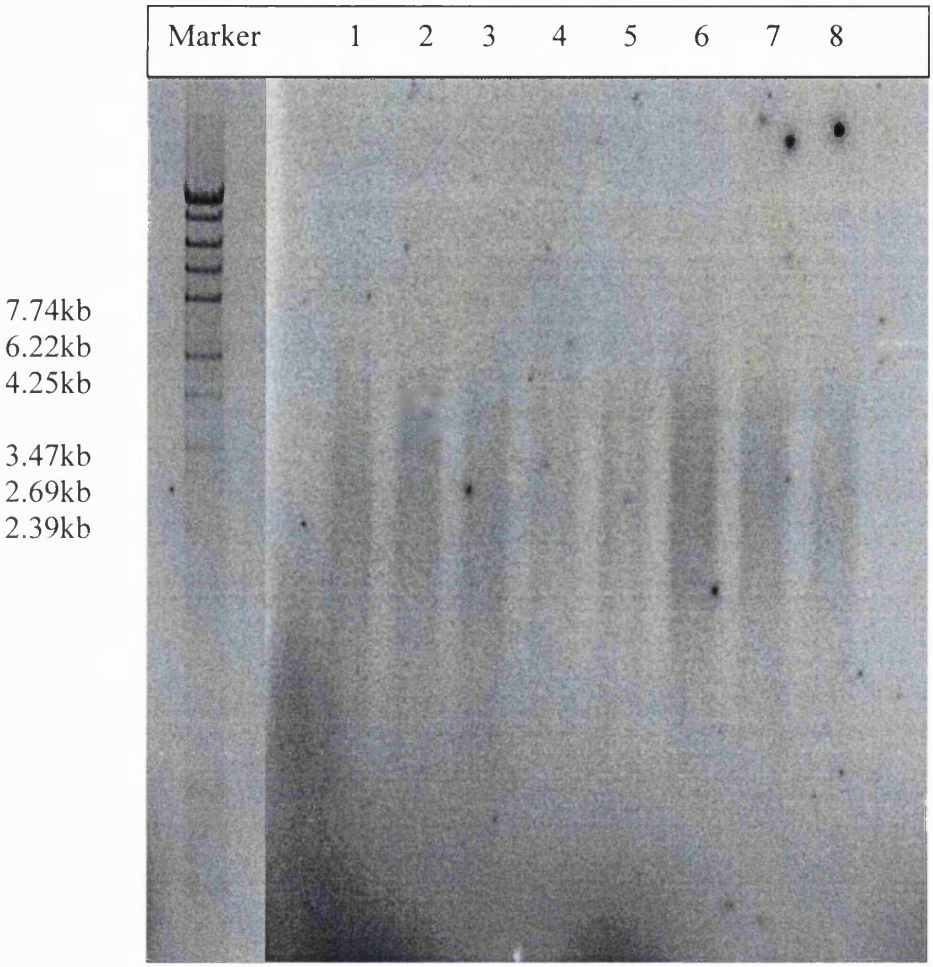

Figure 5.6. A431 DNA was harvested after one and three weeks from untreated cells (lane 1 and 5 respectively), culture treated with 0.5μM cisplatin (lane 2 and 6), 1 μM BRACO19 (lane 3 and 7) and 0.5μM cisplatin+1 μM BRACO19 (lane 4 and 8).

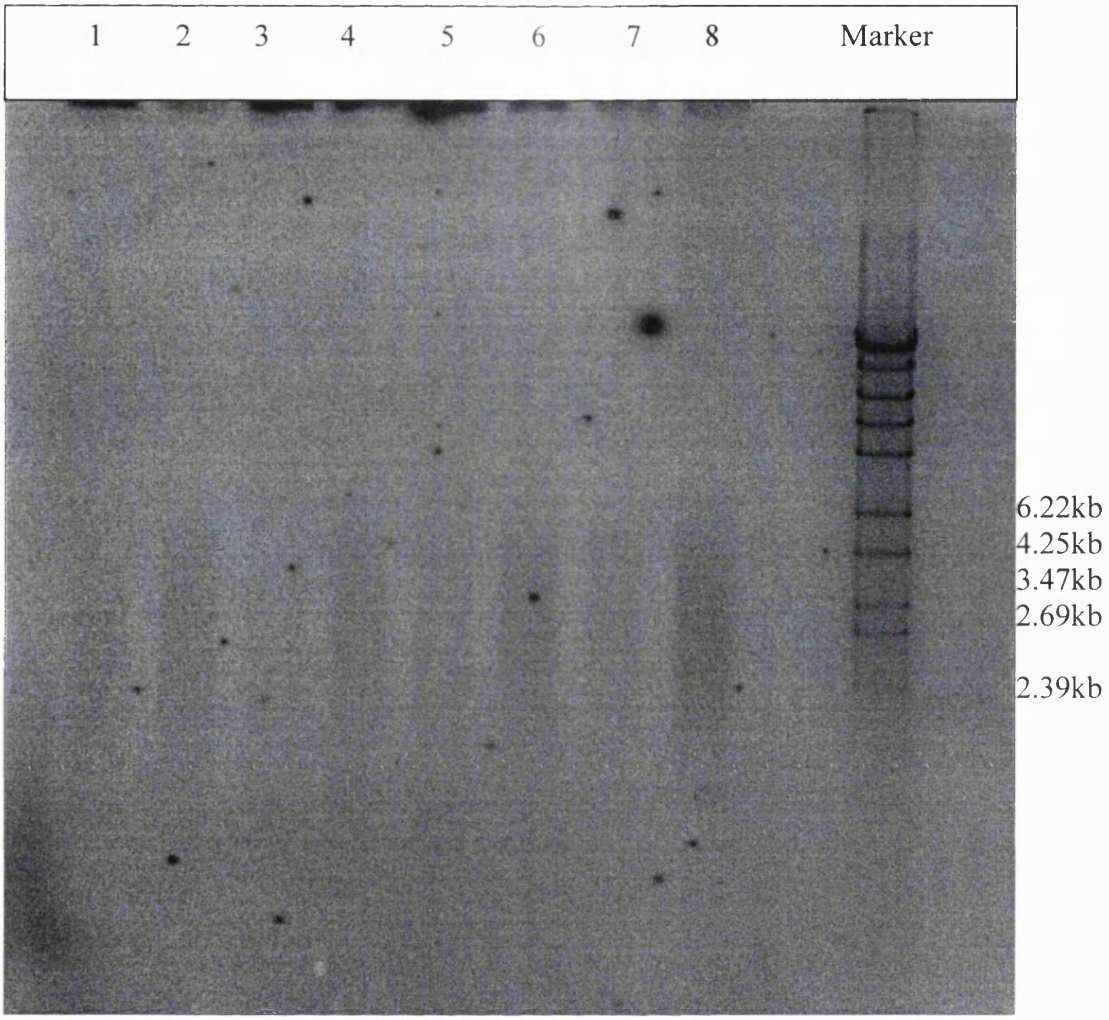

Figure 5.7. A431 DNA was harvested after five, six and seven weeks from untreated cells (lane 1, 3, 5 and 7) and culture treated with 1.5μM BRACO19 (lane 2, 4, 6 and 8). DNA was digested with RsaI and HinfI and hybridised with a ^{32}P labelled oligonucleotide.

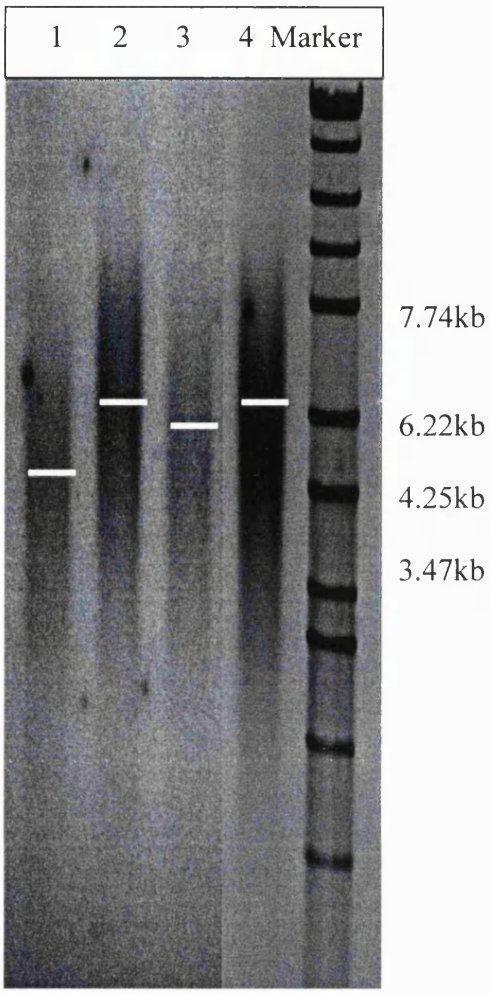

Figure 5.8. A2780 DNA was harvested from untreated cells (lane 4 and 2) for one and five weeks respectively, culture treated with 2μM BRACO19 (lane 3 and 1) for one and five weeks respectively. DNA was digested with RsaI and HinfI and hybridised with a ^{32}P labelled oligonucleotide.

5.3.4 Effect on h-TERT expression and telomerase activity

h-TERT gene expression was studied after two weeks of treatment. Cisplatin treatment in A431 cells did not produce any change in h-TERT expression. On the other hand, BRACO19 produces significant reduction in h-TERT gene expression at 1μM concentration and a very similar effect at 1.5μM concentration. The combination of both agents; 0.5μM cisplatin+1μM BRACO19 showed very similar effects on gene expression as BRACO19 alone (Figure 5.9).

Telomerase activity was measured using the TRAP assay. A431 cells were treated up to two weeks. Both single agents showed reductions in telomerase activity after treatment. Cisplatin showed a reduction of approximately 30% after one week and the same outcome was observed after two weeks of treatment. BRACO19 showed a more marked effect, 35% reduction after one week and 50% reduction after two weeks of treatment. On the other hand, upon combination treatment telomerase activity was inhibited by more than 40% after one week, and more than 65% at the end of two weeks of treatment (Figure 5.10).

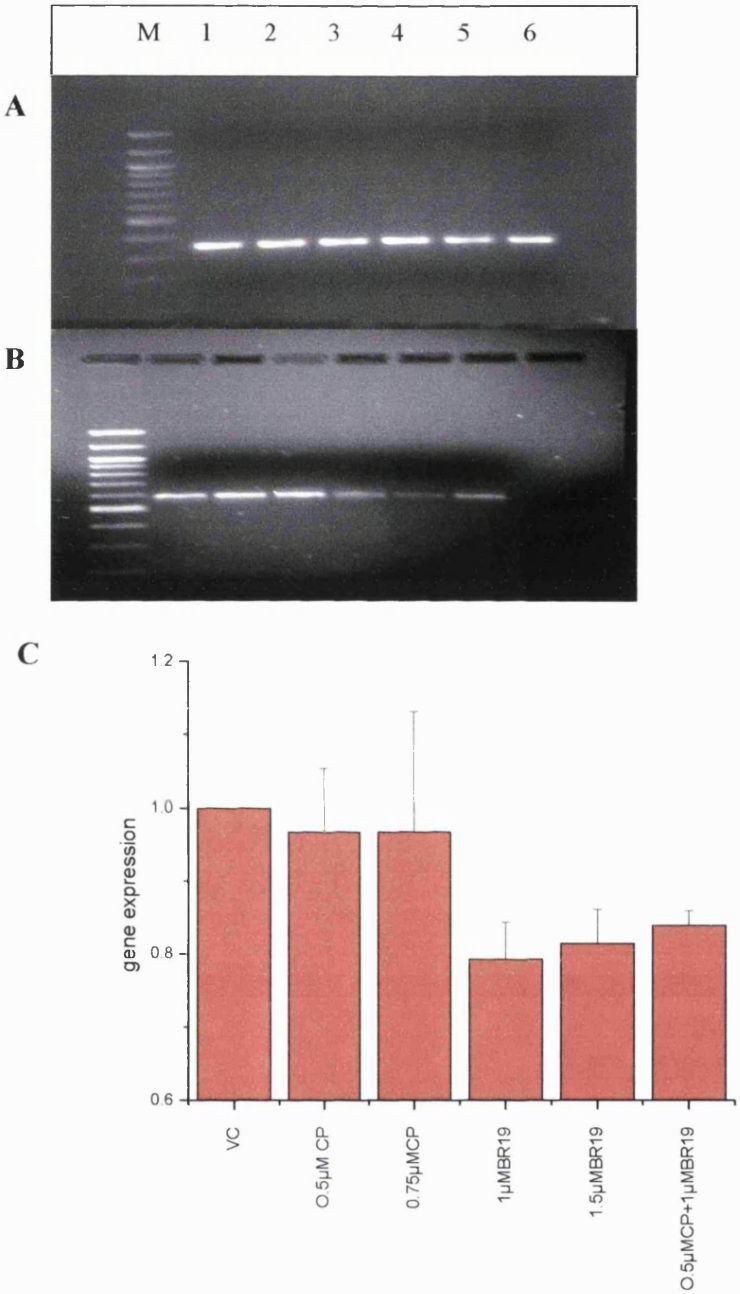

Figure 5.9. The mRNA levels of GAPDH (A) and hTERT (B) were determined by RT-PCR. Marker (M), Vehicle control (lane 1), cells treated during two weeks with 0.5μM cisplatin (lane 2), 0.75 μM cisplatin (lane 3), 1μM BRACO19 (lane 4), 1.5 μM BRACO19 (lane 5), 0.5 μM cisplatin +1μM BRACO19 (lane 6). C. Graph representing gene expression of h-TERT normalized with GAPDH expression

A

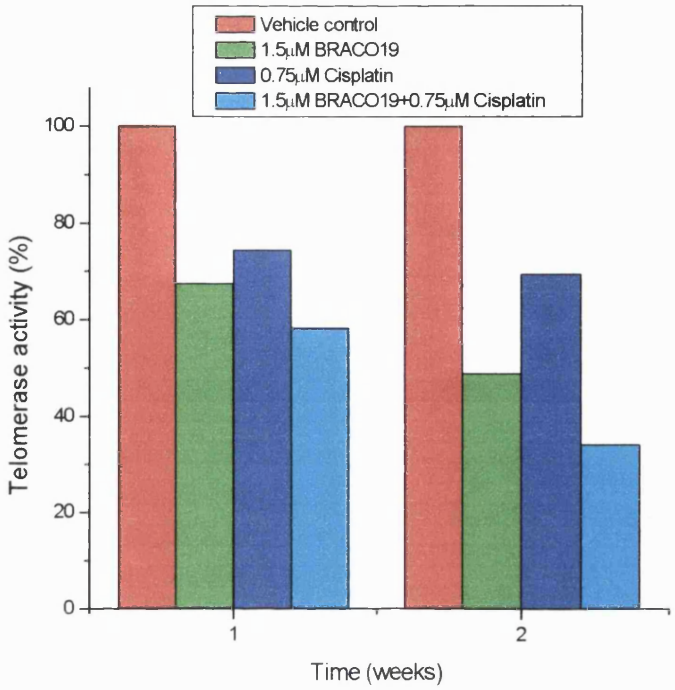

B

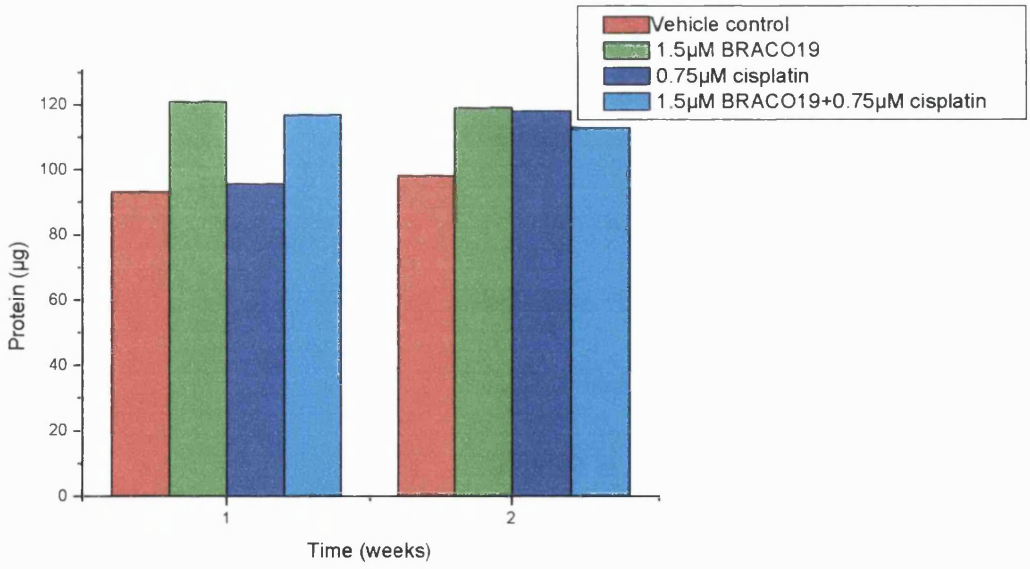

Figure 5.10. A. Telomerase activity in A431 cells treated with BRACO19 or cisplatin as single agents or as a combination for one and two weeks. B. Total cellular protein was extracted from pellets ($5x10^5$cells) and 500ng of protein was subsequently used to measure telomerase activity by the TRAP method.

5.4 Discussion

The effect of cisplatin, BRACO19 or the combination of both agents on DNA led to phosphorylation of H2AX as an early DNA damage response. Remarkably, the combination treatment showed more intense effects compared to single treatments that were at a maximum after 12 hours of exposure. It has been previously shown that cisplatin induces the formation of γH2AX foci as a DNA damage signal. One study showed maximum increase in γH2AX after only 3 hours in Hela cells treated with cisplatin *(Huang et al, 2004)*. The appearance of γH2AX after treatment with cisplatin may occur as a consequence of the double-stranded breaks produced during repair of cisplatin adducts in the DNA. However, the appearance of γH2AX after treatment with BRACO19, may be more related to the effect on telomeres. G-quadruplex binders were designed to bind to G-quadruplexes that may be formed at the 3'-telomeric overhang in order to inhibit the action of telomerase, and produce telomere shortening and therefore senescence or apoptosis. However, they show much more rapid effects than conventional telomerase inhibitors. There is increasing evidence suggesting that these ligands provoke uncapping of the telomeric overhang *(Riou, 2004)*. One of the most potent G-quadruplex stabilising agents, telomestatin, has been shown to provoke delocalisation of POT1 from telomeres. This effect on telomeres was accompanied by DNA damage response with an increase in γH2AX foci, partially localised on the telomeres *(Gomez et al, 2006)*. BRACO19 has been shown to produce delocalisation of POT1 in the HT1080 tumour cell line transfected with GFP-hPOT1 *(Gunaratnam et al, 2007)*. It seems that the effect on telomere capping may produce DNA damage response that can be detected as γH2AX foci. Other G-quadruplex stabilising agents have also been shown to induce phosphorylation of H2AX. The ligand RHPS4 induces the formation of γH2AX foci after short-time treatment. They used telomere probes to demonstrate that these γH2AX foci are located in the telomeres *(Phatak et al, 2007)*. Combination treatment as has been mentioned above produces higher % of γH2AX. Therefore, the combination of both agents induce higher DNA damage response that implicates the up-regulation of DNA repair enzymes such as PARP1 as it has been previously shown in this study (see chapter 4).

The uncapping of the telomere produces the formation of different types of chromosomal abnormalities *(Bolzán and Bianchi, 2006; Murname, 2006)*.

Chromosomes that possess their telomeres unprotected tend to fuse its chromatids. Consequently, they fuse with other chromosomes forming an end-to-end fusion. Different G-quadruplex binders have been proved to produce chromosome abnormalities. In some cases, when the doses of these agents are reduced it is possible to observe long-term effect and these chromosome end-to-end fusions are sometimes accompanied by telomere shortening that could occur due to telomerase inhibition. The triazine derivative compound ligand 12459 has been shown to provoke the formation of chromosomal aberrations in different cell lines such as A549, JFD10 and JFD18 due to an effect on the capping of the telomeres *(Gomez et al, 2003)*. The pentacyclic acridinium compound RHPS4 produces telomere fusions in uterus carcinoma cells UXF1138L. This compound has been shown to displace the telomerase catalytic subunit from the nucleus and it also delocalises POT1 from the telomeres and as a consequence induces DNA damage response and chromosomal fusions *(Phatak et al, 2007; Salvati et al, 2007)*. Telomestatin treatment in SiHa cancer cells produces delocalization of TRF2 from telomeres and loss of telomeric overhang that lead to telomere fusions *(Tahara et al, 2006)*. BRACO19 has been reported to cause telomere fusions in the prostate DU145 cell line *(Incles et al, 2004)*. BRACO19 has also been shown to induce chromosomal abnormalities in UXF1138L *(Burger et al, 2005)*. Upon one week of treatment the number of chromosome abnormalities was not significant for BRACO19 or cisplatin as single treatments. However, the concentrations used in this study did not produce a significant effect on cell viability after one week of treatment. On the other hand, the combination of both compounds produced a dramatic increase in chromosomal abnormalities such as chromosome end-to-end fusions, as a result of the effect of both agents on the telomeres. In agreement with our previous studies (see chapter 2), BRACO19 and cisplatin have synergistic effects.

Inhibition of telomerase activity was found after treatment with both agents and interestingly, a more marked effect was observed following combination treatment. Inhibition of telomerase activity enhances the effect of cisplatin in different cell lines *(Misawa et al, 2002)*. The effect on telomerase activity seems to have a link to the DNA repair machinery. NHOF cells transfected with h-TERT have enhanced DNA repair *(Shin et al, 2004)*, consequently telomerase inhibition could produce a negative effect on DNA repair that leads to the accumulation of cisplatin adducts and explain the

synergism observed. Other studies using human melanoma cells expressing mutant h-TERT characterized by telomere dysfunction showed an enhancement in cisplatin activity. Furthermore, h-TERT gene expression was reduced after BRACO19 treatment and very similar reduction occurred after combination treatment whereas cisplatin treatment in A431 cells did not produce any change in h-TERT expression. At my request, Alan Todd searched for sequences which can potentially form G-quadruplexes on the pattern G_{3-5} $N_{1-7}G_{3-5}$ N_{1-7} G_{3-5} N_{1-7} G_{3-5} in the promoter region of h-TERT. The following region was found:

-109 to -41 5′ CCCCG CCCC GTCCCGACCCC TCCC GGGTCCCCGG
GGGGCGGGGCAGGGCTGGGGAGGGCCCAGGGGCC

CCCAG CCCCCT CCGGGCCCTCCC AGCCCCTCCCC 3′
GGGTCGGGGGAGGCCCGGGAGGGTCGGGGAGGGG

It could be that these G-quadruplexes act by controlling the transcription of h-TERT. Therefore, the down-regulation of h-TERT could be explained as a consequence of the stabilisation of these G-quadruplexes by BRACO19. The existence of several motifs in h-TERT promoter that are able to form G-quadruplex structures has been previously published, and the G-quadruplex ligand 12459 has been shown to have selectivity against these G-quadruplex by the PCR-stop assay *(Gomez et al, 2004)*. Another G-quadruplex ligand the pentacyclic acridine derivative RHPS4, has been shown to produce decrease in h-TERT expression in 21NT cells *(Gowan et al, 2001)*.

Cisplatin produces inhibition of telomerase activity in several human cell lines such as a hepatoma cell line *(Furuta et al, 2003; Zhang et al, 2002)*, ovarian cancer cells *(Kunifuji, 2002)*, testicular cancer *(Burger et al, 1997)*. However, this effect seems to be cell type dependent *(Zhang et al, 2002)*. There are different possible mechanisms that could explain the effect of cisplatin on telomerase activity. One possible explanation is that cisplatin binds to this guanine rich motif in the RNA subunit of telomerase inhibiting the action of telomerase. The second possible theory is that cisplatin binds to G-quadruplexes in the loop regions and prevent the unfolding of the DNA single strand telomeric sequences, also producing inhibition of telomerase *(Redon et al, 2003)*. However, the results published on the effect of cisplatin on telomerase activity are

inconsistent; cisplatin does not produce telomerase inhibition in nasopharyngeal cancer cells *(Ku et al, 1997)*.

The effect on telomere length was also studied in A431 cells. The reason of choosing the 0.5μM cisplatin+1μM BRACO19 combination is that it is not as aggressive and efficient as the 0.75μM cisplatin+1.5μM BRACO19 combination and it may allow the detection of a change in telomere length after a few weeks of treatment due to the effect on telomerase inhibition. However, no differences were observed for either BRACO19 or cisplatin as single agents or the combination. BRACO19 produces telomere shortening in other cells lines after long-term treatment *(Burger et al, 2005; Gunaratnam et al, 2007)*. For that reason, A431 cells were treated with 1.5μM BRACO19 for a longer period of time, up to seven weeks. A431 cells presents very short telomeres ~2.5kb. Nevertheless, there was no telomere shortening after long treatment with BRACO19 in the epidermis carcinoma cell line A431. On the other hand, the long-term effect of BRACO19 in the ovarian carcinoma cell line A2780 was also studied. A2780 cells present longer telomeres than A431 cells ~6kb. A2780 cells were treated with 2μM BRACO19 up to five weeks. This concentration is not very effective in terms of cell growth (see chapter 2); however, it reduces telomere length by ~2kb after five weeks exposure. It seems that the effect of G-quadruplex stabilising agents on telomere length may be either concentration dependent or cell type dependent.

Cisplatin has been shown to produce a decrease in telomere length in several cell lines. High doses of cisplatin in Hela cells did not produce telomere shortening; these treatments activated apoptotic pathways in 12 hours and did not allow cells to complete S-phase. However, lower doses of cisplatin in the same cell line allow cells to complete cell division and lead to telomere shortening before cells undergo apoptosis. *(Ishibashi and Lippard, 1998)*. Cisplatin treatment in BEL-7404 hepatoma cells also led to telomere shortening *(Zhang et al, 2002)*.

One of the advantages of these G-quadruplex stabilising compounds is that they have effects against those cancer cells without telomerase activity which possess an alternative mechanism to maintain their telomeres *(Gowan et al, 2001; Pennarun et al, 2005; Kim et al, 2003)*. However, this can also be seen as a down-side due to the action

being targeted towards telomeres and therefore the adverse effects could be extended to non-cancerous cells. Nevertheless, due to the differences between normal and cancer cells, it is possible to find selectivity against cancer cells. The RHPS4 compound showed selectivity against tumour cells compared to normal cells. The RHPS4 ligand was unable to delocalise POT1 and TRF2 in normal human cells. One of the possible explanations is that cancer cells exhibit a higher proliferating rate. However, highly proliferating normal human peripheral blood lymphocytes were resistance to the same treatment. *(Salvati et al, 2007)*. Telomestatin treatment (5μM) that killed 90% of cancer cells within one week did not show toxicity in normal epithelial and fibroblast cells. Normal cells treated at this concentration were viable up to five weeks. Furthermore, this treatment was shown to induce chromosomal abnormalities and apoptosis only in cancer cells used in this study, but not in normal cells *(Tahara et al, 2006)*. Recent studies have shown that telomerase may be involved in the capping of telomeres *(Masutomi et al, 2005; Sung et al, 2005)*. The uterus UXF1138L cancer cells upon treatment with BRACO19 showed decrease in nuclear h-TERT expression. Therefore, BRACO19 acts by interfering with telomerase capping function *(Burger et al, 2005)*. Another G-quadruplex stabilising agent, the RHPS4 ligand, produced similar result in the same cell line; RHPS4 displaced telomerase catalytic subunit from the nucleus whereas cytoplasmic h-TERT protein signal was more intense after treatment. This is suggesting that these ligands displaced h-TERT from the nucleus to the cytoplasm *(Phatak et al, 2007)*.

Additionally, conventional telomerase inhibitors need a long time lag until effects are apparent, and this is a major problem in cancer therapy. However, this problem is not relevant to G-quadruplex agents that show more rapid effects. In this study it was demonstrated when BRACO19 and cisplatin are used in combination they potentiate their effects on telomeres. Therefore, these agents may have more clinical applicability. Furthermore, the use of these agents in combination with drugs that enhance their effects make an attractive strategy for cancer therapy.

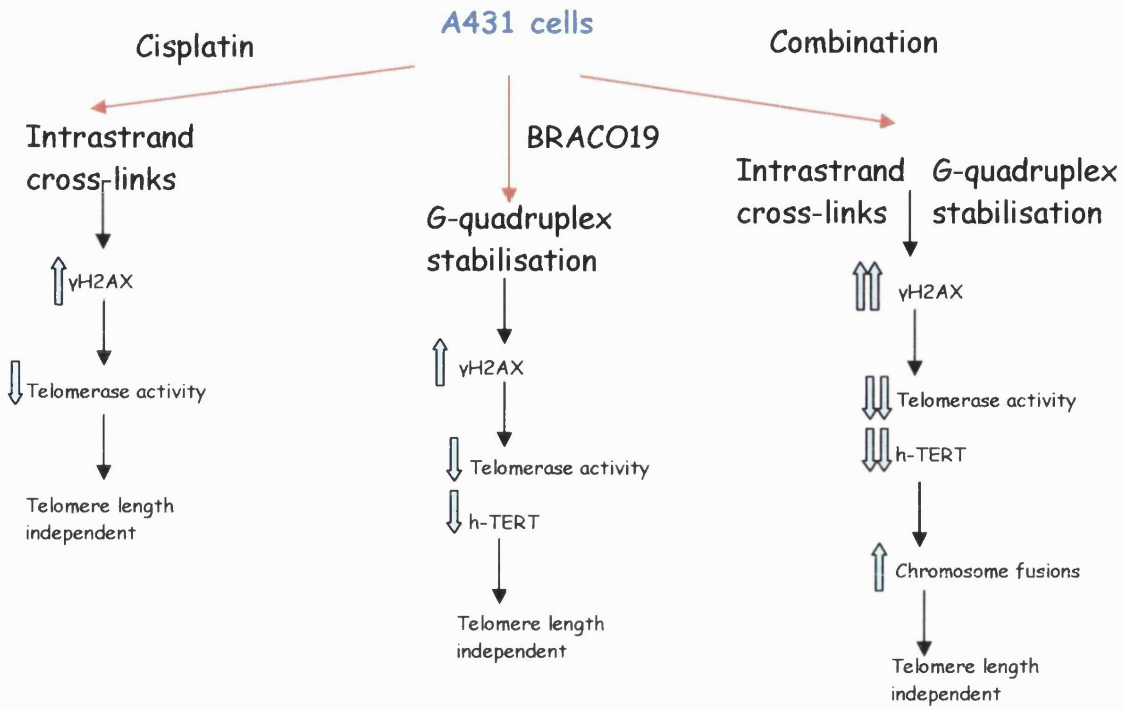

Figure 5.11 Scheme of telomere associated DNA damage response in A431cells following treatment with cisplatin, BRACO19 or the combination of both compounds (see text for details).

Chapter 6- CONCLUSIONS

The aim of this thesis was to study the combination of BRACO19 and cisplatin in various cancer cell lines and to investigate the mechanism of action of both agents in combination.

Combination studies using median-effect plot analysis showed that combining BRACO19 and cisplatin produced synergistic cell kill after 4 days treatment in the different cell lines used in this study; the epidermis carcinoma A431, the breast cancer MCF-7 and the ovarian cell lines A2780 and A2780cis. In this study different ratio of drugs were used in order to find the best combination. Although these cell lines have different sensitivity against this combination treatment all the cell lines followed the same pattern, when the concentration of BRACO19 compared to cisplatin is greater the combination is superior and is synergistic for all of them. Other studies have shown antagonism between cisplatin and another G-quadruplex stabilising agent, the pentacyclic acridine RHPS4 *(Cookson et al, 2005)*. The combination index indicated antagonism when MCF-7 breast cancer cells were treated with a constant ratio of 1:4 (RHPS4:cisplatin). However, results for other ratios were not shown and it could be that changing the ratio by increasing the concentration of RHPS4 would lead to an improved outcome.

Long-term viability studies using sub-cytotoxic concentrations showed definite synergism for A431 and MCF-7 cells, and complete cessation of cell growth after two weeks of treatment for the combination at concentrations for both compounds that do not produce a significant effect when used as single agents. However, the effect of the combination in the ovarian cell lines was additive at the concentrations used in this study. These long-term studies allowed us to investigate if there is a correlation between what was observed after short-term exposure and most importantly to ensure that the effect was maintained.

There is increasing evidence to explain the synergism between these compounds:

1. The effectiveness of cisplatin is correlated with the number of DNA adducts that forms, therefore if there is an agent that interferes with DNA repair machinery, this agent will potentiates the effect of cisplatin *(Rodriges et al, 2004)*.

2. Telomerase activity seems to have a link with the DNA repair machinery (discussed in chapter 2). Telomerase inhibition could produce a negative effect on DNA repair that leads to the accumulation of cisplatin adducts and explain the synergy observed. As a result the indirect effect of BRACO19 on telomerase could have a positive effect on the combination.

3. Furthermore, it has been previously demonstrated that telomere dysfunction more than telomerase inhibition is the principal determinant of chemosensitivity towards cisplatin (discussed in chapter 2). Subsequently a G-quadruplex stabilising agent such as BRACO19 which has a direct effect on the telomere overhang would have a more rapid and effective effect, therefore it would be more appropriate to combine cisplatin with a G-quadruplex stabilising agent than with a conventional telomerase inhibitor.

4. Finally, it is very important to use new strategies in order to avoid the appearance of resistance to treatment. Resistance to cisplatin has been related to telomere elongation and telomerase activity *(Mese et al, 2001)*, consequently, the effect of BRACO19 on telomerase activity and telomeres can be used as a good approach to avoid the appearance of resistance towards cisplatin.

EFFECTS ON TELOMERES AND TELOMERASE

In this study it was demonstrated that the effect of both agents on telomeres and telomerase were potentiated. Upon one week of treatment the number of chromosome abnormalities was not significant for BRACO19 or cisplatin as single treatments. On the other hand, the combination of both compounds produced a dramatic increase in chromosome end-to-end fusions, as a result of the effect of both agents on the telomeres. Inhibition of telomerase activity was found after treatment with both agents and interestingly, a more marked effect was observed following combination treatment. Furthermore, h-TERT gene expression was reduced after BRACO19 treatment and a very similar reduction occurred after combination treatment. In agreement with previous combination index studies, BRACO19 and cisplatin seem to have synergistic effects.

CELL GROWTH INHIBITION STUDIES

In the MCF-7 cell line, there was induction of senescence for both agents and also for the combination. The onset of senescence was time and concentration dependent for both compounds, and the combination showed a more marked effect. However, in the A431 cell line, there was no induction of senescence even at very high concentrations of BRACO19 or cisplatin. It has previously been shown that in order to prevent senescence the two main regulator genes p53 and Rb have to be inactivated *(Smogorzewska and de Lange, 2002)*. However, the inactivation of p53 seems to be sufficient to avoid or delay the appearance of senescence in some cell lines *(Beauséjour et al, 2003)*. A431 cells have a p53 inactive protein mutated at codon 273 *(Lanzi et al, 1998)*, but they have wild-type Rb *(Ahmad et al, 1999)*. Remarkably, A431 cells with dominant-negative TERT do not undergo senescence after telomere shortening and chromosome breakage; cells undergo apoptosis. A431 cells treated with cisplatin produced a very rapid apoptotic response which is caspase 3-dependent, whereas BRACO19 treatment produced necrotic cell death. The combination of both compounds also produced necrotic cell death but it also led to a dramatic decrease in cell proliferation.

G-quadruplex binders show much more rapid effects than conventional telomerase inhibitors, and short-term effects seem to be more related to the action of these ligands in the capping of the telomeres. The uncapping of telomeres is recognised as a DNA

strand break or DNA damage and DNA damage machinery is activated. Due to the action being targeted towards telomeres, these compounds have also effects against those cancer cells without telomerase activity which possess an alternative mechanism to maintain their telomeres *(Gowan et al, 2001; Pennarun et al, 2005; Kim et al, 2003).* This could also be seen as a down-side because the effects could be extended to non-cancerous cells. However, due to the differences between normal and cancer cells, it is possible to find selectivity against cancer cells (discussed in chapter 5). Another advantage of these G-quadruplex binders compared to conventional telomerase inhibitors is that they have very rapid effects and the lag phase problem is non-existent. Therefore, these agents may have more clinical applicability. Furthermore, the uses of these agents in combination with drugs that enhance their effects make them an attractive strategy for cancer therapy.

FUTURE WORK

As has been mention above, the effectiveness of cisplatin is correlated with the number of DNA adducts that form; therefore any agent that interferes with DNA repair machinery will avoid the repair of these adducts and will potentiates the effect of cisplatin. We observed inhibition of telomerase and decrease in h-TERT expression following BRACO19 treatment. Therefore, telomerase inhibition could produce inhibition of DNA repair that leads to the accumulation of cisplatin adducts and explains the synergy observed. In order to corroborate this hypothesis, future work could focus on studying the number of DNA adducts formed following single agent and combination treatment. An increase in the number of DNA adducts in the combination would mean that BRACO19 is actually interfering with the DNA repair machinery.

It seems that when the concentration of BRACO19 compared to cisplatin is greater the combination is superior and is synergistic for all of them. It would be of interest to study if there is actually an interaction between the two compounds. First of all, uptake studies of both agents alone and then in combination could be performed. It would be of importance to measure the amount that has been taken up and therefore, if the uptake of one compound is affecting the uptake of the other compound. It would be also of interest to study if these two agents interact with each other or on the contrary if they are stable after they have been taken up by the cells.

Disruption of the "capped" status of the chromosomes due to the action of a DNA damaging agent or a telomerase inhibitor is recognised as a DNA strand break and can be detected as γH2AX foci. Different G-quadruplex stabilising agents have previously been shown to induce early DNA damage response. The ligand RHPS4 induces the formation of γH2AX foci after short-time treatment and it has been shown that these γH2AX foci are located in the telomeres with the use of telomere probes *(Phatak et al, 2007)*. However, the appearance of γH2AX after treatment with cisplatin may occur as a consequence of the double-stranded breaks produced during repair of cisplatin adducts in the DNA. Cisplatin has selectivity towards guanine bases in the DNA; therefore G-rich regions in the genome such as telomeres are potential targets of cisplatin. In this study we demonstrated that both agents induce a DNA damage response; however, the use of telomere probes could serve to investigate if γH2AX foci formed after BRACO19 or cisplatin treatments are actually located in the telomeres. This will give us much information about how these two compounds interact.

Another point of interest could be the study of the effect of this combination treatment in the A431 cisplatin resistant cell line. The appearance of resistance to cisplatin treatment has limited its use in clinic. The uses of new strategies of treatment which are effective against tumours that have become resistant to cisplatin are of major importance in cancer therapy. A comparative study using both A431 and A431 cisplatin resistant cell lines, firstly comparing the effectiveness of this combination therapy and secondly investigating different possible mechanisms of resistance could give us information about if this therapy could be of utility in these resistant cancers.

Finally, this is an *in vitro* approach that gives an idea of the effectiveness of this combination, and other *in vivo* studies have to be carried out to investigate if there is correlation with what was found here.

REFERENCES

Adjei A. A, Budihardjo I. I, Rowinsky E. K, Kottke T. J, Svingen P. A, Buckwalter C. A, Grochow L. B, Donehower R. C, Kaufmann S. H. Cytotoxic synergy between pyrazoloacridine (NSC 366140) and cisplatin in vitro: inhibition of platinum-DNA adduct removal. *Clinical Cancer Research.* 3, 761-770 (1997).

Agami R, Blandino G, Oren M, Shaul Y. Interaction of c-Abl and p73α and their collaboration to induce apoptosis. *Nature.* 399, 809-813 (1999).

Ahmad N, Gupta S, Mukhtar H. Involvement of retinoblastoma (Rb) and E2F transcription factors during photodynamic therapy of human epidermoid carcinoma cells A431. *Oncogene.* 18, 1891-1896 (1999).

Aliouat-Denis C. M, Dendouga N, van den Wyngaert I, Goehlmann H, Steller U, van de Weyer I, van Slycken N, Andries L, Kass S, Luyten W, Janicot M, Vialard J. E. p53-independent regulation of $p21^{waf1/Cip1}$ expression and senescence by Chk2. *Molecular Cancer Research.* 3, 627-634 (2005).

Ashkenazi A, Dixit V. M. Death Receptors: Signaling and Modulation. *Apoptosis.* 281, 1305-1308 (1998).

Barros L. F, Hermosilla T, Castro J. Necrotic volume increase and the early physiology of necrosis. *Comparative Biochemistry and Physiology Part A.* 130, 401-409 (2001).

Beauséjour C. M, Krtolica A, Galimi F, Narita M, Lowe S. W, Yaswen P, Campisi J. Reversal of human cellular senescence: roles of the p53 and p16 pathways. *The EMBO Journal.* 22, 4212-4222 (2003).

Bellamy W. T. Prediction of response to drug therapy of cancer. A review of in vitro assays. *Drugs.* 44, 690-708 (1992).

Ben-Porath I, Weinberg R. A. The signals and pathways activating cellular senescence. *The International Journal of Biochemistry and Cell Biology.* 37, 961-976 (2005).

Bhatia M. Apoptosis versus necrosis in acute pancreatitis. *AJP Gastrointestinal and Liver Physiology.* 286, 189-196 (2004).

Binz N, Shalaby T, Rivera P, Shin-ya K, Grotzer M. A. Telomerase inhibition, telomere shortening, cell growth suppression and induction of apoptosis by telomestatin in childhood neuroblastoma cells. *European Journal of Cancer.* 41, 2873-2881 (2005).

Biroccio A, Gabellini, C Amodei S, Benassi B, del Bufalo D, Elli R, Antonelli A, D'Incalci M and Zupi G. Telomere dysfunction increases cisplatin and Ecteinascidin-743 sensitivity of melanoma cells. *Molecular Pharmacology.* 63, 632-638 (2003).

Blackburn E. H. Telomere states and cell fates. *Nature.* 408, 53-56 (2000).

Blackburn E. H. Switching and signalling at the telomere. *Cell.* 106, 661-673 (2001).

Boik J. C, Newman R. A, Boik R. J. Quantifying synergism/antagonism using nonlinear mixed-effects modelling: a simulation study. *Statistics in Medicine.* Published on line. (2007).

Boldt S, Weidle U. H, Kolch W. The role of MAPK pathways in the action of chemotherapeutic drugs. *Carcinogenesis*. 23, 1831-1838 (2002).

Bolzán A. D, Bianchi M. S. Telomeres, interstitial telomeric repeat sequences, and chromosomal aberrations. *Mutation Research*. 612, 189-214 (2006).

Bortner C. D, Oldenburg N. B. E, Cidlowski J. A. The role of DNA fragmentation in apoptosis. *Trends in Cell Biology*. 5, 21-26 (1995).

Brabec V, Kasparkova J. Modifications of DNA by platinum complexes relation to resistance of tumors to platinum antitumor drugs. *Drug Resistance Updates*. 8, 131-146 (2005).

Brown J. M, Wouters B. G. Apoptosis, p53, and tumor cell sensitivity to anticancer agents. *Cancer Research*. 59, 1391-1399 (1999).

Burge S, Parkinson G. N, Hazel P, Todd A. K, Neidle S. Survey and summary. Quadruplex DNA: sequence, topology and structure. *Nucleic Acids Research*. 34, 5402-5415 (2006).

Burger A. M, Double J. A, Newell D. R. Inhibition of telomerase activity by cisplatin in human testicular cancer cells. *European Journal of Cancer*. 33, 638-644 (1997).

Burger A. M, Dai F, Schultes C. M, Reszka A. P, Moore M. J, Double J. A, Neidle S. The G-quadruplex-interactive molecule BRACO19 inhibits tumor growth, consistent with telomere targeting and interference with telomerase function. *Cancer Research*. 65, 1489-1496 (2005).

Burkhart B. A, Alcorta D. A, Chiao C, Isaacs J. S, Barrett J. C. Two posttranscriptional pathways that regulate p21 are identified by HPV16-E6 interaction and correlate with life span and cellular senescence. *Experimental Cell Research*. 247, 168-175 (1999).

Campisi J. Cellular senescence as a tumor-suppressor mechanism. *Trends in Cell Biology*. 11, 27-31 (2001).

Carini R, Autelli R, Bellomo G, Dianzani M. U, Albano E. Sodium-mediated cell swelling is associated with irreversible damage in isolated hepatocytes exposed to hypoxia or mitochodrial toxins. *Biochemistry Biophysics Research Community*. 206, 180-185 (1995).

Chen J. L, Blasco M. A, Greider C. W. Secondary structure of vertebrate telomerase RNA. *Cell*. 100, 503-514 (2000).

Chen J. L, Opperman K. K, Greider C. W. A critical stem-loop structure in the CR4-CR5 domain of mammalian telomerase RNA. *Nucleic Acids Research*. 30, 592-597 (2002).

Chen J. L, Greider C. W. An emerging consensus for telomerase RNA structure. *Proceedings of the National Academy of Sciences USA*. 101, 14683-14684 (2004).

Chiu C. P, Dragowska W, Kim N. W, Vaziri H, Yui J, Thomas T. E, Harley C. B, Lansdorp P. M. Differential expression of telomerase activity in hematopoietic progenitors from adult human bone marrow. *Stem Cells*. 14, 239-248 (1996).

Chiu C. P, Harley C. B. Replicative senescence and cell immortality: the role of telomeres and telomerase. *Proceedings of the Society for Experimental Biology and Medicine*. 214, 99-106 (1997).

Chou T. C, Talalay P. Analysis of combined drug effects: a new look at a very old problem. *Trens in Pharmacology Science*. 4, 450-454 (1983)

Chou T. C, Talalay P. Quantitative analysis of dose-effect relationship: The combined effects of multiple drugs on enzyme inhibitors. *Advances in Enzyme Regulation*. 22, 27-44 (1984).

Chou T. C. Theoretical basis, experimental design, and computerized simulation of synergism and antagonism in drug combination studies. *Pharmacological Reviews*. 58, 621-681 (2006).

Chowdhury D, Keogh M. C, Ishii H, Peterson C. L, Buratowski S, Lieberman J. γH2AX dephosphorylation by protein phosphatase 2A facilitates DNA double-strand break repair. *Molecular Cell*. 20, 801-809 (2005).

Cohen G. M, Sun X. M, Snowden R. T, Dinsdale D, Skilleter D. N. Key morphological features of apoptosis may occur in the absence of internucleosomal DNA fragmentation. *Biochemistry*. 286, 331-334 (1992).

Cookson J. C, Dai F, Smith V, Heald R. A, Laughton C. A, Stevens M. F. G, Burger A. M. Pharmacodynamics of the G-quadruplex-stabilizing telomerase inhibitor 3, 11-difluoro-6,8,13-trimethyl-8H-quino(4,3,2-kl)acridium methosulfate (RHPS4) in vitro: activity in human tumor cells correlates with telomere length and can be enhanced, or antagonized, with cytotoxic agents. *Molecular Pharmacology*. 68, 1551-1557 (2005).

Coste F, Malinge J. M, Serre L, Shepard W, Roth M, Leng M, Zelwer C. Crystal structure of a double-stranded DNA containing a cisplatin interstrand cross-link at 1.63 A resolution: hydration at the platinated site. *Nucleic Acids Research*. 27, 1837-1846 (1999).

Counter C. M, Avilion A. A, LeFeuvre C. E, Stewart N. G, Greider C. W, Harley C. B, Bacchetti S. Telomere shortening associated with chromosome instability is arrested in immortal cells which express telomerase activity. *The EMBO Journal*. 11, 1921-1929 (1992).

Cristofalo V. J, Lorenzini A, Allen R. G, Torres C, Tresini M. Replicative senescence: a critical review. *Mechanism of Ageing and Development*. 125, 827-48 (2004).

Crompton M. The mitochondrial permeability transition pore and its role in cell death. *Biochemistry Journal*. 341, 233-249 (1999).

Davis J. T. G-quartets 40 years later: from 5′-GMP to molecular biology and supramolecular chemistry. *Angewandte Chemie International Edition*. 43, 668-698 (2004).

Dantzer F, Giraud-Panis M. J, Jaco I, Ame J. C, Schultz I, Blasco M, Koering C. E, Gilson E, Menissier de Murcia J, de Murcia G, Schreiber V. Functional interaction between Poly(ADP-Ribose)polymerase 2 (PARP-2) and TRF2: PARP activity negatively regulates TRF2. *Molecular and Cellular Biology*. 24, 1595-1607 (2004).

Dijt F. J, Fichtinger-Schepman A-M. J, Berends F, Reedijk J. Formation and repair of ciplatin-induced adducts to DNA in cultured normal and repair-deficient human fibroblast. *Cancer Research*. 48, 6058-6062 (1988).

Dikmen Z. G, Wright W. E, Shay J. W, Gryaznow S. M. Telomerase targeted oligonucleotide thio-phosphoramidates in T24-luc bladder cancer cells. *Cancer Research*. 65, 7866-7873 (2005).

Dimri G. P, Lee X, Basile G, Acosta M, Scott G, Roskelley C, Medrano E. E, Linskens M, Rubelj I, Pereira-Smith O, Peacocke M, Campisi J. A biomarker that identifies senescent human cells in culture and in aging skin in vivo. *Proceedings of the National Academy of Sciences USA*. 92, 9363-9367 (1995).

Dixon I. M, Lopez F, Esteve J P, Tejera A. M, Blasco M. A, Pratviel G, Meunier B. Porphyrin derivatives for telomere binding and telomerase inhibition. *Chemobiochemistry*. 6, 123-132 (2005).

Djojosubroto M. W, Choi Y. S, Lee H. W, Rudolph K. L. Telomeres and telomerase in aging, regeneration and cancer. *Molecules and Cells*. 15, 164-175 (2003).

Du Z, Zhao Y, Li N. Genome-wide analisis reveals regulatory role of G4 DNA in gene transcription. *Genome Research*. 18, 233-241 (2008).

Duquette M. L, Handa P, Vincent J. A, Taylor A. F, Maizels N. Intracellular transcription of G-rich DNAs induces formation of G-loops, novel structures containing G4DNA. *Genes and Development*. 18, 1618-1629 (2004).

Eastmant A, Jennerwein M. M , Nagel D. L. Characterization of bifunctional adducts produced in DNA by trans-diamminedichloroplatinum. *Chemico-Biological Interactions*. 67, 71-80 (1988).

El-Daly H, Kull M, Zimmermann S, Pantic M, Waller C. F, Martens U. M. Selective cytotoxicity and telomere damage in leukaemia cells using the telomerase inhibitor BIBR1532. *Blood*. 105, 1742-1749 (2005).

Elizondo-Riojas M. A, Kozelka J. Unrestrained 5 ns molecular dynamics simulation of a cisplatin-DNA 1, 2-GG adduct provides a rationale for the NMR features and reveals increased conformational flexibility at the platinum binding site. *Journal of Molecular Biology*. 314, 1227-1243 (2001).

Fernandez-Capetillo O, Lee A, Nussenzweig M, Nussenzweig A. H2AX: the histone guardian of the genome. *DNA Repair*. 3, 959-967 (2004).

Ferrari S, Palmerini E. Adjuvant and neoadjuvant combination chemotherapy for osteogenic sarcoma. *Current Opinion in Oncology*. 19, 341-346 (2007).

Fink D, Nebel S, Aebi S, Zheng H, Cenni B, Nehme A, Christen R. D, Howell S, B. The role of DNA mismatch repair in platinum drug resistance. *Cancer Research.* 56, 4881-4886 (1996).

Fulda S, Debatin K. M. Extrinsic versus intrinsic apoptosis pathway in anticancer chemotherapy. *Oncogene.* 25, 4798-47811 (2006).

Furuta M, Nozawa K, Takemura M, Izuta S, Murate T, Tsuchiya M, Yoshida K, Taka N, Nimura Y, Yoshida S. A novel platinum compound inhibits telomerase activity in vitro and reduces telomere length in a human hepatoma cell line. *International Journal of Cancer.* 104, 709-715 (2003).

Galluzzi L, Zamzami N, de La Motte Rouge T, Lemaire C, Brenner C, Kroemer G. Methods for the assessment of mitochondrial membrane permeabilization in apoptosis. *Apoptosis.* 12, 803-13 (2007).

Garnier I. O, Bombard S. GG sequence of DNA and the human telomeric sequence react with *cis*-diammine-diaquaplatinum at comparable rates. *Journal of Inorganic Biochemistry.* 101, 514-524 (2007).

Ghazizadeh M. Cisplatin may induce frataxin expression. *Journal Nippon Medical School.* 70, 367-371 (2003).

Gilley D, Blackburn E. H. The telomerase RNA pseudoknot is critical for the stable assembly of a catalytically active ribonucleoprotein. *Proceedings of the National Academy of Sciences USA.* 96, 6621-6625 (1999).

Gogvadze V, Orrenius S. Mitochondrial regulation of apoptotic cell death. *Chemico-Biological Interactions.* 163, 4-14 (2006).

Goldoni M, Johansson C. A mathematical approach to study combined effects of toxicans in vitro: Evaluation of the Bliss independence criterion and the Loewe additivity model. *Toxicology in Vitro.* 21, 759-769 (2007).

Gomez D, Aouali N, Londoño-Vallejo A, Lacroix L, Mégnin-Chanet F, Lemarteleur T, Douarre C, Shin-ya K, Mailliet P, Trentesaux C, Morjani H, Mergny J. L, Riou J. F. Resistance to the short term antiproliferative activity of the G-quadruplex ligand 12459 is associated with telomerase overexpression and telomere capping alteration. *The Journal of Biological Chemistry.* 278, 50554-50562 (2003).

Gomez M, Wu J, Schreiber V, Dunlap J, Dantzer F, Wang Y, Liu Y. PARP1 is a TRF2 associated Poly(ADP-Ribose) Polymerase and protects eroded telomeres. *Molecular Biology of the Cell.* 17, 1686-1696 (2006).

Gomez D, Lemarteleur T, Lacroix L, Mailliet P, Mergny J. L, Riou J. F. Telomerase downregulation induced by the G-quadruplex ligand 12459 in A549 cells is mediated by hTERT RNA alternative splicing. *Nucleic Acids Research.* 32, 371-379 (2004).

Gomez D, Wenner T, Brassart B, Douarre C, O'Donohue M. F, El Khoury V, Shin-ya K, Morjani H, Trentesaux, Riou J. F. Telomestatin induced telomere uncapping is modulated by POT1 through G-overhang extension in HT1080 human tumor cells. *The Journal of Biological Chemistry.* 281, 38721-38729 (2006).

Gong J. G, Costanzo A, Yang H. Q, Melino G, Kaelin W. G, Levrero M, Wang J. Y. L. The tyrosine kinase c-Abl regulates p73 in apoptotic response to cisplatin-induced DNA damage. *Nature*. 399, 806-809 (1999).

Gonzalez V. M, Fuertes M. A, Alonso C, Perez J.M. Is cisplatin induced cell death always produced by apoptosis?. *Molecular Pharmacology*. 59, 657-663 (2001).

Gowan S. M, Heald R, Stevens M. F. G, Kelland L. R. Potent inhibition of telomerase by small-molecule pentacyclic acridines capable of interacting with G-quadruplexes. *Molecular Pharmacology*. 60, 981-988 (2001).

Gowan S. M, Harrison J. R, Patterson L, Valenti M, Read M. A, Neidle S, Kelland L. R. A G-Quadruplex-Interactive Potent Small-Molecule Inhibitor of Telomerase Exhibiting in vitro and in vivo antitumor activity. *Molecular Pharmacology*. 61, 1154-1162 (2002).

Greco W. R, Bravo G, Parsons J. C. The search for synergy: a critical review from a response surface perspective. *Pharmacological Reviews*. 47, 331-385 (1995).

Greco W. R, Faessel H, Levasseur L. The search for cytotoxic synergy between anticancer agents: a case of Dorothy and the ruby slippers?. *Journal of the National Cancer Institute*. 88, 699-700 (1996).

Greider C. W, Blackburn E. H. Identification of a specific telomere terminal transferase activity in Tetrahymena extracts. *Cell*. 43, 405-413 (1985).

Greider C. W, Blackburn E. H. A telomeric sequence in the RNA of Tetrahymena telomerase required for telomere repeat synthesis. *Nature*. 337, 331-337 (1989).

Greider C. Telomeres do D-loop-T-loop. *Cell*. 97, 419-422 (1999).

Griffith J. D, Comeau L, Rosenfield S, Stansel R. M, Bianchi A, Moss H, Lange T. Mammalian telomeres end in a large duplex loop. *Cell*. 97, 503-514 (1999).

Gunaratnam M, Greciano O, Martins C, Reszka A. P, Schultes C. M, Morjani H, Riou J. F, Neidle S. Mechanism of acridine-based telomerase inhibition and telomere shortening. *Biochemical Pharmacology*. 74, 679-689 (2007).

Ha H. C, Snyder S. H. Poly(ADP-ribose) polymerase is a mediator of necrotic cell death by ATP depletion. *Proceedings of the National Academy of Sciences USA*. 96, 13978-13982 (1999).

Hahn W, Counter C. M, Lundberg A. S, Beijersbergen R. L, Brooks M. W, Weinberg R. A. Creation of human tumour cells with defined genetic elements. *Nature*. 400, 464-468 (1999).

Hahn W, Stewart S. A, Brooks M. W, York S. G, Eaton E, Kurachi A, Beijersbergen R. L, Knoll J. H. M, Meyerson M, Weinberg R. A. Inhibition of telomerase limits the growth of human cancer cells. *Nature*. 5, 1164-1170 (1999).

Han H, Hurley L. H. G-quadruplex DNA: a potencial target for anti-cancer drug design. *Trends in Pharmacologycal Sciences*. 21, 136-142 (2000).

Harley C. B, Futcher A. B, Greider C. W. Telomeres shorten during ageing of human fibroblasts. *Nature*. 345, 458-460 (1990).

Harrison R. J, Cuesta J, Chessari G, Read M. A, Basra S. K, Reszka A. P, Morrell J, Gowan S. M, Incles C. M, Tanious F. A, Wilson W. D, Kelland L. R, Neidle S. Trisubstituted acridines derivatives as potent and selective telomerase inhibitors. *Journal of Medicinal Chemistry*. 46, 4464-4476 (2003).

Haupt Y, Maya R, Kazaz A, Oren M. Mdm2 promotes the rapid degradation of p53. *Nature*. 387, 296-299 (1997).

Hawkins D. S, Demers G. W, Galloway D. A. Inactivation of p53 enhances sensitivity to multiple chemotherapeutic agents. *Cancer Research*. 56, 892-898 (1996).

He Q, Liang C. H, Lippard S. J. Steroid hormones induce HMG1 overexpression and sensitize breast cancer cells to cisplatin and carboplatin. *Proceedings of the National Academy of Sciences USA*. 97, 5768-5772 (2000).

Helt C. E, Cliby W. A, Keng P. C, Bambara R. A, O'Reilli M. A. Ataxia telangiectasia mutated (ATM) and ATM and Rad3-related protein exhibit selective target specificities in response to different forms of DNA damage. *The Journal of Biological Chemistry*. 280, 1186-1192 (2005).

Hemann M. T, Strong M. A, Hao L. Y, Greider C. W. The shortest telomere, not average telomere length, is critical for cell viability and chromosome stability. *Cell*. 107, 67-77 (2001).

Herbig U, Sedivy J. M. Regulation of growth arrest in senescence: telomere damage is not the end of the story. *Mechanism of Ageing and Development*. 127, 16-24 (2006).

Hiyama E, Hiyama K. Telomere and telomerase in stem cells. *British Journal of Cancer*. 96, 1020-1024 (2007).

Hockemeyer D, Sfeir A. J, Shay J. W, Wright W. E, de Lange T. POT1 protects telomeres from a transient DNA damage response and determines how human chromosome ends. *The EMBO Journal*. 24, 2667-2678 (2005).

Holzer A. K, Katano K, Klomp L. W. J, Howell S. B. Cisplatin rapidly down-regulates its own influx transporter hCTR1 in cultured human ovarian carcinoma cells. *Clinical Cancer Research*. 10, 6744-6749 (2004).

Houghtaling B. R, Cuttonaro L, Chang W, Smith S. A dynamic molecular link between the telomere length regulator TRF1 and the chromosome end protector TRF2. *Current Biology*. 14, 1621-1631 (2004).

Huang X, Okafuji M, Traganos F, Luther E, Holden E, Darzynkiewicz Z. Assesment of histone H2AX phosphorylation induced by DNA topoisomerase I and II inhibitors topotecan and mitoxantrone and by the DNA cross-linking agent cisplatin. *Cytometry*. 58, 99-110 (2004).

Huang H. S, Liu Z. M, Ding L, Chang W. C, Hsu P. Y, Wang S. H, Chi C. C, Chuang C. H. Opposite effect of ERK1/2 and JNK on p53-independent p21WAF1/CIP1

activation involved in the arsenic trioxide-induced human epidermoid carcinoma A431 cellular cytotoxicity. *Journal of Biomedical Science.* 13, 113-125 (2006).

Huard S, Moriarty T. J, Autexier C. The C terminus of the human telomerase reverse transcriptase is a determinant of enzyme processivity. *Nucleic Acids Research.* 31, 4059-4070 (2003).

Huppert J. L, Balasubramanian S. Prevalence of quadruplexes in human genome. *Nucleic Acids Research.* 33, 2908-2916 (2005).

Huppert J. L, Balasubramanian S. G-quadruplex in promoters throughout the human genome. *Nucleic Acids Research.* 35, 406-413 (2007).

Incles C. M Schultes C. M, Kempski H, Koehler H, Kelland L. R, Neidle S. A G-quadruplex telomere targeting agent produces p16-associated senescence and chromosomal fusions in human prostate cancer cells. *Molecular Cancer Therapeutics.* 3, 1201-1206 (2004).

Irwin M. S, Kondo K, Marin M. C, Cheng L. S, Hahn W. C, Kaelin W. G. Chemosensitivity linked to p 73 function. *Cancer Cell.* 3, 403-410 (2003).

Ishibashi T, Lippard S. J. Telomere loss in cells treated with cisplatin. *Biochemistry.* 95, 4219-4223 (1998).

Jaco I, Munoz P, Blasco M. A. Role of human Ku86 in telomere lenght maintenance and telomere capping. *Cancer Research.* 64, 7271-7278 (2004).

Jayaraman L, Chandra Moorthy N, Murthy K. G. K, Manley J. L, Bustin M, Prives C. High mobility group protein-1 (HMG-1) is a unique activator of p53. *Genes and Development.* 12, 462-472 (1998).

Jeyapalan J. C, Saretzki G, Leake A, Tilby M. J, von Zglinicki T. Tumour-cell apoptosis after cisplatin treatment is not telomere dependent. *International Jornal of Cancer.* 118, 2727-2734 (2006).

Kaghad M, Bonnet H, Yang A, Creancier L, Biscan J. C, Valent A, Minty A, Chalon P, Lelias J. M, Dumont X, Ferrara P, McKeon F, Caput D. Monoallelically expressed gene related to p53 at 1p36, a region frequently deleted in neuroblastoma and other human cancers. *Cell.* 90, 809-819 (1997).

Kanduc D, Mittelman A, Serpico R, Sinigaglia E, Sinha A. A, Natale C, Santacroce R, Di Corcia M. G, Lucchese A, Dini L, Pani P, Santacroce S, Simone S, Bucci R, Farber E. Cell death: Apoptosis versus necrosis (Review). *International Journal of Oncology.* 21, 165-170 (2002).

Karlseder J, Broccoli D, Dai Y, Hardy S, de Lange T. p53 and ATM-dependent apoptosis induced by telomeres lacking TRF2. *Science.* 283, 1321-1325 (1999).

Kartalou M, Essigmann J. M. Recognition of cisplatin adducts by cellular proteins. *Mutation Research.* 478, 1-21 (2001).

Kaufmann S. H, Peereboom D, Buckwalter C. A, Svingen P. A, Grochow L. B, Donehower R. C, Rowinsky E. K. Cytotoxic effects of topotecan combined with various

anticancer agents in human cancer cell lines. *Journal of the National Cancer Institute.* 88, 734-741 (1996).

Kelland L. Targeting the limitless replicative potential of cancer: the telomerase/telomere pathway. *Clinical Cancer Research.* 13, 4960-4963 (2007).

Kelleher C, Kurth I, Lingner J. Human protection of telomeres 1 (POT1) is a negative regulator of telomerase activity in vitro. *Molecular and Cellular Biology.* 25, 808-818 (2005).

Khosravi-Far R, Esposti M. E. Death receptor signals to mitochondria. *Cancer Biology and Therapy.* 3(11), 1051-1057 (2004).

Kim N. W, Piatyszek M. A, Prowse K. R, Harley C. B, West M. D, Ho P. L, Coviello G. M, Wright W. E, Weinrich S. L, Shay J. W. Specific association of human telomerase activity with immortal cells and cancer. *Science.* 266, 2011-2025 (1994).

Kim H. E, Du F, Fang M, Wang X. Formation of apoptosome is initiated by cytochrome c-induced dATP hydrolysis and subsequent nucleotide exchange on Apaf-1. *Proceedings of the National Academy of Sciences USA.* 102, 17545-17550 (2005).

Kim R. Emi M, Tanabe K, Uchida Y, Arihiro K. The role of apoptotic or nonapoptotic cell death in determining cellular response to anticancer treatment. *Europen Journal of Surgical Oncology.* 32, 269-277 (2006).

Kim M. Y, Gleason-Guzman M, Izbicka E, Nishioka D, Hurley L. H. The different biological effects of telomestatin and TMPyP4 can be attributed to their selectivity for interaction with intramolecular or intermolecular G-quadruplex structures. *Cancer Research.* 63, 3247-3256 (2003).

Kishi K, Doki Y, Yano M, Yasuda T, Fujiwara Y, Takiguhi S, Kim S, Higuchi I, Monden M. Reduced MLH1 expression after chemotherapy is an indicator for poor prognosis in esophageal cancers. *Clinical Cancer Research.* 9, 4368-4375 (2003).

Koeppel F, Riou J. F, Laoui A, Mailliet P, Arimondo P. B, Labit D, Petitgenet O, Helene C, Mergny J. L. Ethidium derivatives bind to G-quartets, inhibit telomerase and act as fluorescent probes for quadruplex. *Nucleic Acids Research.* 29, 1087-1096 (2001).

Ku W. C, Cheng A. J, Wang T. C. Inhibition of telomerase activity by PKC inhibitors in human nasopharyngeal cancer cells in culture. *Biochemistry Biophysics Research Communications.* 241, 730-6 (1997).

Kumar S. Caspase function in programmed cell death. *Cell Death and Differentiation.* 14, 32-43 (2007).

Kunifuji Y, Gotoh S, Abe T, Miura M, Karasaki Y. Down-regulation of telomerase activity by anticancer drugs in human ovarian cancer cells. *Anti-Cancer Drugs.* 13, 595-598 (2002).

de Laat W. L, Jaspers N. G. J, Hoeijmakers J. H. J. Molecular mechanism of nucleotide excision repair. *Genes and Development.* 13, 768-785 (1999).

de Lange T. Shelterin: the protein complex that shapes and safeguards human telomeres. *Genes and Development.* 19, 2100-2110 (2005)..

Lanzi C, Perego P, Supino R, Romanelli S, Pensa T, Carenini N, Colangelo D, Leone R, Apoptoli P, Cassinelli G, Gambetta R. A, Zunino F. Decreased drug accumulation and increased tolerante to DNA damage in tumor cells with a low level of cisplatin resistance. *Biochemical Pharmacology.* 55, 1247-1254 (1998).

Lee S. R, Wong J. M. Y, Collins K. Human telomerase reverse transcriptase motifs required for elongation of a telomeric substrate. *The Journal of Biological Chemistry.* 278, 52531-52536 (2003).

Legassie J. D, Jarstfer M. B. Telomerase as a DNA-dependent DNA polymerase. *Biochemistry.* 44, 14191-14201 (2005).

Legendre F, Bas V, Kozelka J, Chottard J. C. A complete kinetic study of GG versus AG platination suggests that the doubly aquated derivatives of cisplatin are the actual DNA binding species. *Chemistry European Journal.* 6, 2002-2010 (2000).

Li B, Oestreich S, de Lange T. Identification of human Rap1: Implications for telomere evolution. *Cell.* 1001, 471-483 (2000).

Lin J, Ly H, Hussain A, Abraham M, Pearl S, Tzfati Y, Parslow T. G, Blackburn E. H. A universal telomerase RNA core structure includes structured motifs required for binding the telomerase reverse transcriptase protein. *Proceedings of the National Academy of Sciences USA.* 101, 14713-14718 (2004).

Lingner J. Cech T. R. Telomerase and chromosome end maintenance. *Current Opinion in Genetics and Development.* 8, 226-232 (1998).

Lingner J, Hughes T. R, Shevchenko A, Mann M, Lundblad V, Cech T. R. Reverse transcriptase motifs in the catalytic subunit of telomerase. *Science.* 276, 561-567 (1997).

Lu X, Errington J, Curtin N. J, Lunec J, Newell D. R. The impact of p53 status on cellular sensitivity to antifolate drugs. *Clinical Cancer Research.* 7, 2114-2123 (2001).

Makarov V. L, Hirose Y, Langmore J. P. Long G tails at both ends of human chromosomes suggest a C strand degradation mechanism for telomere shortening. *Cell.* 88, 657-666 (1997).

Martins C, Gunaratnam M, Stuart J, Makwana V, Greciano O, Reszka A. P, Kelland L. R, Neidle S Structure-based design of benzylamino-acridine compounds as G-quadruplex DNA telomere targeting agents. *Bioorganic Medicinal Chemistry Letters.* 17, 2293-2298 (2007).

Masutomi K, Possemato R, Wong J. M. Y, Currier J. L, Tothova Z, Manola J. B, Ganesan S, Lansdorp P. M, Collins K, Hahn W. C. The telomerase reverse transcriptase regulates chromatin state and DNA damage response. *Proceedings of the National Academy of Sciences USA.* 102, 8222-8227 (2005).

Matapurkar A, Lazebnik Y. Requirement of cytochrome c for apoptosis in human cells. *Cell Death and Differentiation.* 13, 2062-2067 (2006).

McDonald A. C, Brown R. Induction of p53-dependent and p53-independent cellular responses by topoisomerase 1 inhibitors. *British Journal of Cancer.* 78, 745-751 (1998).
Merlin J. L. Concepts of synergism and antagonism. *Anticancer Research.* 14, 2315-2319 (1994).

Mese H, Sasaki A, Alcalde R. E, Nakayama R. E, Matsumura T. Regulation of apoptosis reduction in the cisplatin-resistance A431 cell line by Bcl-2 and CPP32. *Experimental Chemotherapy.* 46, 69-76 (2000).

Mese H, Sasaki A, Nakayama S. Alcalde R. E, Matsumura T. The role of caspase family protease, caspase 3 on cisplatin-induced apoptosis in cisplatin-resistance A431 cell line. *Cancer Chemotherapy Pharmacology.* 46, 241-245 (2000).

Mese H, Ueyama Y, Suzuki A, Nakayama S, Sasaki A, Hamakawa H, Matsuruma T. Inhibition of telomerase activity as a measure of tumor cell killing by cisplatin in squamous carcinoma cell line. *Chemotherapy.* 47, 136-42 (2001).

Michalakis J, Georgatos S. D, Romanos J, Koutala H, Georgoulias V, Tsiftisis D, Theodoropoulos P. A. Micromolar taxol, with or without hyperthermia, induces mitotic catastrophe and cell necrosis in HeLa cells. *Cancer Chemotherapy Pharmacology.* 56, 615-622 (2005).

Misawa M, Tauchi, Sashida G, Nakajima A, Abe K, Ohyashiki J. H, Ohyashiki K. Inhibition of human telomerase enhance the effect of chemotherapeutic agents in lung cancer cells. *International Journal of Oncology.* 21, 1087-1092 (2002).

Moggs J. G, Szymkowski D. E, Yamada M, Karran P, Wood R. D. Differential human nucleotide excision repair of paired and mispaired cisplatin-DNA adducts. *Nucleic Acids Research.* 25, 480-490 (1997).

Morero J. L, Poleri C, Martin C, Van Kooten M, Chacon R, Rosenberg M. Influence of apoptosis and cell cycle regulator proteins on chemotherapy response and survival in stage IIIA/IIIB NSCLC patients. *Journal of Thoracic Oncology.* 2, 293-298 (2007).

Mukherjee B, Kessinger C, Kobayashi J, Chen B. P. C, Chen D. J, Chatterjee A, Burma S. DNA-PK phosphorylates histone H2AX during apoptotic DNA fragmentation in mammalian cells. *DNA repair.* 5, 575-590 (2006).

Murname J. P. Telomeres and chromosome instability. *DNA Repair.* 5, 1082-1092 (2006).

Muntoni A, Reddel R. R. The first molecular details of ALT in human tumor cells. *Human Molecular Genetics.* 14, 191-196 (2005).

Nagatani G, Nomoto M, Takano H, Ise T, Kato K, Imamura T, Izumi H, Makishima K, Kohno K. Transcriptional activation of the human HMG1 gene in cisplatin-resistance human cancer cells. *Cancer Research.* 61, 1592-1597 (2001).

Neidle S, Parkinson G. Telomere maintenance as a target for anticancer drug discovery. *Nature Reviews Drug Discovery.* 1, 383-393 (2002).

Oganesian L, Bryan T. Physiological relevance of telomeric G-quadruplex formation: a potential drug target. *Bioessays*. 29, 155-165 (2007).

Oniscu A, Sphyris N, Morris R. G, Bader S, Harrison D. J. p73α is a candidate effector in the p53 independent apoptosis pathway of cisplatin damaged primary murine colonocytes. *Journal of Clinical Pathology*. 57, 492-498 (2004).

Opresko P. L, von Kobbe C, Laine J. P, Harrigan J, Hickson I. D, Bohr V. A. Telomere-binding protein TRF2 binds to and stimulates the Werner and Bloom Syndrome Helicases. *The Journal of Biological Chemistry*. 277, 41110-41119 (2002).

Opresko P. L, Mason P. A, Podell E. R, Lei M, Hickson I. D, Cech T. R, Bohr V. A. POT1 stimulated RecQ helicases WRN and BLM to unwind telomeric DNA substrates. *The Journal of Biological Chemistry*. 280, 32069-32080 (2005).

Ou T. M, Lu Y. J, Zhang C, Huang Z. S, Wang X. D, Tan J. H, Chen Y, Ma D. L, Wong K. Y, Tang J. C, Sun-Chi Chan A, Gu L. Q. Stabilization of G-quadruplex DNA and down-regulation of oncogene c-myc by quindoline derivatives. *Journal of Medicinal Chemistry*. 50, 1465-1474 (2007).

Paccagnella A, Favaretto A, Oniga F, Barbieri F, Ceresoli G, Torri W, Villa D, Verusio C, Cetto G. L, Santo A, Pangher V Artioli F, Cacciani G. C, Parodi G, Soresi F, Ghi M. G, Morabito A, Biason R, Giusto M. Mosconi P, Chiarion Sileni V. Cisplatin versus carboplatin in combination with mitomycin and vinblastine in advanced non small cell lung cancer. A multicenter, randomized phase III trial. *Lung Cancer*. 43, 83-91 (2004).

Pennarun G, Granotier C, Gauthier L. R, Gomez D, Hoffschir F, Mandine E, Riou J. F, Mergny J. L, Mailliet P, Boussin F. D. Apoptosis related to telomere instability and cell cycle alterations in human glioma cells treated by new highly selective G-quadruplex ligands. *Oncogene*. 24, 2917-2928 (2005).

Petit T, Bearss D. J, Troyer D. A, Munoz R. M, Windle J. J. p53-independent response to cisplatin and oxaliplatin in MMTV-ras mouse salivary tumors. *Molecular Cancer Therapeutics*. 2, 165-171 (2003).

Phatak P, Cookson J. C, Dai F, Smith V, Gartenhaus R. B, Stevens M. F. G, Burger A. M. Telomere uncapping by the G-quadruplex ligand RHPS4 inhibits clonogenic tumour cell growth in vitro and in vivo consistent with a cancer stem cell targeting mechanism. *British Journal of Cancer*. 96, 1223-1233 (2007).

Pietenpol J. A, Stewart Z. A. Cell cycle checkpoint signalling: cell cycle arrest versus apoptosis. *Toxicology*. 181, 475-481 (2002).

Plooy A. C. M, van Dijk M, Berends F, Lohman P. H. M. Formation and repair of DNA interstrand cross-links in relation to cytotoxicity and unscheduled DNA synthesis induced in control and mutant human cells treated with cis-Diamminedichloroplatinum (II). *Cancer Research*. 45, 4178-4184 (1985).

di Prieto A, Vries E. G. E, Gietema J. A, Spierings D. C. J, de Jong S. Testicular germ cell tumours: The paradigm of chemo-sensitive solid tumours. *The International Journal of Biochemistry and Cell Biology*. 37, 2437-2456 (2005).

Ramadan S, Terrinoni A, Catani M. V, Sayan A. E, Knight R. A, Mueller M, Krammer P. H, Melino G, Candi E. p73 induces apoptosis by different mechanisms. *Biochemical and Biophysical Research Communications*. 331, 713-717 (2005).

Raaphorst G. P, Leblanc J. M, Li L. F. A comparition of response to cisplatin, radiation and combined treatment for cells deficient in recombination repair pathways. *Anticancer Research*. 25, 53-58 (2005).

Read M, Harrison R. J, Romagnoli B, Tanious F. A, Gowan S. H, Reszka A. P, Wilson W. D, Kelland L. R, Neidle S. Structure-based design of selective and potent G quadruplex-mediated telomerase inhibitors. *Proceedings of the National Academy of Sciences USA*. 98, 4844-4849 (2001).

Redon S, Bombard S, Elizondo-Riojas M. A, Chottard J. C. Platinum cross-linding of adenines and guanines on the quadruplex structures of the $AG_3(T_2AG_3)_3$ and $(T_2AG_3)_4$ human telomere sequences in Na^+ and K^+ solutions. *Nucleic Acids Research*. 31, 1605-1613 (2003).

Redon S, Bombard S, Elizondo-Riojas M. A, Chottard J. C. Platination of the $(T_2AG_3)_4$ telomeric sequence: a structural and cross-linking study. *Biochemistry*. 40, 8463-8470 (2001).

Reed J, Gunaratnam M, Beltran M, Reszka A. P, Vilar R, Neidle S. TRAP-LIG, a modified telomere repeat amplification protocol assay to quantitate telomerase inhibition by small molecules. *Analytical Biochemistry*. Published on line. (2008).

Reedijk J. Why does cisplatin reach guanine-N7 with competing S-donor ligands available in the cell?. *Chemistry Review*. 99, 2499-2510 (1999).

Reedijk J. New clues for platinum antitumor chemistry: kinetically controlled metal binding to DNA. *Proceedings of the National Academy of Sciences USA*. 100, 3611-3616 (2003).

Reles A, Wen W. H, Schmider A, Gee C, Runnebaum I. B, Kilian U, Jones L. A, El-Naggar A, Minguillon C, Schonborn I, Reich O, Kreienberg R, Lichtenegger W, Press M. F. Correlation of p53 mutations with resistance to platinum-based chemotherapy and shortened survival in ovarian cancer. *Clinical Cancer Research*. 7, 2984-2997 (2001).

Rennicke A, Voigt W, Mueller T, Fruehauf A, Schmoll H. J, Beyer C, Dempke W. Resistance mechanism following cisplatin and oxaliplatin treatment of the human teratocarcinoma cell line 2102EP. *Anticancer Research*. 25, 1147-1156 (2005).

Reynolds C. P, Maurer B. J. Evaluating response to antineoplastic drug combination in tissue culture models. *Methods in Molecular Medicine*. 110, 173-183 (2005).

Rezler E. M, Bearss D. J, Hurley L. H. Telomeres and telomerases as drug targets. *Current Opinion in Pharmacology*. 2, 415-423 (2002).

Rheinwald J. G, Hahn W. C, Ramsey M. R, Wu J.Y, Guo Z, Tsao H, De Luca M, Catricala C, O'Toole K. M. A two-stage, p16 and p53 dependent keratinocyte senescence mechanism that limits replicative potential independent of telomere status. *Molecular and Cellular Biology*. 22, 5157-5172 (2002).

Riou J. F. G-Quadruplex interacting agents targeting the telomeric G-overhang are more than simple telomerase inhibitors. *Current Medicinal Chemistry.* 4, 439-443 (2004).

Rodriges M, Barbosa Junior F, Perussi J. R. Dipyridamole increases the cytotoxicity of cisplatin in human larynx cancer cells *in vitro*. *Brazilian Journal of Medical and Biological Research.* 37, 591-599 (2004).

Rogakou E. P, Pilch D. R, Orr A. H, Ivanova V. S, Bonner W. M. DNA double-stranded breaks induce histone H2AX phosphorylation on serine 139. *Journal of Biological Chemistry.* 273, 5858-5868 (1998).

Rogakou E. P, Boon C, Redon C, Bonner W. M. Megabase chromatin domains involved in DNA double-strand breaks in vivo. *The Journal of Cell Biology.* 146, 905-915 (1999).

Rogakou E, Nieves-Neira W, Boon C, Pommier Y, Bonner W. M. Initiation of DNA fragmentation during apoptosis induces phosphorilation of H2AX histone at serine 139. *The Journal of Biological Chemistry.* 275, 9390-9395 (2000).

Roninson I. B. Tumor cell senescence in Cancer Treatment. *Cancer Research.* 63, 2705-2715 (2003).

Rosenberg B. Fundamental studies with cisplatin. *Cancer.* 55, 2303-2316 (1985).

Rossetti L, Franceschin M, Schirripa S, Bianco A, Ortaggi G, Savino M. Selective interactions of perylene derivatives having different side chains with inter- and intramolecular G-quadruplex DNA structures. A correlation with telomerase inhibition. *Bioinorganic and Medicinal Chemistry Letters.* 15, 413-420 (2005).

Rudin C. M, Yang Z, Schumaker L. M, VanderWeele D. J, Newkirk K, Egorin M. J, Zuhowski E. G, Cullen K. J. Inhibition of glutathione synthesis reverses Bcl-2-mediated cisplatin resistance. *Cancer Research.* 63, 312-318 (2003).

Salvati E, Leonetti C, Rizzo A, Scarsella M, Mottolese M, Galati R, Sperduti I, Stevens M. F. G, D'Incalci M, Blasco M, Chiorino G, Bauwens S, Horard B, Gilson E, Stoppacciaro A, Zupi G, Biroccio A. Telomere damage induced by the G-quadruplex ligand RHPS4 has an antitumor effect. *The Journal of Clinical Investigation.* 117, 3236-3247 (2007).

Samimi G, Fink D, Varki N. M, Husain A, Hoskins W. J, Alberts D. S, Howell S. B. Analysis of MLH1 and MDH2 expression in ovarian cancer before and after platinum drug-based chemotherapy. *Clinical Cancer Research.* 6, 1415-1421 (2000).

Schaffitzel C, Berger I, Postberg J, Hanes J, Lipps H. J, Plückthun. In vitro generated antibodies specific for telomeric guanine-quadruplex DNA react with Stylonychia lemnae macronuclei. *Proceedings of the National Academy of Sciences USA.* 98, 8572-8577 (2001).

Schmidt M, Fan Z. Protection against chemotherapy-induced cytotoxicity by cyclin-dependent kinase inhibitors (CKI) in CKI-responsive cells compared with CKI-unresponsive cell. *Oncogene.* 20, 6164-6171 (2001).

Schuler M, Green D. R. Transcription, apoptosis and p53: catch-22. *Trends in Genetics.* 21, 182-187 (2005).

Schultes C, Guyen B, Cuesta J, Neidle S. Synthesis, biophysical and biological evaluation of 3,6-bis-amidoacridines with extended 9-anilino substituents as potent G-quadruplex-binding telomerase inhibitors. *Bioorganic Medicinal Chemistry Letters.* 14, 4347-4351 (2004).

Sedletska Y, Giraud-Panis M. J, Malinge J. M. Cisplatin is a DNA-damaging antitumour compound triggering multifactorial biochemical responses in cancer cells: importance of apoptotic pathways. *Current Medicinal Chemistry Anticancer Agents.* 5, 251-265 (2005)

Seimiya H, Muramatsu Y, Ohishi T, Tsuruo T. Tankyrase 1 as a target for telomere-directed molecular cancer therapeutics. *Cancer Cell.* 7, 25-37 (2005).

Selvakumaran M, Pisarcik D. A, Bao R, Yeung A. T, Hamilton T. C. Enhanced cisplatin cytotoxicity by disturbing the nucleotide excision repair pathway in ovarian cancer cell lines. *Cancer Research.* 63, 1311-1316 (2003).

Shafer R. H, Smirnov I. Biological aspects of DNA/RNA quadruplex. *Biopolymers.* 56, 209-227 (2001).

Shammas M. A, Shmookler Reis R. J, Li C, Koley H, Hurley L. H, Anderson K. C, Munshi N. C. Telomerase inhibition and cell growth arrest after telomestatin treatment in multiple myeloma. *Clinical Cancer Research.* 10, 770-776 (2004).

Shay J. W, Bacchetti S. A survey of telomerase activity in human cancer. *European Journal of Cancer.* 33, 787-791 (1997).

Shay J. W, Wright W, E. Telomerase therapeutics for cancer: challenges and new directions. *Nature Reviews Drug Discovery.* 5, 577-584 (2006).

Shi Y. Mechanical aspects of apoptosome assembly. *Current Opinion in Cell Biology.* 18, 677-684 (2006).

Shin K. H, Kang M. K, Dicterow E, Kameta A, Baluda M. A, Park N. H. Introduction of human telomerase reverse transcriptase to normal human fibroblast enhances DNA repair capacity. *Clinical Cancer Research.* 10, 2551-2560 (2004).

Simonsson T, Pecinka P, Kubista M. DNA tetraplex formation in the control region of c-*myc*. *Nucleic Acids Research.* 26, 1167-1172 (1998).

Siwkowski A. M, Madge L. A, Koo S, McMillan E. L, Monia B. P, Pober J. S, Baker B. F. Effects of antisense oligonucleotide-mediated depletion o tumor necrosis factor (TNF) receptor 1 associated death domain on TNF receptor gene expression. *Molecular Pharmacology.* 66, 572-579 (2004).

Skehan P, Storeng R, Scudiero D, Monks A, Mc Mahou J, Vistica D, Warren J. T, Bokesch H, Kenney S, Boyd M. R. New colorimetric cytotoxicity assay for anticancer-drug screening. *Journal of the National Cancer Institute.* 82, 1107-1112 (1990).

Smith J. R, Pereira-Smith O. M. Replicative senescence: implications for in vivo aging an tumor suppression. *Science*. 273, 63-67 (1996).

Smogorzewska A, van Seensel B, Bianchi A, Oelmann S, Schaefer M, Schnapp G, de Lange T. Control of human telomere length by TRF1 and TRF2. *Molecular and Cellular Biology*. 20, 1659-1668 (2000).

Smogorzewska A, de Lange T. Different damage signaling pathways in human and mouse cells. *The EMBO Journal*. 21, 4338-4348 (2002).

Spurgers K. B, Gold D. L, Coombes K. R, Bohnenstiehl N. L, Mullins B, Meyn R. E, Logothetis C. J, McDonnell T. J. Identification of cell cycle regulatory genes as principal targets of p53-mediated transcriptional repression. *Journal of Biological Chemistry*. 281, 25134-25142 (2006).

van Steensel B, de Lange T. Control of telomere length by the human telomeric protein TRF1. *Nature*. 385, 740-743 (1997).

Stordal B, Pavlakis N, Davey R. Oxaliplatin for the treatment of cisplatin-resistant cancer: A systematic review. *Cancer Treatment Review*. 33, 347-357 (2007).

Sugimura M, Sagae S, Ishioka S, Nishioka Y, Tsukada K, Kudo R. Mechanisms of paclitaxel-induced apoptosis in an ovarian cancer cell line and its paclitaxel-resistance clone. *Oncology*. 66, 53-61 (2004).

Sundquist W. I, Klug A. Telomeric DNA dimerizes by formation of guanines tetrads between hairpin loops. *Nature*. 342, 825-829 (1989).

Sung Y. H, Choi Y. S, Cheong C, Lee H. W. The pleiotropy of telomerase against cell death. *Molecular Cells*. 19, 303-309 (2005).

Tabuko K, Izumiyama-Shimomura N, Honma N, Sawabe M, Arai T, Kato M, Oshimura M, Nakamura K. I. Telomere lengths are characteristic in each human individual. *Experimental Gerontology*. 37, 523-531 (2002).

Takahara P. M, Rosenzweig A. C, Frederick C. A, Lippard S. J. Crystal structure of double-stranded DNA containing the major adduct of the anticancer drug cisplatin. *Nature*. 377, 649-652 (1995).

Tahara H, Shin-ya K, Seimiya H, Yamada H, Tsuruo T, Ide T. G-Quadruplex stabilization by telomestatin induces TRF2 protein dissociation from telomeres and anaphase bridge formation accompanied by loss of the 3' telomeric overhang in cancer cells. *Oncogene*. 25,1955-1966 (2006)

Takahashi A, Ohnishi T. Does γ-H2AX foci formation depend on the presence of DNA double strand breaks?. *Cancer Letters*. 229, 171-179 (2006).

Tanaka H, Mendonca M. S, Bradshaw P. S, Hoelz D. J, Malkas L. H, Meyn M. S. DNA damage-induced phosphorylation of the human telomere-associated protein TRF2. *Proceedings of the National Academy of Sciences USA*. 102, 15539-15544 (2005).

Tarsounas M, Munoz P, Claas A, Smiraldo P. G, Pittman D. L, Blasco M. A, West S. C. Telomere maintenance requires the RAD51D recombination/repair protein. *Cell.* 117, 337-347 (2004).

Tauchi T, Shin-ya K, Sashida G, Sumi M, Okabe S, Ohyashiki J. H, Ohyashiki K. Telomerase inhibition with a novel G-quadruplex-interactive agent, telomestatin: in vitro and in vivo studies in acute leukemia. *Oncogene.* 25, 5719-5725 (2006).

Theimer C. A, Blois C. A, Feigon J. Structure of the human telomerase RNA pseudoknot reveals conserved tertiary interactions essential for function. *Molecular Cell.* 17, 671-682 (2005).

Thornberry N. A, Lazebnik Y. Caspases: Enemies Within. *Apoptosis.* 281, 1312-1316 (1998).

To K. K. W, Ho Y. P, Au-Yeung S. C. F. Synergistic interaction between platinum-based antitumor agents and demethylcantharidin. *Cancer Letters.* 223, 227-237 (2005).

Todd A. K, Johnston M, Neidle S. Highly prevalent putative quadruplex sequence motifs in human DNA. *Nucleic Acids Research.* 33, 2901-2907(2005).

Todd A. K, Haider S. M, Parkinson G. N, Neidle S. Sequence occurrence and structural uniqueness of a G-quadruplex in the human c-kit promoter. *Nucleic Acids Research.* 35, 5799-5808 (2007).

Tomaska L, McEachern M. J, Nosek J. Alternatives to telomerase: keeping linear chromosomes via telomeric circles. *FEBS Letters.* 567, 142-146 (2004).

Uezono T, Maruyama W, Matsubara K, Naoi M, Shimizu K, Saito O, Ogawa K, Mizukami H, Hayase N, Shiono H. Norharman, an indoleamine-derived beta-carboline, but not Trp-P-2, a gamma-carboline, induces apoptotic cell death in human neuroblastoma SH-SY5Y cells. *Journal of Neuronal Transmission.* 108, 943-953 (2001).

Vikhanskaya F, D`Incalci M, Broggini M. p73 competes with p53 and attenuates its response in a human ovarian cancer cell line. *Nucleic Acids Research.* 28, 513-519 (2000).

Verdun R. E, Karlseder J. Replication and protection of telomeres. *Nature.* 447, 924-931 (2007).

Vogelstein B, Lane D, Levine A. J. Surfing the p53 network. *Nature.* 408, 307-310 (2000).

Vogiatzi P, Cassone M, Abbadessa G, Claudio P. P. The limitless role of p53 in cell cycle machinery. Good or bad news?. *Cancer Biology and Therapy.* 5, 1090-1093 (2006).

Voortman J, Smit E. F, Honeywell R, Kuenen B. C, Peters G. J, van de Velde H. Giaccone G. A parallel dose-escalation study of weekly and twice weekly bortezomib in combination with gemcitabine and cisplatin in the first-line treatment of patients with advanced solid tumors. *Clinical Cancer Research.* 13, 3642-3651 (2007).

Wang D, Lippard S. J. Cellular processing of platinum anticancer drugs. *Nature Reviews Drug Discovery*. 4, 307-320 (2005).

Wang F, Podell E. R, Zaug A. J, Yang Y, Baciu P, Cech T. R, Lei M. The POT1-TPP1 telomere complex is a telomerase processivity factor. *Nature*. 445, 506-510 (2007).

White L. K, Wright W. E, Shay J. W. Telomerase inhibitors. *Trends in Biotechnology*. 19, 114-120 (2001).

Williams J, Lucas P. C, Griffith K. A, Choi M, Fogoros S, Hu Y. Y, Liu J. R. Expression of Bcl-xl in ovarian carcinoma is associated with chemoresistance and recurrent disease. *Gynecologic Oncology*. 96, 287-295 (2005).

Woo R. A, McLure K. G, Lees-Miller S. P, Rancourt D. E, Lee P. W. K. DNA-dependent protein kinase acts upstream of p53 in response to DNA damage. *Nature*. 394, 700-704 (1998).

Wood C. M, Nicholson J. M, Lambert S. J, Chantalat L, Reynolds C. D, Baldwin J. P. High-resolution structure of the native histone octamer. *Structural Biology and Crystallization Communications*. 61, 541-545 (2005).

Wozniak K, Blasiak J. Recognition and repair of DNA-cisplatin adducts. *Acta Biochimica Polonica*. 49, 583-596 (2002).

Xue C, Haber M, Flemming C, Marshall G. M, Lock R. B, MacKenzie K. L, Gurova K. V, Norris M. D, Gudkov A. V. p53 determines multidrug sensitivity of childhood neuroblastoma. *Cancer Research*. 67, 10351-10360 (2007).

Yamada M, O'Regan E, Brown R, Karran P. Selective recognition of a cisplatin-DNA adduct by human mismatch repair proteins. *Nucleic Acids Research*. 25, 491-495 (1997).

Yunmbam M. K, Guo Y, Miller M. R, Yu J. J. Combinatorial treatment of ovarian cancer cells with harringtonine and cisplatin results in increased cisplatin-DNA adducts. *Oncology Reports*. 11, 833-838 (2004).

Zamble D.B, Lippard S. J. Cisplatin and DNA repair in cancer chemotherapy. *Trends in Biochemical Sciences*. 20, 435-439 (1995).

Zahler A. M, Williamson J. R, Cech T. R, Prescott D. M. Inhibition of telomerase by G-quartet DNA structures. *Nature*. 350, 718-720 (1991).

Zhang X, Mar V, Zhou W. Harrington L, Robinson M. O. Telomere shortening and apoptosis in telomerase-inhibited human tumor cells. *Genes and Development*. 13, 2388-2398 (1999).

Zhang R. G, Zhang R. P, Wang X, Wang X. W, Xie H. Effects of cisplatin on telomerase activity and telomere length in BEL-7404 human hepatoma cells. *Cell Research*. 12, 55-62 (2002).

Zhao W, Lin Z. X, Zhang Z. Q. Cisplatin-induced premature senescence with concomitant reduction of gap junctions in human fibroblast. *Cell Research.* 14, 60-66 (2004).

Zhou J. M, Zhu X. F, Lu Y. J, Deng R, Huang Z. S, Mei Y. P, Wang Y, Huang W. L, Liu Z. C, Gu L. Q, Zeng Y. X. Senescence and telomere shortening induced by novel G-quadruplex interactive agents, quindoline derivatives, in human cancer cell lines. *Oncogene.* 25, 503-511 (2005).

Zhu X. D, Niedernhofer L, Kuster B, Mann M, Hoeijmakers J. H. J, de Lange T. ERCC1/XPF removes the 3'overhang from uncapped telomeres and represses formation of telomeric DNA-containing double minute chromosomes. *Molecular Cell.* 12, 1489-1498 (2003).

Zhong W. X, Ditsworth D, Bauer D. E, Wang Z. Q, Thompson C. B. Alkylating DNA damage stimulates a regulated form of necrotic cell death. *Genes and Development.* 18, 1272-1282 (2004).